Midwest States' Regional Pooled Fund Research Program
Fiscal Year 2001-2002 (Year 12)
Research Project Number SPR-3 (017)
NDOR Sponsoring Agency Code RPFP-02-02

Phase III Development of a Short-Radius Guardrail for Intersecting Roadways

Submitted by

Cody S. Stolle
Undergraduate Research Assistant

Karla A. Polivka, M.S.M.E., E.I.T.
Research Associate Engineer

Robert W. Bielenberg, M.S.M.E., E.I.T.
Research Associate Engineer

John D. Reid, Ph.D.
Professor

Ronald K. Faller, Ph.D., P.E.
Research Assistant Professor

John R. Rohde, Ph.D., P.E.
Associate Professor

Dean L. Sicking, Ph.D., P.E.
Professor and MwRSF Director

MIDWEST ROADSIDE SAFETY FACILITY
University of Nebraska-Lincoln
527 Nebraska Hall
Lincoln, Nebraska 68588-0529
(402) 472-6864

Submitted to

Midwest States' Regional Pooled Fund Program

Nebraska Department of Roads
1500 Nebraska Highway 2
Lincoln, Nebraska 68502

MwRSF Research Report No. TRP-03-183-07

December 6, 2007

Technical Report Documentation Page

1. Report No.	2.	3. Recipient's Accession No.
TRP-03-183-07		

4. Title and Subtitle	5. Report Date
Phase III Development of a Short-Radius Guardrail for Intersecting Roadways	December 6, 2007
	6.

7. Author(s)	8. Performing Organization Report No.
Stolle, C.S., Polivka, K.A., Bielenberg, R.W., Reid, J.D., Faller, R.K., Rohde, J.R., and Sicking, D.L.	TRP-03-183-07

9. Performing Organization Name and Address	10. Project/Task/Work Unit No.
Midwest Roadside Safety Facility (MwRSF) University of Nebraska-Lincoln 527 Nebraska Hall Lincoln, NE 68588-0529	11. Contract © or Grant (G) No. SPR-3(017)

12. Sponsoring Organization Name and Address	13. Type of Report and Period Covered
Midwest States' Regional Pooled Fund Program Nebraska Department of Roads 1500 Nebraska Highway 2 Lincoln, Nebraska 68502	Final Report 2005-2007
	14. Sponsoring Agency Code RPFP-02-02

15. Supplementary Notes

16. Abstract (Limit: 200 words)

This research study consisted of the development and testing of a short-radius guardrail system for protection of hazards near intersecting roadways and capable of meeting the Test Level 3 (TL-3) impact conditions of the NCHRP Report No. 350 criteria. A short-radius system was designed and consisted of a curved and slotted thrie beam nose section with two adjacent slotted thrie beam sections supported by breakaway posts. One side of the system was attached to a TL-3 steel post approach transition while the other attached to a TL-2 end terminal.

A series of two full-scale crash tests were conducted on the short-radius guardrail system. The first test on the short-radius system was conducted as a modified version of NCHRP Report No. 350 Test Designation 3-31. As such, the impact was oriented at an angle of 0 degrees to the roadway, but the impact point was altered to force the vehicle to move directly down the primary side of the system. This was believed to be a more critical impact condition than provided by the standard test 3-31. In test SR-5, a 2,001-kg (4,412-lb) pickup truck impacted the short-radius with its center aligned with post no. 1P at an speed of 101.8 km/h (63.2 mph) and at an angle of -0.3 degrees. The pickup truck was safety redirected, and test SR-5 was judged acceptable according to NCHRP Report No. 350. The second test on the short-radius system was conducted according to NCHRP Report No. 350 Test Designation 3-30. Prior to running test SR-6, the short-radius was modified by altering the upstream anchor for the primary side. Bogie testing was conducted on the modified anchor to insure that the design generated appropriate anchor loads. In test SR-6, an 893-kg (1,969-lb) small car impacted the short-radius guardrail at a speed of 99.4 km/h (61.8 mph) and at an angle of 0.8 degrees on the center of the curved nose of the system. This test was judged unacceptable according to NCHRP Report No. 350 criteria due to excessive ridedown decelerations.

After review of the full-scale tests, it was evident that the short-radius guardrail system showed significant improvement over the original system developed by the Midwest Roadside Safety Facility, but further development was required.

17. Document Analysis/Descriptors	18. Availability Statement
Highway Safety, Guardrail Longitudinal Barrier, Short-Radius Barrier, Intersection Protection, Roadside Appurtenances, Crash Test, Compliance Test	No restrictions. Document available from: National Technical Information Services, Springfield, Virginia 22161

19. Security Class (this report)	20. Security Class (this page)	21. No. of Pages	22. Price
Unclassified	Unclassified	227	

DISCLAIMER STATEMENT

The contents of this report reflect the views of the authors who are responsible for the facts and the accuracy of the data presented herein. The contents do not necessarily reflect the official views or policies of the state highway departments participating in the Midwest States' Regional Pooled Fund Program nor the Federal Highway Administration. This report does not constitute a standard, specification, or regulation.

ACKNOWLEDGMENTS

The authors wish to acknowledge several sources that made a contribution to this project: (1) the Midwest States' Regional Pooled Fund Program funded by the California Department of Transportation, Connecticut Department of Transportation, Illinois Department of Transportation, Iowa Department of Transportation, Kansas Department of Transportation, Minnesota Department of Transportation, Missouri Department of Transportation, Montana Department of Transportation, Nebraska Department of Roads, New Jersey Department of Transportation, Ohio Department of Transportation, South Dakota Department of Transportation, Texas Department of Transportation, Wisconsin Department of Transportation, and Wyoming Department of Transportation for sponsoring this project; (2) Martin Snow and Universal Steel for donating the slotted nose section of guardrail; and (3) MwRSF personnel for constructing the barriers and conducting the crash tests.

A special thanks is also given to the following individuals who made a contribution to the completion of this research project.

Midwest Roadside Safety Facility

J.C. Holloway, Research Manager
C.L. Meyer, Research Engineer II
A.T. Russell, Laboratory Mechanic II
K.L. Krenk, Field Operations Manager
A.T. McMaster, Laboratory Mechanic I
Undergraduate and Graduate Assistants

California Department of Transportation

Gary Gauthier, Roadside Safety Research Specialist
Wes Lum, P.E., Office Chief National Liaison

Connecticut Department of Transportation

Dionysia Oliveira, Transportation Engineer 3

Illinois Department of Transportation

David Piper, P.E., Highway Policy Engineer

Iowa Department of Transportation

David Little, P.E., Assistant District Engineer
Deanna Maifield, Methods Engineer

Kansas Department of Transportation

Ron Seitz, P.E., Bureau Chief
Rod Lacy, P.E., Road Design Leader

Minnesota Department of Transportation

Jim Klessig, Implementation Liaison
Mohammad Dehdashti, P.E., Design Standard Engineer
Michael Elle, P.E., Design Standard Engineer

Missouri Department of Transportation

Joseph G. Jones, Technical Support Engineer

Montana Department of Transportation

Susan Sillick, Research Bureau Chief

Nebraska Department of Roads

Amy Starr, Research Engineer
Phil TenHulzen, P.E., Design Standards Engineer
Jodi Gibson, Research Coordinator

New Jersey Department of Transportation

Kiran Patel, P.E., P.M.P, C.P.M, Deputy State Transportation Engineer

Ohio Department of Transportation

Dean Focke, P.E., Roadway Safety Engineer

South Dakota Department of Transportation

David Huft, Research Engineer
Bernie Clocksin, Lead Project Engineer

Texas Department of Transportation

Mark Bloschock, P.E., Supervising Design Engineer
Mark Marek, P.E., Design Engineer

Wisconsin Department of Transportation

John Bridwell, Standards Development Engineer
Patrick Fleming, Standards Development Engineer

Wyoming Department of Transportation

William Wilson, P.E., Standards Engineer

Federal Highway Administration

John Perry, P.E., Nebraska Division Office
Danny Briggs, Nebraska Division Office

Dunlap Photography

James Dunlap, President and Owner

TABLE OF CONTENTS

Page

TECHNICAL REPORT DOCUMENTATION PAGE i

DISCLAIMER STATEMENT iii

ACKNOWLEDGMENTS iv

TABLE OF CONTENTS vii
List of Figures ix
List of Tables xiv

1 INTRODUCTION 1
1.1 Problem Statement 1
1.2 Objective 2
1.3 Scope 2

2 NCHRP 350 TESTING AND EVALUATION CRITERIA 3
2.1 Test Requirements 3
2.2 Evaluation Criteria 4

3 TEST CONDITIONS 8
3.1 Test Facility 8
3.2 Vehicle Tow and Guidance System 8
3.3 Test Vehicles 8
3.4 Data Acquisition Systems 9
3.4.1 Accelerometers 9
3.4.2 Rate Transducers 12
3.4.3 High-Speed Photography 12
3.4.4 Pressure Tape Switches 18

4 DESIGN MODIFICATIONS, TEST NO. SR-5 21

5 SHORT-RADIUS DESIGN DETAILS 26
5.1 Design Details 26

6 CRASH TEST NO. SR-5 60
6.1 Test SR-5 60
6.2 Test Description 60
6.3 System and Component Damage 61
6.4 Vehicle Damage 62
6.5 Occupant Risk Values 63
6.6 Discussion 63

7 DISCUSSION AND COMPONENT TESTING 89
7.1 Design Modification 89
7.2 Component Test 89

8 SHORT-RADIUS DESIGN MODIFICATIONS 94

9 CRASH TEST NO. SR-6 105
9.1 Test SR-6 105
9.2 Test Description 105
9.3 System and Component Damage 106
9.4 Vehicle Damage 107
9.5 Occupant Risk Values 108
9.6 Discussion 108

10 SUMMARY AND CONCLUSIONS 129

11 FUTURE DEVELOPMENT 133

12 REFERENCES 134

13 APPENDICES 137
APPENDIX A
English-Unit System Drawings, Test SR-5 138
APPENDIX B
Test Summary Sheets in English Units 163
APPENDIX C
Occupant Compartment Deformation Data, Test SR-5 166
APPENDIX D
Accelerometer and Rate Transducer Data Analysis, Test SR-5 170
APPENDIX E
Metric-Unit System Drawings, Test SR-6 178
APPENDIX F
English-Unit System Drawings, Test SR-6 198
APPENDIX G
Accelerometer and Rate Transducer Data Analysis, Test SR-6 218
APPENDIX H
Accelerometer and Rate Transducer Data Analysis, Test SR-6 220

List of Figures

Page

1. Full-Scale Crash Test Matrix 6
2. Test Vehicle, Test SR-5 10
3. Vehicle Dimensions, Test SR-5 11
4. Test Vehicle, Test SR-6 13
5. Vehicle Dimensions, Test SR-6 14
6. Vehicle Target Locations, Test SR-5 15
7. Vehicle Target Locations, Test SR-6 16
8. Location of High-Speed Cameras, Test SR-5 19
9. Location of High-Speed Cameras, Test SR-6 20
10. Comparison of Full-Scale Test and LS-DYNA Simulation Model, Test No. SR-4 24
11. LS-DYNA Simulations of Test SR-4 and SR-5 25
12. Short-Radius Overall System Layout 31
13. Short-Radius Secondary Side System Layout 32
14. Short-Radius Primary Side System Layout 33
15. Cable Release Layout 34
16. Primary Side Cable Anchor Detail 35
17. Anchor Cable and Release Cable Details 36
18. Nose Cable Details 37
19. MGS Timber Posts and Foundation Tube and Thrie Beam Foundation Tube Details 38
20. Post Details 39
21. MGS CRT and BCT Post Details 40
22. Thrie Beam CRT and BCT Post Details 41
23. Iowa Steel Post Transition, Post Nos. 14P-19P Details 42
24. Primary Side End Anchorage Details 43
25. Anchorage Post Details 44
26. Thrie Beam Slot Pattern No. 1 45
27. Thrie Beam Slot Pattern No. 2 46
28. Thrie Beam Bend Radius No. 1 47
29. Thrie Beam Bend Radius No. 2 48
30. Thrie Beam Bend Radius No. 3 49
31. Cable Release Bracket 50
32. Cable Release Bracket Part Details 51
33. Cable Release Base Details 52
34. Cable Release Base Part Details 53
35. Cable Release Lever Kicker Details 54
36. Short-Radius System Details 55
37. Short-Radius System Details 56
38. Short-Radius Nose Section Details 57
39. Short-Radius Cable Anchor Details 58
40. Short-Radius Post Details 59
41. Summary of Test Results and Sequential Photographs, Test SR-5 65

42. Vehicle Trajectory and Final Position, Test SR-5 66
43. Additional Sequential Photographs, Test SR-5 67
44. Additional Sequential Photographs, Test SR-5 68
45. Additional Sequential Photographs, SR-5 69
46. Additional Sequential Photographs, Test SR-5 70
47. Documentary Photographs, Test SR-5 71
48. Documentary Photographs, Test SR-5 72
49. Impact Location, Test SR-5 73
50. Vehicle Trajectory and Final Position, Test SR-5 74
51. System Damage, Test SR-5 75
52. System Damage, Test SR-5 76
53. Damage to Nose Section, Test SR-5 77
54. Rail Damage Between Post Nos. 3P through 7P, Test SR-5 78
55. Cable Anchor Damage, Test SR-5 79
56. Nose Cable Damage, Test SR-5 80
57. Post No. 1S Damage, Test SR-5 81
58. Post Nos. 1P through 4P Damage, Test SR-5 82
59. Post No. 5P Damage, Test SR-5 83
60. Post No. 6P Damage, Test SR-5 84
61. Soil Failure, Test SR-5 85
62. Vehicle Damage, Test SR-5 86
63. Vehicle Damage, Test SR-5 87
64. Vehicle Damage, Test SR-5 88
67. Load Cell Data, Test SRA-1 93
68. System Details, Test SR-6 95
69. Secondary Side Details, Test SR-6 96
70. Primary Side Details, Test SR-6 97
71. Primary Side Cable Anchor Detail, Test SR-6 98
72. Secondary Side Cable Anchor Details, Test SR-6 99
73. BCT Cable and Anchorage Part Details, Test SR-6 100
74. MGS and Thrie Beam Foundation Tubes, Test SR-6 101
75. Post Details, Test SR-6 102
78. Summary of Test Results and Sequential Photographs, Test SR-6 110
79. Vehicle Trajectory and Final Position, Test SR-6 111
80. Additional Sequential Photographs, Test SR-6 112
82. Additional Sequential Photographs, Test SR-6 114
83. Additional Sequential Photographs, Test SR-6 115
84. Documentary Photographs, Test SR-6 116
85. Documentary Photographs, Test SR-6 117
86. Impact Location, Test SR-6 118
87. Vehicle Trajectory and Final Position, Test SR-6 119
88. System Damage, Test SR-6 120
89. System Damage, Test SR-6 121
90. Post Nos. 1S Through 3S Damage, Test SR-6 122

91. Post Nos. 1P through 6P Damage, Test SR-6 123
92. Post Nos. 6P through 8P Damage, Test SR-6 124
93. Vehicle Damage, Test SR-6 125
94. Vehicle Damage, Test SR-6 126
95. Windshield Damage, Test SR-6 127
96. Occupant Compartment Damage, Test SR-6 128
97. Summary of Short-Radius Guardrail Impacts 131
A-1. Short-Radius Design Details (English), Test SR-5 139
A-2. Secondary Side Design Details (English), Test SR-5 140
A-3. Primary Side Design Details (English), Test SR-5 141
A-4. Cable Release Lever Attachment Details (English), Test SR-5 142
A-5. Primary Side End Anchorage Details (English), Test SR-5 143
A-6.Anchor Cable and Release Cable Details (English), Test SR-5 144
A-7. Nose Cable Anchor Plate Details (English), Test 145
A-8. MGS and Thrie Beam Foundation Tube Details (English), Test 146
A-9. Wood Post Details, Post Nos. 1P, 1S, 2P-13P, 2S-5S,6S-8S, and 9S-10S (English), Test SR-5 147
A-10. MGS CRT and BCT Post Details (English), Test SR-5 148
A-11. Thrie Beam Timber Post Details (English), Test SR-5 149
A-12. Iowa Steel Post Transition Details, Post Nos. 14P-19P (English), Test SR-5 150
A-13. Primary Side End Anchorage Details (English), Test SR-5 151
A-16. Anchorage Post Details (English), Test SR-5 152
A-15. Rail Slot Pattern No. 1 Details (English), Test SR-5 153
A-16. Rail Slot Pattern No. 2 Details (English), Test SR-5 154
A-17. Rail Curvature, Rail Section No. 1 (English), Test SR-5 155
A-18. Rail Curvature, Rail Section Nos. 2 and 3 (English), Test SR-5 156
A-19. Rail Curvature, Rail Section No. 4 (English), Test SR-5 157
A-20. Cable Release Bracket, Part A (English), Test SR-5 158
A-21. Cable Release Bracket Details (English), Test SR 159
A-22. Cable Release Base (English), Test SR-5 160
A-23. Cable Release Base Details (English), Test SR-5 161
A-24. Cable Release Lever Kicker Details (English), Test SR-5 162
B-1. Summary of Test Results and Sequential Photographs (English), Test SR-5 164
B-2. Summary of Test Results and Sequential Photographs (English), Test SR-6 165
C-1.Occupant Compartment Deformation Data - Set 1, Test SR-5 167
C-2.Occupant Compartment Deformation Data - Set 2, Test SR-5 168
C-3.Occupant Compartment Deformation Index (OCDI), Test SR-5 169
D-1. Graph of Longitudinal Deceleration, Test SR-5 171
D-2. Graph of Longitudinal Occupant Impact Velocity, Test SR-5 172
D-3. Graph of Longitudinal Occupant Displacement, Test SR-5 173
D-4. Graph of Lateral Deceleration, Test SR-5 174
D-5. Graph of Lateral Occupant Impact Velocity, Test SR-5 175
D-6. Graph of Lateral Occupant Displacement, Test SR-5 176
D-7. Graph of Roll, Pitch, and Yaw Angular Displacements, Test SR-5 177

E-1. Short-Radius Design Details, Test SR-6 179
E-2. Secondary Side Design Details, Test SR-6 180
E-3. Primary Side Design Details, Test SR-6 181
E-4. Primary Side End Anchorage Details, Test SR-6 182
E-5. Cable Anchor Details, Test SR-6 183
E-6. Cable Anchor Details, Test SR-6 184
E-7. Nose Cable Anchor Plate Details, Test SR-6 185
E-8. MGS and Thrie Beam Foundation Tube Details, Test SR-6 186
E-9. Wood Post Details, Test SR-6 187
E-10. Wood Post Details, Test SR-6 188
E-11. Wood Post Details, Test SR-6 189
E-12. Iowa Steel Post Transition Details, Test SR-6 190
E-13. Primary Side End Anchorage Details, Test SR-6 191
E-14. Anchorage Post Details, Test SR-6 192
E-15. Rail Slot Pattern Details, Rail Section No. 1, Test SR-6 193
E-16. Rail Slot Pattern Details, Rail Section No. 2, Test SR-6 194
E-17. Rail Curvature, Rail Section No. 1, Test SR-6 195
E-18. Rail Curvature, Rail Section Nos. 2 and 3, Test SR-6 196
E-19. Rail Curvature, Rail Section No. 4, Test SR-6 197
F-1. Short-Radius Design Details (English), Test SR 199
F-2. Secondary Side Design Details (English), Test SR-6 200
F-3. Primary Side Design Details (English), Test SR 201
F-4. Primary Side End Anchorage Details (English), Test SR 202
F-5. Cable Anchor Details (English), Test SR 203
F-7. Nose Cable Anchor Plate Details (English), Test SR 205
F-8. MGS and Thrie Beam Foundation Tube Details (English), Test SR 206
F-9. Wood Post Details (English), Test SR 207
F-10. Wood Post Details (English), Test SR 208
F-11. Wood Post Details (English), Test SR 209
F-12. Iowa Steel Post Transition Details (English), Test SR 210
F-13. Primary Side End Anchorage Details (English), Test SR 211
F-14. Anchorage Post Details (English), Test SR-6 212
F-15. Rail Slot Pattern Details, Rail Section No. 1 (English), Test SR-6 213
F-16. Rail Slot Pattern Details, Rail Section No. 2 (English), Test SR 214
F-17. Rail Curvature, Rail Section No. 1 (English), Test SR-6 215
F-18. Rail Curvature, Rail Section Nos. 2 and 3 (English), Test SR-6 216
F-19. Rail Curvature, Rail Section No. 4 (English), Test SR-6 217
G-1. Occupant Compartment Deformation Index (OCDI), Test SR-6 218
H-1. Graph of Longitudinal Deceleration, Test SR-6 221
H-2. Graph of Longitudinal Occupant Impact Velocity, Test SR-6 222
H-3. Graph of Longitudinal Occupant Displacement, Test SR-6 223
H-4. Graph of Lateral Deceleration, Test SR-6 224
H-5. Graph of Lateral Occupant Impact Velocity, Test SR-6 225
H-6. Graph of Lateral Occupant Displacement, Test SR-6 226

H-7. Graph of Roll, Pitch, and Yaw Angular Displacements, Test SR-6 227

List of Tables

Page

1. NCHRP Report 350 Evaluation Criteria for 2000P Pickup Truck and 820C Small Car Tests 7
2. Bogie Test Summary, Test SRA-1 93
3. Summary of Safety Performance Evaluation Results 132

1 INTRODUCTION

1.1 Problem Statement

A short-radius guardrail is a common safety treatment for situations where driveways or secondary roadways intersect a high-speed roadway near a bridge. Short-radius guardrail systems involve a curved section of guardrail placed around the corner of the intersecting roadway with tangent sections on each end that parallel the respective roadways. The tangent sections of guardrail found along the primary roadway are generally attached to an approach guardrail transition and then anchored to a bridge rail, while the sections found along the secondary roadway are generally attached to a guardrail end terminal. A short-radius guardrail system is intended to perform in a similar manner to a bullnose median barrier or a crash cushion. For example, when a high-angle impact occurs in the curved portion of the system, the vehicle is to be captured and brought to a controlled stop. In addition, the system must be capable of redirecting impacting vehicles along the tangent sections of the guardrail installation.

Recently, the members of the Midwest States' Regional Pooled Fund Program contracted with the Midwest Roadside Safety Facility (MwRSF) to develop a new short-radius guardrail design that would meet the Test Level 3 (TL-3) criteria set forth in NCHRP Report No.350 (1). Previously, MwRSF conducted a review of past NCHRP Report No. 230 (2) short-radius designs, identified the important design considerations for such a system, and developed an initial design concept for a TL-3 short-radius system (3). Furthermore, MwRSF conducted a series of four full-scale crash tests on this short-radius system (4). Phase III of this research, described herein, consisted of further analysis, design, and full-scale testing of the short-radius system.

1.2 Objective

The objective of this research study was to evaluate the safety performance of the short-radius guardrail system through full-scale crash testing and modify the design, as necessary, in order to improve its safety performance. The system's safety performance was evaluated according to the TL-3 criteria set forth in NCHRP Report No. 350.

1.3 Scope

Two full-scale crash tests of the short-radius guardrail system were conducted in order to reach the research objective. The first test utilized a 3/4-ton pickup truck weighing approximately 2,000 kg (4,409 lb), and the second test utilized a small car weighing approximately 820 kg (1,808 lb). The first test, a modification of NCHRP Report No. 350 test designation 3-31, was performed at a target impact speed of 100 km/h (62.1 mph) and at an angle of 0 degrees with the centerline of the vehicle aligned with the centerline of the first post on the primary roadway side of the system. The second test, NCHRP Report No. 350 test designation 3-30, was performed at a target impact speed of 100 km/h (62.1 mph) and at an angle of 0 degrees on the center of the curved nose of the system. The test results were analyzed, evaluated, and documented. Conclusions and recommendations were then made that pertain to the safety performance of the short-radius guardrail design.

2 NCHRP 350 TESTING AND EVALUATION CRITERIA

2.1 Test Requirements

Due to the nature of potential impacts into the curved section of a short-radius guardrail system, it was believed necessary to classify the system as either a terminal or crash cushion in order to determine the appropriate NCHRP Report No. 350 crash tests and evaluation criteria. A short-radius guardrail should be defined as a non-gating device and must fulfill the requirements for non-gating terminals and crash cushions. A non-gating device is designed to contain and redirect a vehicle when impacted downstream from the end of the device. According to NCHRP Report No. 350, non-gating end terminals and crash cushions must be subjected to eight full-scale vehicle crash tests, five using a 2,000-kg (4,409-lb) pickup truck and three using an 820-kg (1,808-lb) small car. The required 2,000-kg (4,409-lb) pickup truck crash tests for a Test Level 3 (TL-3) device are:

(1) Test Designation 3-31 consisted of a 100 km/h (62.2 mph) impact at a nominal angle of 0 degrees on the tip of the barrier nose.
(2) Test Designation 3-33 consisted of a 100 km/h (62.2 mph) impact at a nominal angle of 15 degrees on the tip of the barrier nose.
(3) Test Designation 3-37 consisted of a 100 km/h (62.2 mph) impact at a nominal angle of 20 degrees on the beginning of the Length-of-Need (LON).
(4) Test Designation 3-38 consisted of a 100 km/h (62.2 mph) impact at a nominal angle of 20 degrees on the Critical Impact Point (CIP).
(5) Test Designation 3-39 consisted of a 100 km/h (62.2 mph) reverse direction impact at an angle of 20 degrees one half of the LON from the end of the terminal.

The required 820-kg (1,808-lb) small car crash tests for a TL-3 device are:

(1) Test Designation 3-30 consisted of a 100 km/h (62.2 mph) impact at a nominal angle of 0 degrees on the tip of the barrier nose with a ¼-point offset.
(2) Test Designation 3-32 consisted of a 100 km/h (62.2 mph) impact at a nominal angle of 15 degrees on the tip of the barrier nose.
(3) Test Designation 3-36 consisted of a 100 km/h (62.2 mph) impact at a nominal impact angle of 15 degrees on the beginning of the LON.

Of the eight recommended NCHRP Report No. 350 compliance tests, it was deemed that

only five crash tests were necessary for evaluating the short-radius system's safety performance. Two length of need tests, 3-36 and 3-37, were not conducted because previous testing has shown that thrie beam guardrail is capable of meeting the length of need requirements found in the safety standards. Similarly, the reverse direction impact test was not tested. Test 3-39 calls for a reverse direction impact of a 2,000-kg (4,409-lb) pickup truck on a point at the length of the terminal divided by two. Thus, based on previous experience with straight thrie beam guardrail testing, it was believed that test 3-39 was unnecessary. A diagram showing the impact location for the seven of the eight crash tests is shown in Figure 1. Test no. 3-39 is not shown because the LON for the system was unknown at this time. In addition, the critical impact point is defined for non-gating terminals as the point along the installation where it is unknown whether the guardrail will capture or redirect the impacting vehicle, and the modification of test 3-31 is a more critical impact scenario than test 3-39.

2.2 Evaluation Criteria

Evaluation criteria for full-scale vehicle crash testing are based on three appraisal areas: (1) structural adequacy; (2) occupant risk; and (3) vehicle trajectory after collision. The criteria for structural adequacy are intended to evaluate a barrier's ability to contain, redirect, or allow controlled penetration in a predictable manner. Occupant risk criteria evaluate the degree of hazard to which the occupants in the impacting vehicle are affected by impact with the barrier system. Vehicle trajectory after collision is a measure of the potential for the vehicle, upon redirection, to encroach into adjacent traffic lanes and cause subsequent multi-vehicle accidents. This criterion also indicates the potential safety hazard for the occupants of the impacting vehicle associated with secondary collisions with other fixed objects. These three evaluation criteria are defined in Table

1. The full-scale vehicle crash test was conducted and reported in accordance with the evaluation procedures provided in NCHRP Report No. 350.

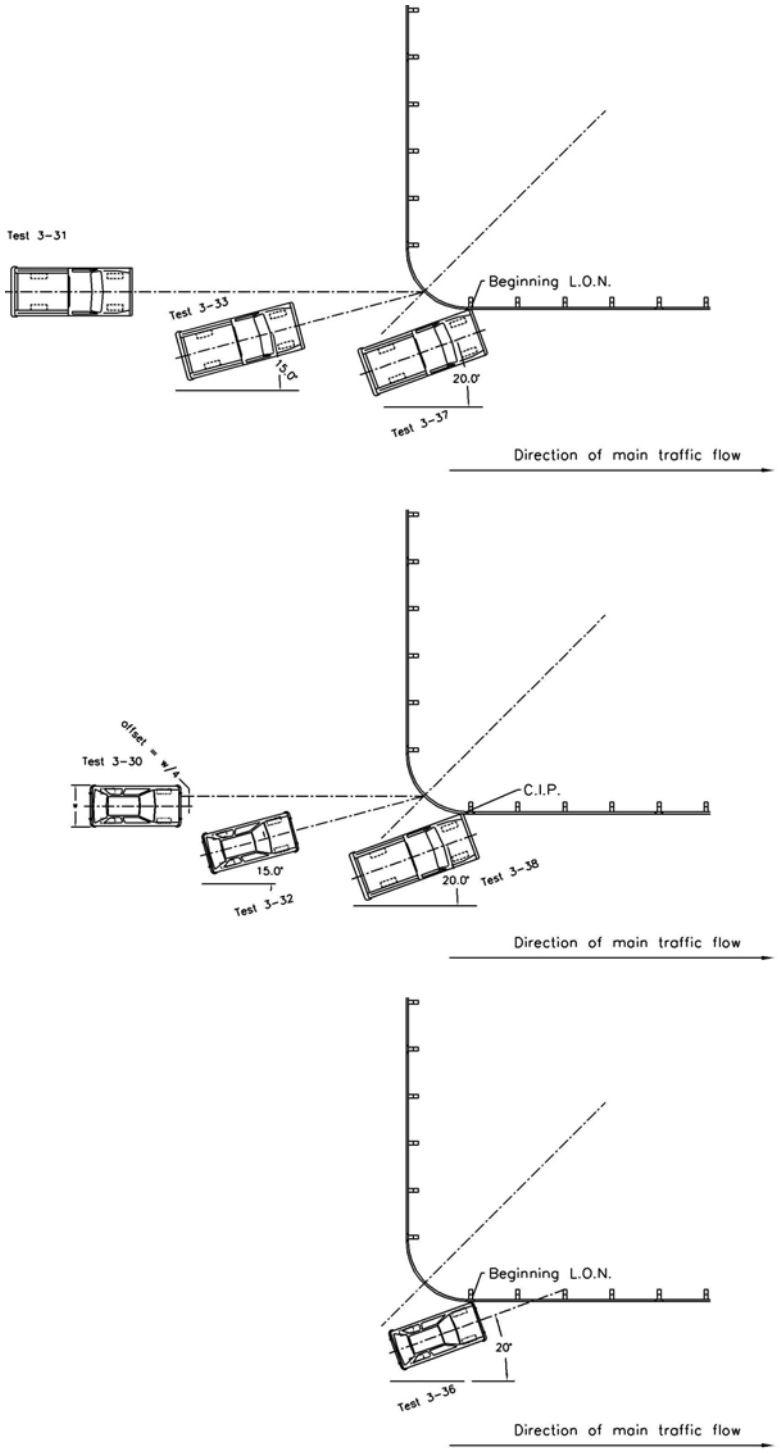

Figure 1. Full-Scale Crash Test Matrix

Table 1. NCHRP Report 350 Evaluation Criteria for 2000P Pickup Truck and 820C Small Car Tests

Evaluation Factors	Evaluation Criteria	Applicable Tests
Structural Adequacy	A. Test article should contain and redirect the vehicle; the vehicle should not penetrate, underride, or override the installation although controlled lateral deflection of the test article is acceptable.	3-37 3-38
	C. Acceptable test article performance may be by redirection, controlled penetration, or controlled stopping of the vehicle.	3-30 3-31 3-32 3-33 3-39
Occupant Risk	D. Detached elements, fragments or other debris from the test article should not penetrate or show potential for penetrating the occupant compartment, or present an undue hazard to other traffic, pedestrians, or personnel in a work zone. Deformations of, or intrusions into, the occupant compartment that could cause serious injuries should not be permitted.	ALL
	F. The vehicle should remain upright during and after collision although moderate roll, pitching, and yawing are acceptable.	ALL
	H. Occupant impact velocities should satisfy the following: **Occupant Impact Velocity Limits** Component — Preferred — Maximum Longitudinal and Lateral — 9 m/s (29.5 ft/s) — 12 m/s (39.4 ft/s)	3-30 3-31 3-32 3-33 3-36
	I. Occupant ridedown accelerations should satisfy the following: **Occupant Ridedown Acceleration Limits (Gs)** Component — Preferred — Maximum Longitudinal and Lateral — 15 Gs — 20 Gs	3-30 3-31 3-32 3-33 3-36
Vehicle Trajectory	K. After collision it is preferable that the vehicle's trajectory not intrude into adjacent traffic lanes.	ALL
	L. The occupant impact velocity in the longitudinal direction should not exceed 12 m/s (39.4 ft/s) and the occupant ridedown acceleration in the longitudinal direction should not exceed 20 Gs.	3-37 3-38 3-39
	M. The exit angle from the test article preferably should be less than 60 percent of the test impact angle, measured at the time the vehicle lost contact with the device.	3-36 3-37 3-38 3-39
	N. Vehicle trajectory behind the test article is acceptable.	3-30 3-31 3-32 3-33 3-39

3 TEST CONDITIONS

3.1 Test Facility

The testing facility is located at the Lincoln Air-Park on the northwest (NW) side of the Lincoln Municipal Airport and is approximately 8.0 km (5.0 miles) NW of the University of Nebraska-Lincoln.

3.2 Vehicle Tow and Guidance System

A reverse cable tow system with a 1:2 mechanical advantage was used to propel the test vehicle. The distance traveled and the speed of the tow vehicle were one-half that of the test vehicle. The test vehicle was released from the tow cable before impact with the short-radius system. A digital speedometer was located on the tow vehicle to increase the accuracy of the test vehicle impact speed.

A vehicle guidance system developed by Hinch (5) was used to steer the test vehicle. A guide-flag, attached to the front-left wheel and the guide cable, was sheared off before impact with the longitudinal barrier. The 9.5-mm (3/8-in.) diameter guide cable was tensioned to approximately 13.3 kN (3 kips), and supported laterally and vertically every 30.48 m (100 ft) by hinged stanchions. The hinged stanchions stood upright while holding up the guide cable, but as the vehicle was towed down the line, the guide-flag struck and knocked each stanchion to the ground. The vehicle guidance systems for test nos. SR-5 and SR-6 were approximately 335 m (1,100 ft) and 238 m (780 ft) long, respectively.

3.3 Test Vehicles

For test no. SR-5, a 1997 Ford F-250 ¾-ton pickup truck was used as the test vehicle. The test inertial and gross static weights were 2,001 kg (4,412 lbs). The test vehicle is shown in Figure

2, and vehicle dimensions are shown in Figure 3.

For test no. SR-6, a 1996 Geo Metro small car was used as the test vehicle. The test inertial and gross static weights were 818 kg (1,803 lbs) and 893 kg (1,969 lbs), respectively. The test vehicle is shown in Figure 4, and vehicle dimensions are shown in Figure 5.

The longitudinal component of the center of gravity was determined using the measured axle weights. The location of the final centers of gravity are shown in Figures 3 through 7.

Square, black and white-checkered targets were placed on the vehicle to aid in the analysis of the high-speed videos, as shown in Figures 6 through 7. Round, checkered targets were placed on the center of gravity on the left-side and right-side doors and on the roof of the vehicle. The remaining targets were located for reference so that they could be viewed from the high-speed cameras for film analysis.

The front wheels of the test vehicle were aligned for camber, caster, and toe-in values of zero so that the vehicle would track properly along the guide cable. Two 5B flash bulbs were mounted on both the hood and roof of the vehicle to pinpoint the time of impact with the barrier system on the high-speed videos. The flash bulbs were fired by a pressure tape switch mounted on the front face of the bumper. A remote controlled brake system was installed in the test vehicle so the vehicle could be brought safely to a stop after the test.

3.4 Data Acquisition Systems

3.4.1 Accelerometers

One triaxial piezoresistive accelerometer system with a range of ±200 Gs was used to measure the acceleration in the longitudinal, lateral, and vertical directions at a sample rate of 10,000 Hz. The environmental shock and vibration sensor/recorder system, Model EDR-4M6, was

Figure 2. Test Vehicle, Test SR-5

Date: 04/04/2005 Test Number: SR-5 Model: 2000P/F250

Make: FORD Vehicle I.D.#: 1FTEF2763VKC80261

Tire Size: LT 255/70 R16 Year: 1997 Odometer: 129555

*(All Measurements Refer to Impacting Side)

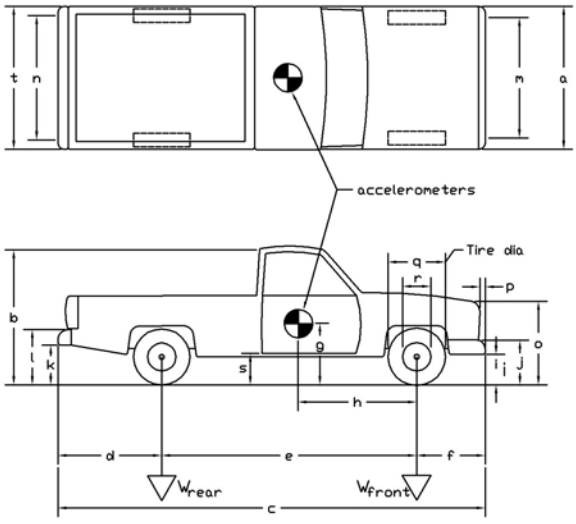

Vehicle Geometry – mm (in.)

a	1899 (74.75)	b	1854 (73.0)
c	5823 (229.25)	d	730 (28.75)
e	3524 (138.75)	f	1441 (56.75)
g	667 (26.25)	h	1521 (59.875)
i	495 (19.5)	j	724 (28.5)
k	508 (20.0)	l	711 (28.0)
m	1654 (65.125)	n	1664 (65.5)
o	1016 (40.0)	p	95 (3.75)
q	756 (29.75)	r	441 (19.375)
s	429 (16.875)	t	1880 (74.0)

Wheel Center Height Front 359 (14.125)

Wheel Center Height Rear 362 (14.25)

Wheel Well Clearance (FR) 876 (34.5)

Wheel Well Clearance (RR) 921 (36.25)

Engine Type 8 CYL. GAS

Engine Size 4.6 L

Transmission Type:

(Automatic) or Manual

FWD or (RWD) or 4WD

Weights kg (lbs)	Curb	Test Inertial	Gross Static
W_{front}	1074 (2368)	1127 (2485)	1127 (2485)
W_{rear}	787 (1736)	874 (1927)	874 (1927)
W_{total}	1862 (4105)	2001 (4412)	2001 (4412)

Note any damage prior to test: None

Figure 3. Vehicle Dimensions, Test SR-5

developed by Instrumented Sensor Technology (IST) of Okemos, Michigan and includes three differential channels as well as three single-ended channels. The EDR-4 was configured with 6 MB of RAM memory and a 1,500 Hz lowpass filter. Computer software, “DynaMax 1 (DM-1)” and “DADiSP”, was used to analyze and plot the accelerometer data.

A backup triaxial piezoresistive accelerometer system with a range of ±200 Gs was also used to measure the acceleration in the longitudinal, lateral, and vertical directions at a sample rate of 3,200 Hz. The environmental shock and vibration sensor/recorder system, Model EDR-3, was developed by Instrumental Sensor Technology (IST) of Okemos, Michigan. The EDR-3 was configured with 256 kB of RAM memory and a 1,120 Hz lowpass filter. Computer software, “DynaMax 1 (DM-1)” and “DADiSP”, was used to analyze and plot the accelerometer data.

3.4.2 Rate Transducers

An Analog Systems 3-axis rate transducer with a range of 1,200 degrees/sec in each of the three directions (pitch, roll, and yaw) was used to measure the rates of motion of the test vehicle. The rate transducer was mounted inside the body of the EDR-4M6 and recorded data at 10,000 Hz to a second data acquisition board inside the EDR-4M6 housing. The raw data measurements were then downloaded, converted to the appropriate Euler angles for analysis, and plotted. Computer software, "DynaMax 1" and "DADiSP," was used to analyze and plot the rate transducer data.

3.4.3 High-Speed Photography

For test no. SR-5, two high-speed Photron video cameras, one high-speed AOS VITcam video camera, and one high-speed Red Lake E/Cam video camera, all with operating speeds of 500 frames/s, were used to film the crash test. Seven Canon digital video cameras, with a standard operating speed of 29.97 frames/s, were also used to film the crash test. A high-speed Photron video

Figure 4. Test Vehicle, Test SR-6

Date: 10/06/05 Test Number: SR-6 Model: 820C – Metro

Make: Geo Vehicle I.D.#: 2C1MP239XT6786381

Tire Size: P155/80R13 Year: 1996 Odometer: 28040

*(All Measurements Refer to Impacting Side)

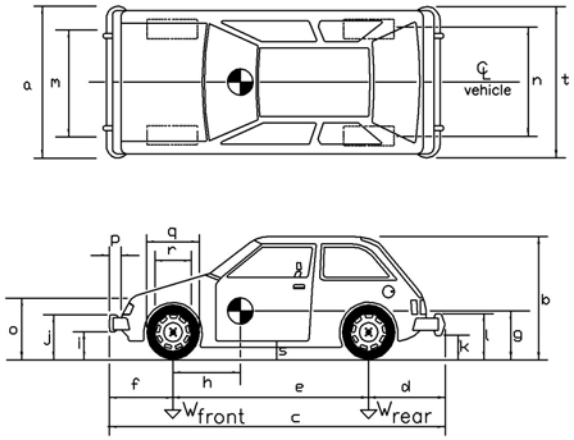

Vehicle Geometry – mm (in.)

a	1562 (61.0)	b	1416 (55.75)
c	3778 (148.75)	d	597 (23.5)
e	2362 (93.0)	f	781 (30.75)
g	546 (21.5)	h	806 (31.75)
i	425 (16.75)	j	533 (21.0)
k	343 (13.5)	l	660 (26.0)
m	1365 (53.75)	n	1327 (52.25)
o	572 (22.5)	p	95 (3.75)
q	559 (22.0)	r	365 (14.375)
s	311 (12.25)	t	1549 (61.0)

Wheel Center Height 260 (10.25)

Engine Type 4 CYL. GAS

Engine Size 1.3 L

Transmission Type:

Automatic or (Manual)

(FWD) or RWD or 4WD

Weights kg (lbs)	Curb	Test Inertial	Gross Static
W_{front}	511 (1127)	538 (1187)	575 (1267)
W_{rear}	264 (581)	279 (616)	318 (702)
W_{total}	775 (1708)	817 (1802)	893 (1969)

Note any damage prior to test: NONE

Figure 5. Vehicle Dimensions, Test SR-6

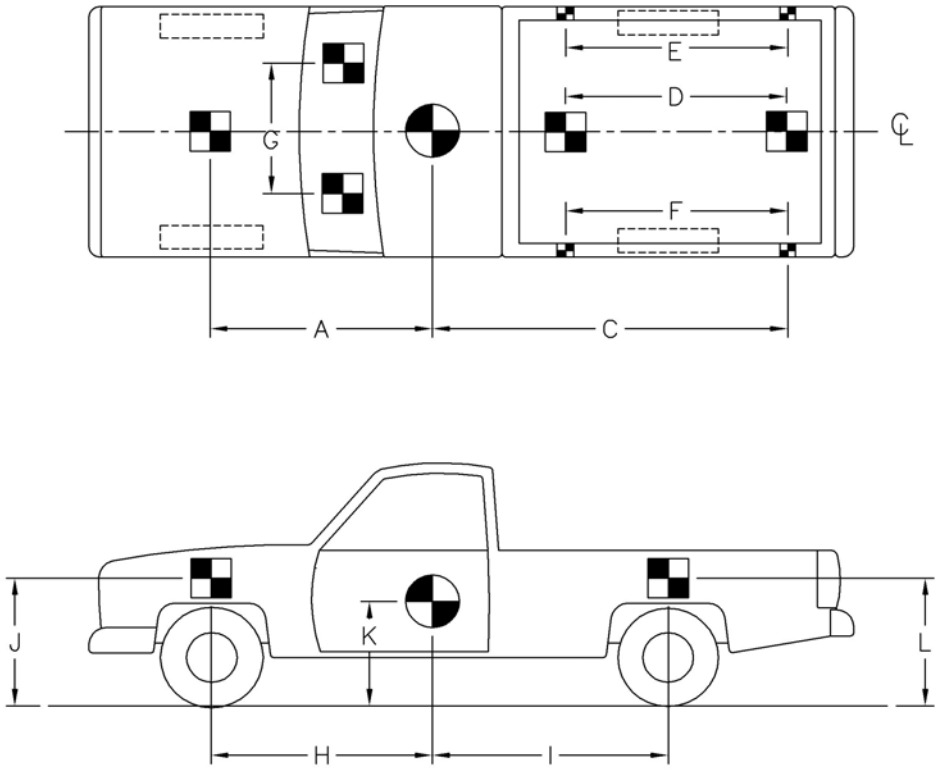

TEST #: SR-5

TARGET GEOMETRY -- mm (in.)

A	1702 (67.0)	D	1676 (66.0)	G	794 (31.25)	J	975 (38.375)
B	-----	E	2178 (85.75)	H	1521 (59.875)	K	667 (26.25)
C	2629 (103.5)	F	2178 (85.75)	I	2003 (78.875)	L	1026 (40.375)

Figure 6. Vehicle Target Locations, Test SR-5

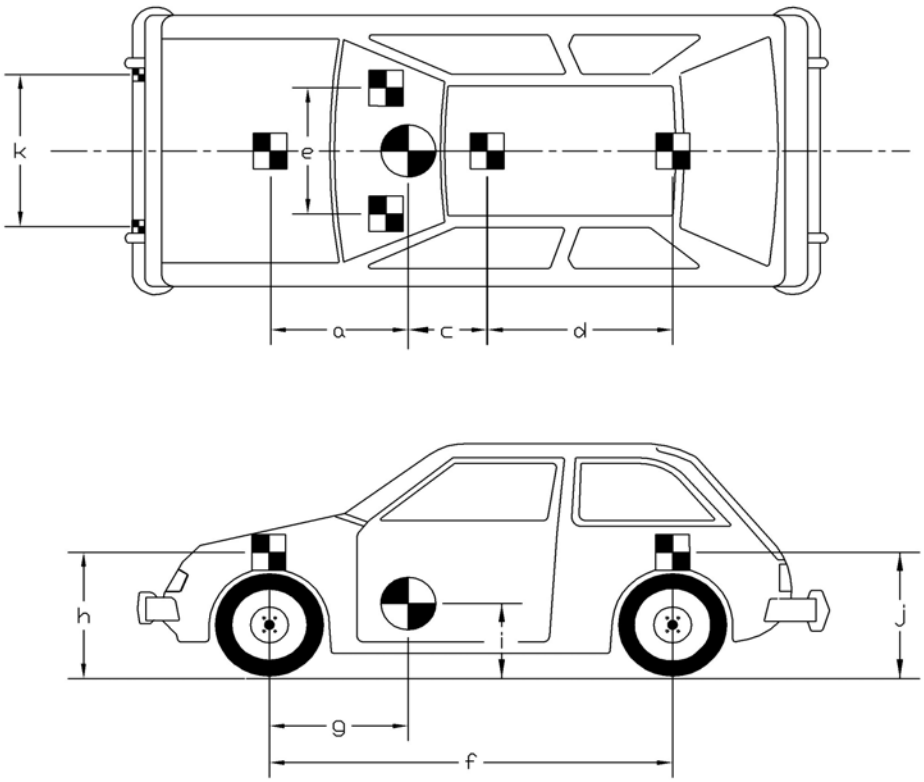

TEST #: SR-6

TARGET GEOMETRY -- mm (in.)

a	1426 (56.125)	b	----	c	527 (20.75)	d	749 (29.5)
e	724 (28.5)	f	2362 (93.0)	g	806 (31.75)	h	737 (29.0)
i	546 (21.5)	j	775 (30.5)	k	933 (36.75)		

Figure 7. Vehicle Target Locations, Test SR-6

camera, with a wide angle 12.5-mm lens, and a Canon digital video camera were placed above the installation to provide a field of view perpendicular to the ground. An additional Photron video camera and a Canon digital video camera were placed downstream from impact and provided a field of view parallel to the system. An AOS high-speed video camera, a Canon digital video camera, and a Nikon 8700 digital camera were placed downstream and offset to the left of the impact point and had an angled view of the impact. An E/Cam video camera and a Canon digital video camera were placed downstream and to the right of the impact point and provided an angled view of the impact. One Canon digital video camera was placed to the right of the impact point and another one was placed to the left of the impact point. Another Canon digital video camera was placed upstream and to the right of the impact point. A schematic of all twelve camera locations for test SR-5 is shown in Figure 8.

For test no. SR-6, three high-speed AOS VITcam cameras and one high-speed Red Lake E/cam video camera, all with operating speeds of 500 frames/s, were used to film the crash test. Five Canon digital video cameras and one JVC digital video cameras, with a standard operating speed of 29.97 frames/s, were also used to film the crash test. An AOS high-speed video camera,with a wide-angled 12.5-mm lens, and a Canon digital video camera were a placed above the installation to provide a field of view perpendicular to the ground. Another high-speed AOS video camera, a Canon digital video camera, and a Nikon 8700 digital camera were placed downstream from impact and provided a field of view parallel to the system. One E/cam high-speed video camera and a Canon digital video camera were placed downstream and offset to the right from impact and had an angled view of the impact. An AOS video camera and a Canon digital video camera were placed upstream and to the right from impact and provided an angled view of the impact. A Canon digital

video camera was placed farther upstream from impact and another one was placed to the left from impact. A JVC digital video camera was placed slightly downstream and left from impact. A schematic of all ten camera locations for test SR-6 is shown in Figure 9.

The Photron and AOS videos and E/cam videos were analyzed using the ImageExpress MotionPlus software and Redlake Motion Scope software, respectively. Actual camera speed and camera divergence factors were considered in the analysis of the high-speed video.

3.4.4 Pressure Tape Switches

For test nos. SR-5 and SR-6, five pressure-activated tape switches, spaced at 2-m (6.56-ft) intervals, were used to determine the speed of the vehicle before impact. Each tape switch fired a strobe light which sent an electronic timing signal to the data acquisition system as the vehicle's right-front tire passed over it. Test vehicle speed was determined from electronic timing mark data recorded using TestPoint software. Strobe lights and high-speed video analysis are used only as a backup in the event that vehicle speed cannot be determined from the electronic data.

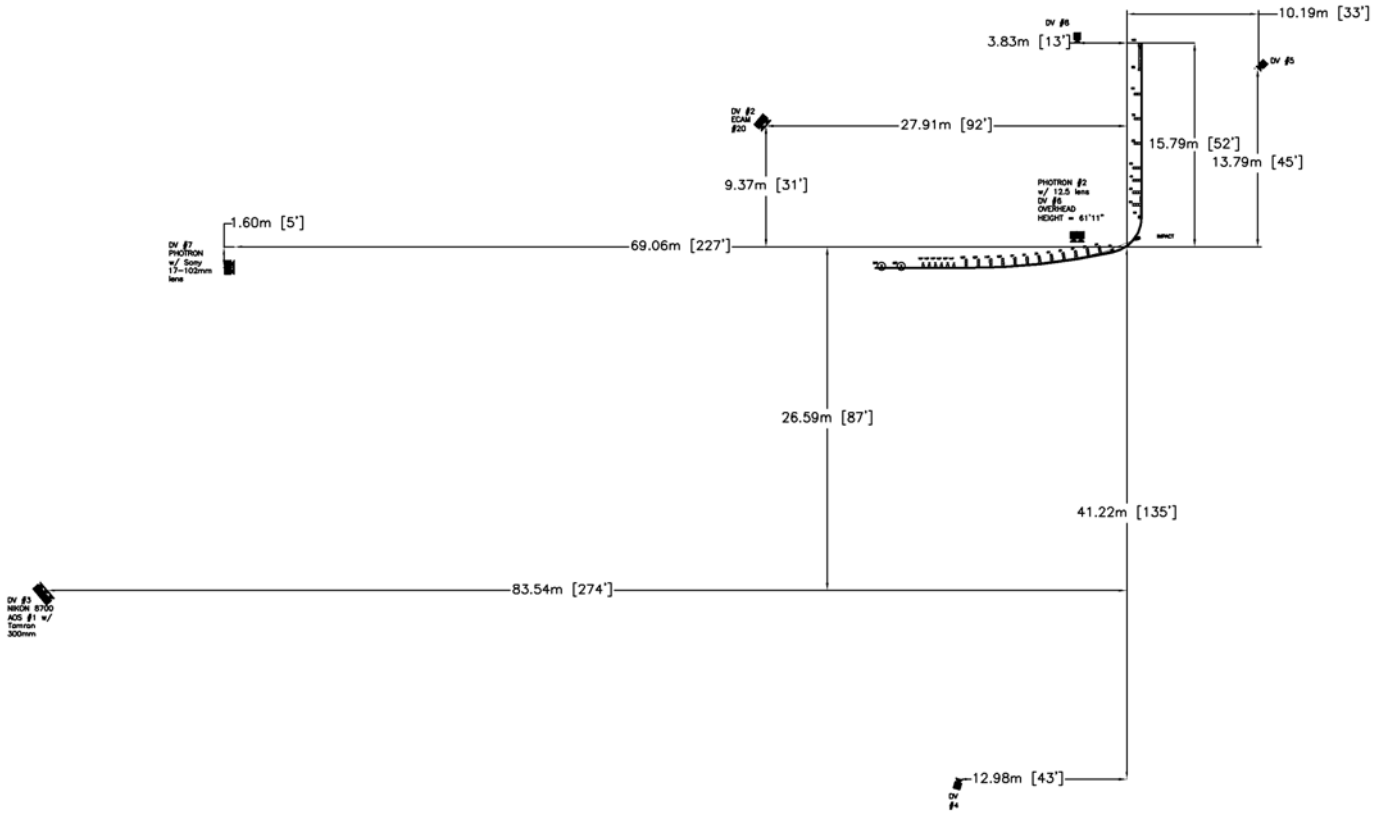

Figure 8. Location of High-Speed Cameras, Test SR-5

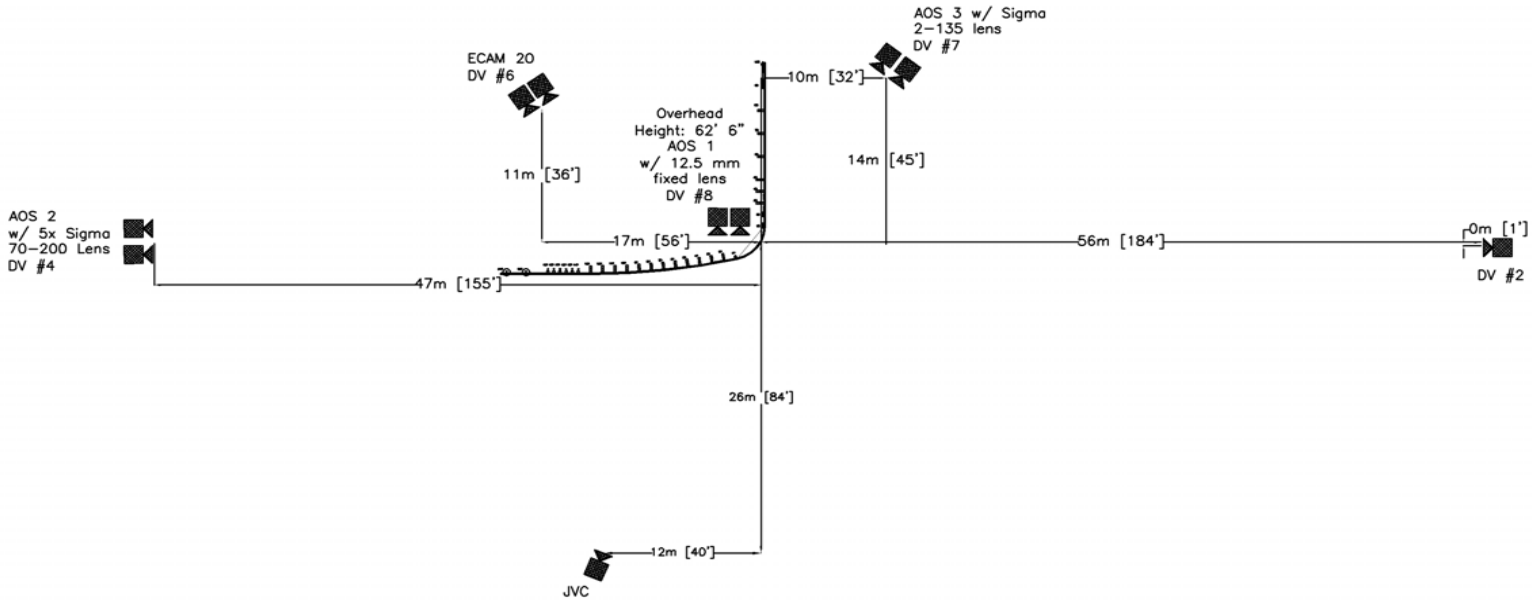

Figure 9. Location of High-Speed Cameras, Test SR-6

4 DESIGN MODIFICATIONS, TEST NO. SR-5

Prior to conducting full-scale test no. SR-5, the researchers reviewed the results of the previous failed test, test no. SR-4, in order to determine design changes that would improve the performance of the system. The failure of test SR-4 to meet the safety performance criteria was directly attributed to the intrusion and snagging of the thrie beam guardrail into the wheel well region of the pickup truck. Through the initial portion of the impact, the thrie beam guardrail was impacted by the left-front corner of the vehicle and deflected toward the inside of the short-radius guardrail system. After approximately 0.300 sec, the leading edge of the impacted guardrail slid past the left-front corner and into the wheel well. The intruding guardrail punched a large hole in the floor pan of the occupant compartment, thus causing a rapid deceleration and yaw of the vehicle. The intrusion of the thrie beam was caused by the combination of the orientation of the impact vehicle, the geometry of the system, and the lack of upstream tension in the guardrail. Because the cable anchorage at post no. 1P was disengaged almost immediately, there was little or no upstream tension in the flared guardrail section. Therefore, the vehicle moved downstream along the system with very little redirection. This in turn led to the intrusion of the thrie beam into the wheel-well region.

The most obvious design modification that was deemed necessary prior to performing test no. SR-5 was to redesign the upstream anchorage to remain effective even if post no. 1P becomes disengaged. However, implementation of such an anchor in the short-radius system presented several hurdles. First, the new anchorage needed to be almost tangent to the primary side in order to develop tension effectively during an impact event. Second, the anchorage needed to remain in place for redirection and release for impacts on the nose of the system where the vehicle is intended

to be captured. Thus, some form of a trigger mechanism must be used to release the cable anchorage when necessary. This trigger mechanism would most likely need to be outside the nose or linked away from nose in order to be effective.

LS-DYNA computer simulation was conducted in order to evaluate the potential effectiveness of a redesigned anchorage that developed upstream tension throughout the impact event. The first step in that analysis was to conduct a simulation of test no. SR-4 and compare the simulation results with the physical test. Sample results from that analysis are shown in Figure 10. The results showed that the simulation model compared well with the physical test in terms of the system deformation and truck redirection. The model captured the loss of tension and the vehicle pocketing within the guardrail that was observed in test no. SR-4. The model became unstable prior to the time in the impact where the guardrail knee entered the wheel well and impacted the firewall in the test, but the results demonstrated that the model could effectively reproduce the correct behavior of the short-radius system with the existing anchorage design.

The second step in the analysis was to compare the results from the SR-4 simulation with the results from a computer simulation where the upstream anchorage remained intact. Thus, a second model was simulated with an upstream anchorage on the primary side that would not release when post no. 1P fractured. The results of that simulation and comparison with the simulation of test no. SR-4 are shown in Figure 11. The comparison of the two computer models showed a clear improvement in the behavior of the system with the anchorage remaining intact. The model with the intact anchorage demonstrated improved upstream tension in the rail and much lower evidence of the pocketing that caused the failure in test no. SR-4.

Based on this analysis, the researchers decided to develop a secondary anchorage for the

primary side of the short-radius system that was connected to a release lever placed in front of the nose of the system. The design allowed the anchor to be released during impacts on or near the nose of the system while remaining in place during impacts on the side of the system. Full-details for the secondary anchor are provided in a subsequent section.

The researchers also decided to lower the top height of the thrie beam rail in the short-radius system from 854 mm (31.625 in.) to 787 mm (31 in.). The thrie beam rail height had been raised to 854 mm (31.625 in.) prior to test no. SR-4 in order to improve the capture of the pickup truck and to aid the pickup truck in smoothly redirecting near the splice in the thrie beam at post no. 1P. However, review of the results of test no. SR-4 showed that the increased height did not significantly improve the capture of the pickup truck, and that the addition of the flare to the primary side of the system eliminated any issue with the redirection and/or interlock of the pickup truck with the splice a t post no. 1P. In addition, it was believed that returning the height of the system to a more standard 787 mm (31 in.) would improve the compatibility of the system with the recently developed MGS system and existing 813-mm (32-in.) high bridge rail designs.

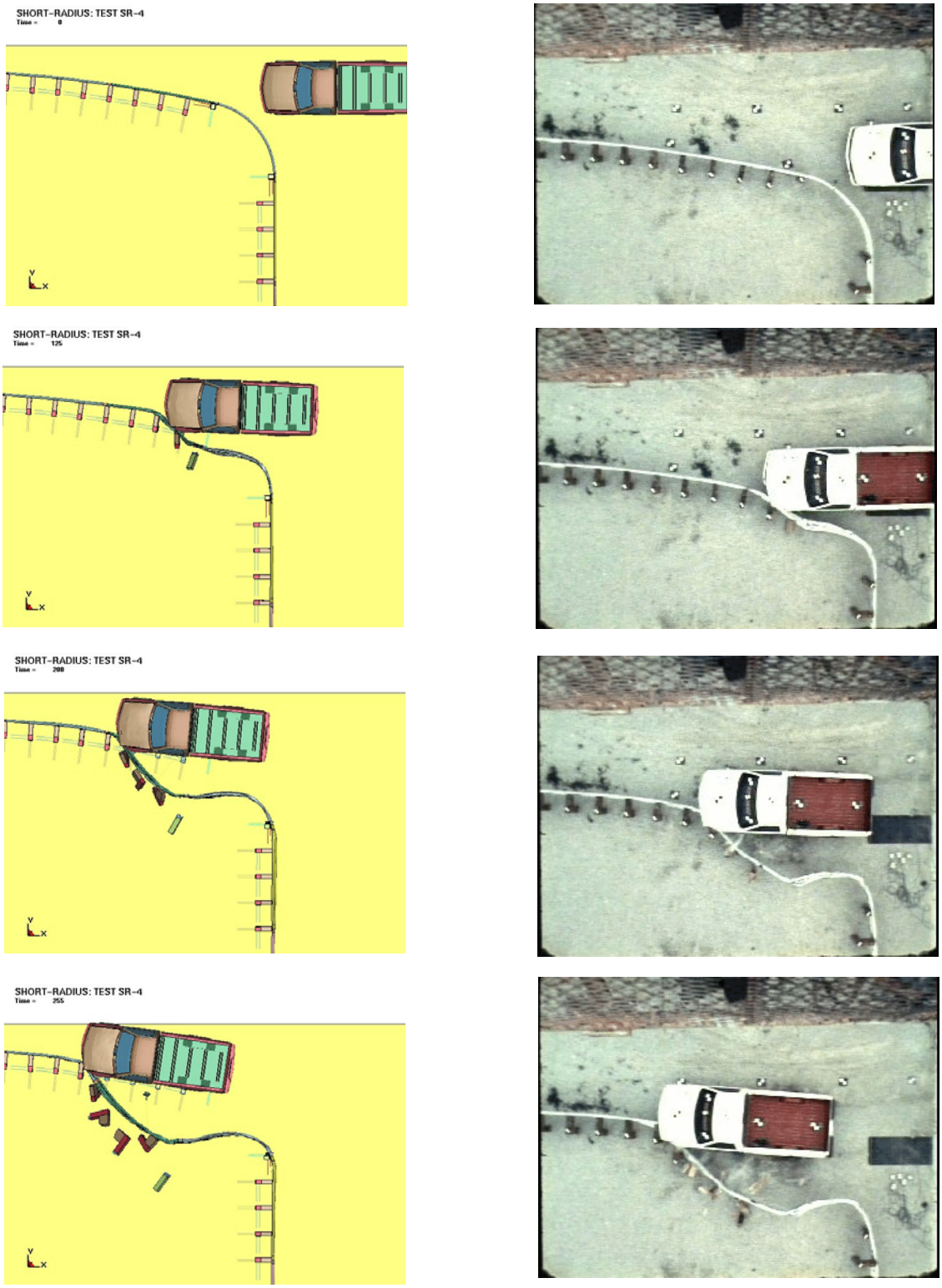

Figure 10. Comparison of Full-Scale Test and LS-DYNA Simulation Model, Test No. SR-4

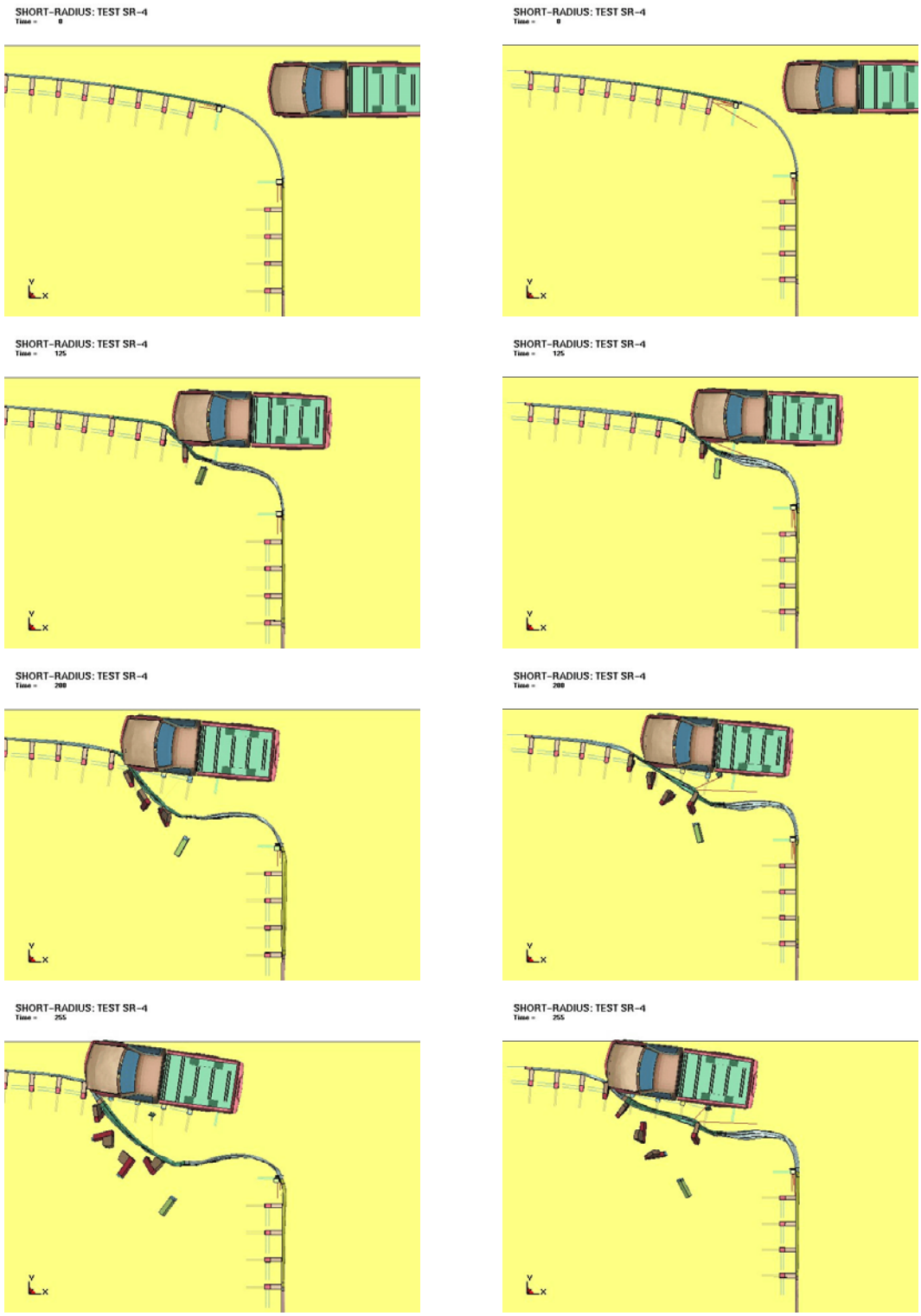

No upstream anchor - SR-4 **With upstream anchor**

Figure 11. LS-DYNA Simulations of Test SR-4 and SR-5

5 SHORT-RADIUS DESIGN DETAILS

The design of the short-radius guardrail system for test no. SR-5 was based on previous research conducted on short-radius systems discussed during Phase I and Phase II of this research (6-12). Full details on the considerations and parameters that shaped the design of the short-radius guardrail system can be found in both reports. Experience gained by the MwRSF researchers during the development of the bullnose median barrier system (13-17) was also applied.

5.1 Design Details

After reviewing the Midwest Regional Pooled Fund member states' standards and the results of the previously tested short-radius systems, a 2,769-mm (9-ft 1-in.) radius design was selected for use in the current study. The small radius reduced the overall size of the system and allowed for easier application of the design to a variety of intersections. The nose section was formed using one 3,810-mm (12-ft 6-in.) long, curved section of thrie beam guardrail.

The midsection of the short-radius system was designed without a post at the centerline of the nose since the end post typically rotates backwards after impact, thus creating a potential for the vehicle to vault over the rail. It was determined that a nose section without the centerline post would have sufficient structural strength to maintain the shape of the rail without rail sagging while also reducing the vaulting hazard. Design details are shown in Figures 12 through 35. The corresponding English-unit drawings are shown in Appendix A. Photographs of the short-radius guardrail system test installation are shown in Figures 36 through 40.

The layout of the modified design concept for the short-radius guardrail system is shown in Figures 12 through 14. For the short-radius system, the nose section consists of a 2,769-mm (9-ft 1-in.) radius nose section adjacent to a parabolic flare on the primary side and tangent on the

secondary side. The primary roadway side is 15,240 mm (50 ft) long, while the side along the secondary roadway is 13,335 mm (43 ft - 9 in.) long. After post no. 14P on the primary roadway side of the system, a 3,810-mm (12-ft 6-in.) long approach guardrail transition system was used to adapt the short-radius system to a thrie beam bridge rail. Details on the approach guardrail transition, used in combination with a safety shape bridge rail, can be found in previous publications by MwRSF (18-19). Actual installations of the short-radius guardrail system could use any NCHRP Report No. 350 approved approach guardrail transition. On the downstream end of the secondary roadway side, timber posts measuring 140 mm wide x 190 mm deep x 1,080 mm long (5.5 in. x 7.5 in. x 42.5 in.) were placed in 1,829-mm (6-ft) long steel foundation tubes were part of an anchor system designed to replicate the capacity of a tangent guardrail terminal.

The system was configured with twenty-one wood posts - thirteen positioned along the primary roadway prior to the transition section and eight placed along the secondary roadway prior to the end terminal. Starting from the radius, the first post on each side of the system was a 140 mm wide by 190 mm deep by 1,187 mm long (5.5 in. x 7.5 in. x 46.75 in.) Breakaway Cable Terminal (BCT) post set in 2,438-mm (8-ft) long foundation tubes. No blockout was used at post no. 1 on either side of the radius. Post nos. 2P through 13P along the primary roadway and post nos. 2S and 5S along the secondary roadway were 1,981-mm (78-in.) long CRT posts. Each of these posts included double 152-mm wide by 203-mm deep by 357-mm long (6-in. x 8-in. x 14-in.) wood blockouts to space the rail away from the post. The front blockouts on the double blockout posts were chamfered at a 25-degree angle from the middle of the front face of the blockout to the bottom. Post spacing along the primary side of the roadway, between posts nos. 2P and 13P, was 952.5 mm (37.5 in.), but followed the parabolic flare, as shown in Figure 14. Post spacing for all posts up to

post no. 5S along the secondary roadway was 952.5 mm (37.5 in.). The top mounting height of the rail was 787 mm (31 in.), as measured from the ground surface. Post nos. 2P through 13P along the primary roadway and post nos. 2S through 5S along the secondary roadway had a soil embedment depth of 1,168 mm (46 in.). Post nos. 6S through 8S along the secondary roadway had a soil embedment depth of 1,016 mm (40 in.) Details of these posts are shown in Figure 19 through 24.

A cable anchor system was attached between the thrie beam and post no. 1 on each side of the system in order to develop the tensile strength of the thrie beam guardrail downstream from the nose section. An additional cable anchor assembly for the primary side was added to supplement the cable anchor system at post no. 1, as detailed in the previous section. Details of all three anchor systems are shown in Figure 15 through 18.

The five guardrail sections used in the short-radius system consisted of 2.67-mm (12-gauge) steel thrie beam. The 3,810-mm (12-ft 6-in.) long sections were spliced together using a standard, bolted lap splice on each interior end. The nose section, rail section nos. 2, 3, and 4 on the primary side, and rail section no. 2 on the secondary side were cut with slots in the valleys. The nose section of the rail (rail section no. 1) consisted of a 3,810-mm (12-ft 6-in.) long beam bent into a 2,769-mm (9-ft 1-in.) radius. The nose section was cut with slots in the valleys to aid in vehicle capture, as shown in Figure 26. There were six primary 699-mm (27.5-in.) long slots centered about the midspan of the rail, three in each valley. The primary slots were divided from one another by 25-mm (1-in.) wide slot tabs. Eight additional smaller 251-mm (9.875-in.) long slots, four on each end of the rail section, were also cut with a 51-mm (2-in.) wide slot tab between them. All slots were 19-mm wide. Rail section nos. 2, 3, and 4 were curved along the parabolic flare on the primary roadway side, and rail section no. 2 was straight along the secondary roadway side. These sections were cut

with a different pattern of slots, as shown in Figure 30. The slot pattern for these sections consisted of two sets of six 298-mm (11.75-in.) long slots centered between the post slots. The slots were separated by 251-mm (9.875-in.) wide slot tabs, which provided one and one-half slots per valley between posts. The remaining section of thrie beam guardrail along the primary roadway was not slotted.

A 2.67-mm (12-gauge) thrie beam to W-beam transition section was placed between post nos. 5S and 6S along the secondary roadway. The transition section was necessary in order to end the guardrail with a simulated tangent W-beam guardrail end terminal.

A set of steel retention cables were attached to the back of the nose section to contain impacting vehicles in the event of rail rupture. A 4.4-m (14-ft 4.75-in.) long by 15.9-mm (0.625-in.) diameter cable was added behind the top and middle humps of the thrie beam nose section. A 6x25 cable was chosen with the intent that one of the two cables would be capable of containing the impacting vehicle. It is noted that the steel cables were only placed behind rail section no. 1. This was done because it was believed that the rail sections beyond the nose section would remain active and intact throughout the impact event. Therefore, the use of longer cable lengths was not deemed necessary. The cables were attached to the guardrail using three 6-mm (0.25-in.) diameter U-bolts per cable to fix the cables behind the top and middle humps of the thrie beam. The ends of each cable were fitted with “Cold Tuff” buttons and clamped between formed steel plates located at the guardrail splice at post no. 1 on each side. The “Cold Tuff” buttons were swaged-grip button ferrules. As such, any similarly sized swaged-grip button ferrule could be substituted into the design. The cable plate and the cable detail are shown in Figure 18, while the assembly details are shown in Figure 15.

An end anchorage was developed for the primary roadway side of the short-radius system in order to simulate the anchorage provided by the bridge rail in an actual installation, as shown in Figure 10. This anchorage was for test purposes only. The anchorage consisted of a pair of 2,032-mm (80-in.) long, W152x37.2 (W6x25) steel posts embedded 1,245 mm (49 in.) into a reinforced concrete base. The reinforced concrete bases consisted of 610-mm (24-in.) diameter concrete cylinders set in the ground, as shown in Figure 24. Reinforcement of the cylinders consisted of a pre-formed, circular, 559-mm (22-in.) diameter welded wire mesh cage. A 10-gauge section of thrie beam was mounted on the posts and spliced to the end of the bridge transition to complete the anchorage.

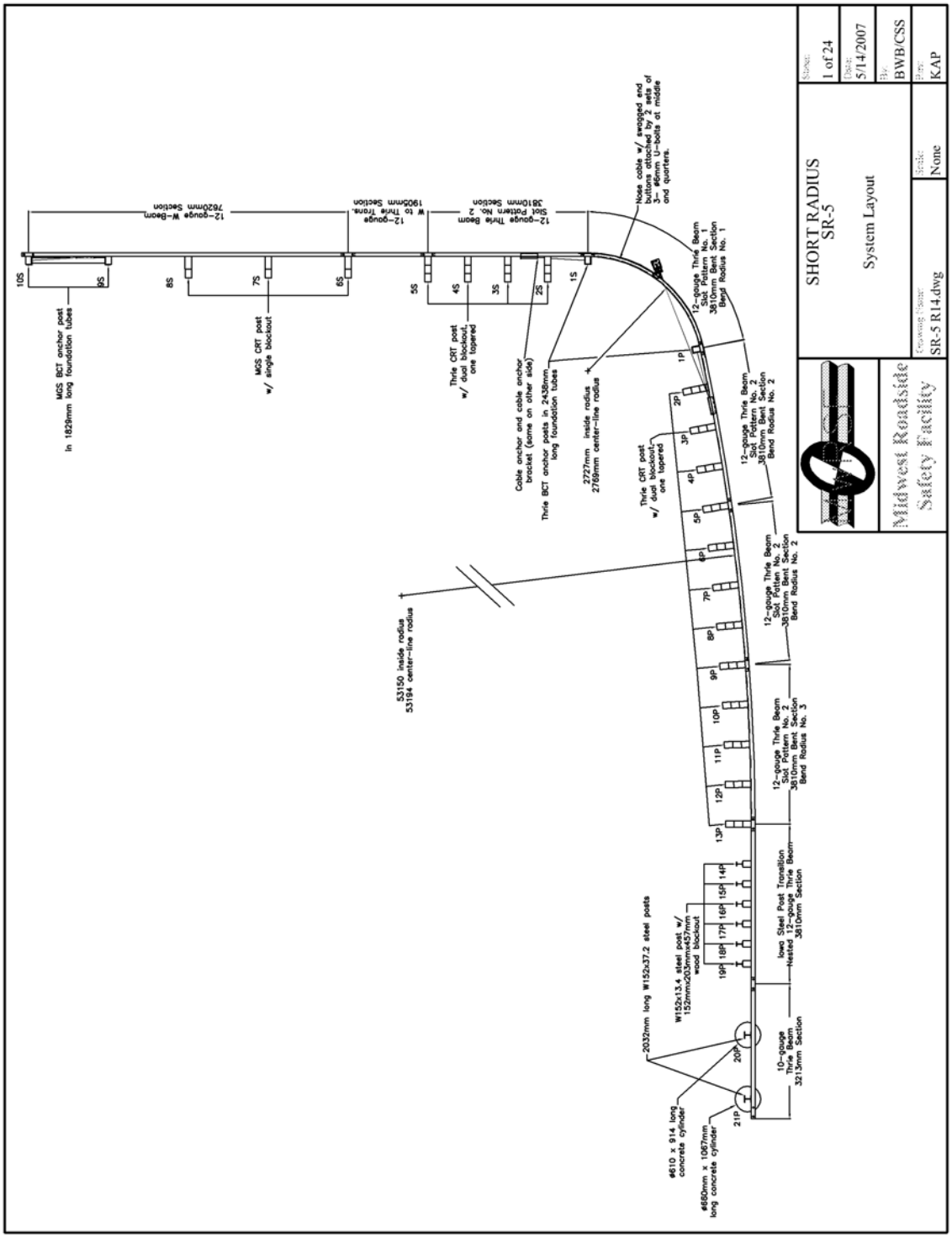

Figure 12. Short-Radius Overall System Layout

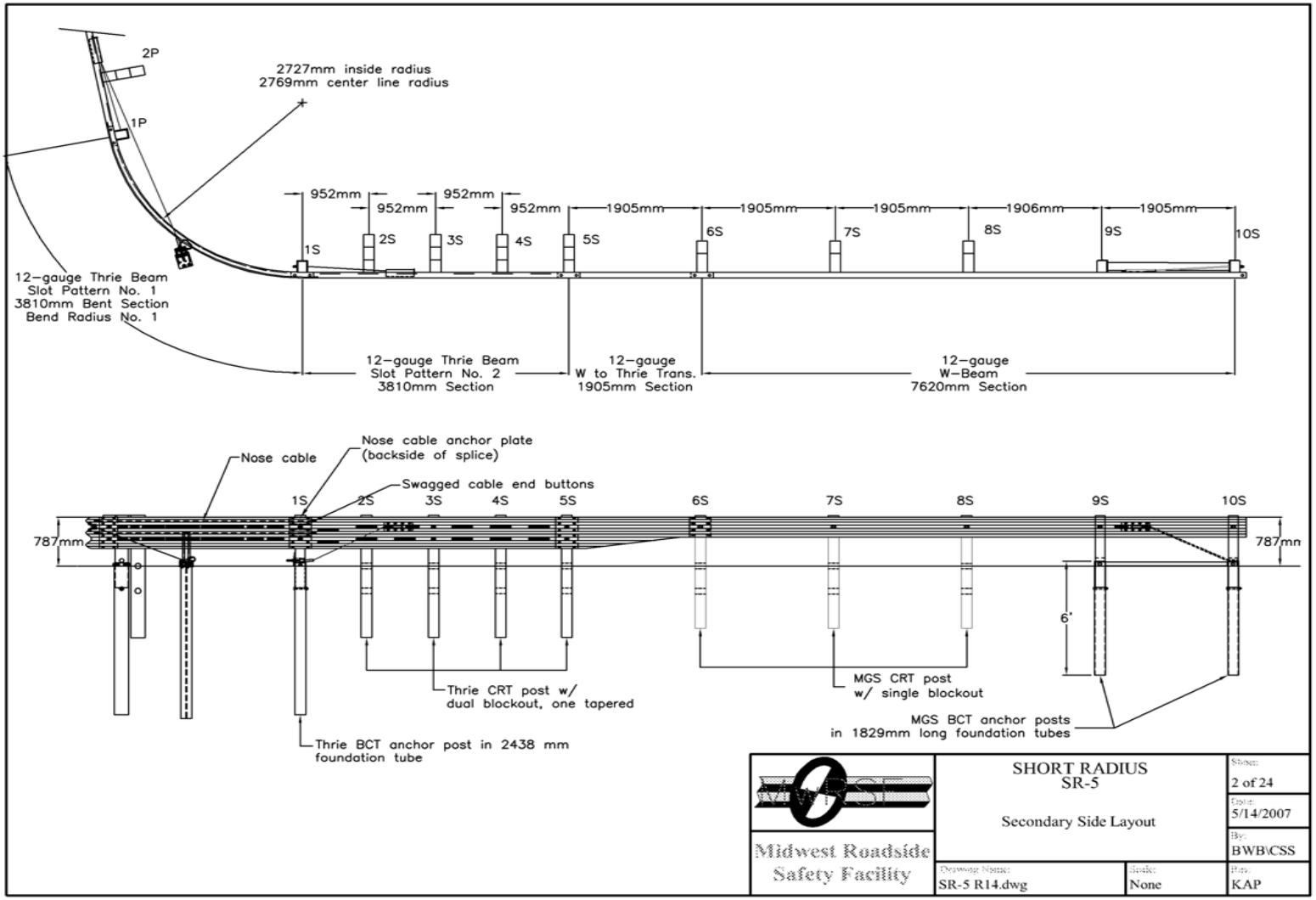

Figure 13. Short-Radius Secondary Side System Layout

X Location with respect to the center of Post no. 13P
Y Location with respect to the backside of the rail at post no. 13P

Post No.	Front Face D.S. Edge		Front Face U.S. Edge	
	X	Y	X	Y
1P	11254	1210	11395	1235
2P	10258	1413	10408	1443
3P	9330	1238	9481	1265
4P	8396	1080	8547	1103
5P	7455	935	7606	959
6P	6526	811	6677	830
7P	5580	702	5731	721
8P	4645	611	4797	625
9P	3700	537	3853	548
10P	2757	478	2910	487
11P	1816	438	1969	443
12P	870	413	1022	416
13P	76	406	76	406

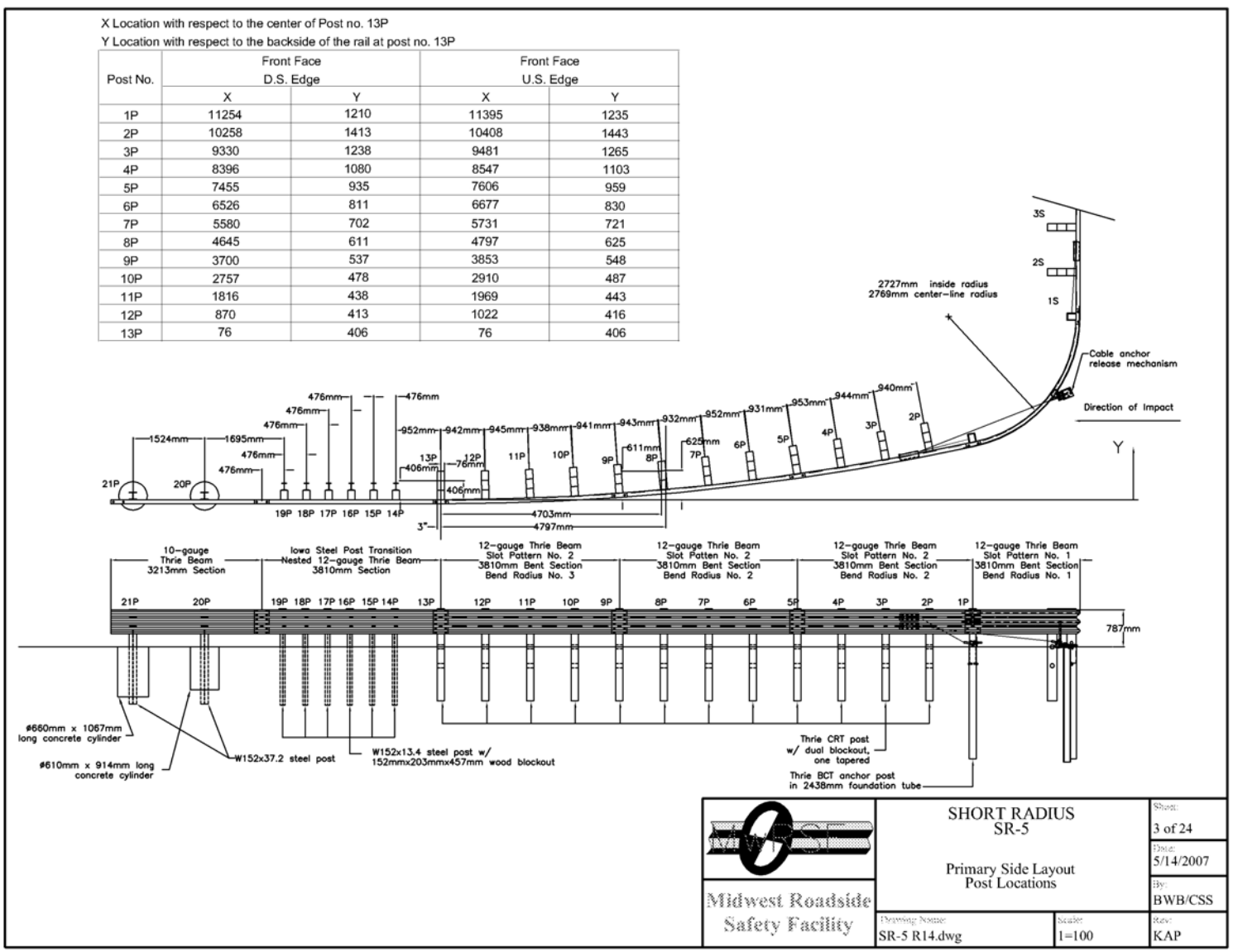

Figure 14. Short-Radius Primary Side System Layout

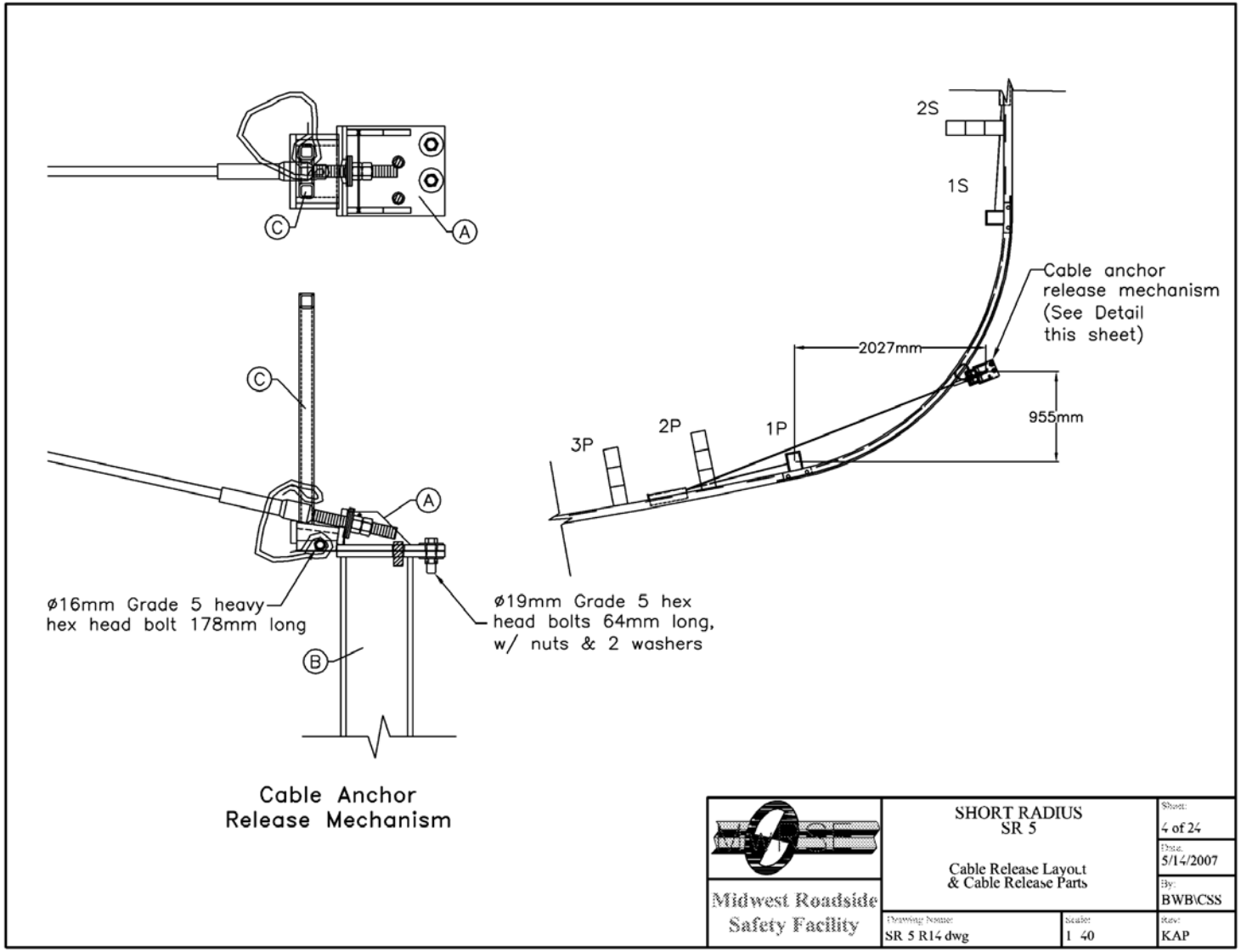

Figure 15. Cable Release Layout

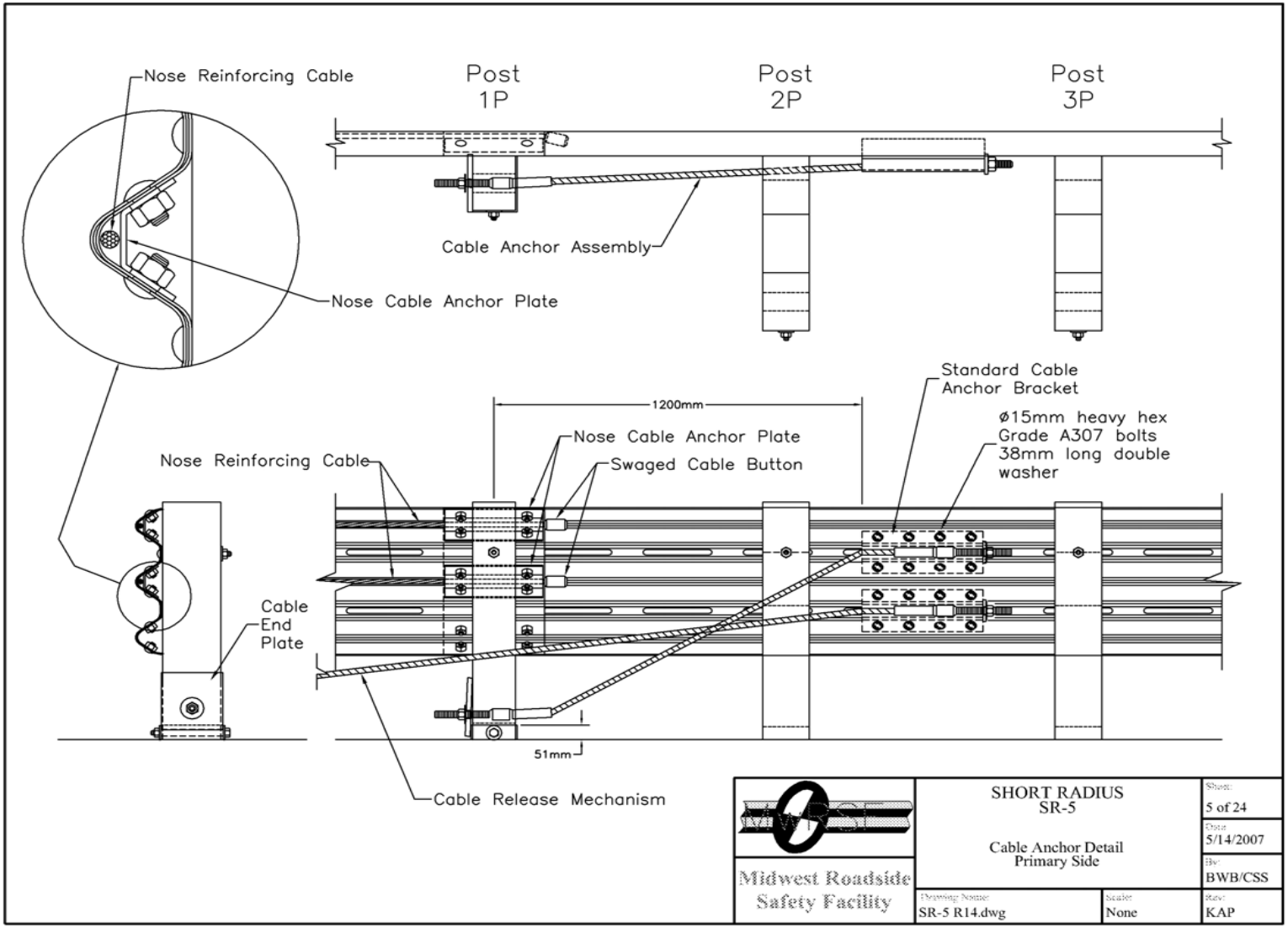

Figure 16. Primary Side Cable Anchor Detail

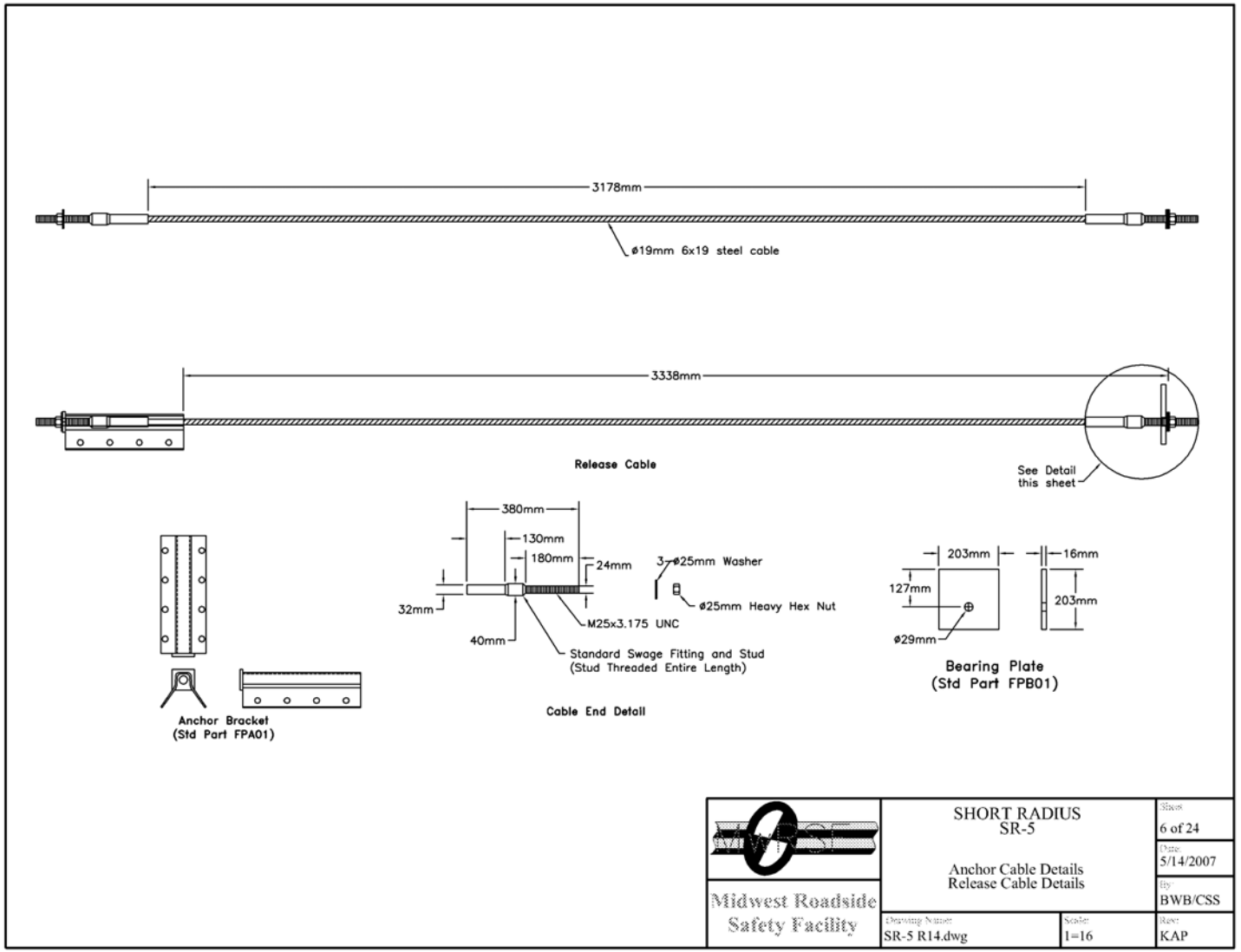

Figure 17. Anchor Cable and Release Cable Details

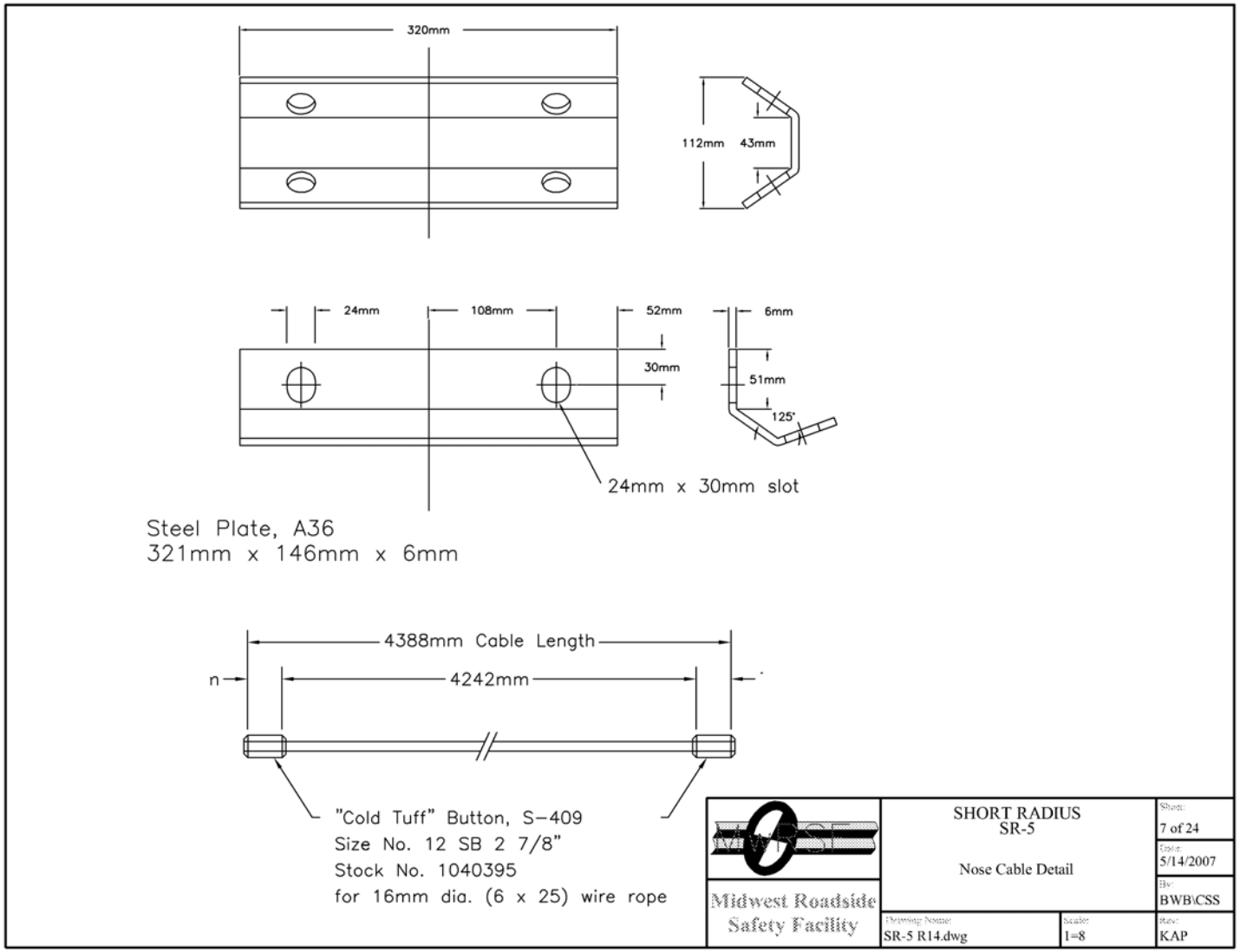

Figure 18. Nose Cable Details

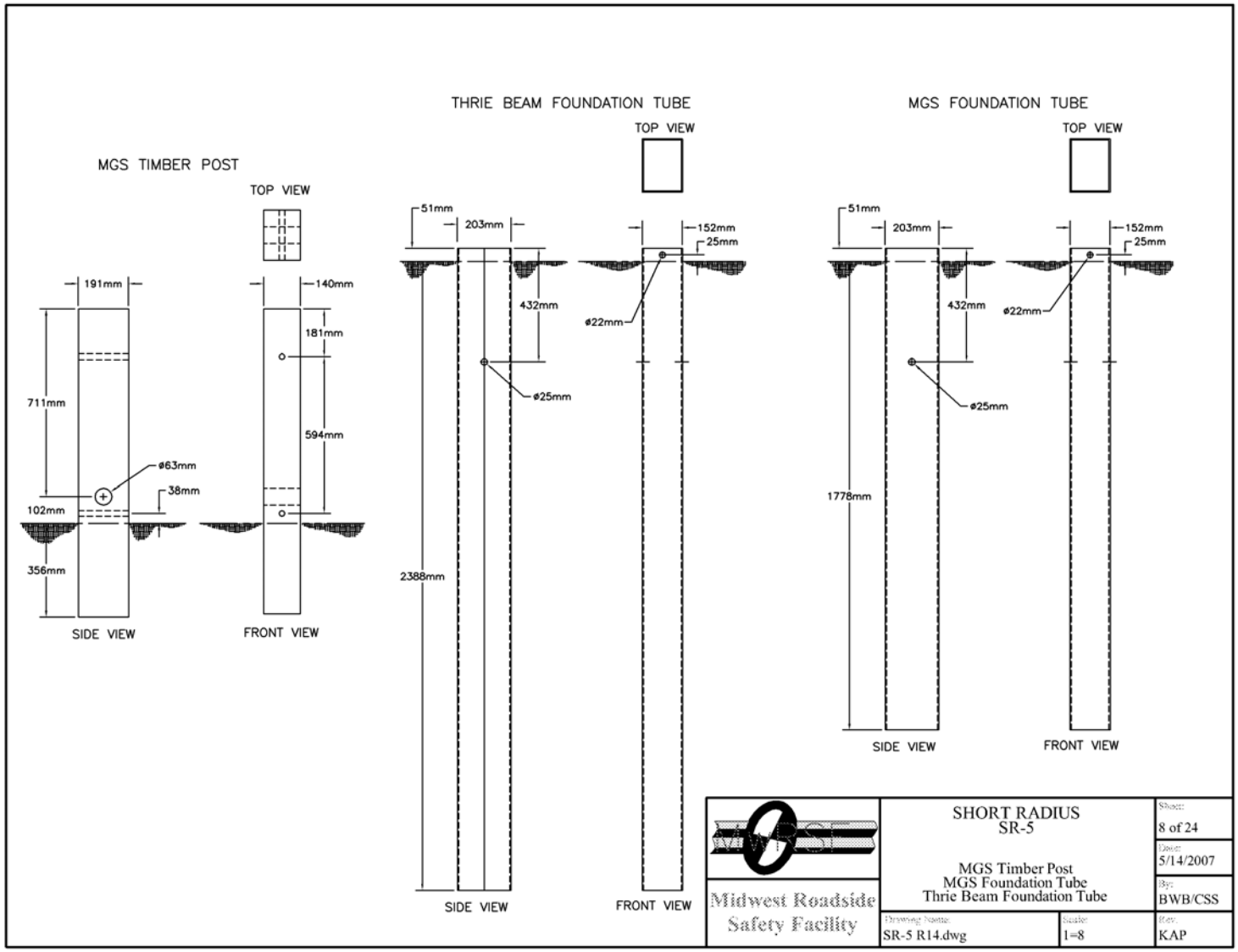

Figure 19. MGS Timber Posts and Foundation Tube and Thrie Beam Foundation Tube Details

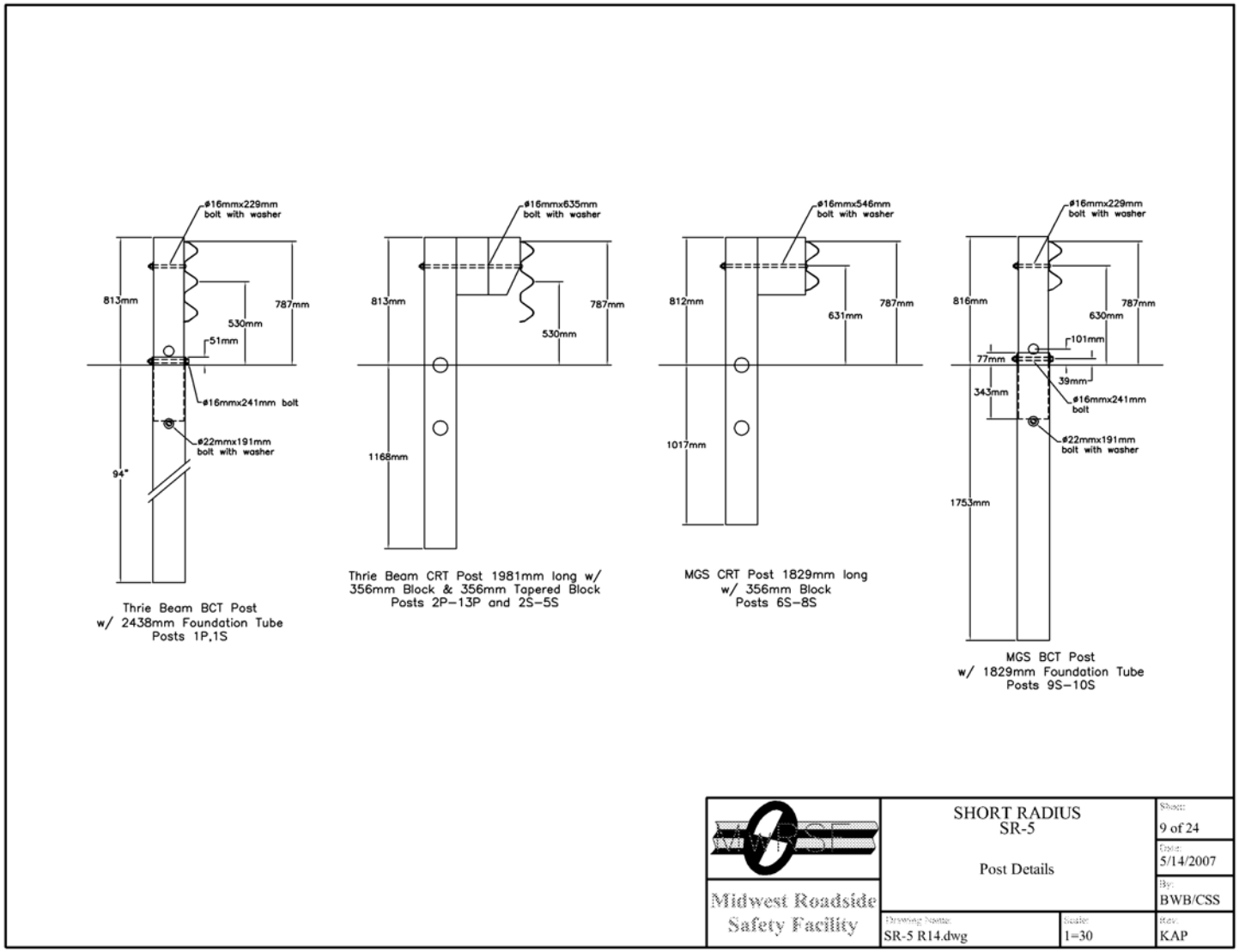

Figure 20. Post Details

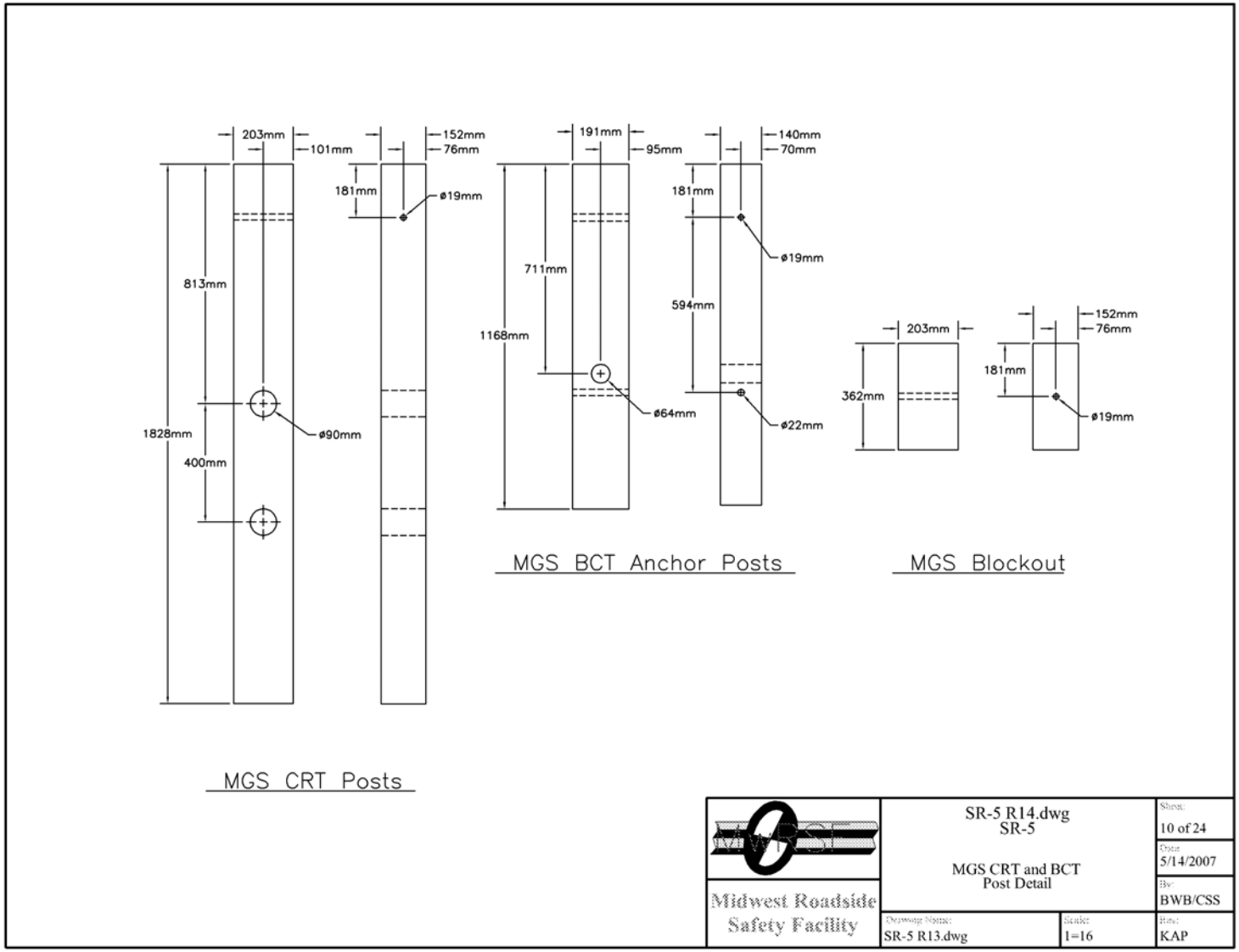

Figure 21. MGS CRT and BCT Post Details

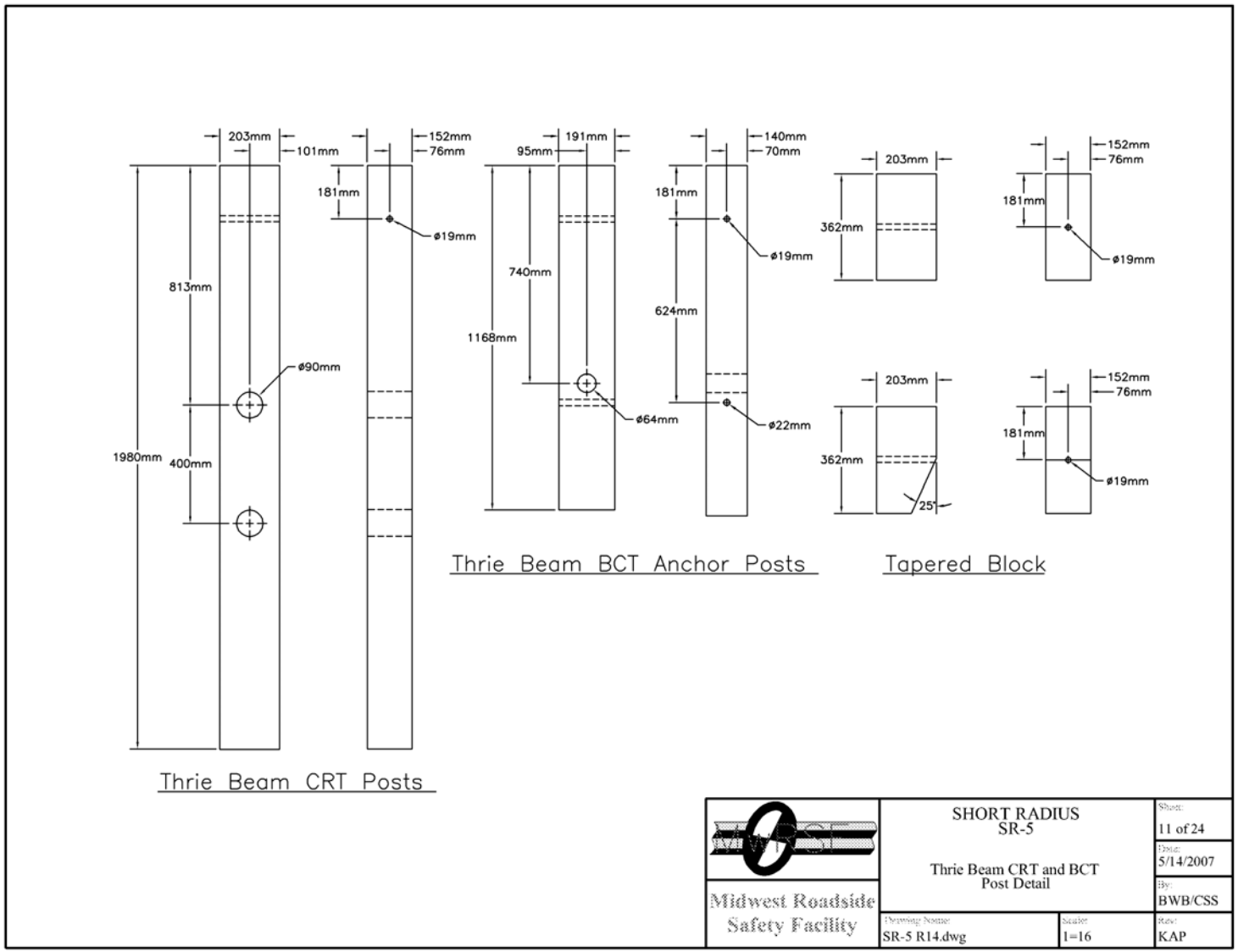

Figure 22. Thrie Beam CRT and BCT Post Details

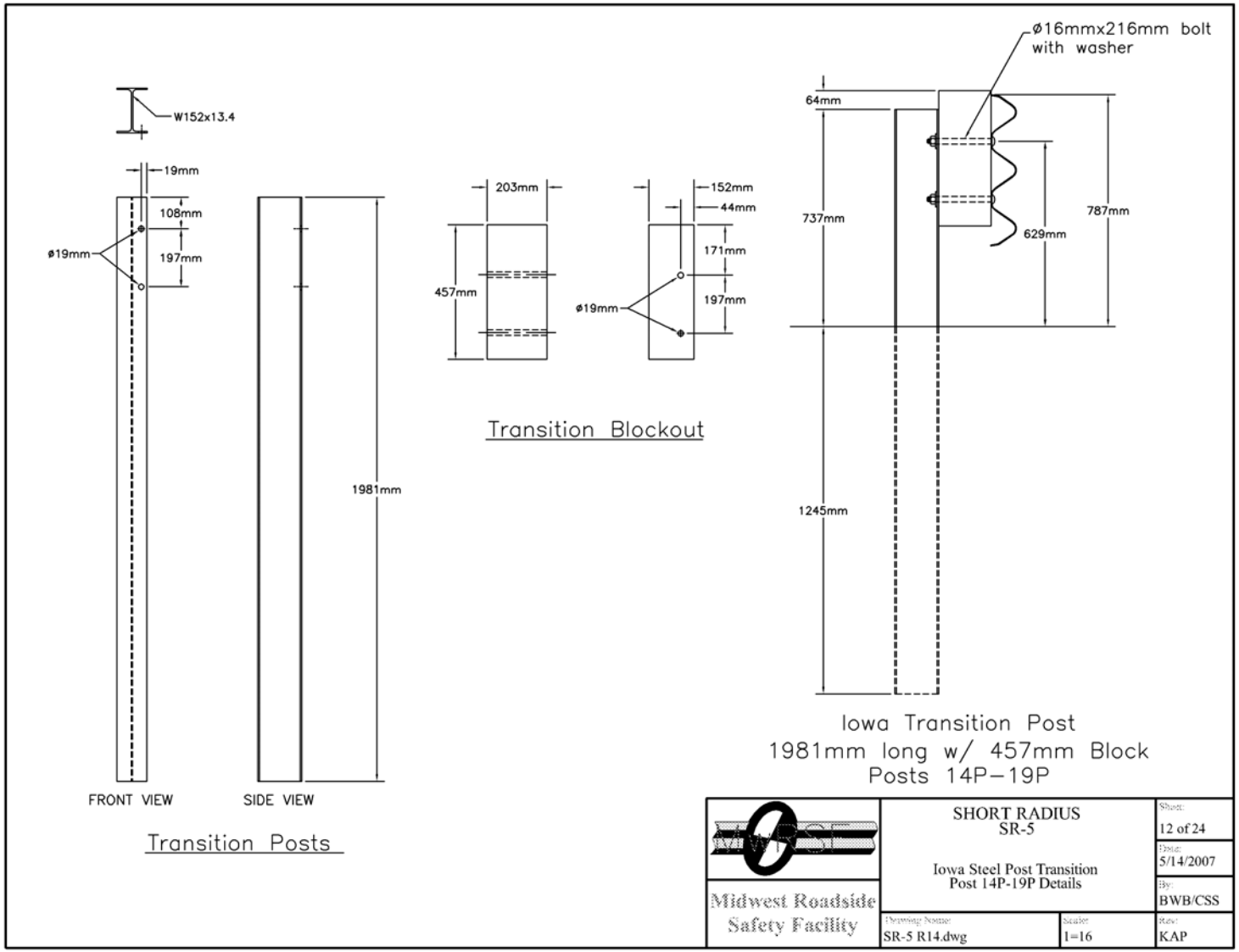

Figure 23. Iowa Steel Post Transition, Post Nos. 14P-19P Details

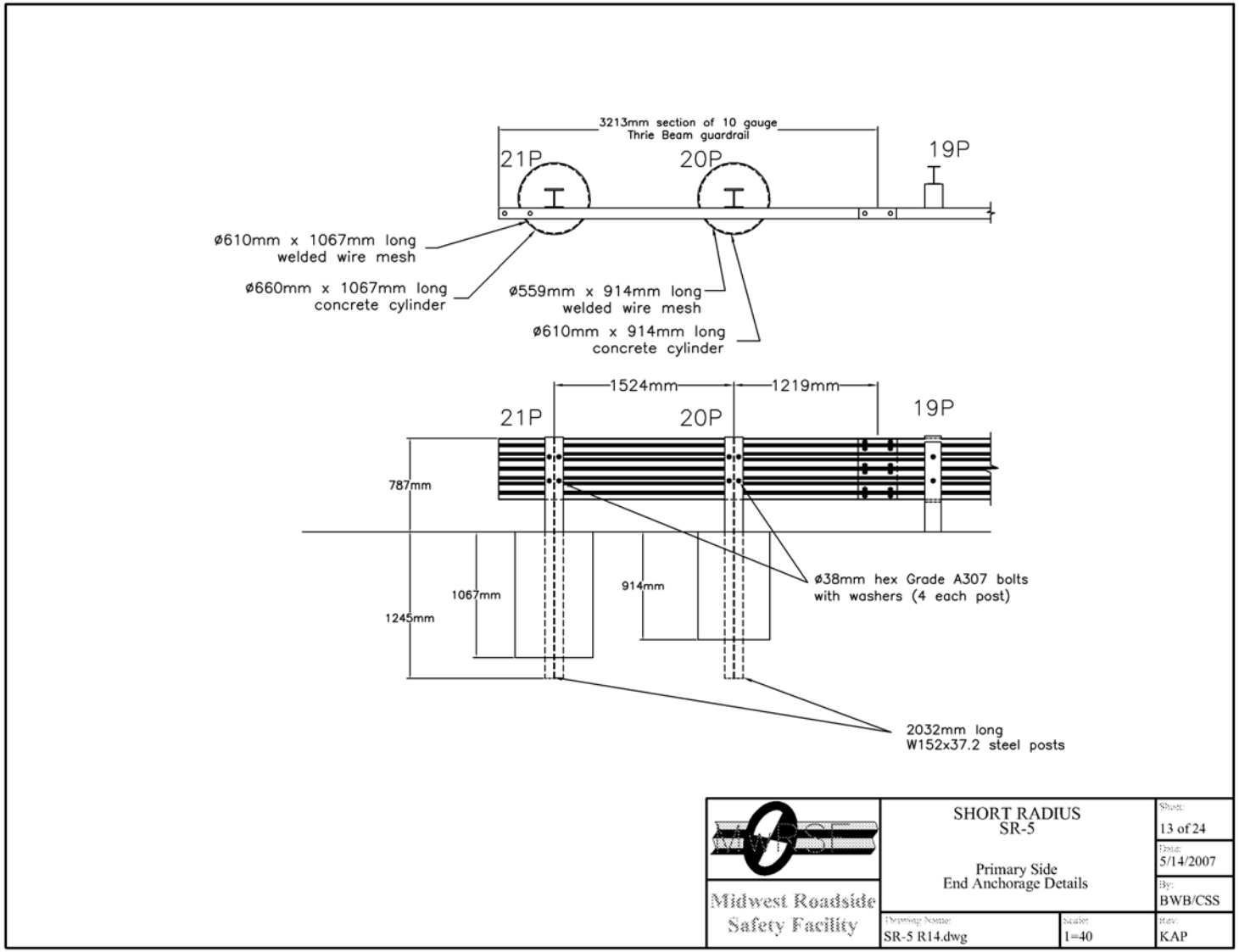

Figure 24. Primary Side End Anchorage Details

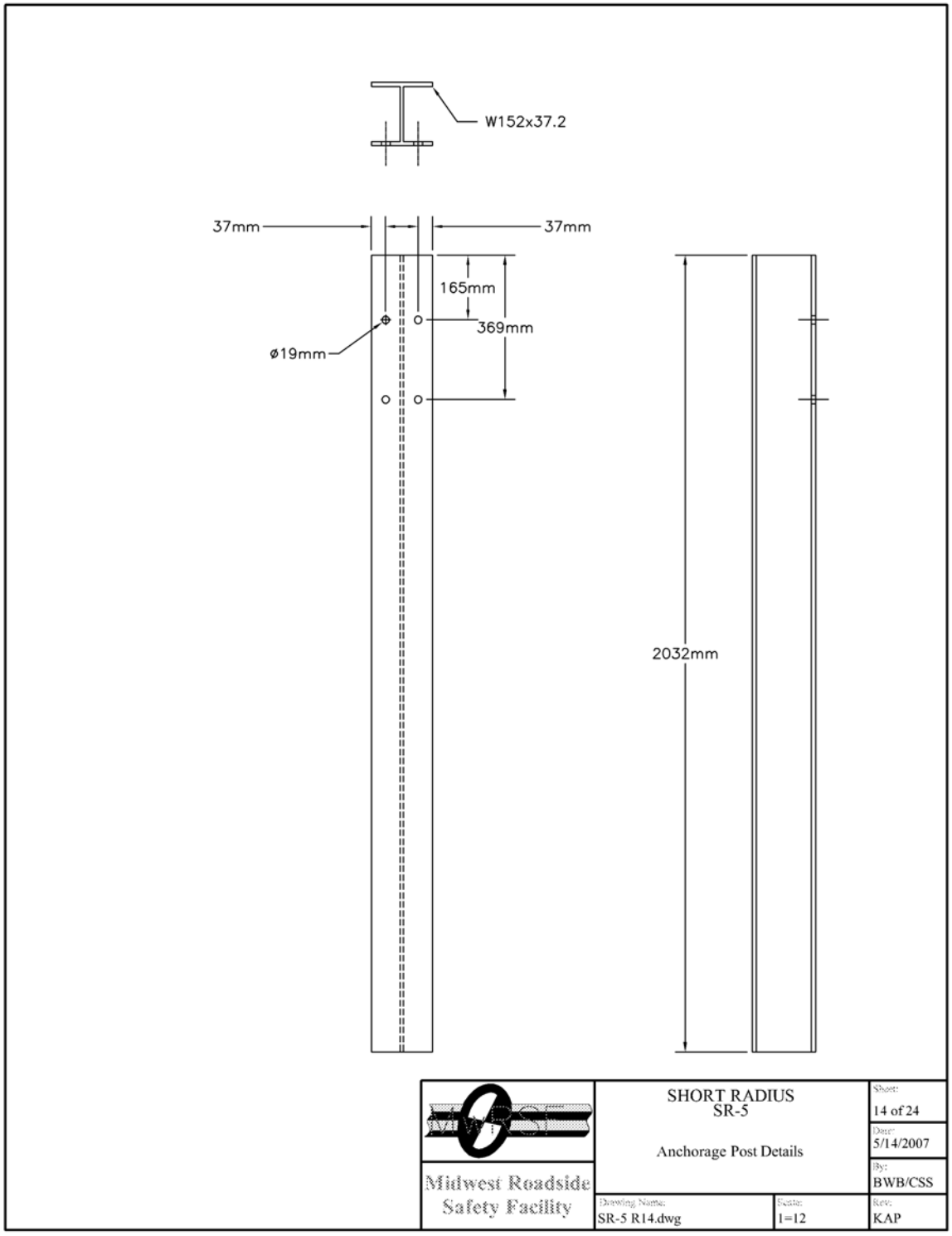

Figure 25. Anchorage Post Details

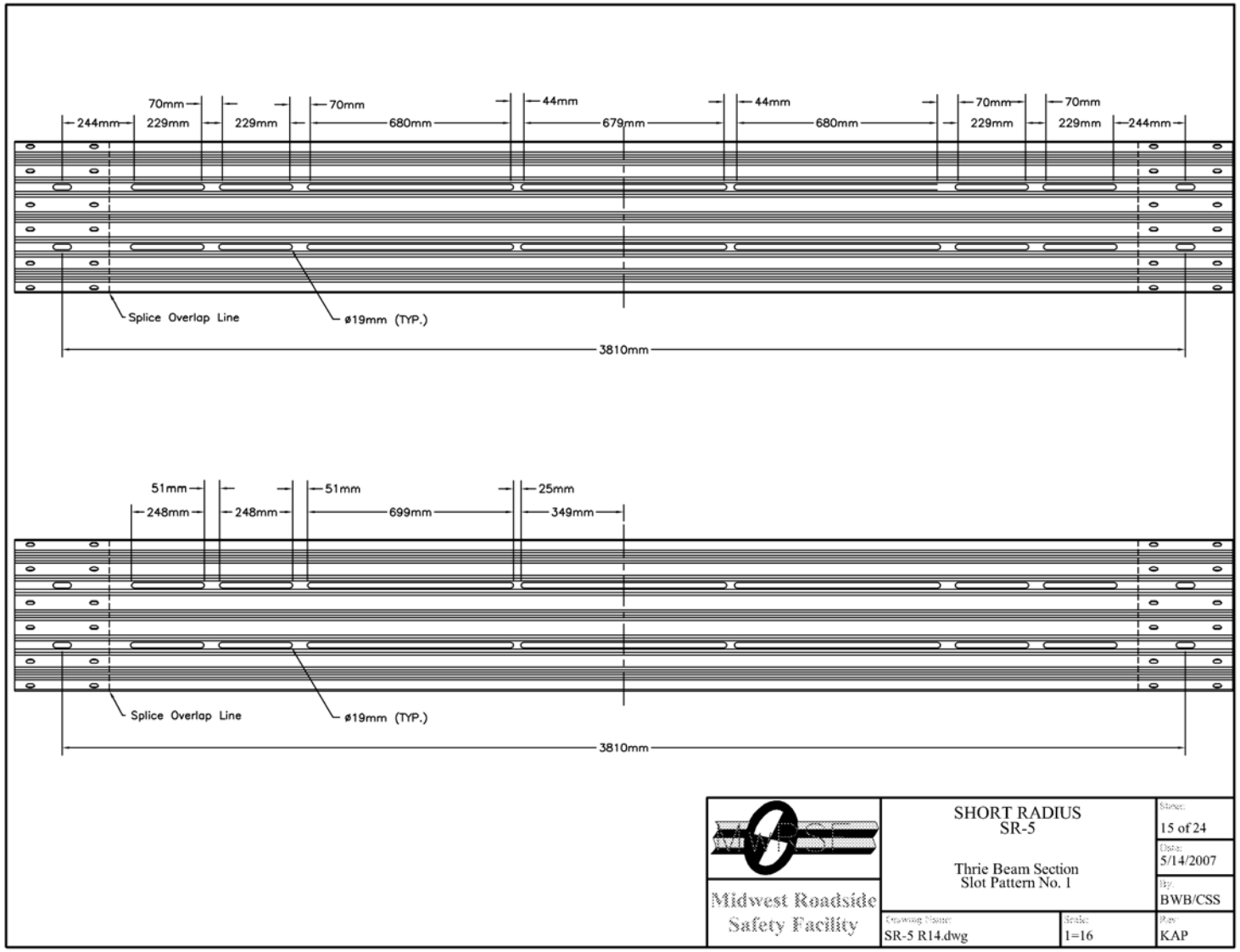

Figure 26. Thrie Beam Slot Pattern No. 1

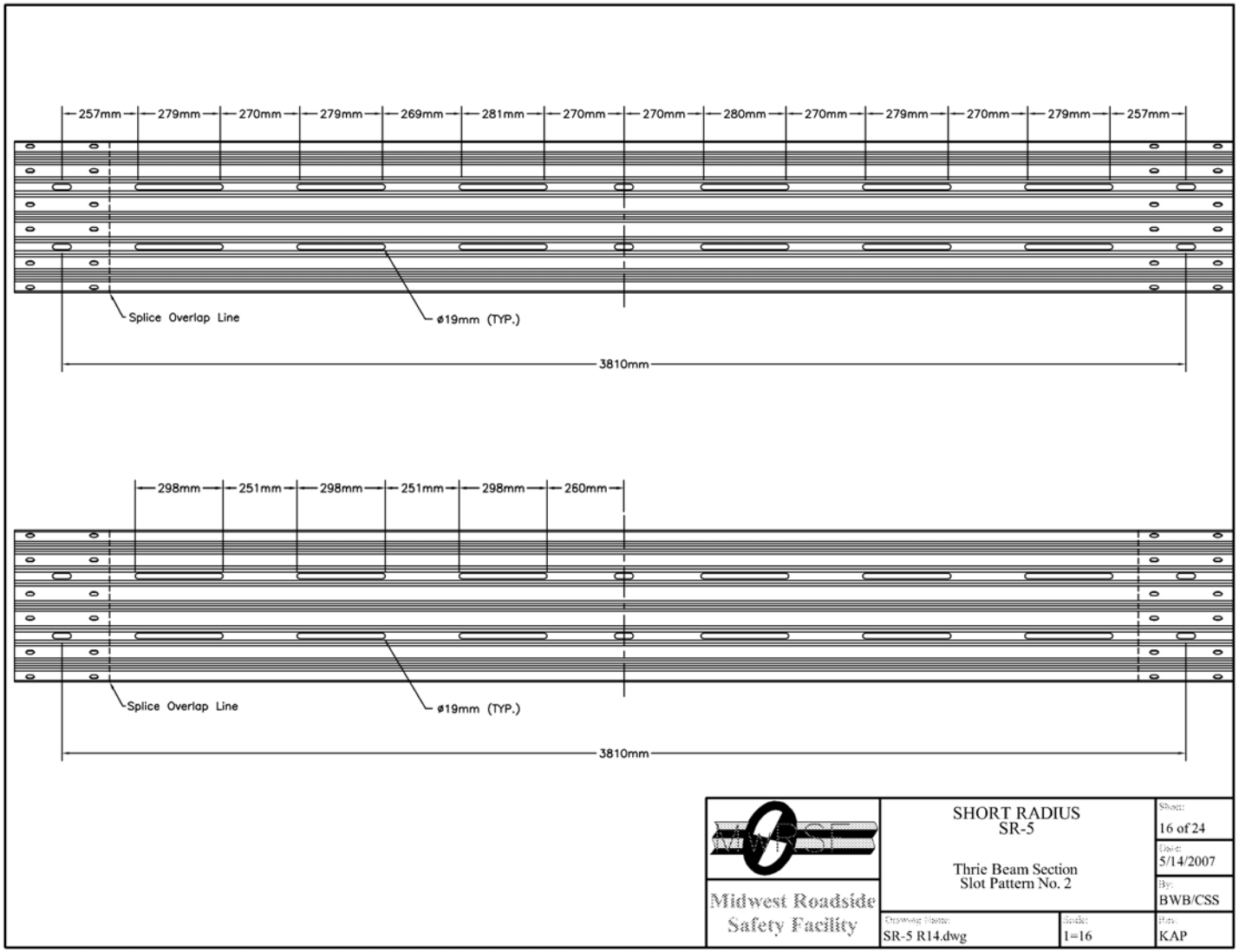

Figure 27. Thrie Beam Slot Pattern No. 2

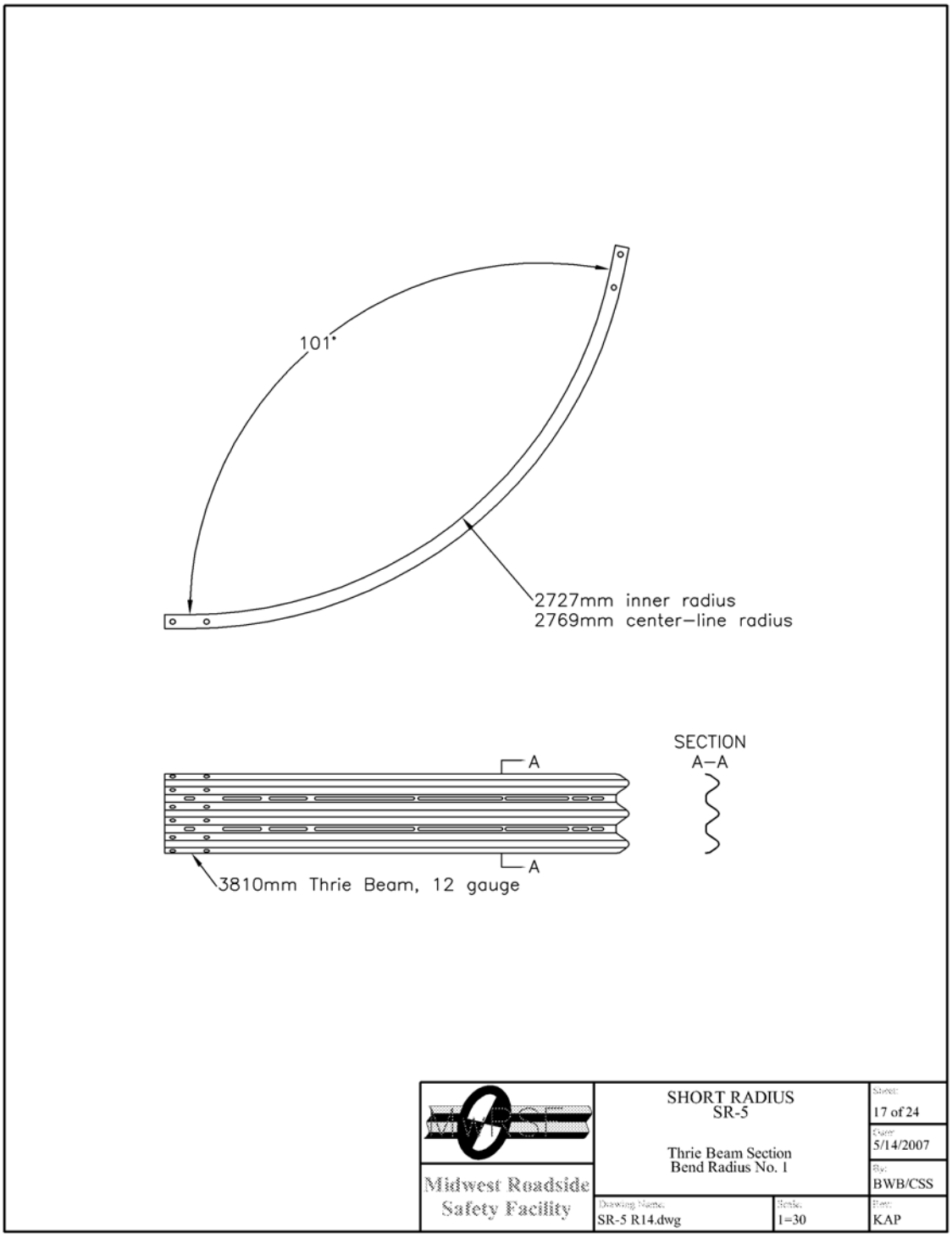

Figure 28. Thrie Beam Bend Radius No. 1

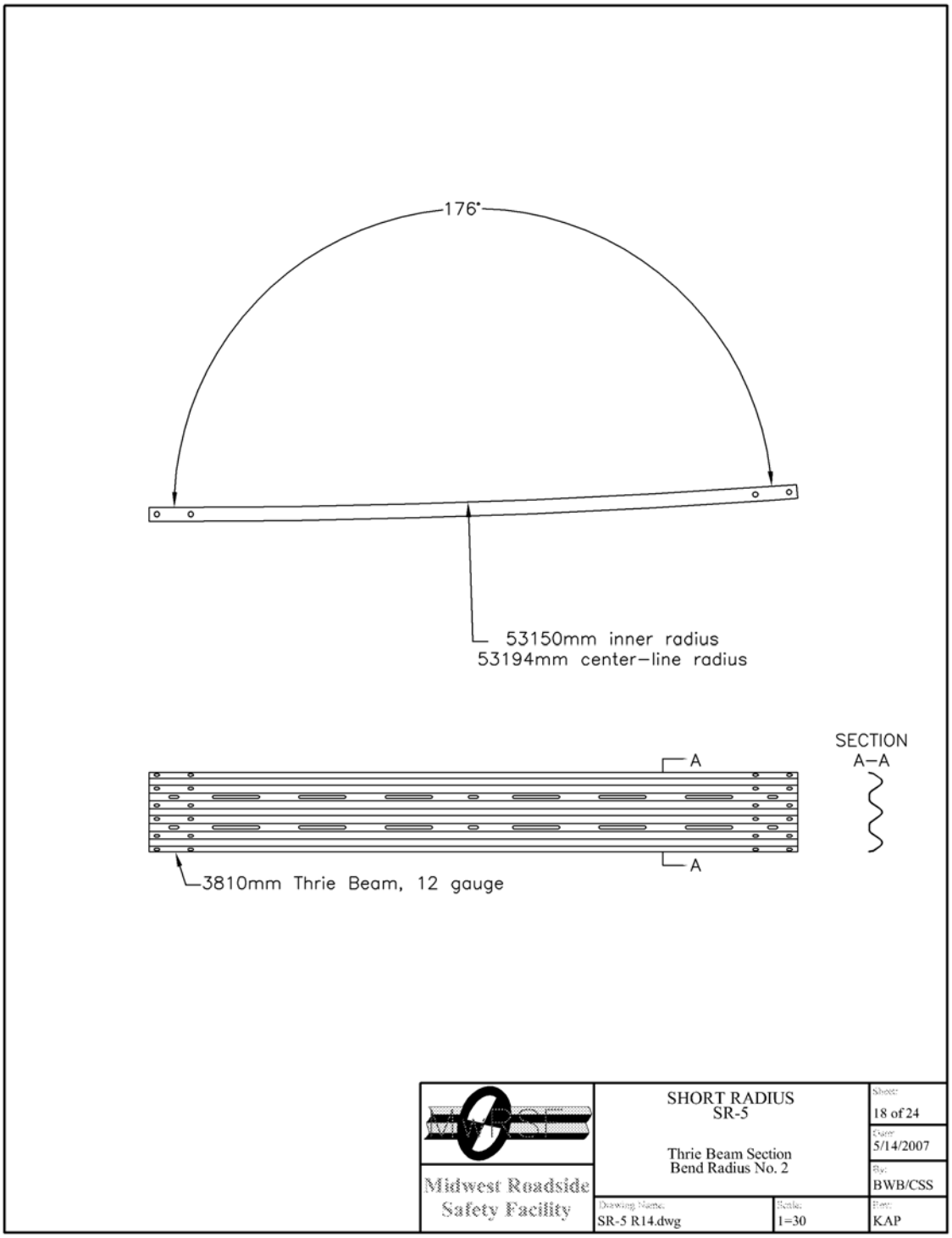

Figure 29. Thrie Beam Bend Radius No. 2

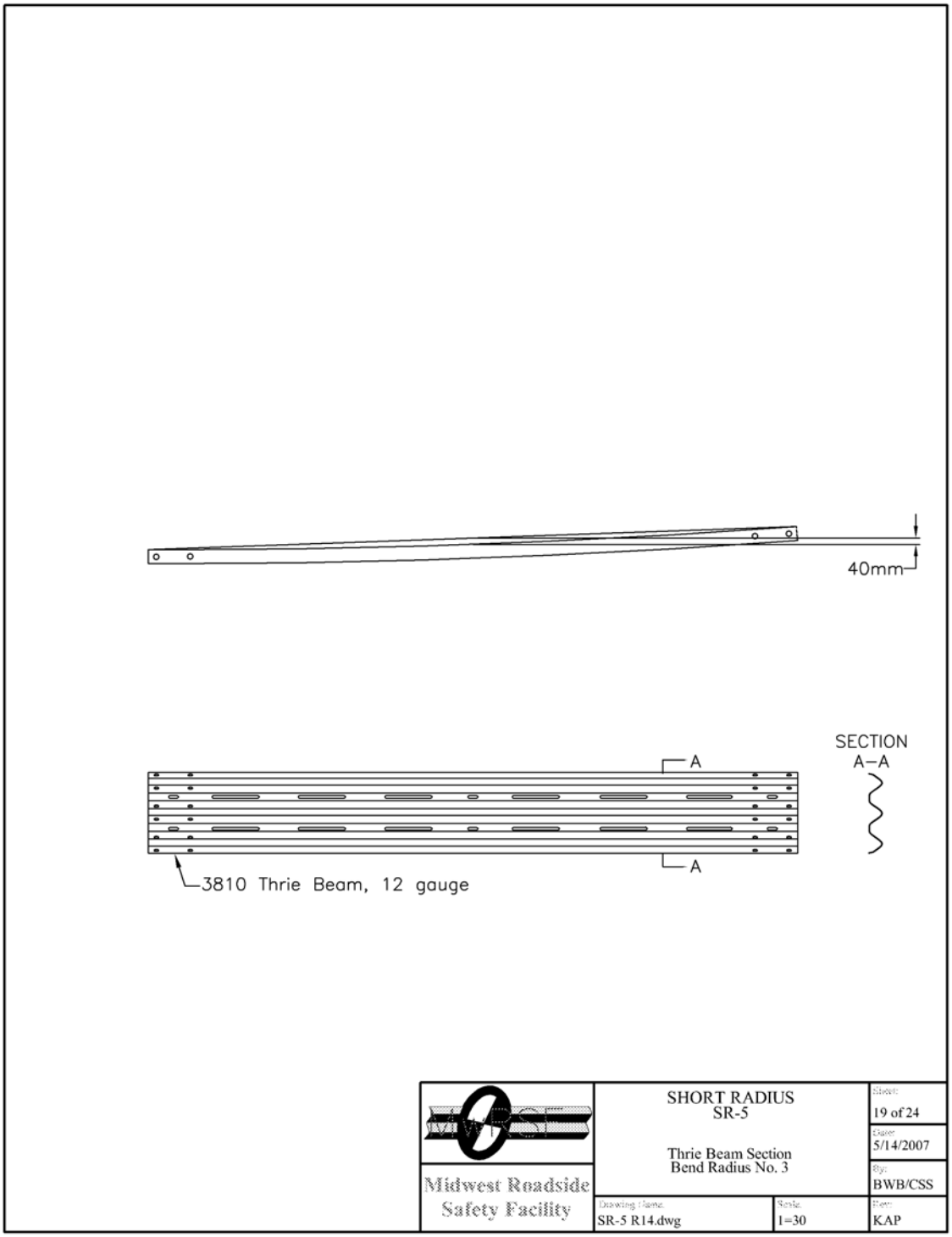

Figure 30. Thrie Beam Bend Radius No. 3

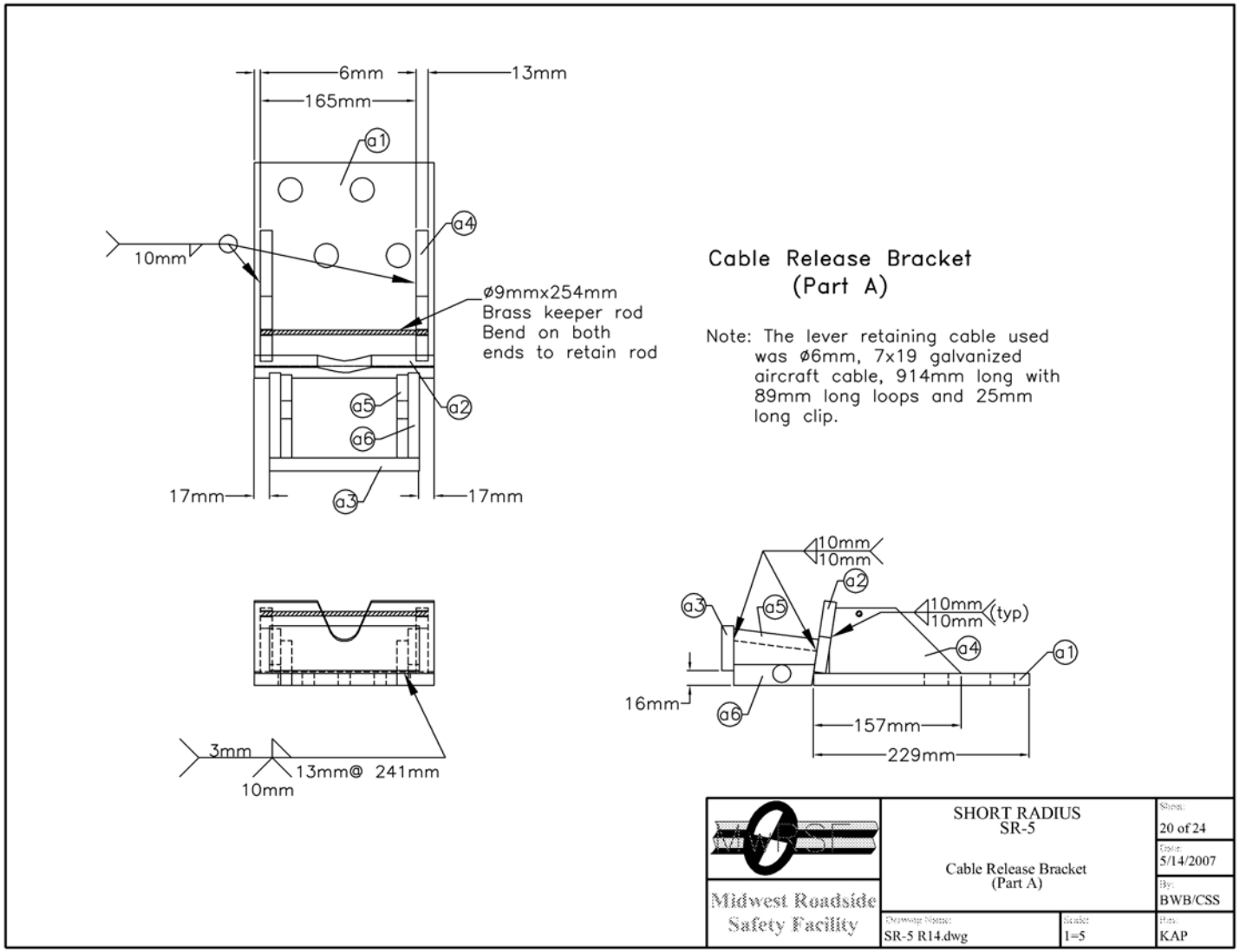

Figure 31. Cable Release Bracket

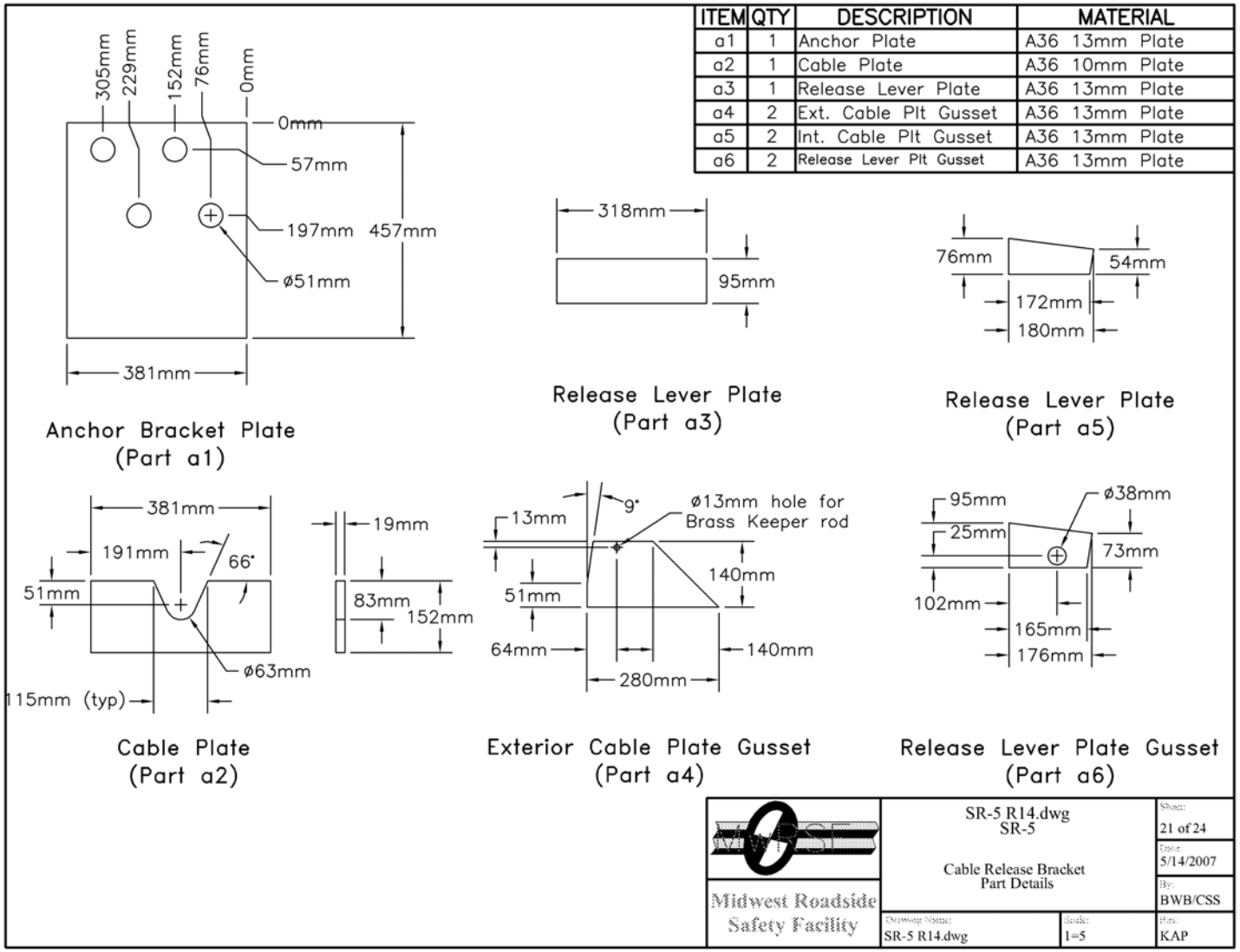

Figure 32. Cable Release Bracket Part Details

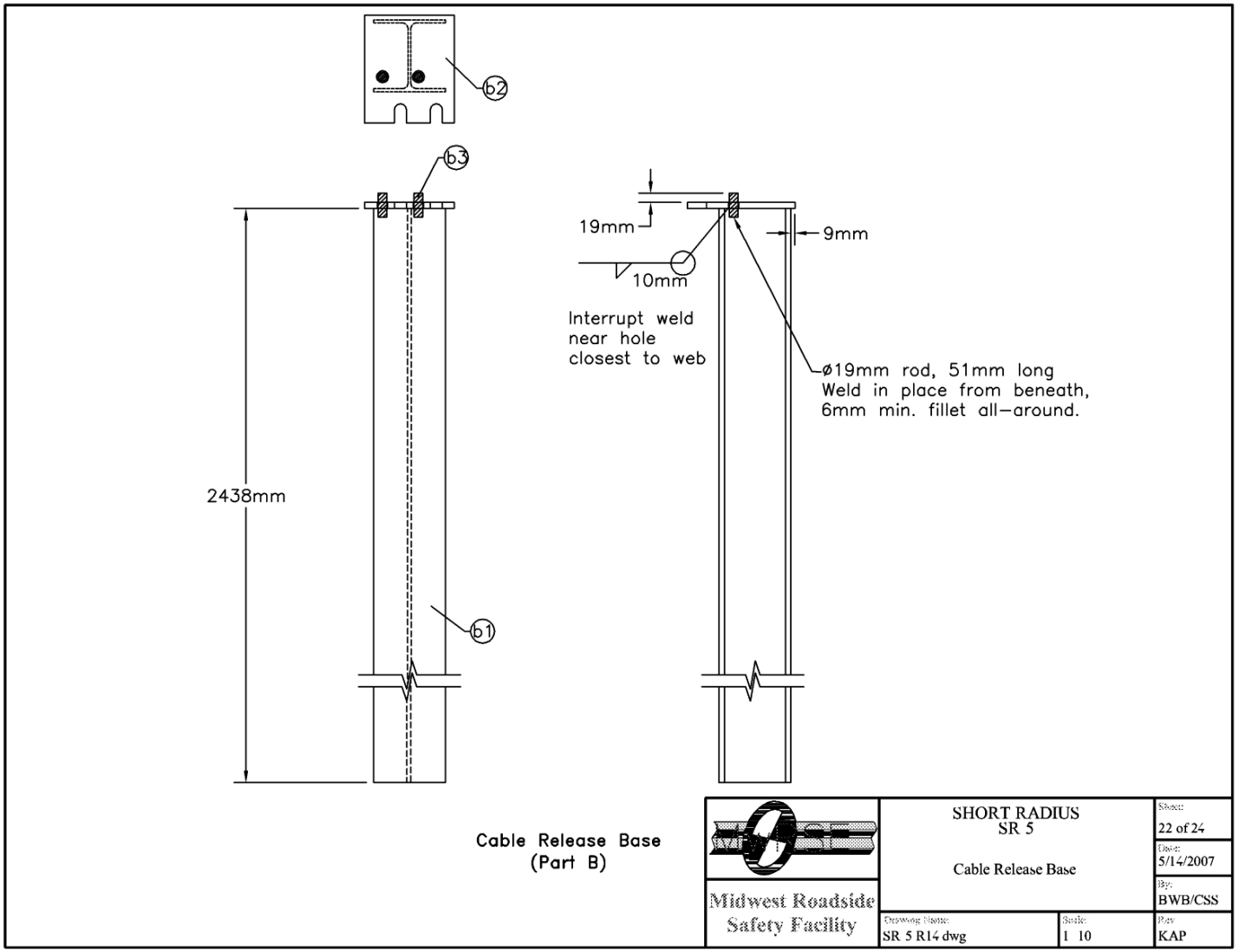

Figure 33. Cable Release Base Details

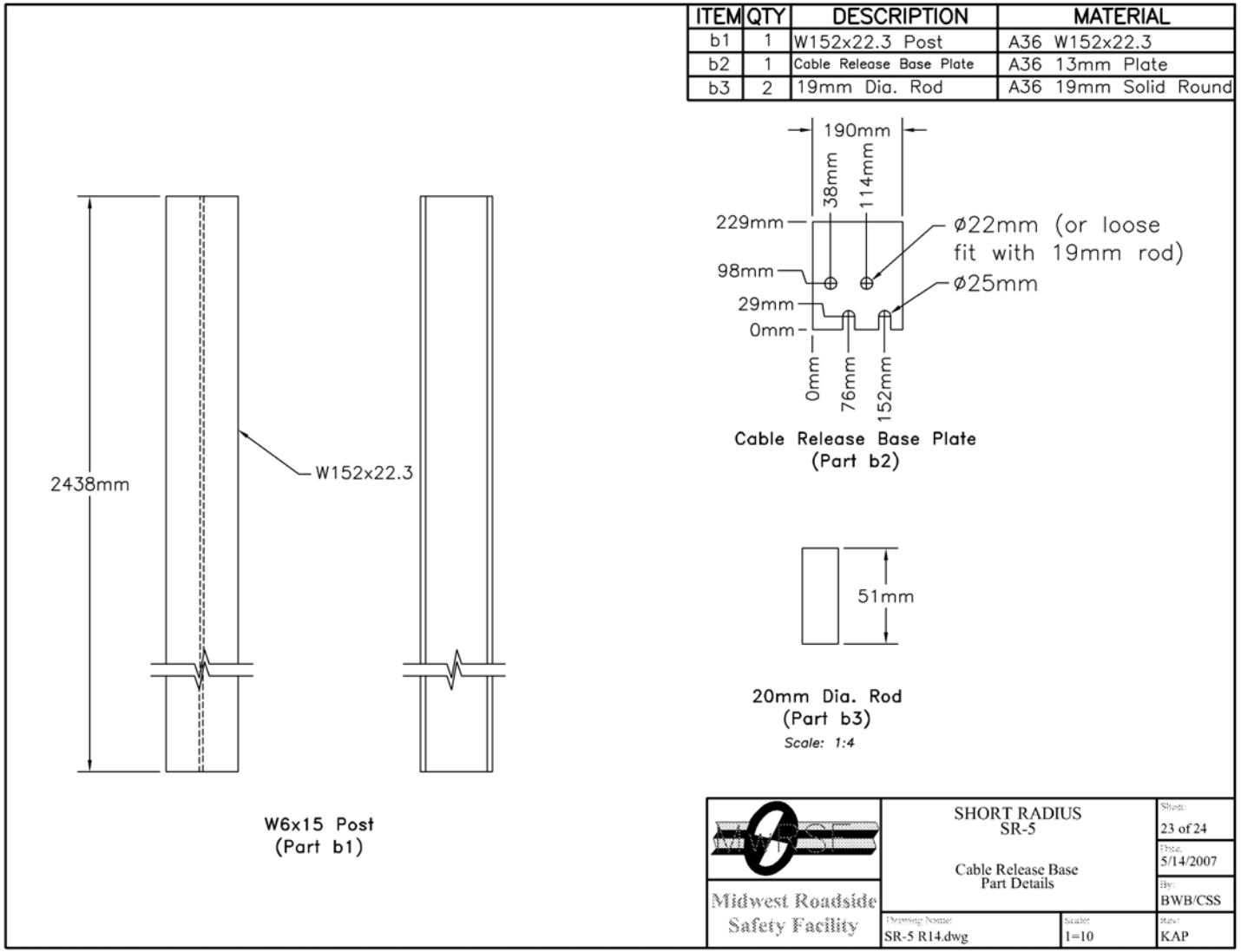

Figure 34. Cable Release Base Part Details

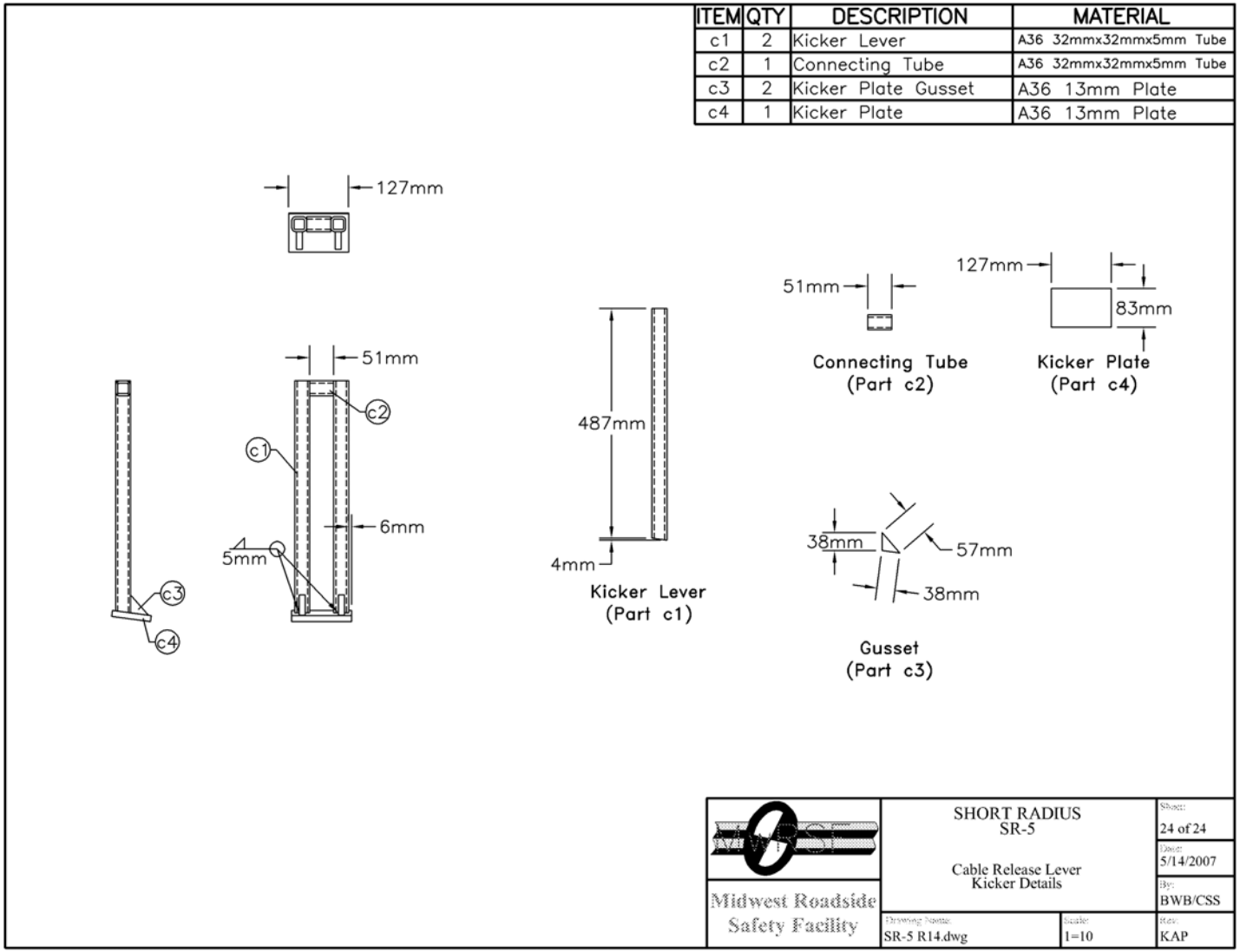

Figure 35. Cable Release Lever Kicker Details

Figure 36. Short-Radius System Details

Figure 37. Short-Radius System Details

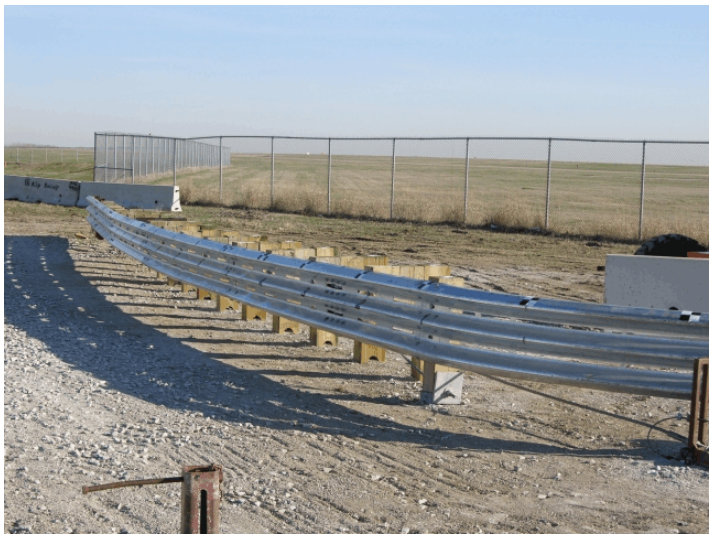

Figure 38. Short-Radius Nose Section Details

Figure 39. Short-Radius Cable Anchor Details

Figure 40. Short-Radius Post Details

6 CRASH TEST NO. SR-5

6.1 Test SR-5

Test SR-5 was conducted as a modified version of NCHRP Report No. 350 Test Designation 3-31. The 2,001-kg (4,411-lb) pickup truck impacted the short-radius guardrail at a speed of 101.8 km/h (63.2 mph) and at an angle of 0.9 degrees. Due to the parabolic flare, the impact location for this test aligned the centerline of the pickup truck with the back face of post no. 13P. A summary of the test results and sequential photographs are shown in Figure 41. Additional sequential photographs are shown in Figures 43 through 46. Documentary photographs of the crash test are shown in Figures 47 and 48.

6.2 Test Description

The right-front corner of the test vehicle impacted the curved nose section of the short-radius guardrail system just upstream of post no. 1P, as shown in Figure 49. Upon impact, the front of the pickup truck deformed the curved nose section inward. At 0.034 sec, the thrie beam guardrail around the right-front corner of the bumper deformed upward and wrapped around the front of the pickup truck. At this same time, the right-front quarter panel crushed inward due to rail contact. At 0.062 sec, the right-front corner of the pickup truck contacted post no. 1P which fractured at the ground. At 0.086 sec, the guardrail continued to capture the pickup truck's front bumper. At this same time, post no. 2P deflected backward. At 0.102 sec, the pickup truck contacted post no. 2P which fractured at the ground. By 0.120 sec, the right-front corner of the pickup truck's hood deformed upward, and the quarter-panel continued crushing below it. At this same time, the pickup truck began to redirect. At 0.156 sec, the pickup truck contacted post no. 3P which deflected backward. At this same time, post no. 1P was still attached to the rail. At 0.170 sec, the hood's right-front corner, the right-front

quarter panel, and the right-front corner of the bumper continued to deform as the rail continued to flatten. At 0.182 sec, the pickup truck contacted post no. 4P which rotated slightly backward in the soil. At 0.190 sec, a gap between the right-front corner of the hood and the quarter panel formed, and the pickup truck rolled slightly counter-clockwise away from the system. At 0.216 sec, the top of the right-side door separated from the frame and bent outward at the door trim. At 0.276 sec, vehicle continued to be redirected, and the front bumper was located at post no. 7P. At 0.468 sec, the pickup truck exited the system with a resultant velocity of 85.4 km/h (53.1 mph) and at an angle of 12.6 degrees. The pickup truck came to rest 41.9 m (137 ft - 6 in.) downstream from impact and 10.8 m (35 ft - 6 in.) laterally away from the primary side, as shown in Figure 42. It should be noted that the secondary anchor remained in place throughout the vehicle contact and successfully developed upstream tension necessary to redirect the vehicle. The trajectory and final position of the pickup truck are shown in Figure 50.

6.3 System and Component Damage

Damage to the short-radius system was moderate, as shown in Figures 51 through 61. Post no. 1P fractured at the foundation tube but remained attached to the rail. Post nos. 2P through 3P fractured at ground level and disengaged from the rest of the system. The tapered blockout at post no. 2P disengaged from the post. Post no. 4P fractured approximately 178 mm (7 in) below the groundline and disengaged from the system. Post no. 5P cracked at the groundline and rotated backwards in the soil. Post no. 6P sustained a 229-mm (9-in.) long crack through the transverse hole and rotated backward in the soil. Post no. 7P also rotated backward in the soil.

Contact marks were found on all three corrugations between the impact location on the rail and post no. 7P. The rail was flattened and deformed between the center of the nose section and post

no. 2P. Rail flattening also was found between post nos. 3P and 5P. Rail bending was observed along curved nose section. Additional rail bending was found at post nos. 3P, 4P, and 6P through 8P. The post bolts released from the rail at post nos. 2P through 4P. Significant post bolt rail deformation was found at post no. 6P. The rail slots between post nos. 3P and 4P were folded and closed by rail flattening and deformation. The rail was deformed backwards and the bottom corrugation deformed upward between post nos. 3P and 7P.

The anchor bracket on the secondary side was deformed. The cable anchor release lever was released and lying next to the bracket. This suggested that the anchor did not release until after the vehicle exited the system, and that the anchor was likely released during elastic rebound of the guardrail. The cable anchor release brackets and cable anchor plate were bent upwards. The cable was separated from the cable brackets at posts nos. 1P and 1S. The BCT bearing plates were bent but remained attached to post no. 1S and pulled through the transverse hole in post no. 1P.

6.4 Vehicle Damage

Exterior vehicle damage was minimal, as shown in Figures 62 through 64. Occupant compartment deformations to the right side and center of the floorboard were judged insufficient to cause serious injury to the vehicle occupants. Maximum longitudinal deflections of 13 mm (0.5 in.) were located near the left side of the right-side floorboard. Maximum lateral deflections of 25 mm (1 in.) were located near the right-front corner of the right-side floor pan. Maximum vertical deflections of 38 mm (1.5 in.) were located near the center of the right-side floorboard. Complete occupant compartment deformations and the corresponding locations are provided in Appendix C.

The right-front bumper corner was deformed inward and encountered significant dents and scratches. The right side of the grill was also deformed inward and fractured around the headlight.

The right-front turn signal cover was fractured and disengaged from the vehicle. The right-front quarter panel was crushed inward and wheel well was severely deformed. The entire right side of the vehicle sustained dents and scratches. The top of the right-side door was jarred open and it could not be opened nor closed. The right-front upper and lower ball joints fractured. The right-side steering arm fractured at the spindle. The right-side lower A-frame control arm was bent. The right-front wheel was separated from the vehicle and encountered significant scratches, dents, deformations, and gouges on both the inside and outside of the rim. The right-rear tire also encountered minor abrasions, but the rim remained undamaged. The spare tire under the vehicle was scratched and torn. The exhaust was fractured, and the gas tank was dented. The left side and rear of the vehicle, the hood, and all window glass remained undamaged.

6.5 Occupant Risk Values

The longitudinal and lateral occupant impact velocities were determined to be 4.07 m/s (13.37 ft/s) and 3.18 m/s (10.43 ft/s), respectively. The maximum 0.010-sec average occupant compartment ridedown decelerations in the longitudinal and lateral directions were 5.72 Gs and 5.37 Gs, respectively. It is noted that the occupant impact velocities (OIVs) and the occupant ridedown decelerations (ORDs) were within the suggested limits provided in NCHRP Report No. 350. The THIV and PHD values were determined to be 4.96 m/s (16.27 ft/s) and 7.35 Gs, respectively. The results of the occupant risk, as determined from the accelerometer data, are summarized in Figure 65. Results are shown graphically in Appendix D. The results from the rate transducer are shown graphically in Appendix D.

6.6 Discussion

The analysis of the test results for test SR-5, showed that the short-radius guardrail system

adequately contained and redirected the 2000P vehicle with controlled lateral displacements of the barrier system. There were no detached elements nor fragments which showed show potential for penetrating the occupant compartment nor presented undue hazard to other traffic. Deformations of, or intrusion into, the occupant compartment that could have caused serious injury did not occur. The test vehicle did not penetrate nor ride over the guardrail system and remained upright during and after the collision. Vehicle roll, pitch, and yaw angular displacements were noted, but they were determined acceptable because they did not adversely influence occupant risk safety criteria nor cause rollover. After collision, the vehicle's trajectory did not intrude into adjacent traffic lanes. Therefore, test no. SR-5 conducted on the short-radius guardrail system was determined to be acceptable according to the TL-3 safety performance criteria found in NCHRP Report No. 350.

0.000 sec | 0.104 sec | 0.216 sec | 0.342 sec | 0.484 sec

- Test Number SR-5
- Date 4/4/2005
- Test Article
  - Type . . . . . Short-Radius Guardrail
  - Key Elements . . . Four 3,810-mm long curved and slotted thrie beam guardrail sections (parabolic flare)
    One 3,810-mm long straight thrie beam guardrail section
    787 mm top rail height
    18 breakaway posts
    Iowa steel post transition
    Simulated tangent W-beam guardrail end terminal
    Additional upstream anchor for primary side
  - Orientation . . . . . Centerline truck with back of post no. 13P
- Soil Type . . . . . Grading B - AASHTO M 147-65 (1990)
- Vehicle Model . . . . . 1997 Ford F-250 pickup truck
  - Curb . . . . . 1,862 kg
  - Test Inertial . . . . . 2,001 kg
  - Gross Static . . . . . 2,001 kg
- Vehicle Speed
  - Impact . . . . . 101.8 km/h
  - Exit . . . . . 85.4 km/h
- Vehicle Angle
  - Impact . . . . . 0.9 deg
  - Exit . . . . . 12.6 deg
- Vehicle Stability . . . . . Satisfactory
- Occupant Ridedown Deceleration (10 msec avg.)
  - Longitudinal . . . . . 5.72 Gs < 20 Gs
  - Lateral (not required) . . . . . 5.37 Gs < 20 Gs
- Occupant Impact Velocity
  - Longitudinal . . . . . 4.07 m/s < 12 m/s
  - Lateral (not required) . . . . . 3.18 m/s < 12 m/s
- THIV (not required) . . . . . 4.96 m/s
- PHD (not required) . . . . . 7.35 Gs
- Vehicle Damage
  - TAD[20] 1-FR-3
  - SAE[21] 1-FRAW5
- Vehicle Stopping Distance 41.92 m downstream
  10.84 m right
- Test Article Damage . . . . . Moderate
- Maximum Deflections
  - Permanent Set . . . . . 1,483 mm
  - Dynamic . . . . . 2,219 mm
  - Working Width . . . . . 2,260 mm laterally from primary side

Figure 41. Summary of Test Results and Sequential Photographs, Test SR-5

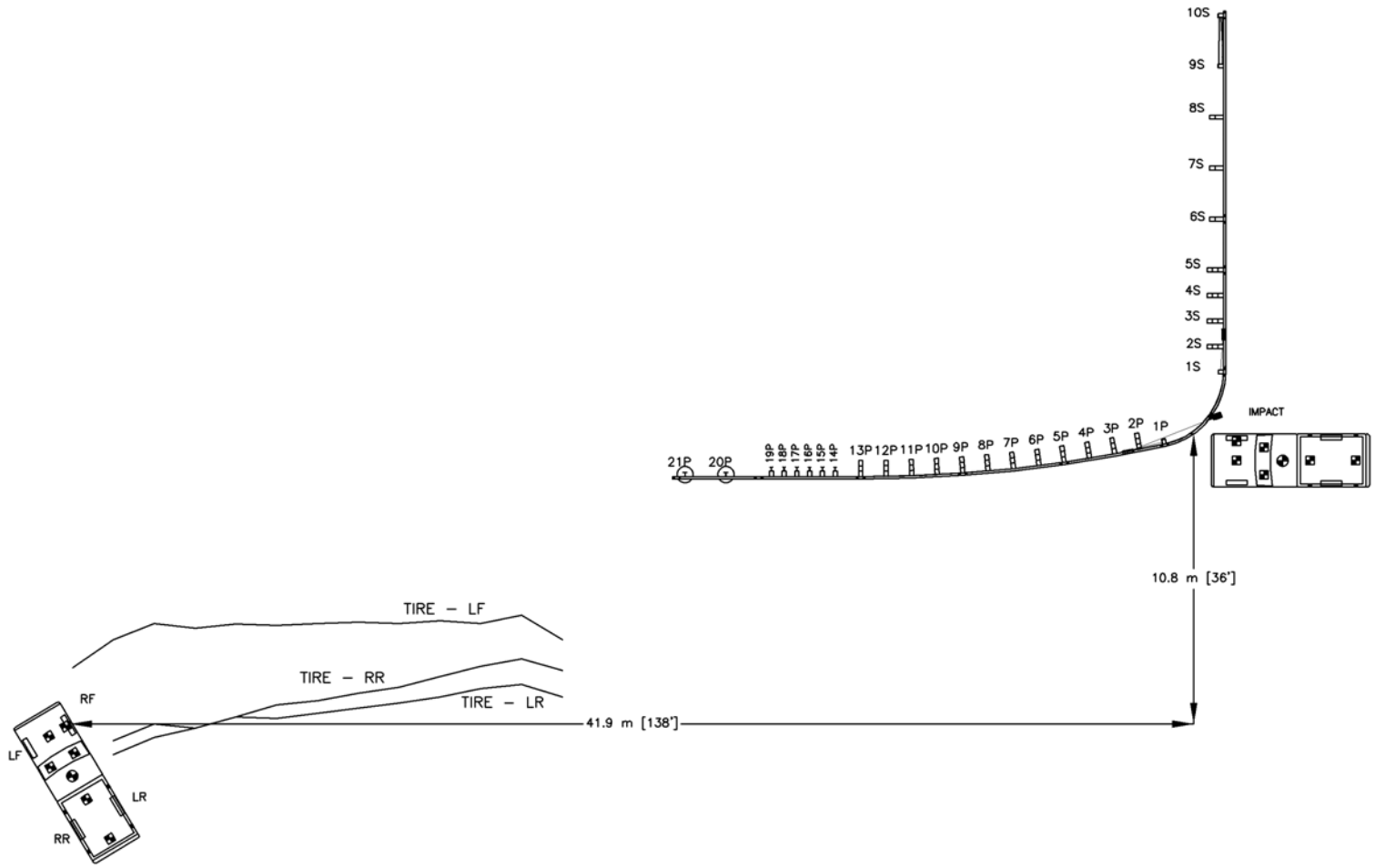

Figure 42. Vehicle Trajectory and Final Position, Test SR-5

0.000 sec

0.000 sec

0.102 sec

0.108 sec

0.212 sec

0.186 sec

0.312 sec

0.266 sec

0.390 sec

0.384 sec

0.574 sec

0.508 sec

Figure 43. Additional Sequential Photographs, Test SR-5

0.000 sec

0.110 sec

0.190 sec

0.276 sec

0.376 sec

0.570 sec

Figure 44. Additional Sequential Photographs, Test SR-5

0.000 sec

0.000 sec

0.100 sec

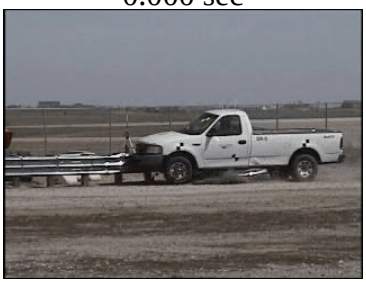

0.100 sec

0.200 sec

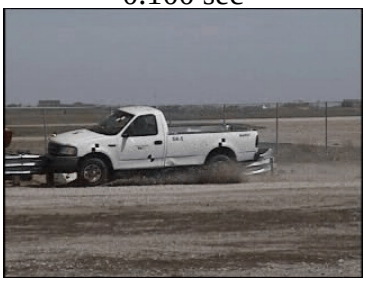

0.200 sec

0.300 sec

0.300 sec

0.400 sec

0.400 sec

Figure 45. Additional Sequential Photographs, SR-5

0.000 sec

0.000 sec

0.334 sec

0.167 sec

0.667 sec

0.334 sec

1.001 sec

0.501 sec

1.335 sec

0.834 sec

1.668 sec

1.168 sec

Figure 46. Additional Sequential Photographs, Test SR-5

Figure 47. Documentary Photographs, Test SR-5

Figure 48. Documentary Photographs, Test SR-5

Figure 49. Impact Location, Test SR-5

Figure 50. Vehicle Trajectory and Final Position, Test SR-5

Figure 51. System Damage, Test SR-5

Figure 52. System Damage, Test SR-5

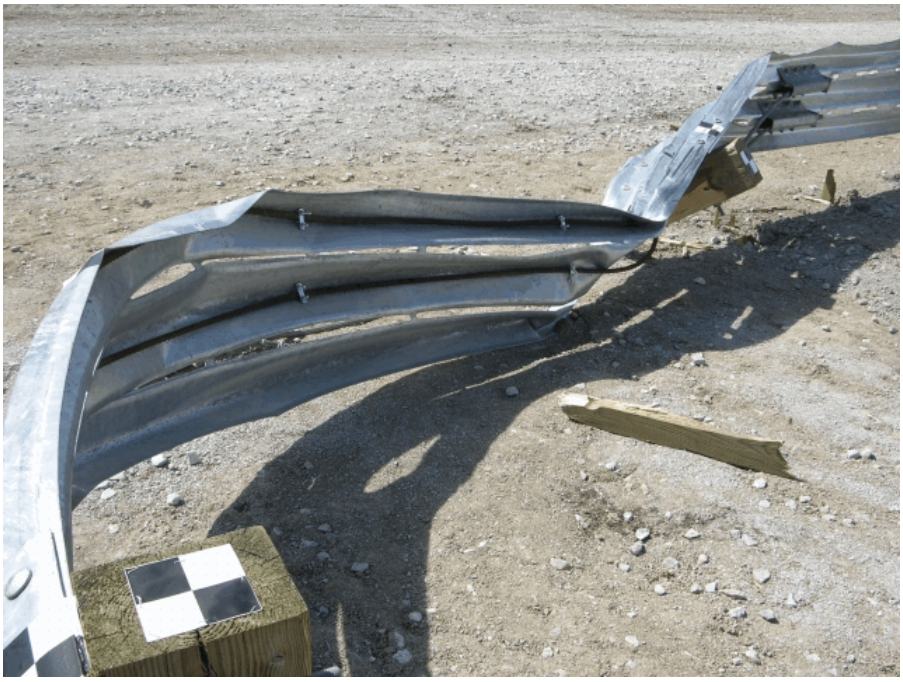

Figure 53. Damage to Nose Section, Test SR-5

Figure 54. Rail Damage Between Post Nos. 3P through 7P, Test SR-5

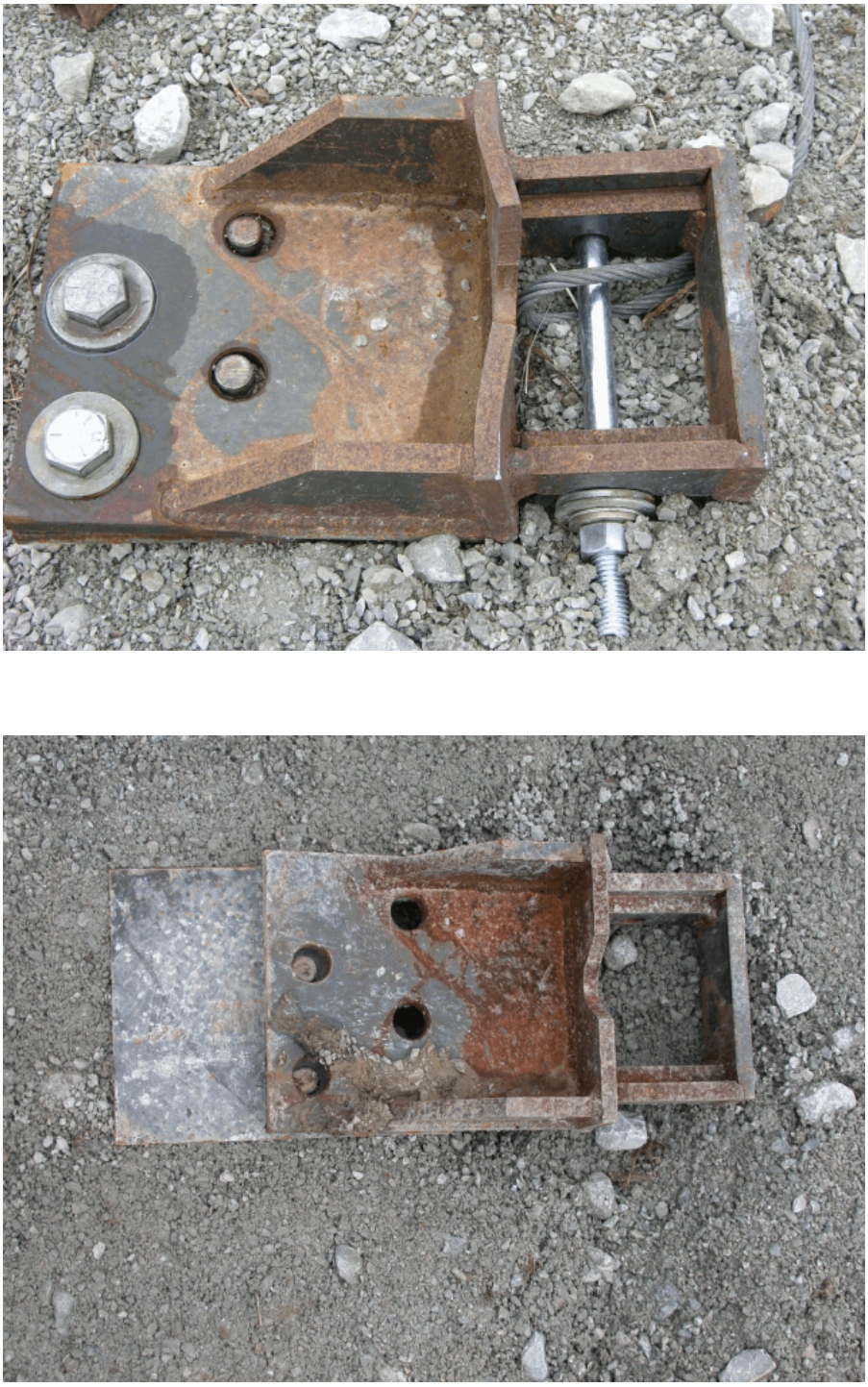

Figure 55. Cable Anchor Damage, Test SR-5

Figure 56. Nose Cable Damage, Test SR-5

Figure 57. Post No. 1S Damage, Test SR-5

Figure 58. Post Nos. 1P through 4P Damage, Test SR-5

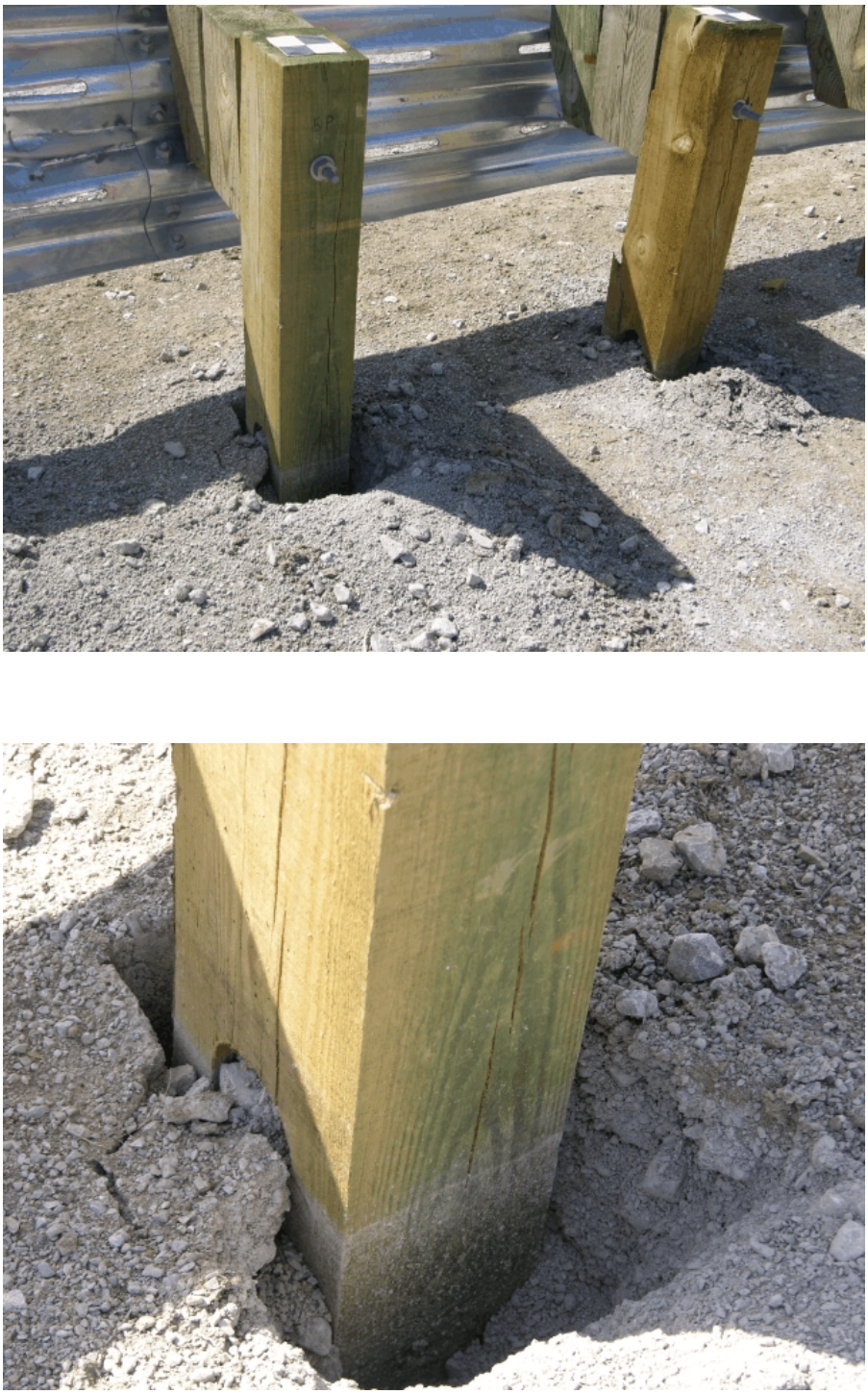

Figure 59. Post No. 5P Damage, Test SR-5

Figure 60. Post No. 6P Damage, Test SR-5

Figure 61. Soil Failure, Test SR-5

Figure 62. Vehicle Damage, Test SR-5

Figure 63. Vehicle Damage, Test SR-5

Figure 64. Vehicle Damage, Test SR-5

7 DISCUSSION AND COMPONENT TESTING

Following a review of the successful test results of SR-5, a Midwest States Pooled Fund Program member had concerns about the location of the cable release mechanism. Many felt that the location of the lever in front of the guardrail system would be a hindrance for mowing crews. Therefore, they requested that the system be redesigned in order to move the cable release mechanism behind the guardrail or eliminate it all together.

7.1 Design Modification

Due to the request by the states, modifications were made to the system to eliminate the cable release mechanism and implement a different method to develop the tensile strength of the thrie beam guardrail downstream from the nose section. In order to eliminate the cable release mechanism, the cable anchor assembly on the primary side was lengthened and oriented differently within the system. The cable came around the traffic face of the first post on the primary side and then terminated in the first post on the secondary side. Thus, the anchorage termination for the secondary side moved downstream one post. A cable bracket was located at the ground line of post no. 1 on the primary side which held the cable down and developed the necessary tensile strength. Based on previous tests, it was believed that post no. 1S would activate in a similar manner to the release mechanism used in test SR-5. The new cable anchor assembly would act to anchor the primary side for redirection impacts, while post no. 1S would always be expected to fracture in capture events.

7.2 Component Test

With the proposed modification to the mechanism used to develop the thrie beam guardrail's tensile strength downstream from the nose section, a bogie test on the modification was performed

to determine the amount of load the new design could withstand. The first post on both the primary and secondary sides was installed with the cable anchor bracket and cable attached as shown in Figure 65.

The 2,082-kg (4,589-lb) bogie, attached to the cable, was pulled away from the installed posts to determine the maximum load the system could withstand and the amount of deformation imparted to the cable anchor bracket at the bottom of the primary-side post. The bogie speed was 34.66 km/h (21.54 mph). The posts experienced moderate movement in the soil as shown in Figure 66. In addition, the cable anchor bracket did not experience any deformations. The maximum load was found to be approximately 35 kips as shown in the load curve in Figure 67. Previous experience and testing of guardrail cable anchorages has demonstrated that the loads found for the new SR anchorage were consistent with past guardrail anchorage loads in the 35 kip range. This suggested that the revised short-radius anchorage would be sufficient for redirective impacts on the primary side of the system. Test results are shown in Table 2.

Figure 65. Bogie Test Setup, Test No. SRA-1

Figure 66. Bogie Test Results, Test No. SRA-1

Table 2. Bogie Test Summary, Test SRA-1

Bogie Test Summary				
Test Information	Purpose			
	Load Test of Redesigned Cable Anchor System with Cable Placed Between 2 BCT Posts			
Post Details	BCT Posts in Galvanized Foundation Tube			
	Posts: 140mmx191mmx1178mm (5.5"x7.5"x46")		Foundation Tube: 152mmx203mmx2388mm (6"x8"x96")	
Test Results	Weight	Speed	Max Load	Result
	2082 kg (4589 lb)	34.67 kph (21.54 mph)		Posts moved in soil; shackle displaced

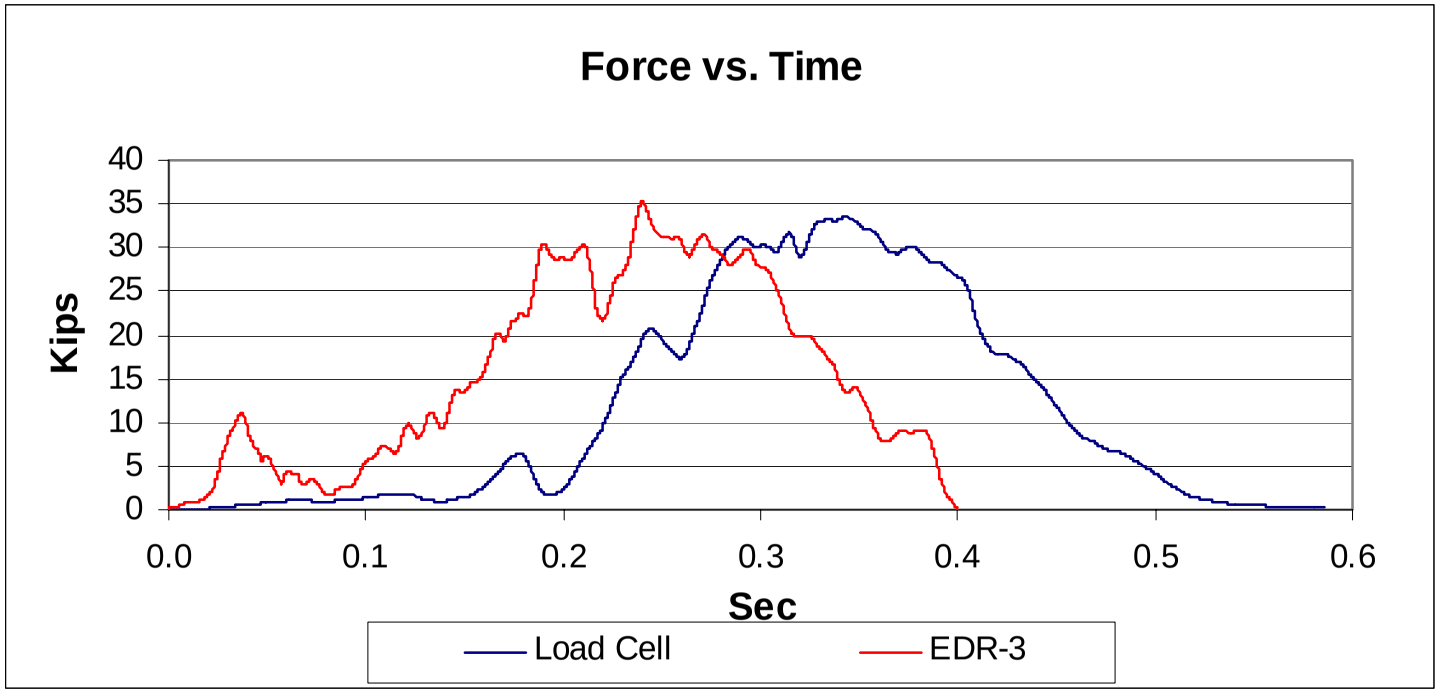

Figure 67. Load Cell Data, Test SRA-1

8 SHORT-RADIUS DESIGN MODIFICATIONS

The modified short-radius guardrail system was identical to the previous system except for the method used to develop the tensile strength of the thrie beam guardrail downstream from the nose section. The cable anchor assembly on the primary side was lengthened and oriented differently within the system thereby removing the cable release mechanism from the traffic side of the system. The cable came around the traffic face of the first post on the primary side and then terminated in the first post on the secondary side, as shown in Figures 68 through 72. The existing anchorage on the secondary side was located at post no. 2S. This change shifted the location of the anchorage one post downstream on the secondary side. A cable bracket was located at the ground line of post no. 1 on the primary side which held the cable down and developed the necessary tensile strength, as shown in Figures 71 and 74. Photographs of the modified system are shown in Figures 76 and 77.

Because component testing of the new anchorage had demonstrated its capacity to develop appropriate tensile loads for redirection purposes, the next test, test SR-6, was conducted according to NCHRP test designation 3-30. This test would test the ability of the redesigned short-radius system to capture an impacting vehicle as well as to evaluate the performance of the new anchorage release with the 820C vehicle.

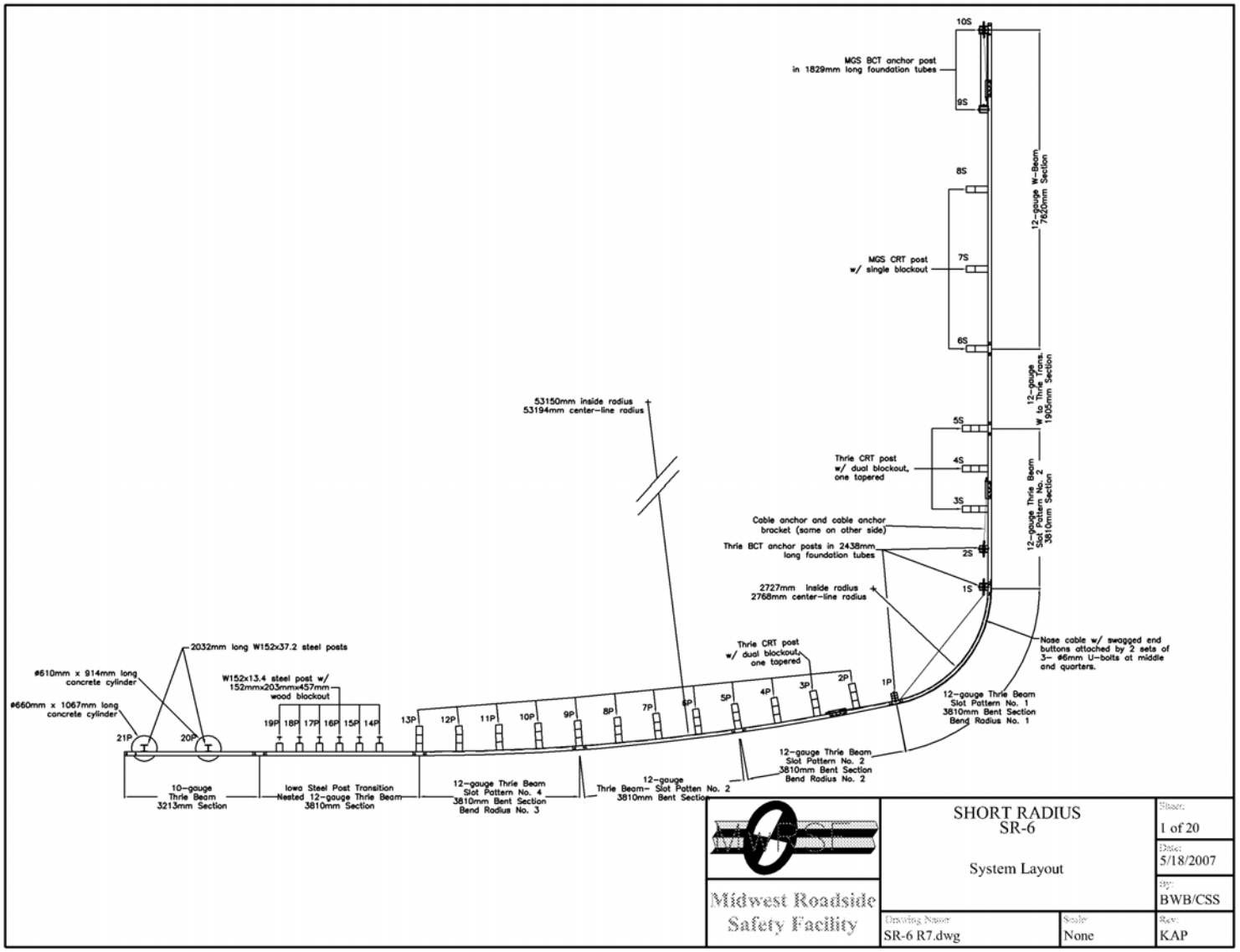

Figure 68. System Details, Test SR-6

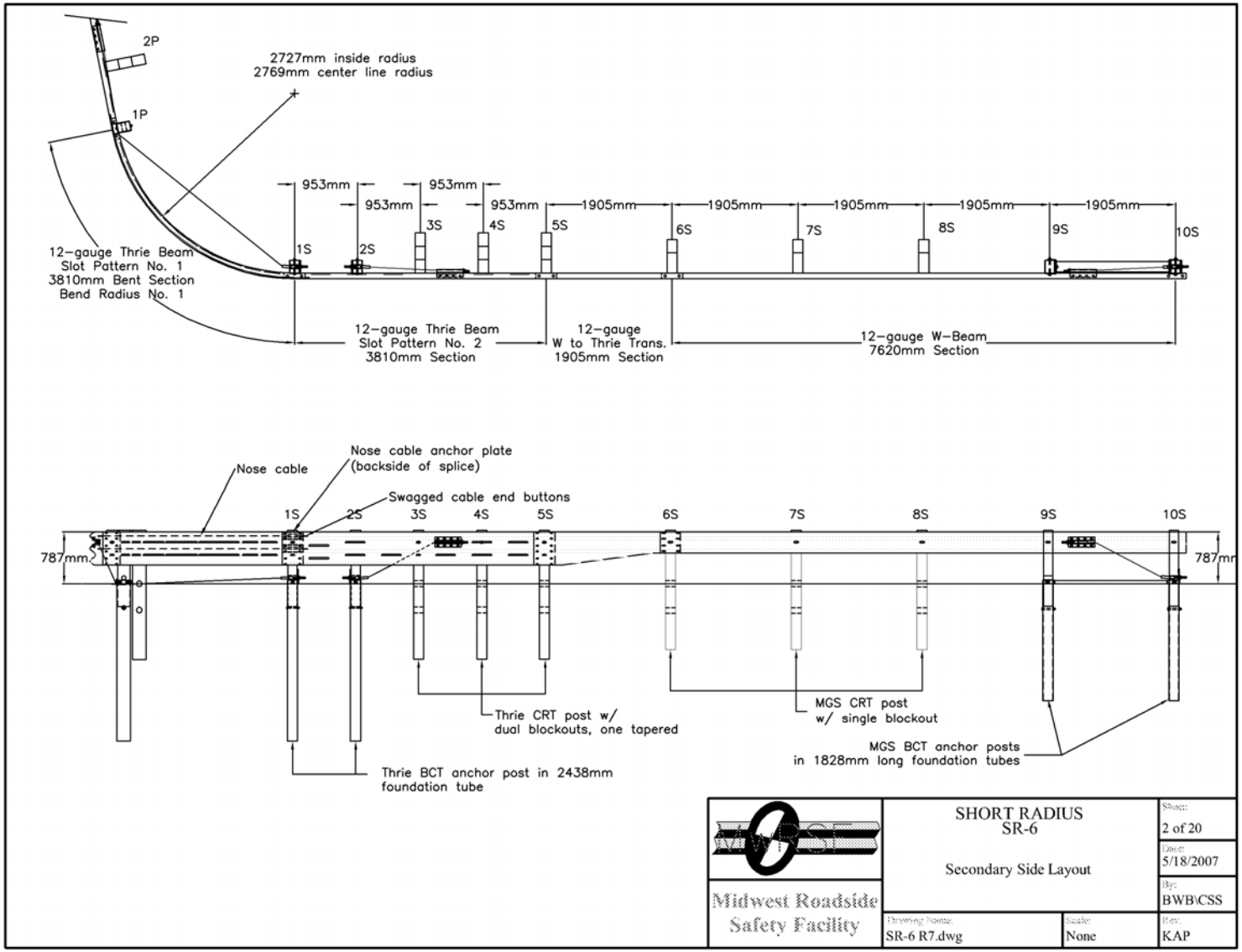

Figure 69. Secondary Side Details, Test SR-6

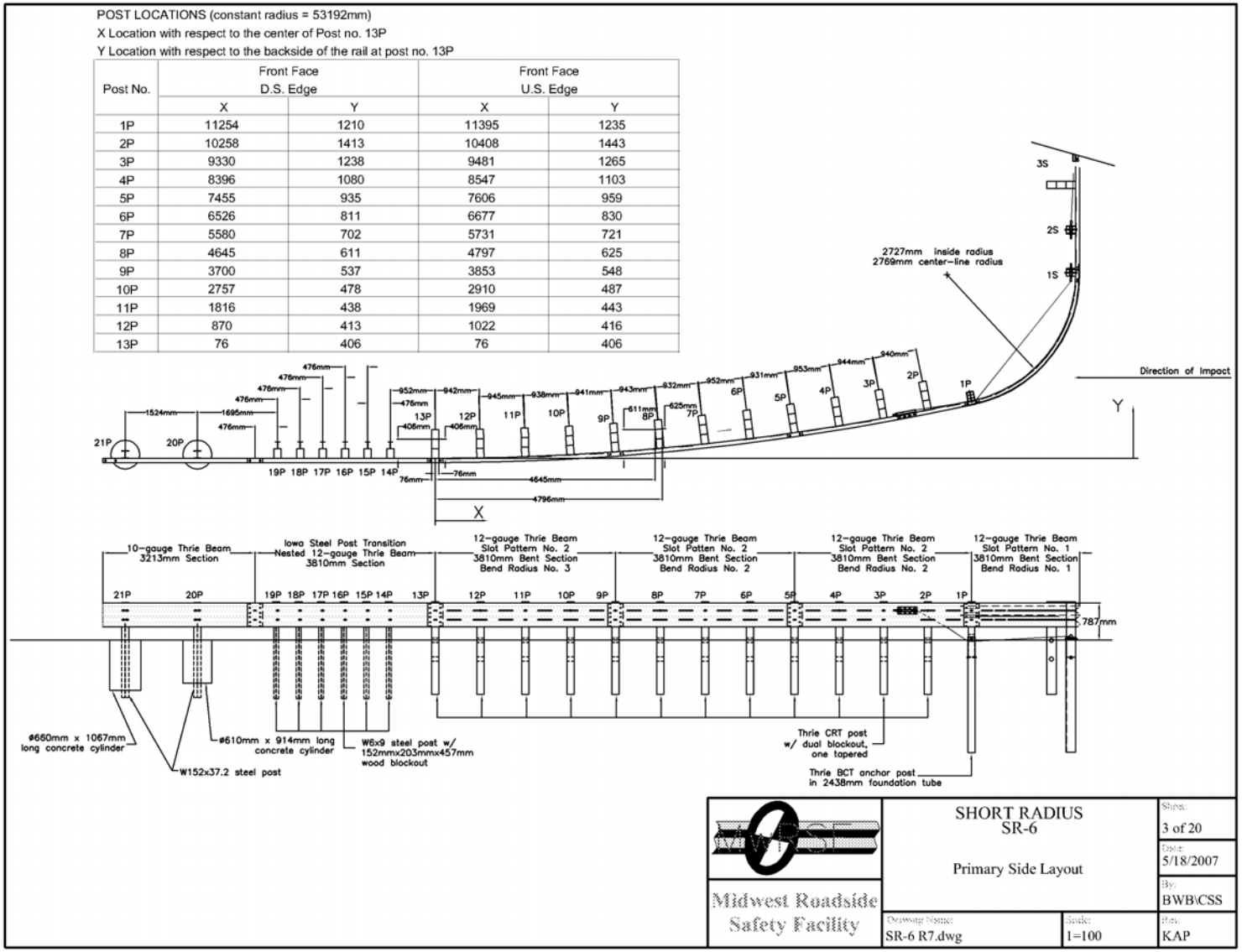

Figure 70. Primary Side Details, Test SR-6

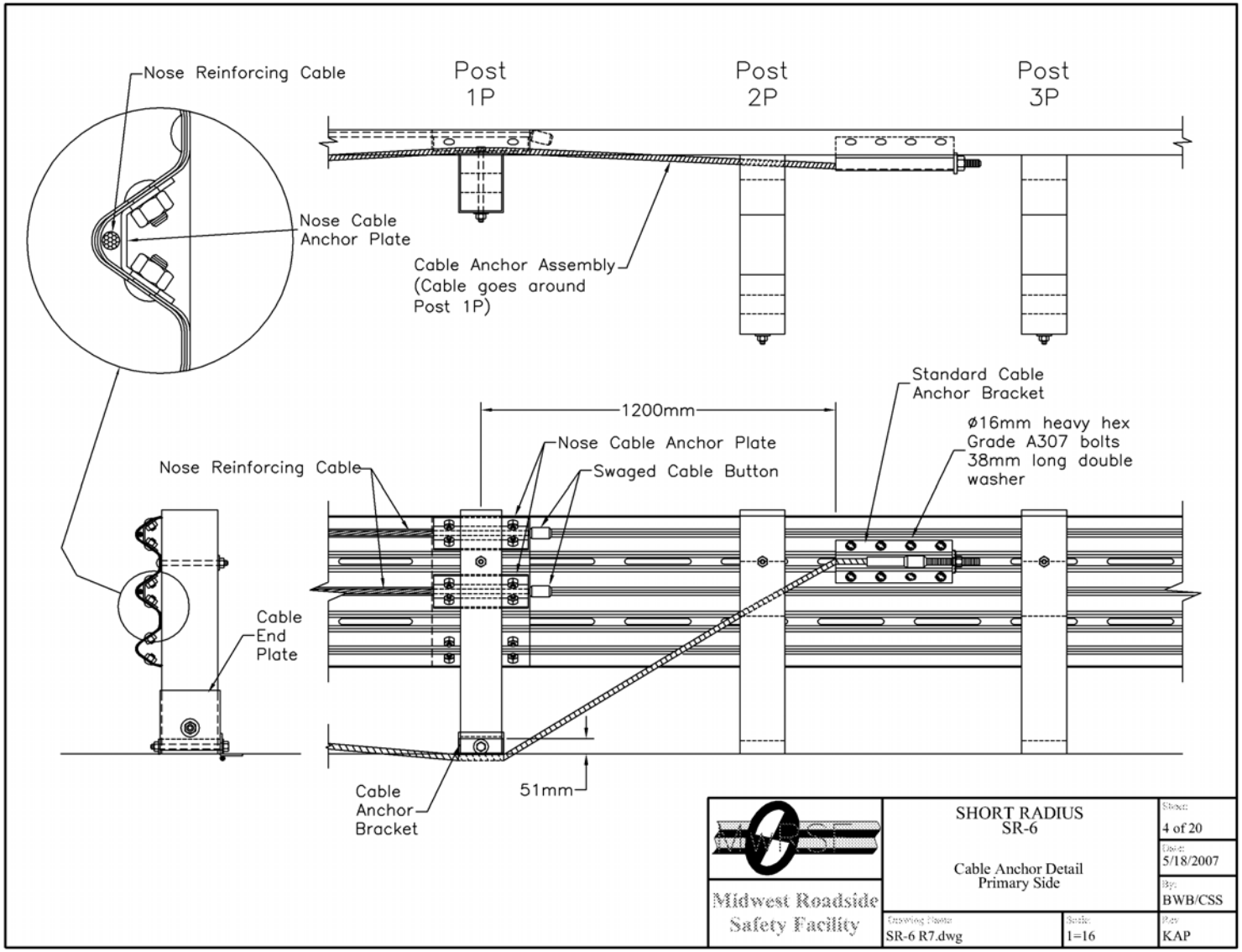

Figure 71. Primary Side Cable Anchor Detail, Test SR-6

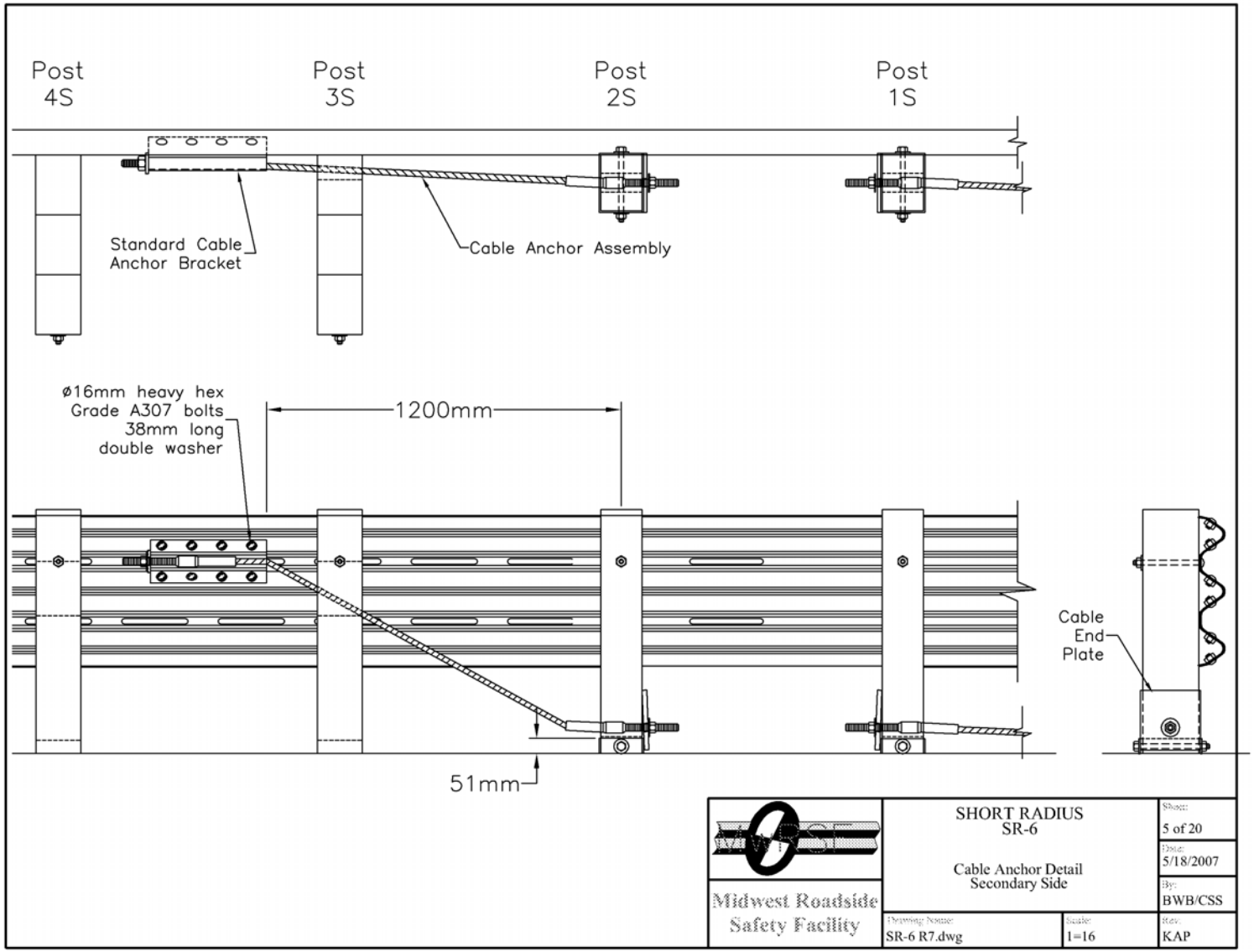

Figure 72. Secondary Side Cable Anchor Details, Test SR-6

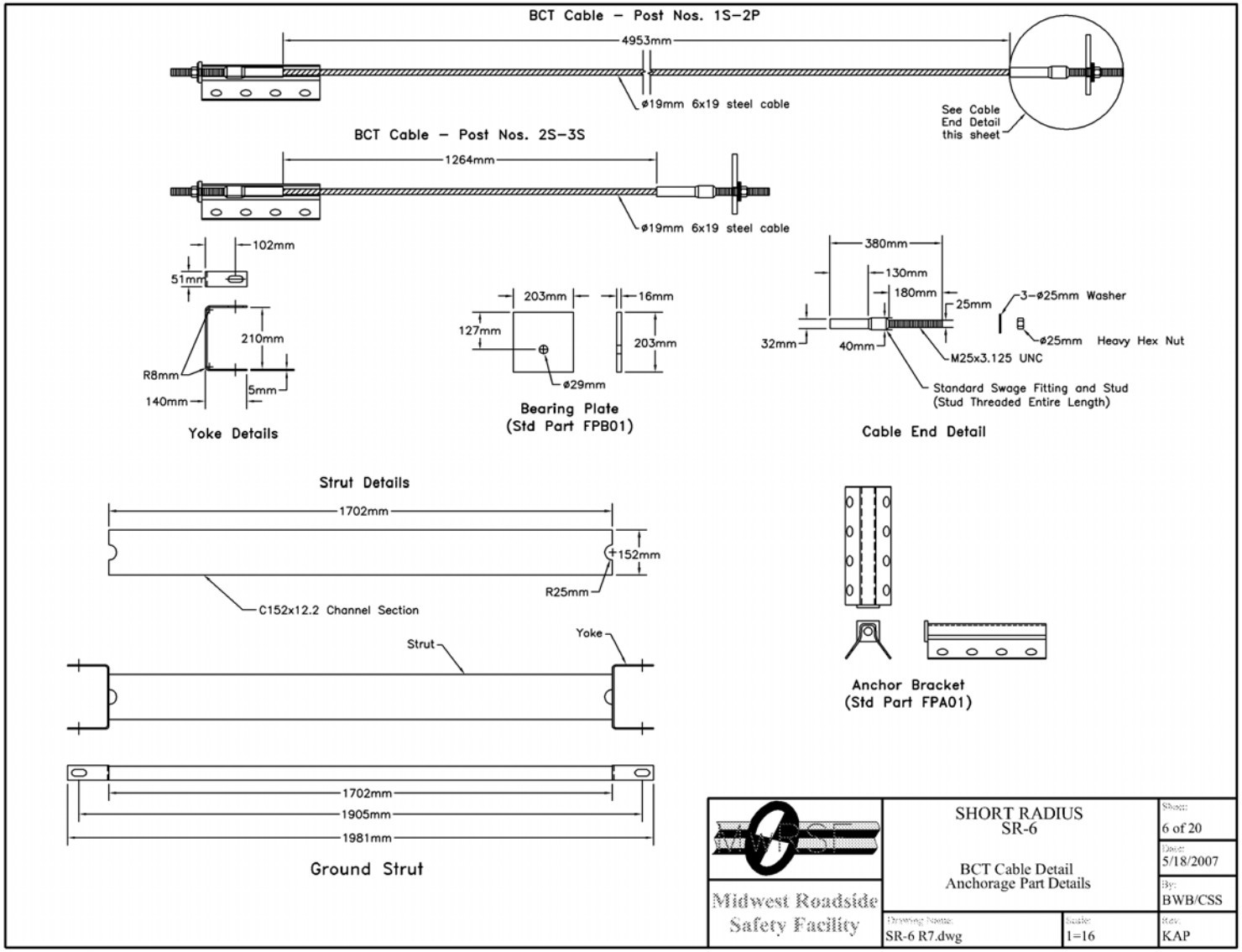

Figure 73. BCT Cable and Anchorage Part Details, Test SR-6

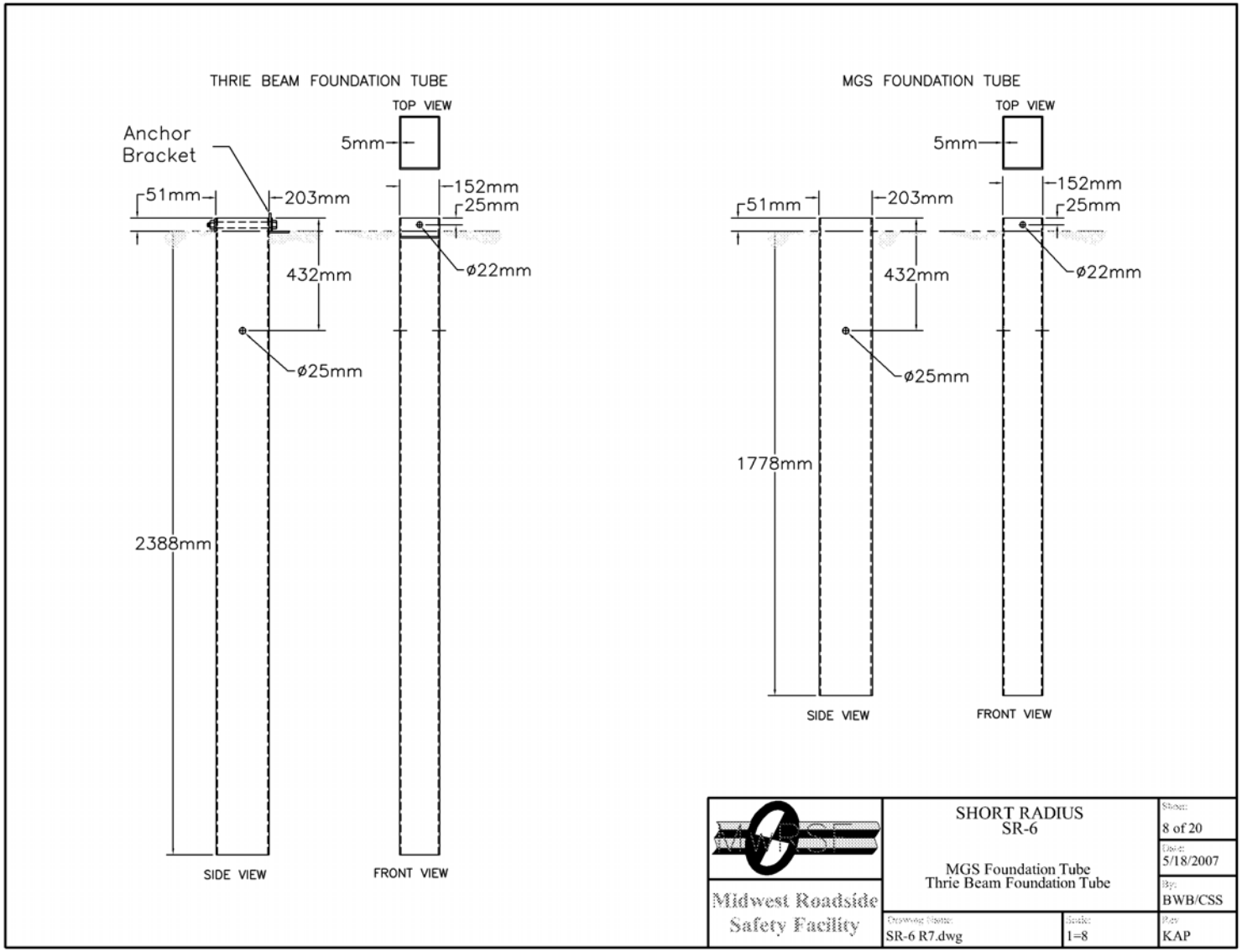

Figure 74. MGS and Thrie Beam Foundation Tubes, Test SR-6

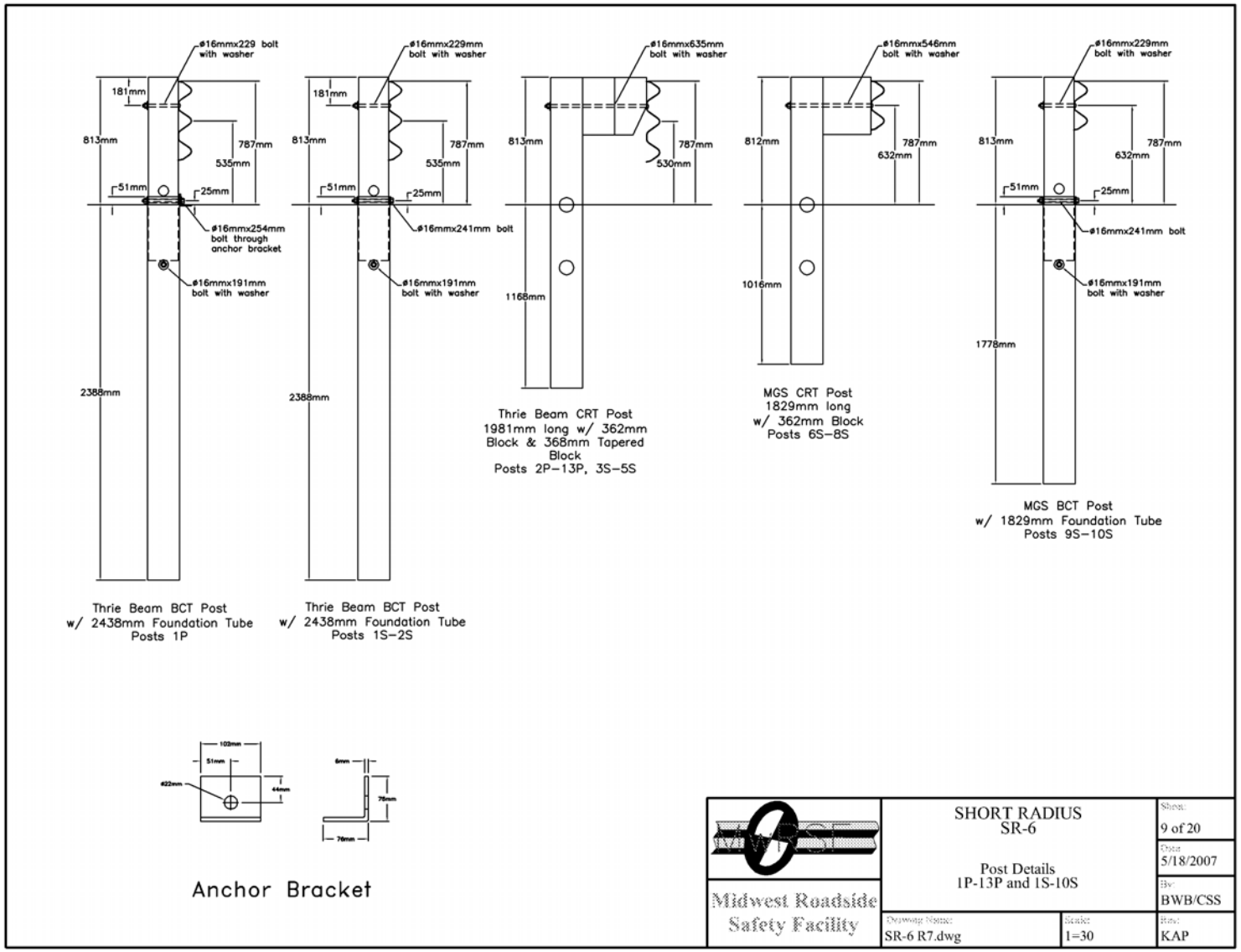

Figure 75. Post Details, Test SR-6

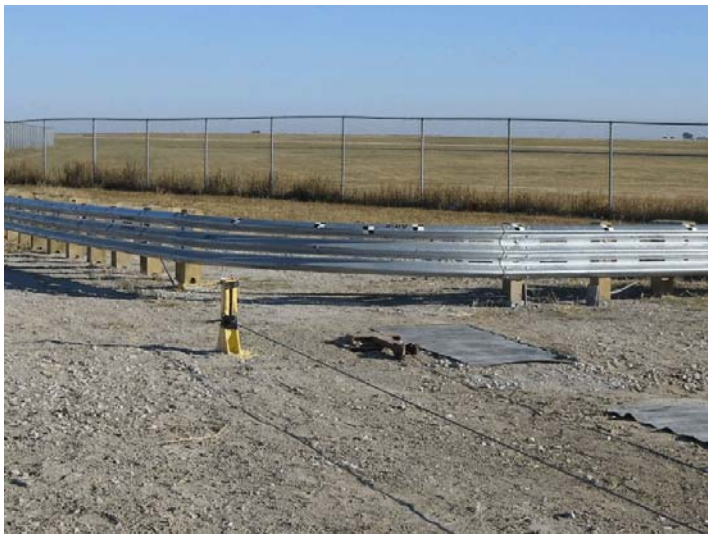

Figure 76. System Modifications, Test SR-2

Figure 77. System Modifications, Test SR-6

9 CRASH TEST NO. SR-6

9.1 Test SR-6

Test SR-6 was conducted according to NCHRP Report No. 350 Test Designation 3-30. The 893-kg (1,969 lb) small car impacted the short-radius guardrail at a speed of 99.4 km/h (61.8 mph) and at an angle of 0.8 degrees. The impact location for this test aligned the right-front quarter point of the small car with the centerline of the curved nose section. A summary of the test results and the sequential photographs are shown in Figure 78. Additional sequential photographs are shown in Figures 80 through 83. Documentary photographs of the crash test are shown in Figures 84 through 85.

9.2 Test Description

The test vehicle impacted the curved nose section of the short-radius guardrail system, as shown in Figure 86. Upon impact, the right-front corner of the small car deformed as well as the curved nose section. At 0.022 sec, a buckle point formed at the quarter point on the secondary side of the curved nose section. At 0.032 sec, the curved nose section buckled near its midpoint, and the front of the hood was pushed up. At this same time, post no. 1S bent back in the sleeve. At 0.044 sec, the right-front corner of the hood deformed inward. As the vehicle continued downstream, a tear propagated through one of the slot tabs of the nose section, and the rail continued to crush and flatten. At 0.052 sec, buckle points occurred at both quarter points of the first section of rail on the primary side and at post nos. 1P and 3P. At 0.070 sec, the hood deformed, and a crease formed near the middle of the hood. At this same time, buckle points formed at post nos. 1S and 1P. At 0.082 sec, post no. 1P fractured at ground level and rotated downstream. At 0.104 sec, post no. 1S fractured at ground level, and the primary side cable anchor was released. At 0.124 sec, the front bumper of

the small car impacted post no. 2P which bent downstream and twisted away from the rail. At 0.146 sec, post no. 2P fractured completely, and the thrie beam rail had spread across the entire front end of the small car. At 0.160 sec, the hood of the car bent completely in half. At this same time, the rail disengaged from post nos. 3P and 4P. Also at this same time, the small car yawed clockwise, and the vehicle began to be captured in the system. At approximately 0.180 sec, the thrie beam rail was pushed up and over the front face of the vehicle as the small car continued into the short-radius system. The capture of the system was reduced to the interlocking of the thrie beam with the hood and "A" pillars of the small car. At 0.196 sec, the blockout at post no. 2P fractured and disengaged from the system. At 0.236 sec, the front of the car continued to crush and yaw. At 0.288 sec, post no. 3P fractured and disengaged from the system. At 0.314 sec, the blockout at post no. 3P contacted post no. 4P, and additional rail kinks and buckle points formed. At 0.436 sec, the car's hood contacted the windshield. At 0.510 sec, all rail deformation ceased, and the car continued to travel under the rail. At 0.546 sec, major windshield cracking occurred. At 0.678 sec, the hood collapsed onto the windshield. At this same time, the car came to a stop due to resistance by the rail. At 0.770 sec, the small car came to rest 4.51 m (14 ft - 10 in.) downstream from impact and 1.47 m (4 ft - 10 in.) right from the impact point, as shown in Figure 79. The trajectory and final position of the small car are shown in Figure 87.

9.3 System and Component Damage

Damage to the short-radius system was moderate, as shown in Figures 88 through 92. Post nos. 1P and 1S fractured at the foundation tube. Post no. 1P disengaged from the rest of the system and post no. 1S remained attached to the rail. Post no. 2P fractured at ground level and disengaged from the rest of the system. Post nos. 3P and 4P also fractured at ground level and disengaged from

the rest of the system. Post no. 5P twisted downstream and encountered a small crack at ground level. The blockout at post no. 5P disengaged from the rail, but remained attached to the post.

Contact marks were found between the center of the nose section and post no. 3P. The rail was flattened and deformed between post nos.1S and 3P. Rail buckling was found along the curved nose section. Additional rail buckling was found at post nos. 1P through 5P and between post nos. 5P and 8P. The post bolt released from the rail at post nos. 6P through 8P. The lower corrugation encountered a 178-mm (7-in.) long tear 2,134 mm (3 ft) downstream from the impact point. Another 178-mm (7-in) long tear occurred on the middle corrugation of the nose section between the primary-side quarter point and the center of the rail. All rail slots were bent and deformed on the primary side. Minor post bolt slot deformation occurred at post nos. 3P through 7P. The galvanization was removed the nose section.

Damage to the cable anchorage systems was minimal, as shown in Figure 90. The cable bracket at post no. 1P was bent and released the cable. The cable end plates at post nos. 1S and 2S remained attached to the posts. Both nose cables were stretched and the primary side ends disengaged from the rail.

9.4 Vehicle Damage

Exterior vehicle damage was extensive, as shown in Figures 93 through 96. Occupant compartment deformations were negligible, as shown in Figure 96. Complete occupant compartment deformations and the corresponding locations are provided in Appendix G.

The left-front and right-front quarter panels were severely crushed and deformed inward toward the wheel wells and encountered tearing of the sheet metal. The front bumper was also deformed and torn and disengaged from the vehicle due to fractured front bumper mounts. The hood

was folded in half and pushed back into the windshield. Contact marks were found on the right-front wheel rim and hubcap. The front frame was dented and crushed inward. The undercarriage sustained scratches and dents. The radiator and coolant valves and cases were crushed and dented. The radiator fan and belts were disengaged and broken. The engine block was displaced backwards and to the left. The windshield was crushed and sustained extensive "spider-web" cracking throughout. Deformation of the windshield exceeded 76 mm (3 in.) near the center of the glass on the left side. In addition, there were two small holes in the center of the windshield where the hood penetrated the glass. The right-rear and left-rear sides, the rear, and all other window glass remained undamaged.

9.5 Occupant Risk Values

The longitudinal and lateral occupant impact velocities were determined to be -9.40 m/s (-30.85 ft/s) and 0.13 m/s (0.41 ft/s), respectively. The maximum 0.010-sec average occupant compartment ridedown decelerations in the longitudinal and lateral directions were -20.73 Gs and 12.05 Gs, respectively. It should be noted that the occupant impact velocities (OIVs) and the lateral occupant ridedown decelerations (ORDs) were within the suggested limits provided in NCHRP Report No. 350. However, the longitudinal occupant ridedown decelerations were above the maximum limits provided in NCHRP Report No. 350. The THIV and PHD values were determined to be 9.44 m/s (30.97 ft/s) and 23.97 Gs, respectively. The results of the occupant risk data, as determined from the accelerometer data, are summarized in Figure 78. Results are shown graphically in Appendix H. The results from the rate transducer are shown graphically in Appendix H.

9.6 Discussion

The analysis of the test results for test SR-6 showed that the short-radius guardrail system

impacted with the 820C vehicle adequately contained the vehicle and brought the vehicle to a stop. Detached elements and fragments did not penetrate nor presented undue hazard to other traffic but showed potential for penetrating the occupant compartment. Deformations of, or intrusion into, the occupant compartment that could have caused serious injury did occur due to the penetration of the hood through the windshield which was crushed inward greater than 76 mm (3 in.). The test vehicle remained upright during and after the collision. Vehicle roll, pitch, and yaw angular displacements were noted, but they were determined acceptable because they did not adversely influence occupant risk safety criteria nor cause rollover. After collision, the vehicle's trajectory did not intrude into adjacent traffic lanes. The longitudinal occupant ridedown decelerations were not within the maximum limits provided in NCHRP Report No. 350. Therefore, test no. SR-6 conducted on the short-radius guardrail system was determined to be unacceptable according to the TL-3 safety performance criteria found in NCHRP Report No. 350 due to the excessive longitudinal occupant ridedown deceleration and excessive windshield crush and penetration.

0.000 sec 0.079 sec 0.172 sec 0.313 sec 0.404 sec

- Test Number SR-6
- Date 10/7/2005
- Test Article
  - Type . . . . . Short-Radius Guardrail
  - Key Elements . . . . . Four 3,810-mm long curved and slotted thrie beam guardrail sections (parabolic flare)
One 3,810-mm long straight thrie beam guardrail section
813 mm top rail height
18 breakaway posts
Iowa steel post transition
Simulated tangent W-beam guardrail end terminal
Cable anchor for primary side tension development
  - Orientation . . . . . Right quarter-point vehicle with centerline nose
- Soil Type . . . . . Grading B - AASHTO M 147-65 (1990)
- Vehicle Model . . . . . 1996 Geo Metro
  - Curb . . . . . 775 kg
  - Test Inertial . . . . . 818 kg
  - Gross Static . . . . . 893 kg
- Vehicle Speed
  - Impact . . . . . 99.4 km/h
  - Exit . . . . . NA (Did not exit)
- Vehicle Angle
  - Impact . . . . . 0.8 deg
  - Exit . . . . . NA (Did not exit)
- Vehicle Stability . . . . . Satisfactory
- Occupant Ridedown Deceleration (10 msec avg.)
  - Longitudinal . . . . . -20.73 Gs > 20Gs
  - Lateral . . . . . 12.05 Gs < 20 Gs
- Occupant Impact Velocity
  - Longitudinal . . . . . -9.40 m/s < 12 m/s
  - Lateral . . . . . 0.13 m/s < 12 m/s
- THIV (not required) . . . . . 9.44 m/s
- PHD (not required) . . . . . 23.97 Gs
- Vehicle Damage . . . . . Extensive
  - TAD[20] 12-FD-6
  - SAE[21] 12-FDAW6
- Vehicle Stopping Distance 4.51 m downstream
1.47 m right
- Test Article Damage . . . . . Moderate
- Test Article Deflections
  - Permanent Set . . . . . 2,325 mm
  - Dynamic . . . . . 2,522 mm
  - Working Width . . . . . 6.5 m downstream of secondary side
4.0 m right of primary side

Figure 78. Summary of Test Results and Sequential Photographs, Test SR-6

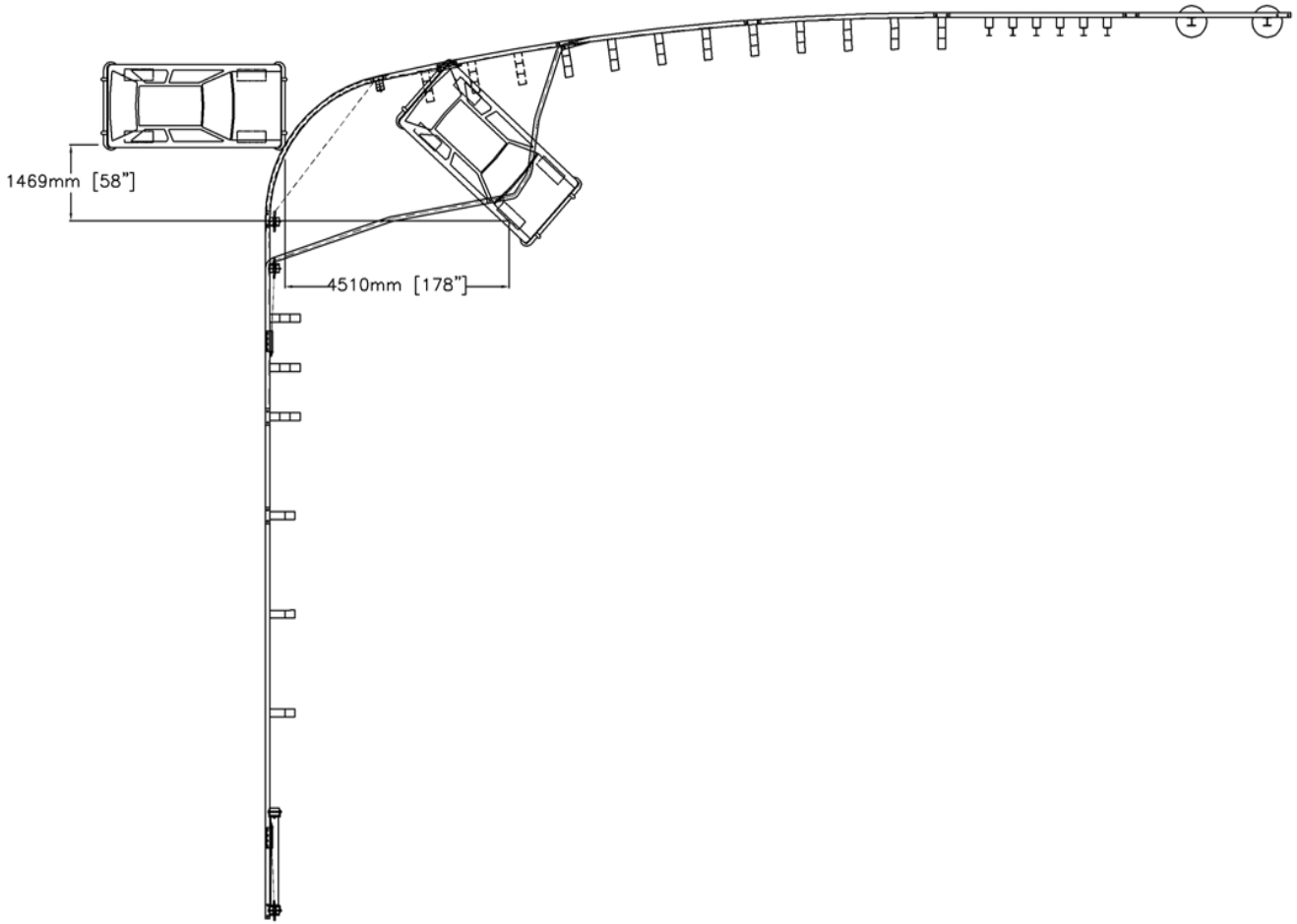

Figure 79. Vehicle Trajectory and Final Position, Test SR-6

0.000 sec

0.376 sec

0.058 sec

0.450 sec

0.120 sec

0.528 sec

0.184 sec

0.596 sec

0.254 sec

0.696 sec

0.316 sec

Figure 80. Additional Sequential Photographs, Test SR-6

0.000 sec

0.370 sec

0.052 sec

0.442 sec

0.100 sec

0.552 sec

0.160 sec

0.624 sec

0.224 sec

0.826 sec

0.286 sec

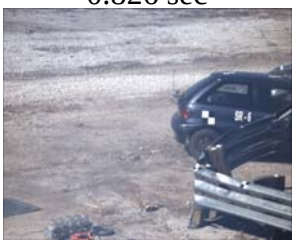
1.122 sec

Figure 81. Additional Sequential Photographs, Test SR-6

0.000 sec

0.000 sec

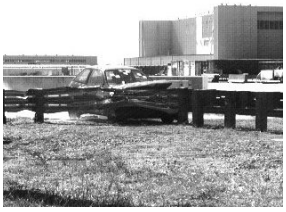

0.052 sec

0.067 sec

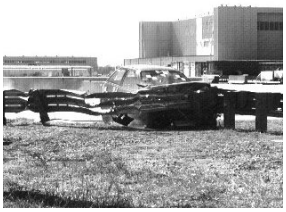

0.140 sec

0.167 sec

0.228 sec

0.234 sec

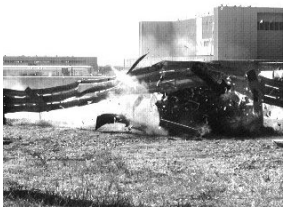

0.356 sec

0.300 sec

0.478 sec

0.367 sec

Figure 82. Additional Sequential Photographs, Test SR-6

0.000 sec

0.000 sec

0.133 sec

0.067 sec

0.200 sec

0.167 sec

0.234 sec

0.234 sec

0.367 sec

0.334 sec

0.434 sec

0.501 sec

Figure 83. Additional Sequential Photographs, Test SR-6

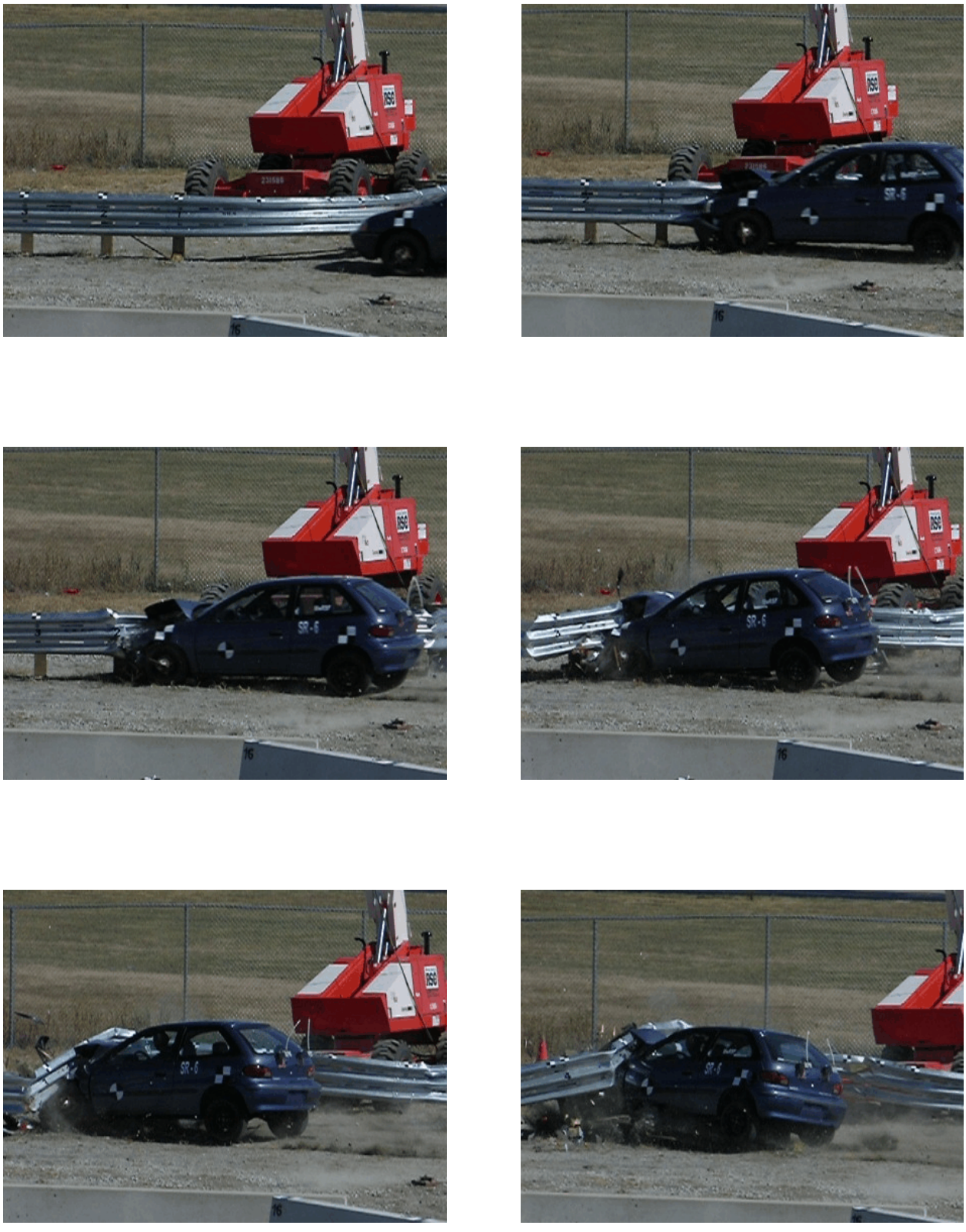

Figure 84. Documentary Photographs, Test SR-6

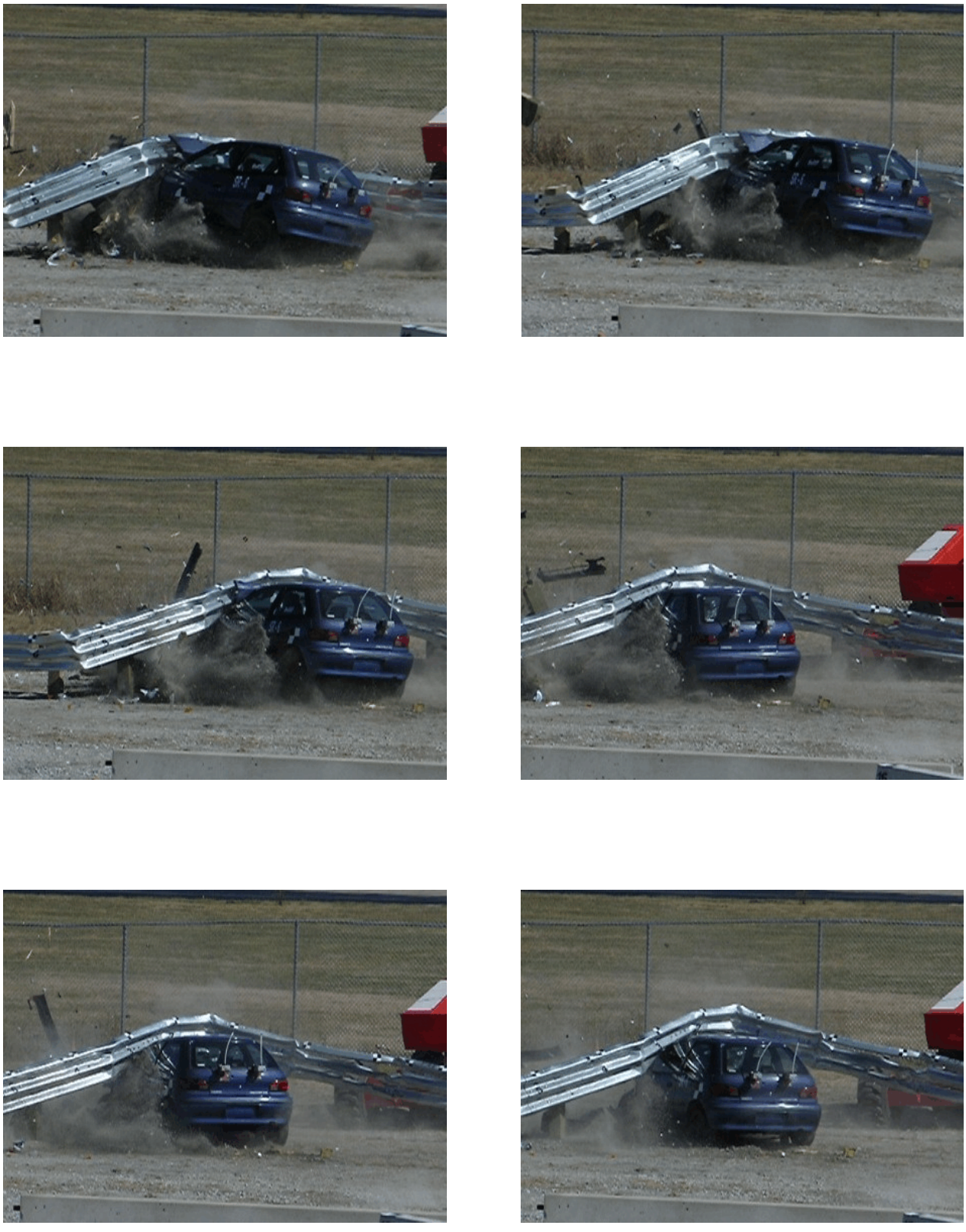

Figure 85. Documentary Photographs, Test SR-6

Figure 86. Impact Location, Test SR-6

Figure 87. Vehicle Trajectory and Final Position, Test SR-6

Figure 88. System Damage, Test SR-6

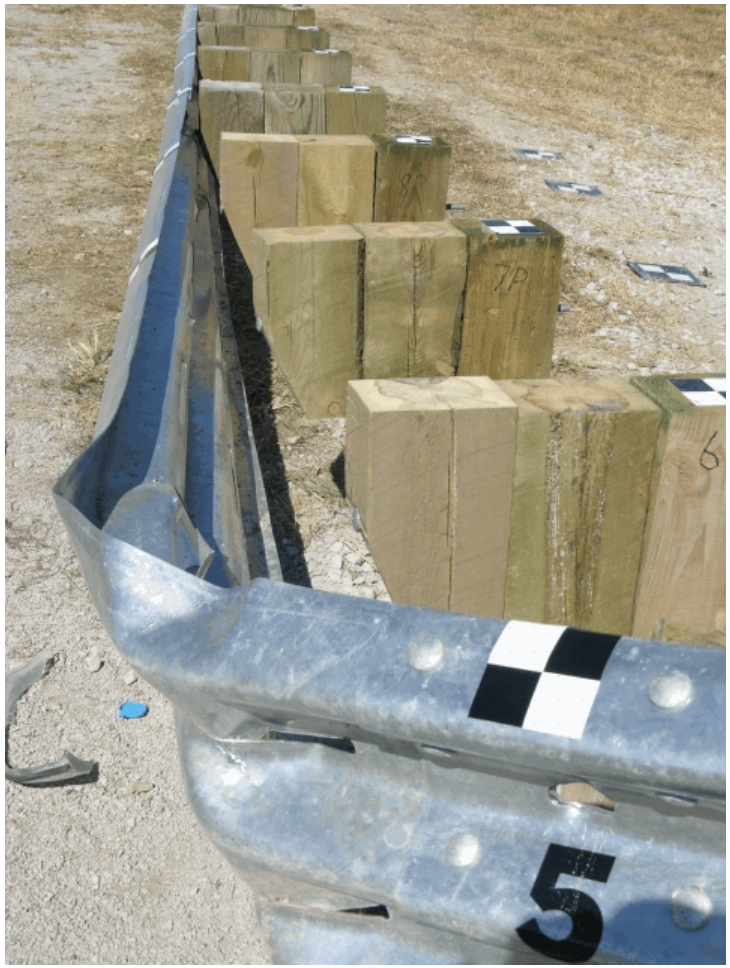

Figure 89. System Damage, Test SR-6

Figure 90. Post Nos. 1S Through 3S Damage, Test SR-6

Figure 91. Post Nos. 1P through 6P Damage, Test SR-6

Figure 92. Post Nos. 6P through 8P Damage, Test SR-6

Figure 93. Vehicle Damage, Test SR-6

Figure 94. Vehicle Damage, Test SR-6

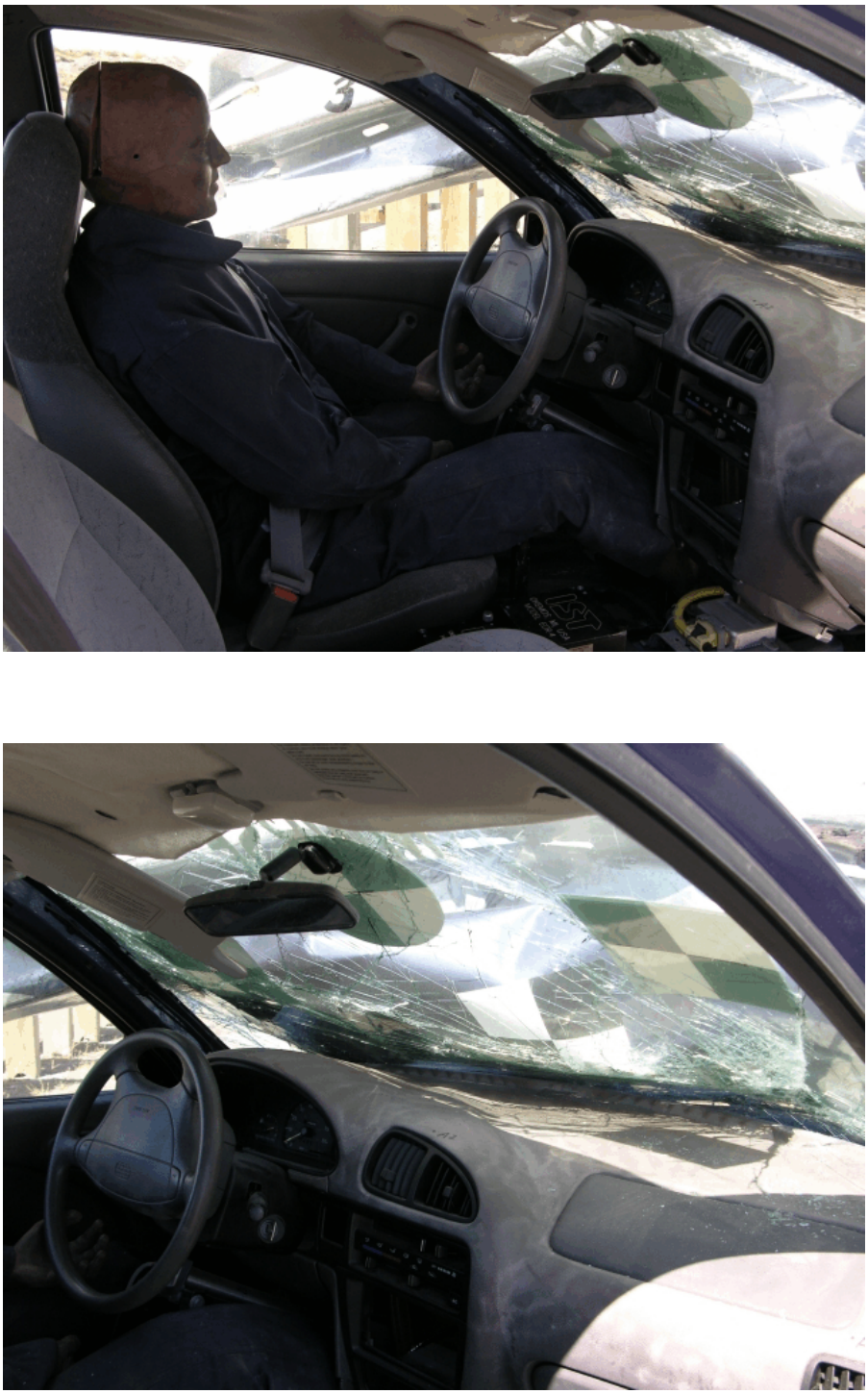

Figure 95. Windshield Damage, Test SR-6

Figure 96. Occupant Compartment Damage, Test SR-6

10 SUMMARY AND CONCLUSIONS

The Phase III development of a TL-3 short-radius guardrail system for intersecting roadways began with the construction of a barrier system consisting of a curved and slotted thrie beam nose section, two adjacent curved, slotted thrie beam sections, and breakaway CRT posts. One side of the system attached to a TL-3 steel post approach guardrail transition while the other side attached to a TL-2 guardrail end terminal. A schematic of the impact conditions for test nos. SR-5 and SR-6 is shown in Figure 97. A summary of the safety performance evaluation is provided in Table 3.

Test SR-5 was conducted according to a modified version of NCHRP Report No. 350 Test Designation 3-31. The short-radius system was modified prior to test SR-5 to include a primary side anchor to retain tension in the system. Due to the parabolic flare, the impact location for this test aligned the centerline of the pickup truck with the back face of post no. 13P. In this test, a 2,001-kg (4,411-lb) pickup truck impacted the short-radius guardrail system at a speed of 101.8 km/h (63.2 mph) and at an angle of 0.9 degrees. The results of test SR-5 were deemed acceptable according to NCHRP Report No. 350 criteria.

Due to maintenance concerns by the Pooled Fund states, design modifications were made to remove the cable release mechanism from the traffic side of the system for the primary side anchorage. The cable anchor assembly on the primary side was lengthened and oriented differently within the system thereby removing the cable release mechanism from the traffic side of the system. The cable traversed around the traffic face of the first post on the primary side and then terminated in the first post on the secondary side. A cable bracket was located at the ground line of post no. 1 on the primary side to hold the cable down. Component testing of the new anchorage demonstrated that it developed appropriate tensile loads. In order to evaluate the new anchorage, the subsequent

test was chosen as a small car impact at the nose of the short-radius system.

Test SR-6 was conducted according to NCHRP Report No. 350 Test Designation 3-30. The impact location for this test aligned the right-front quarter pont of the small car with the centerline of the nose of the short-radius system. In this test, an 893-kg (1969-lb) small car impacted the short-radius guardrail system at a speed of 99.4 km/h (61.8 mph) and at an angle of 0.8 degrees. During this test, the thrie beam guardrail partially captured the small car, and caused rapid deceleration which resulted in excessive occupant ridedown decelerations. In addition, the hood penetrated and caused the windshield to intrude into the occupant compartment. Therefore, based on these results, test SR-6 was deemed unacceptable according to NCHRP Report No. 350 criteria.

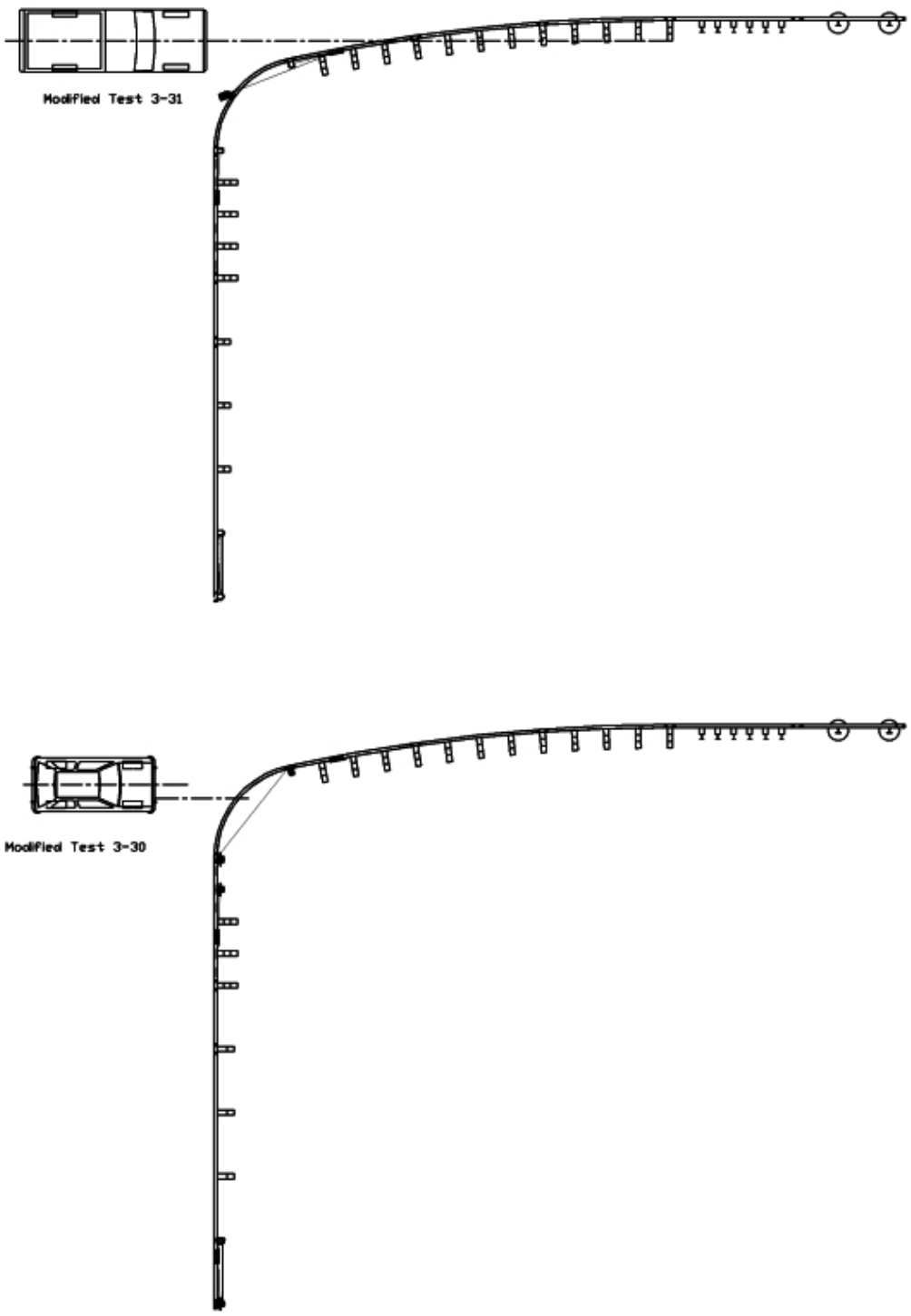

Figure 97. Summary of Short-Radius Guardrail Impacts

Table 3. Summary of Safety Performance Evaluation Results

Evaluation Factors	Evaluation Criteria	Test SR-5	Test SR-6
Structural Adequacy	A	NA	NA
	C	S	S
Occupant Risk	D	S	U
	F	S	S
	H	S	S
	I	S	U
Vehicle Trajectory	K	S	S
	L	NA	NA
	M	NA	NA
	N	S	S
NCHRP Report No. 350 Test Level		TL-3	TL-3
NCHRP No. 350 Test Designation		3-31	3-30
Pass/Marginal/Fail		PASS	FAIL

S - Satisfactory
M - Marginal
U - Unsatisfactory
NA - Not Applicable

11 FUTURE DEVELOPMENT

The development of a TL-3 short-radius guardrail system for intersecting roadways has proven through numerous crash tests and various impact conditions to be extremely difficult. The modified short-radius concept has displayed tremendous improvement and very promising results over the previous designs.

However, due to the rapidly changing vehicle fleet over the course of the last decade, a revision to NCHRP Report No. 350 is in progress. Test vehicles with increased weight and raised centers of gravity are being recommended for the revised criteria. Thus, it was proposed that the development of the short-radius system proceed according to the Update to NCHRP 350, including using the new vehicle types. Following a successful testing program with the proposed vehicles, there would not be any need to retest this system under the revised guidelines once they are implemented, and the short-radius system would be better suited to the needs of the current vehicle fleet.

12 REFERENCES

1. Ross, H. E. Jr., D. L. Sicking, R. A. Zimmer, and J. D. Michie, *Recommended Procedures for the Evaluation of Highway Features*, NCHRP Report No. 350, Transportation Research Board, Washington, D. C., 1993.

2. Michie, Jarvis D., *Recommended Procedures for the Safety Performance Evaluation of Highway Appurtenances*, NCHRP Report No. 230, Transportation Research Board, Washington, D.C., March 1981.

3. Bielenberg, R.W., Reid, J.D., Faller, R.K., Rohde, J.R., Sicking, D.L., Keller, E.A., Holloway, J.C., *Concept Development of a Short-Radius Guardrail System for Intersecting Roadways*, Final Report to the Midwest States' Regional Pooled Fund Program, Transportation Research Report No. TRP-03-100-00, Project No. SPR-3(017)-Year 8, Midwest Roadside Safety Facility, University of Nebraska-Lincoln, September 12, 2000.

4. Bielenberg, R.W., Faller, R.K., Holloway, J.C., Reid, J.D., Rohde, J.R., and Sicking, D.L., *Phase II Development of a Short-Radius Guardrail System for Intersecting Roadways*, Final Report to the Midwest States' Regional Pooled Fund Program, Transportation Research Report No. TRP-03-137-03, Project No. SPR-3(017)-Year 11, Midwest Roadside Safety Facility, University of Nebraska-Lincoln, September 9, 2003.

5. Hinch, J., Yang, T-L, and Owings, R., *Guidance Systems for Vehicle Testing*, ENSCO, Inc., Springfield, VA 1986.

6. Bronstad, M.E., L.R. Calcote, M. H. Ray, and J.B. Mayer, *Guardrail-Bridge Rail Transition Designs, Volume I*, Report No. FHWA/RD-86/178, Southwest Research Institute, San Antonio, Texas, April 1988.

7. Bronstad, M.E., Ray, M.H., Mayer, J.B., Jr., and McDevitt, C.F., *W-Beam Approach Treatment at Bridge Rail Ends Near Intersecting Roadways*, Transportation Research Record No. 1133, Transportation Research Board, National Research Council, Washington, D.C., 1987.

8. Mayer, J.B., *Full-Scale Crash Testing of Approach Guardrail for Yuma County Public Works Department*, Final Report, Project No. 06-2111, Southwest Research Institute, San Antonio Texas, 1989.

9. *1989 Guide Specifications for Bridge Railings*, American Association of State Highway and Transportation Officials, Washington, D.C., 1989.

10. Ross, H.E. Jr., Bligh, R.P., Parnell, C.B., *Bridge Railing End Treatments at Intersecting Streets and Drives*, Report No. FHWA TX-91/92-1263-1F, Texas Transportation Institute, College Station, Texas, August 1992.

11. Bligh, Roger P., Hayes E. Ross, Jr., and Dean C. Alberson, *Short-Radius Thrie Beam Treatment for Intersecting Streets and Drives*, Report No. FHWA/TX-95/1442-1F, Texas Transportation Institute, College Station, Texas, November 1994.

12. *Curved W-Beam Guardrail Installations at Minor Roadway Intersections*, Federal Highway Administration (FHWA), U.S. Department of Transportation, Technical Advisory T 5040.32, April 13, 1992.

13. Bielenberg, B.W., Faller, R.K., Reid, J.D., Rohde, J.R., Sicking, D.L., and Keller, E.A., *Concept Development of a Bullnose Guardrail System for Median Applications*, Final Report to the Midwest States' Regional Pooled Fund Program, Transportation Research Report No. TRP-03-73-98, Project No. SPR-3(017)-Year 7, Midwest Roadside Safety Facility, University of Nebraska-Lincoln, May 22, 1998.

14. Bielenberg, B.W., Reid, J.D., Faller, R.K., Rohde, J.R., Sicking, D.L., Keller, E.A., and Holloway, J.C., *Phase II Development of a Bullnose Guardrail System for Median Applications*, Final Report to the Midwest States' Regional Pooled Fund Program, Transportation Research Report No. TRP-03-78-98, Project No. SPR-3(017)-Years 7 and 8, Midwest Roadside Safety Facility, University of Nebraska-Lincoln, December 18, 1998.

15. Bielenberg, B.W., Reid, J.D., Faller, R.K., Rohde, J.R., Sicking, D.L., Keller, E.A., Holloway, J.C., and Supencheck, L., *Phase III Development of a Bullnose Guardrail System for Median Applications*, Final Report to the Midwest States' Regional Pooled Fund Program, Transportation Research Report No. TRP-03-95-00, Project No. SPR-3(017)-Years 7 and 8, Midwest Roadside Safety Facility, University of Nebraska-Lincoln, June 1, 2000.

16. Reid, J. R. and Bielenberg, B. W., *Using LS-DYNA Simulation to Solve a Design Problem: A Bullnose Guardrail Example*, Paper No. 99-0554, Transportation Research Record No. 1690, Transportation Research Board, Washington, D.C., November 1999.

17. Bielenberg, R.W., Reid, J.D., and Faller, R.K., *NCHRP Report No. 350 Compliance Testing of a Bullnose Median Barrier System*, Paper No. 01-0204, Transportation Research Record No. 1743, Transportation Research Board, Washington, D.C., January 2001.

18. Faller, R.K., Reid, J.D., and Rohde, J.R., *Approach Guardrail Transition for Concrete Safety Shape Barriers*, Transportation Research Record No. 1647, Transportation Research Board, Washington, D.C., November 1998.

19. Faller, R.K., Reid, J.D., Rohde, J.R., Sicking, D.L., and Keller, E.A., *Two Approach Guardrail Transitions for Concrete Safety Shape Barriers*, Final Report to the Midwest States' Regional Pooled Fund Program, Transportation Research Report No. TRP-03-69-98, Project No. SPR-3(017)-Year 6, Midwest Roadside Safety Facility, University of Nebraska-Lincoln, May 15, 1998.

20. *Vehicle Damage Scale for Traffic Investigators*, Second Edition, Technical Bulletin No. 1, Traffic Accident Data (TAD) Project, National Safety Council, Chicago, Illinois, 1971.

21. *Collision Deformation Classification - Recommended Practice J224 March 1980*, Handbook Volume 4, Society of Automotive Engineers (SAE), Warrendale, Pennsylvania, 1985.

13 APPENDICES

APPENDIX A

English-Unit System Drawings, Test SR-5

Figure A-1. Short-Radius Design Details (English)
Figure A-2. Secondary Side Short-Radius Design Details (English)
Figure A-3. Primary Side Short-Radius Design Details (English)
Figure A-4. Primary Side End Anchorage Details (English)
Figure A-5. Cable Release Lever Attachment Details (English)
Figure A-6. Anchor Cable and Release Cable Details (English)
Figure A-7. Nose Cable Anchor Plate Details (English)
Figure A-8. MGS and Thrie Beam Foundation Tube Details (English)
Figure A-9. Wood Post Details, Post Nos. 1P, 1S, 2P-13P, 2S-5S,6S-8S, and 9S-10S (English)
Figure A-10. Wood Post Details (English)
Figure A-11. Wood Post Details (English)
Figure A-12. Iowa Steel Post Transition Details, Post Nos. 14P-19P (English)
Figure A-13. Primary Side End Anchorage Details (English)
Figure A-14. Anchorage Post Details (English)
Figure A-15. Rail Slot Pattern No. 1 Details (English)
Figure A-16. Rail Slot Pattern No. 2 Details (English)
Figure A-17. Rail Curvature, Rail Section No. 1 (English)
Figure A-18. Rail Curvature, Rail Section Nos. 2 and 3 (English)
Figure A-19. Rail Curvature, Rail Section No. 4 (English)
Figure A-20. Cable Release Bracket, Part A (English)
Figure A-21. Cable Release Bracket Details (English)
Figure A-22. Cable Release Base (English)
Figure A-23. Cable Release Base Details (English)
Figure A-24. Cable Release Lever Kicker Details (English)

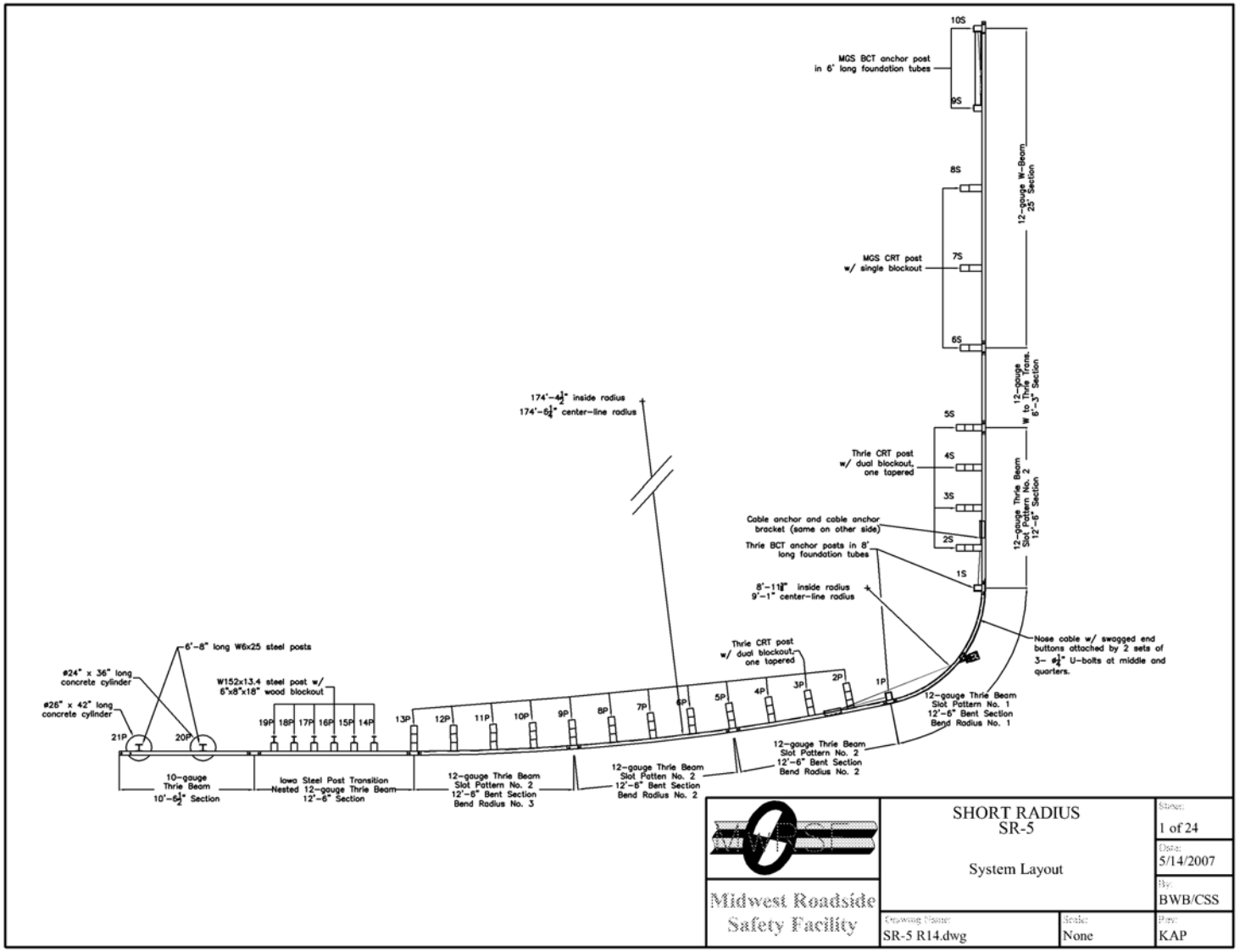

Figure A-1. Short-Radius Design Details (English), Test SR-5

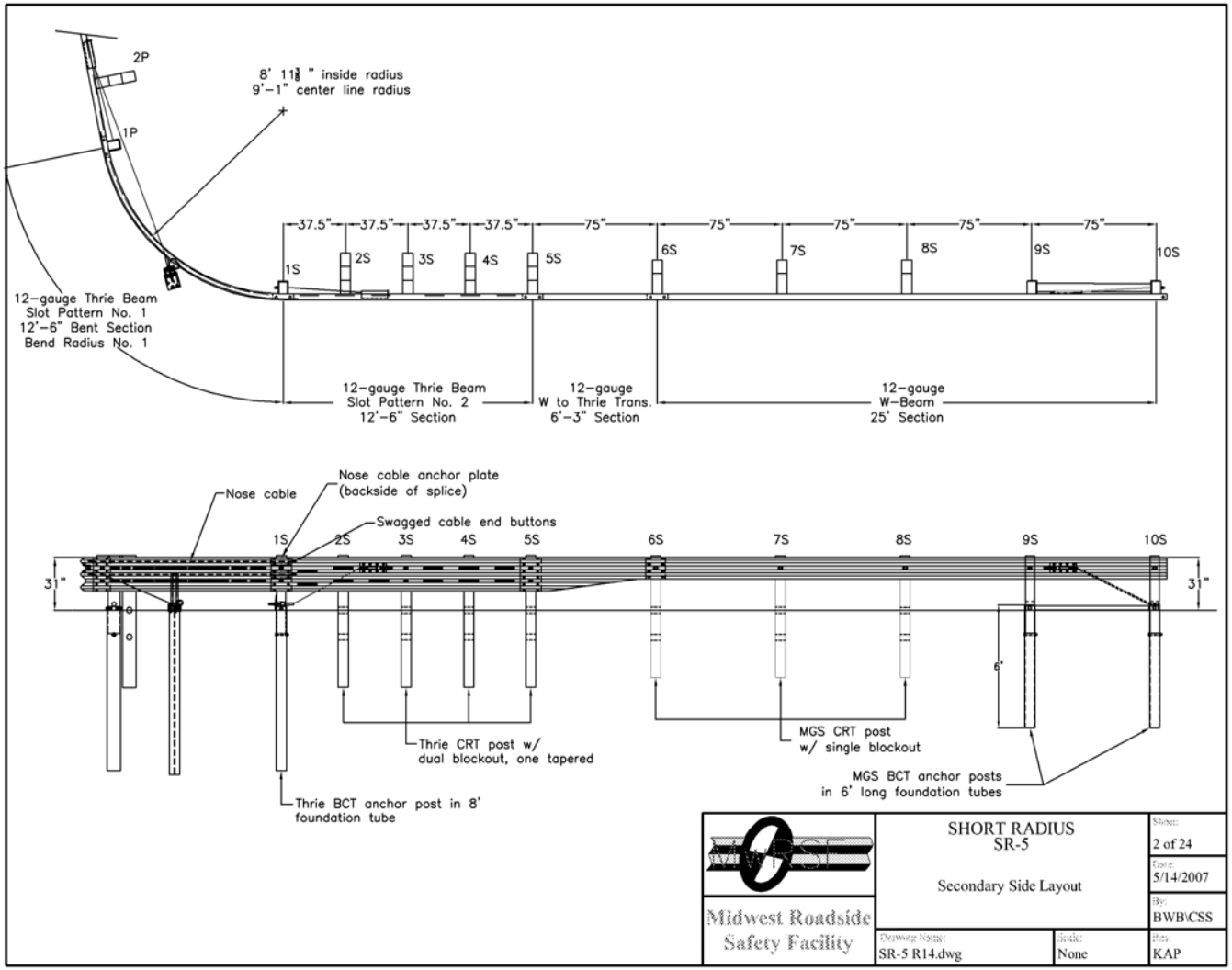

Figure A-2. Secondary Side Design Details (English), Test SR-5

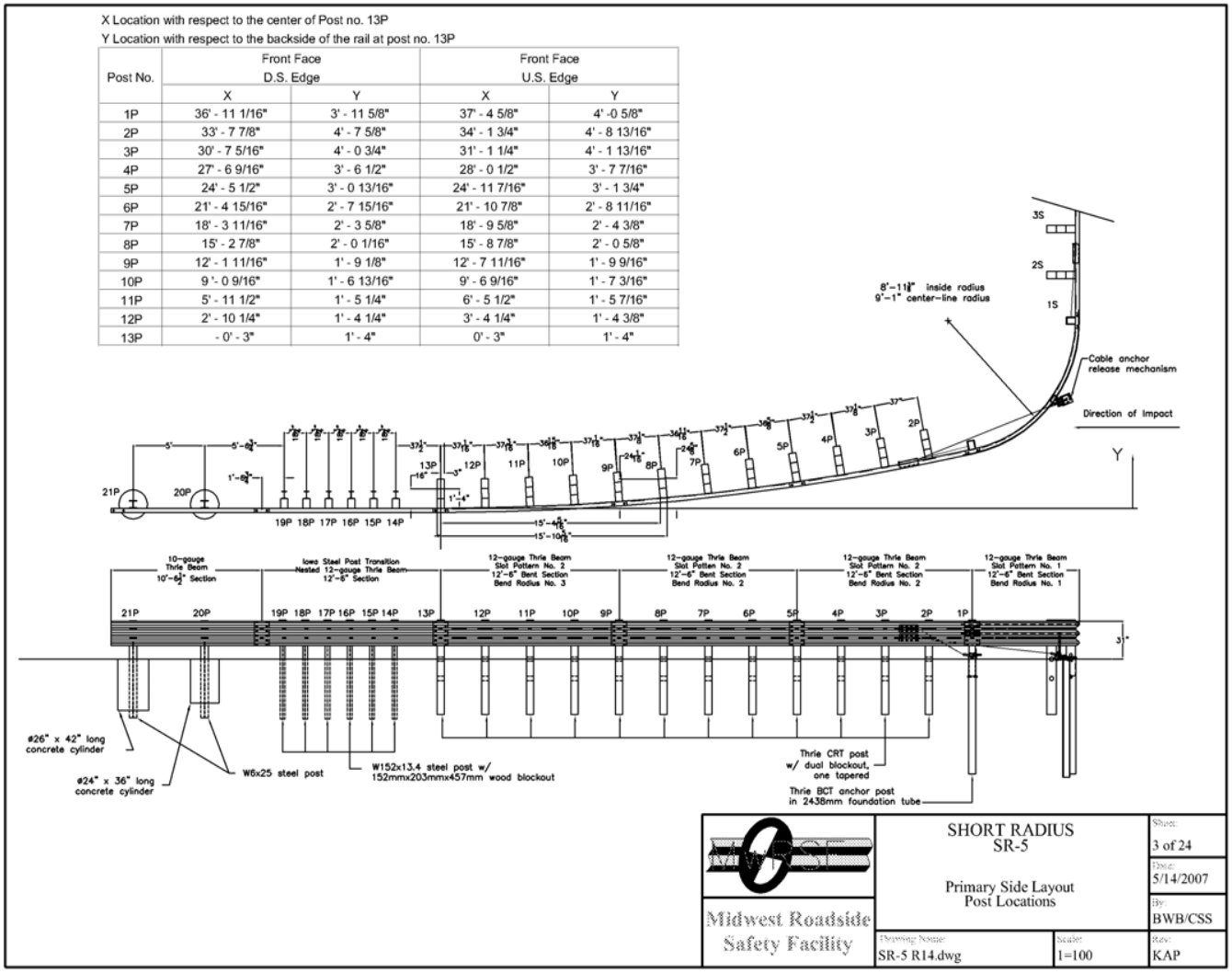

Figure A-3. Primary Side Design Details (English), Test SR-5

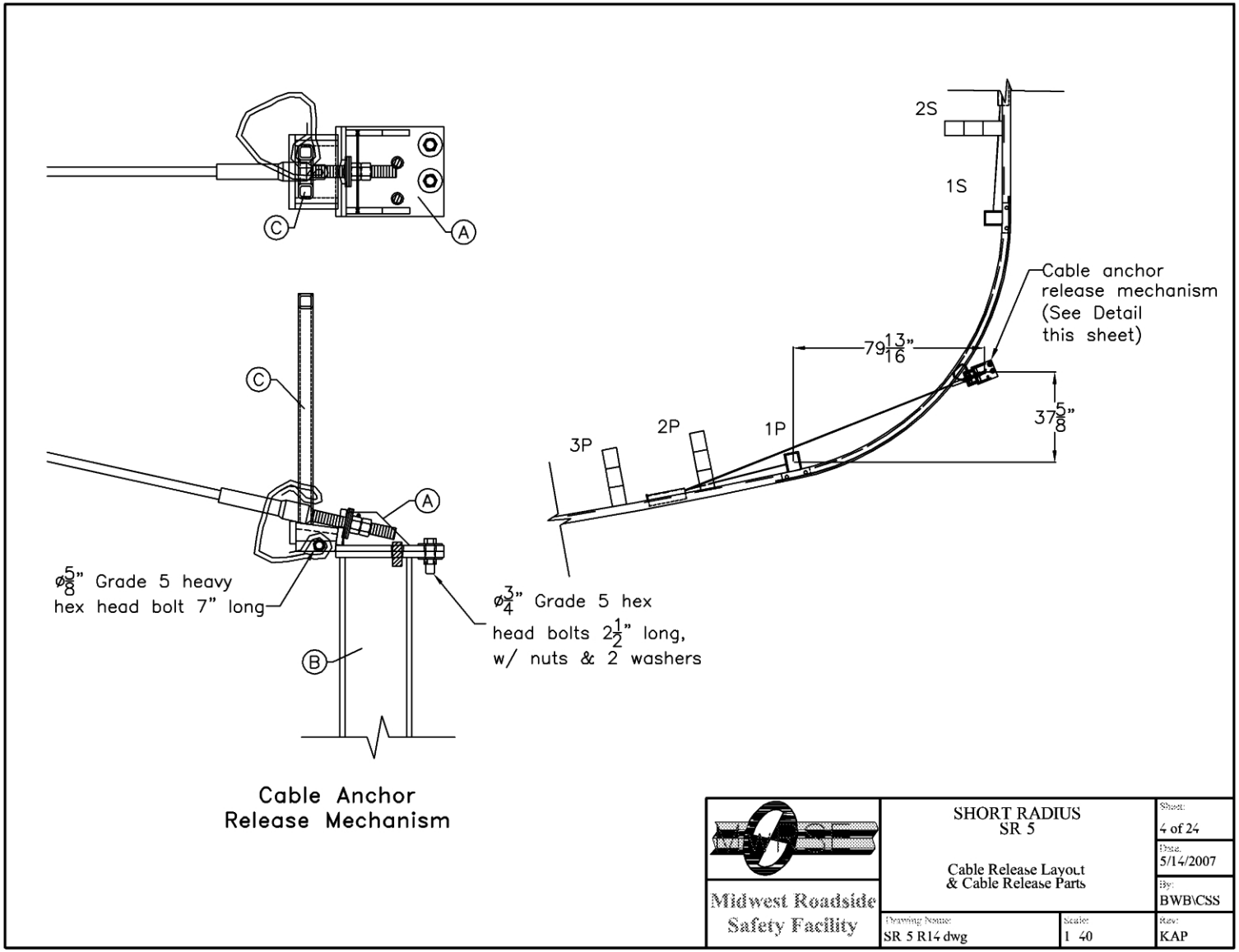

Figure A-4. Cable Release Lever Attachment Details (English), Test SR-5

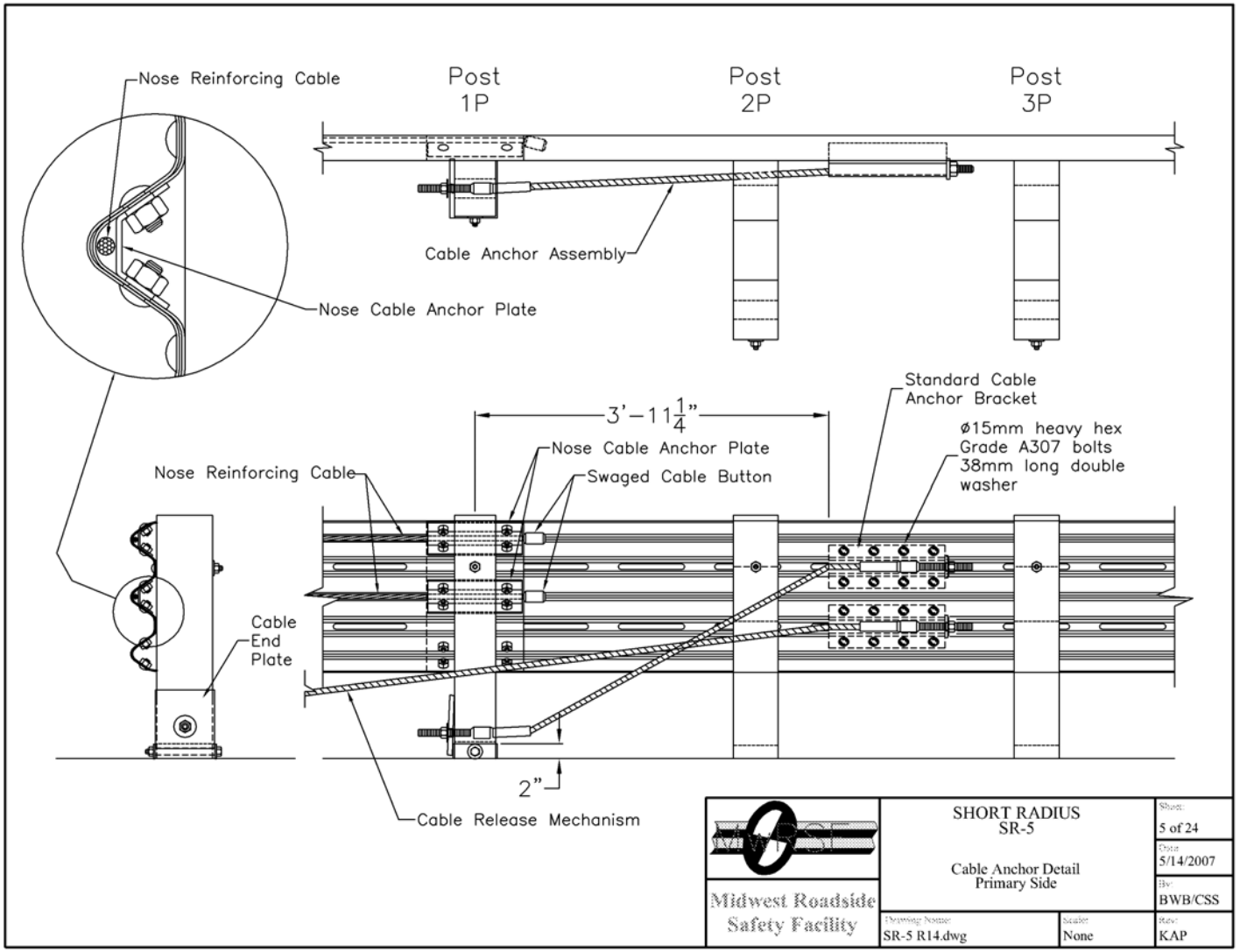

Figure A-5. Primary Side End Anchorage Details (English), Test SR-5

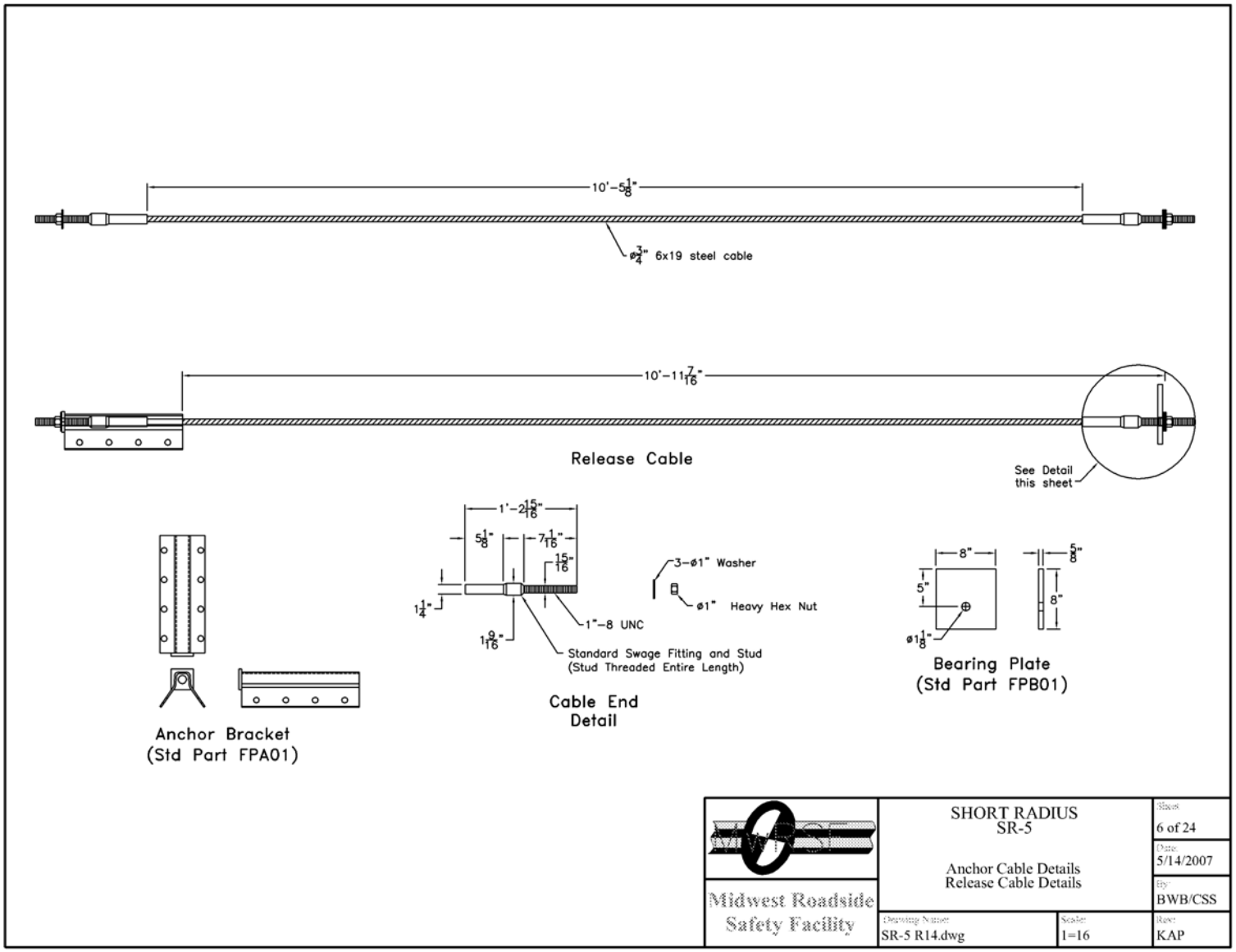

Figure A-6.Anchor Cable and Release Cable Details (English), Test SR-5

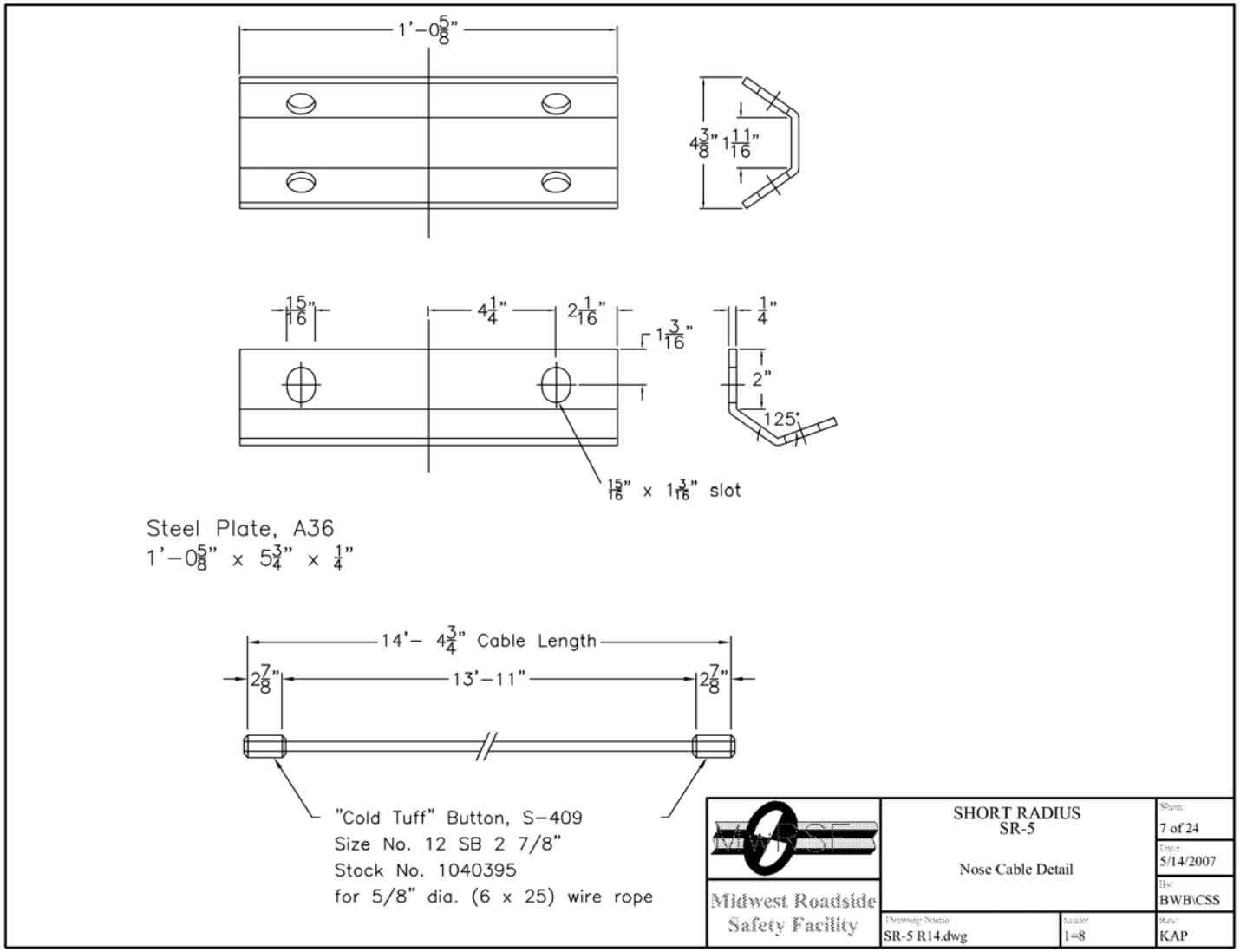

Figure A-7. Nose Cable Anchor Plate Details (English), Test SR-5

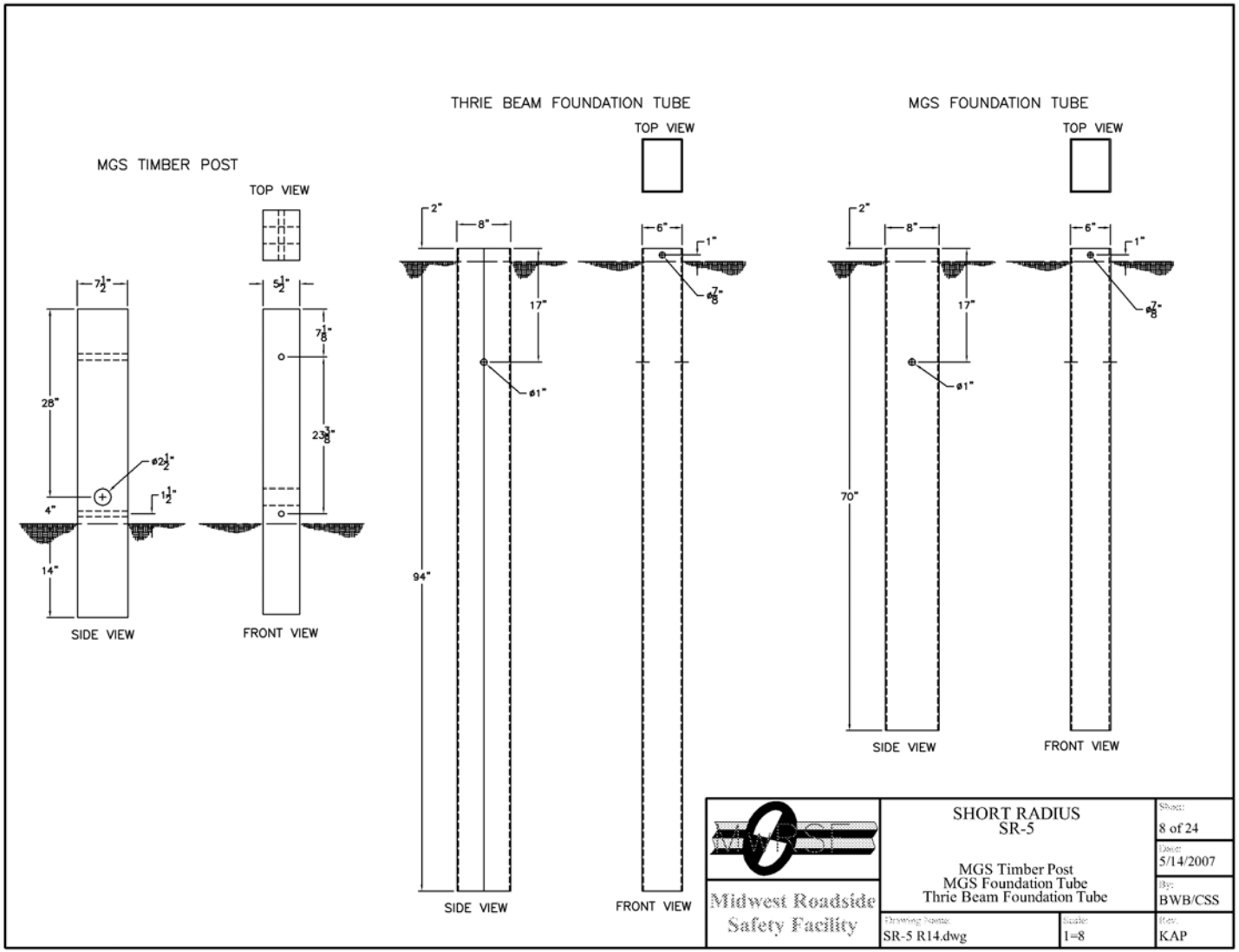

Figure A-8. MGS and Thrie Beam Foundation Tube Details (English), Test SR-5

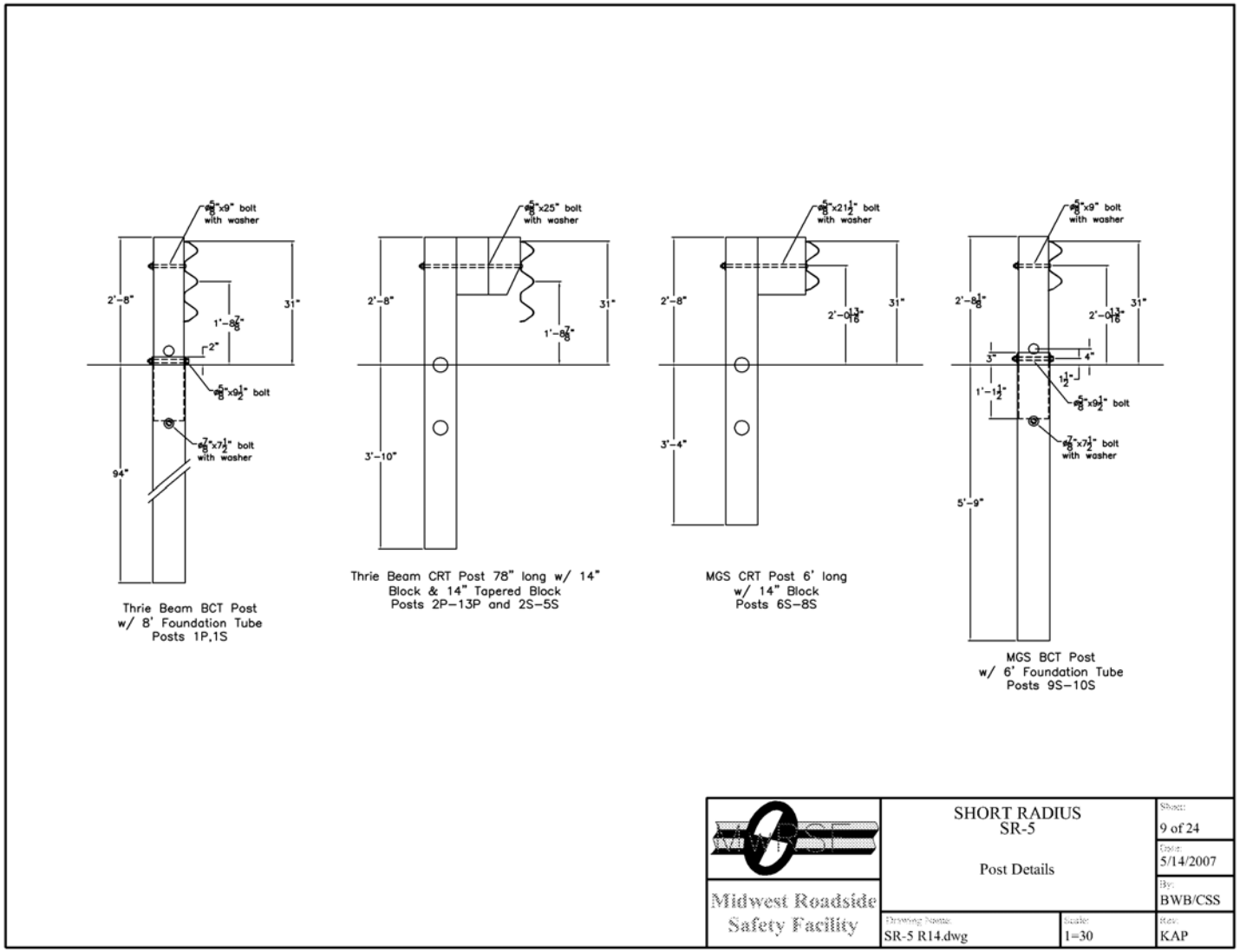

Figure A-9. Wood Post Details, Post Nos. 1P, 1S, 2P-13P, 2S-5S,6S-8S, and 9S-10S (English), Test SR-5

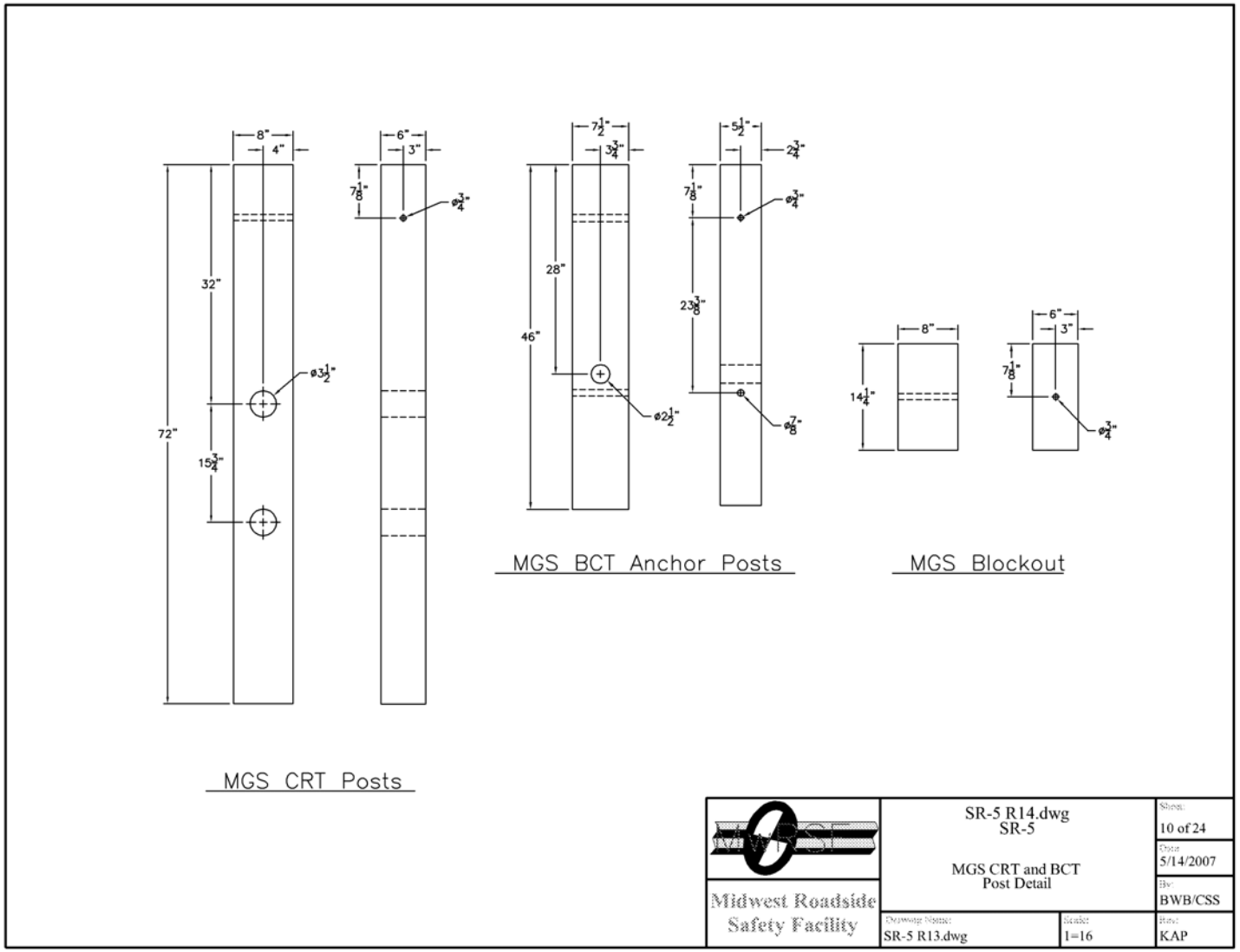

Figure A-10. MGS CRT and BCT Post Details (English), Test SR-5

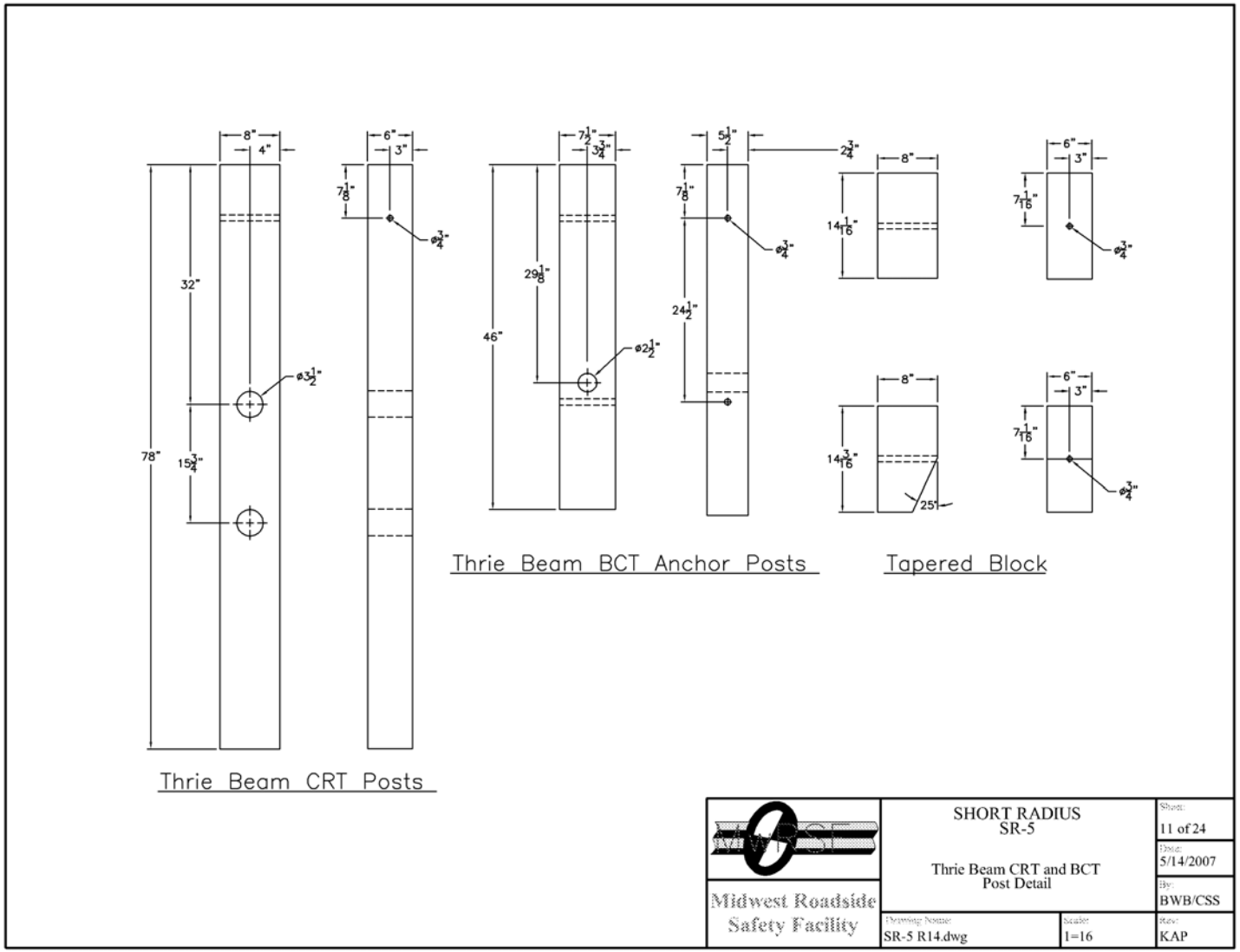

Figure A-11. Thrie Beam Timber Post Details (English), Test SR-5

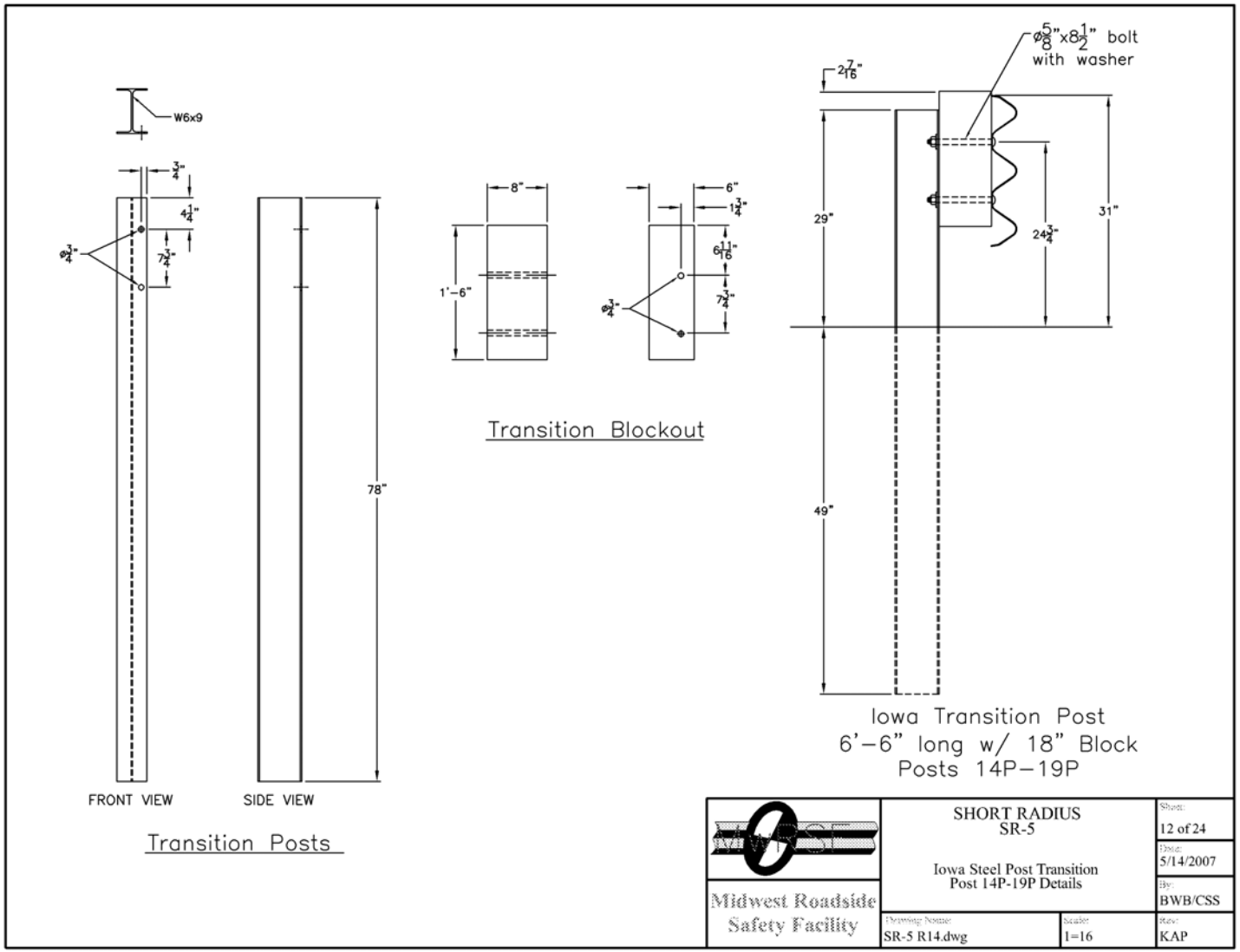

Figure A-12. Iowa Steel Post Transition Details, Post Nos. 14P-19P (English), Test SR-5

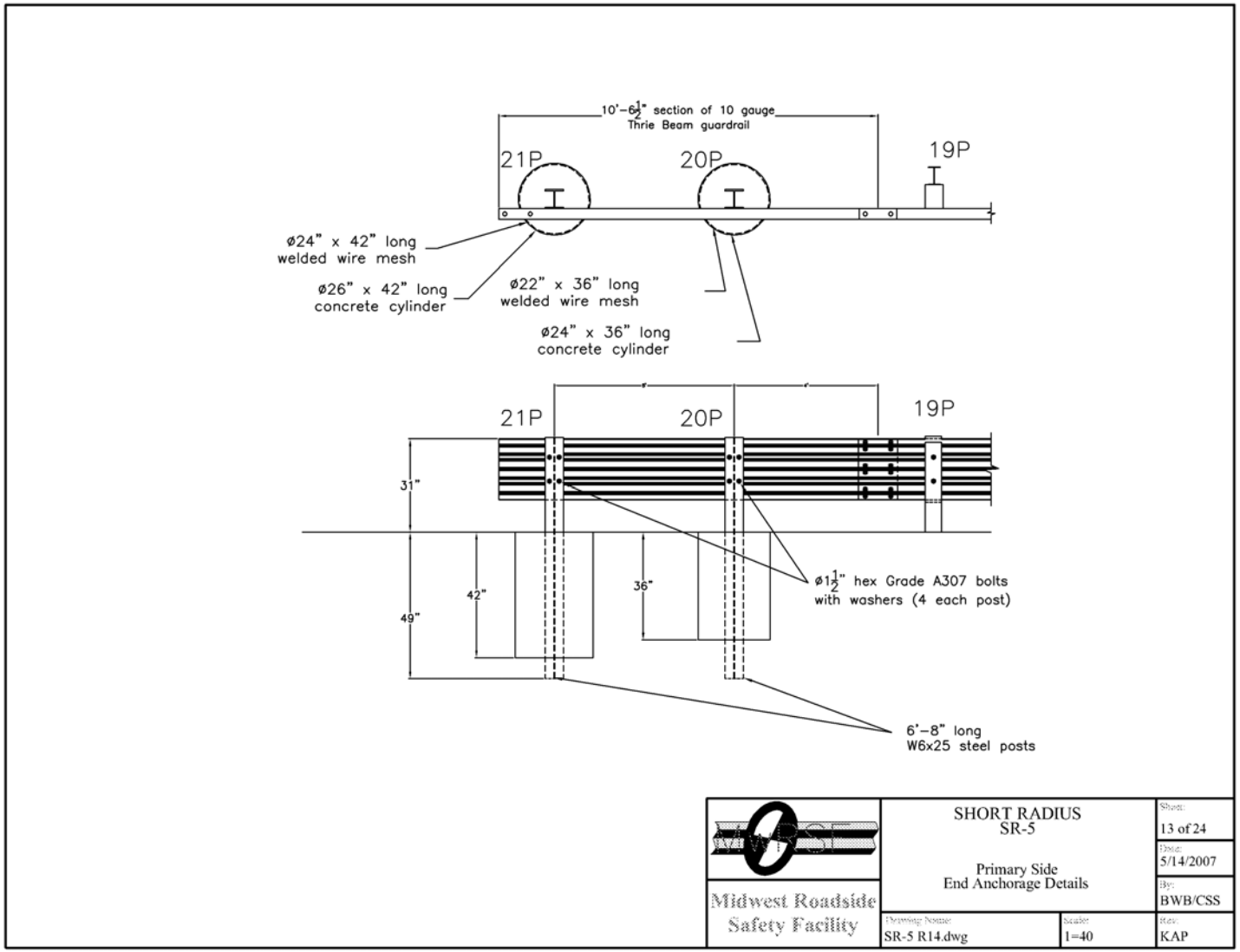

Figure A-13. Primary Side End Anchorage Details (English), Test SR-5

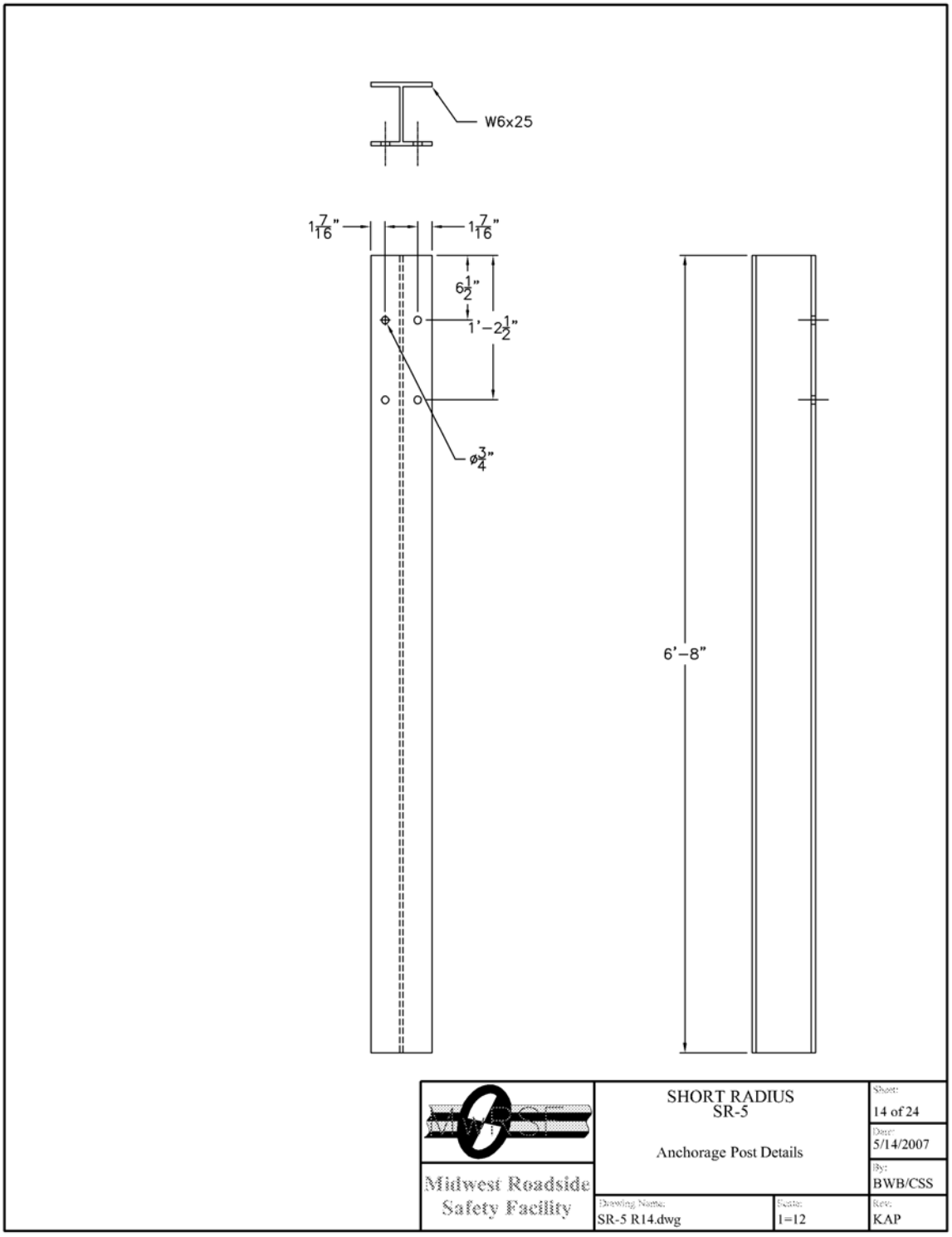

Figure A-16. Anchorage Post Details (English), Test SR-5

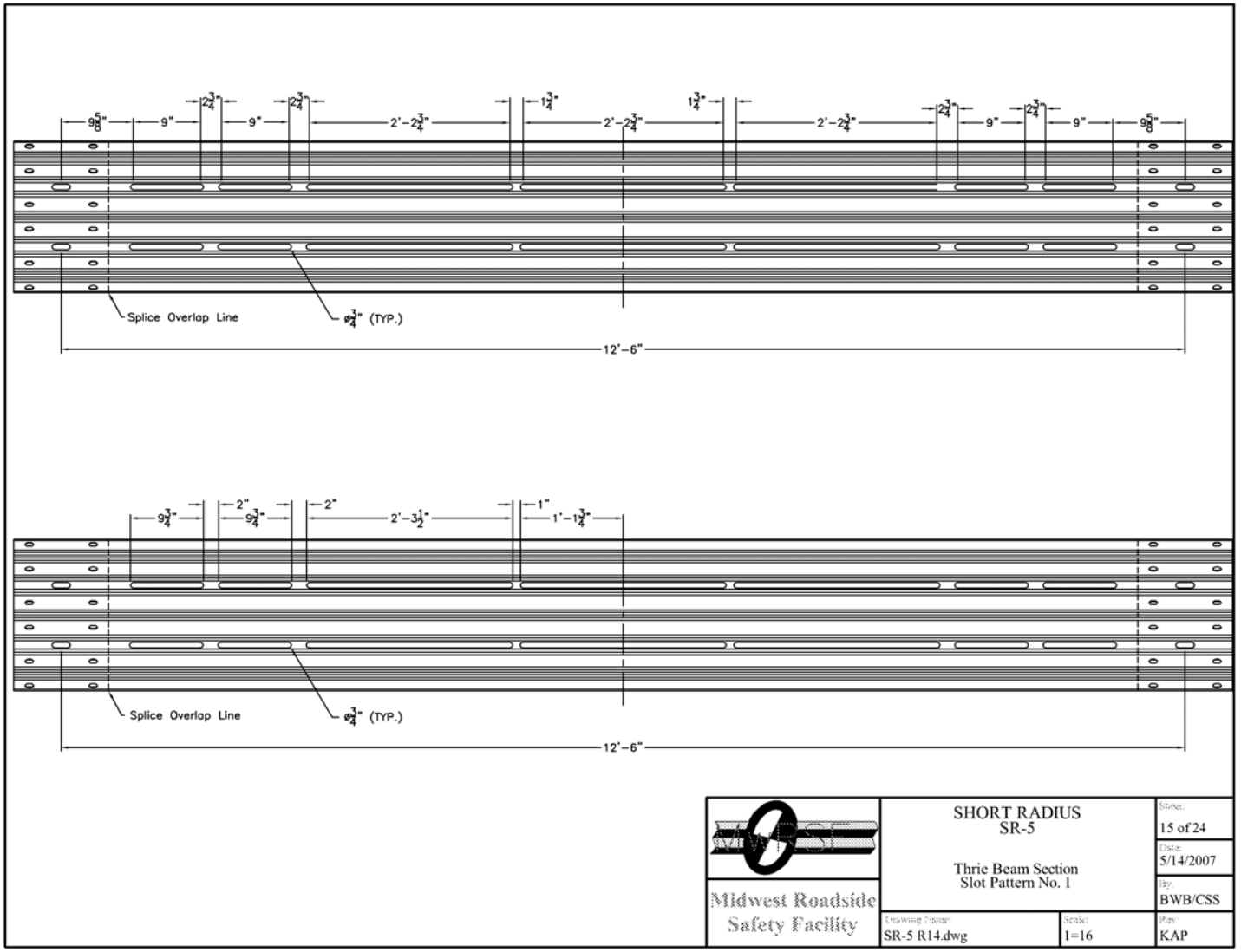

Figure A-15. Rail Slot Pattern No. 1 Details (English), Test SR-5

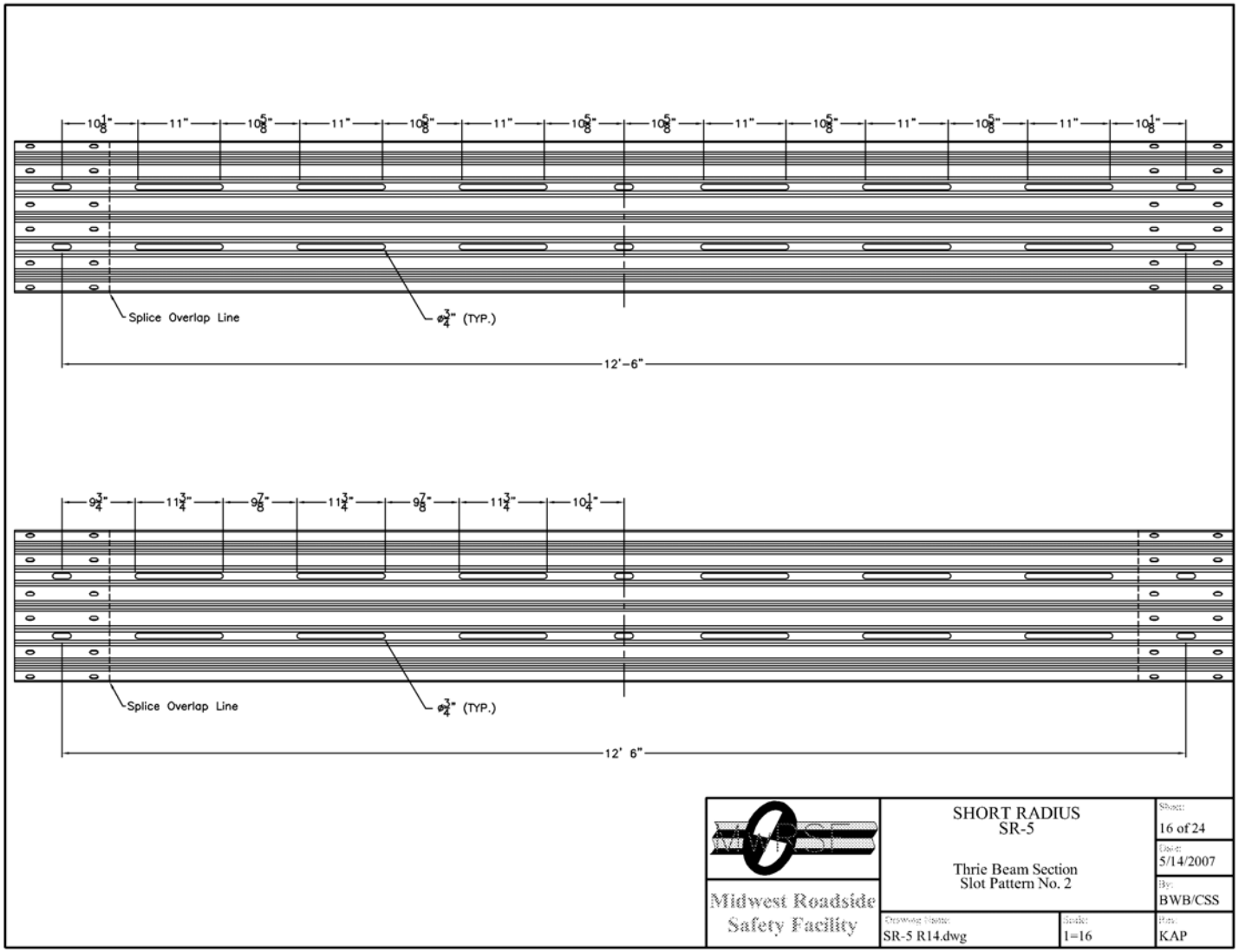

Figure A-16. Rail Slot Pattern No. 2 Details (English), Test SR-5

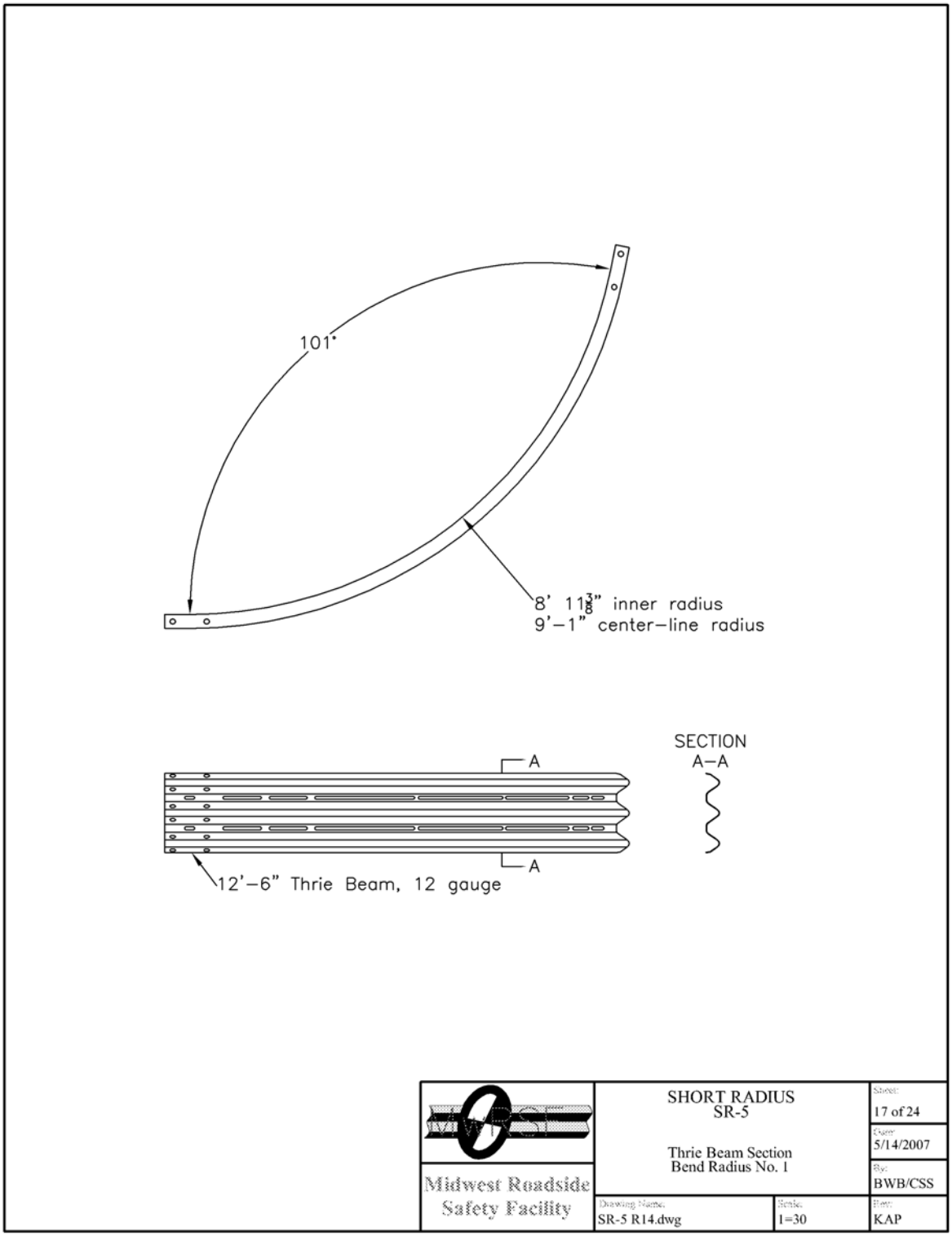

Figure A-17. Rail Curvature, Rail Section No. 1 (English), Test SR-5

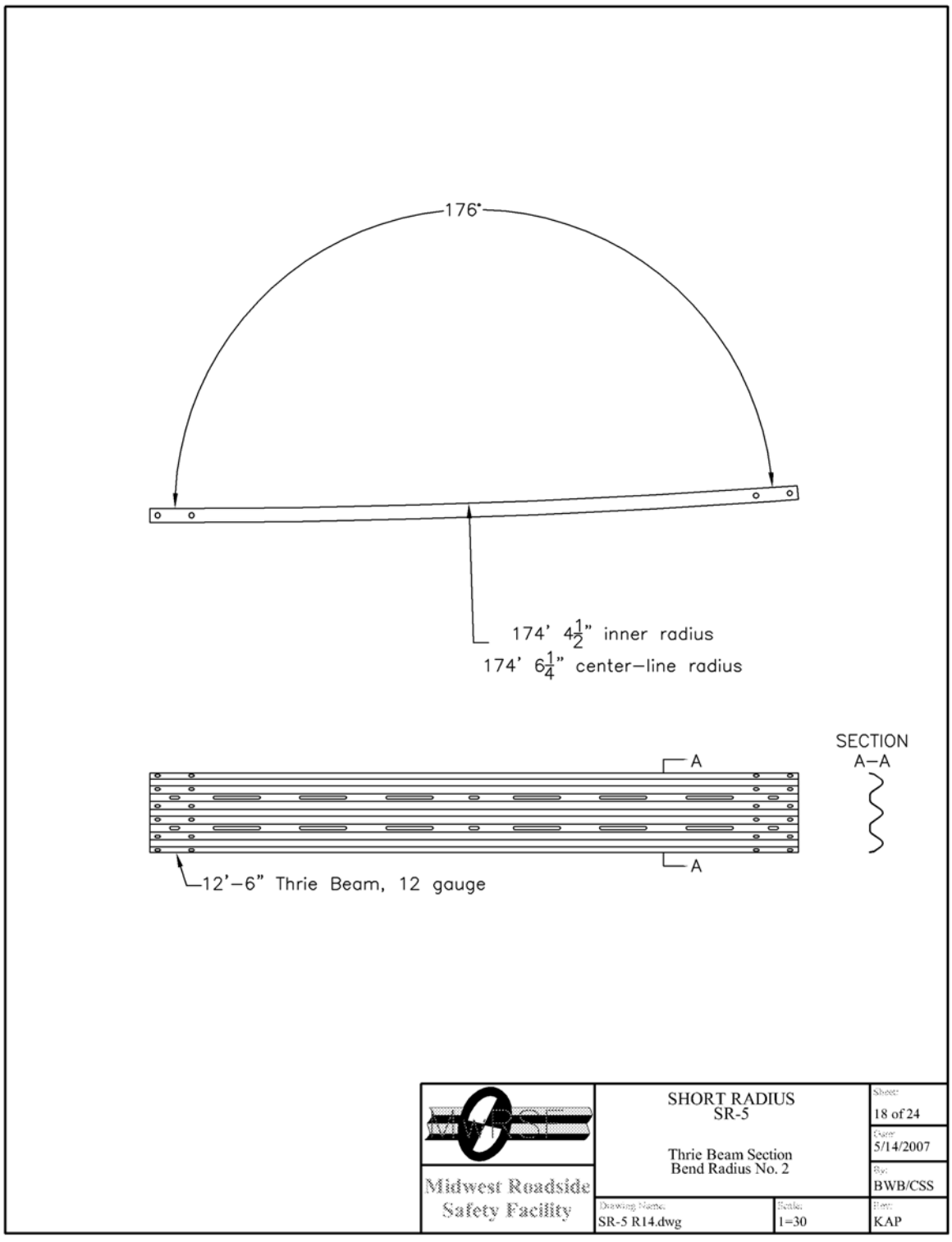

Figure A-18. Rail Curvature, Rail Section Nos. 2 and 3 (English), Test SR-5

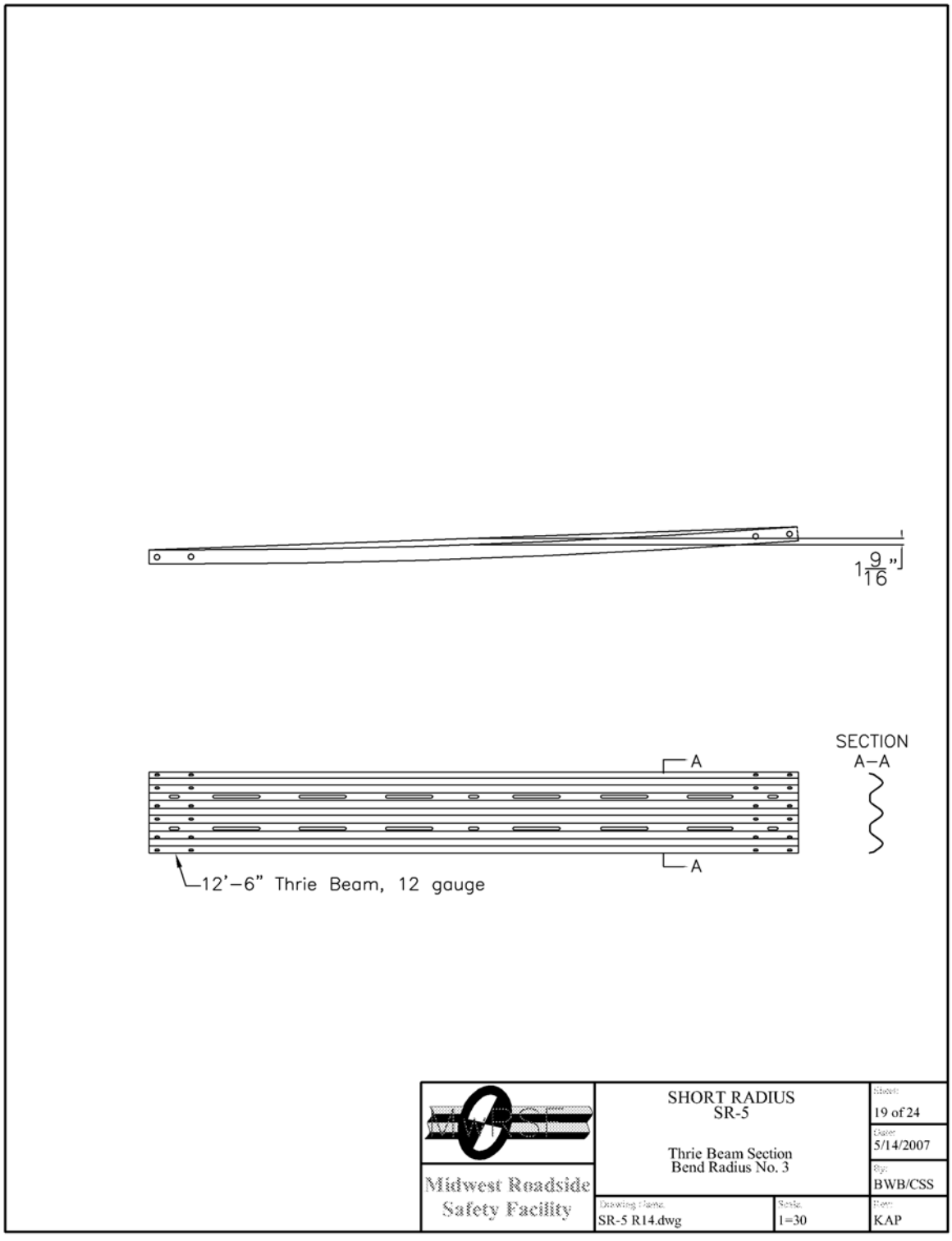

Figure A-19. Rail Curvature, Rail Section No. 4 (English), Test SR-5

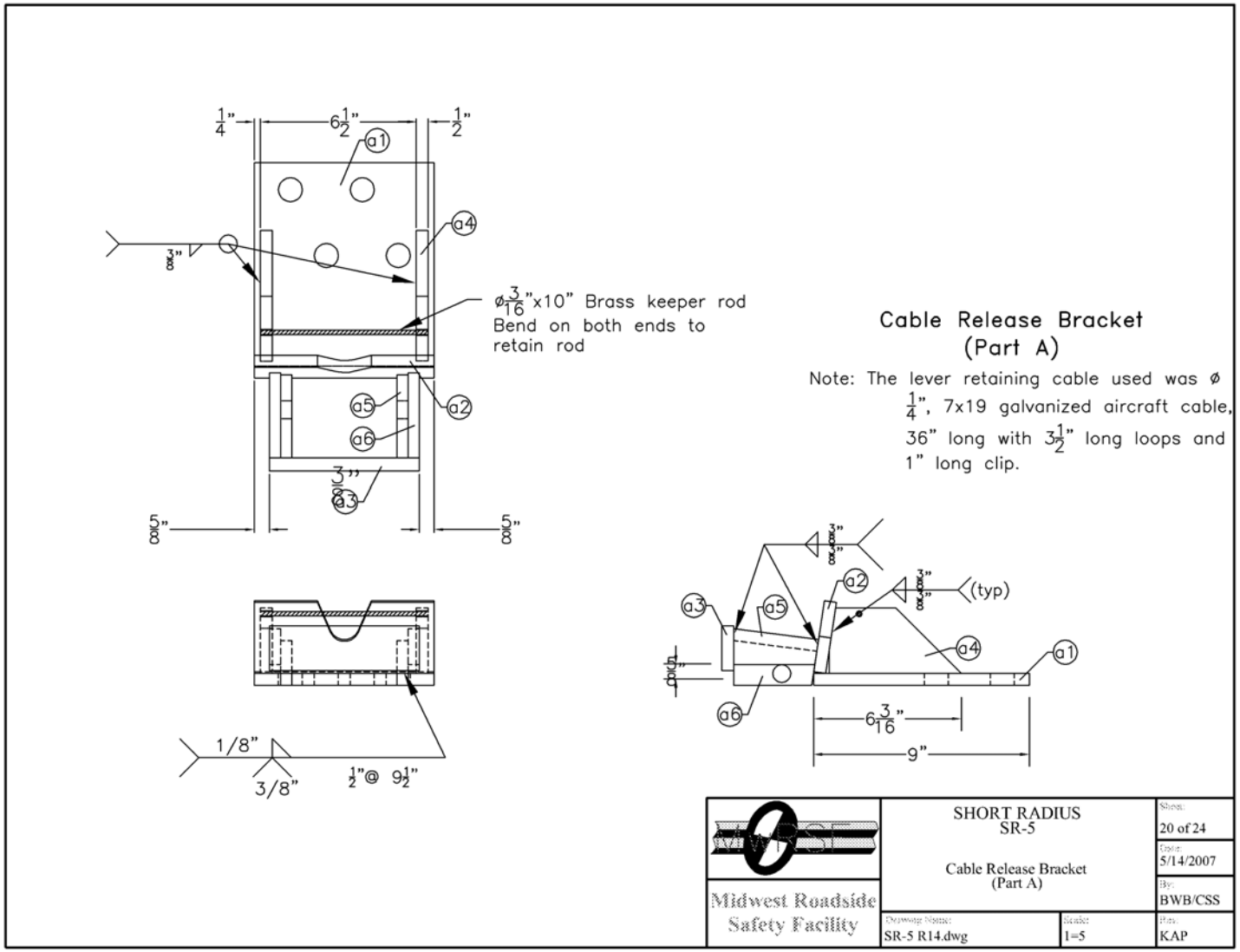

Figure A-20. Cable Release Bracket, Part A (English), Test SR-5

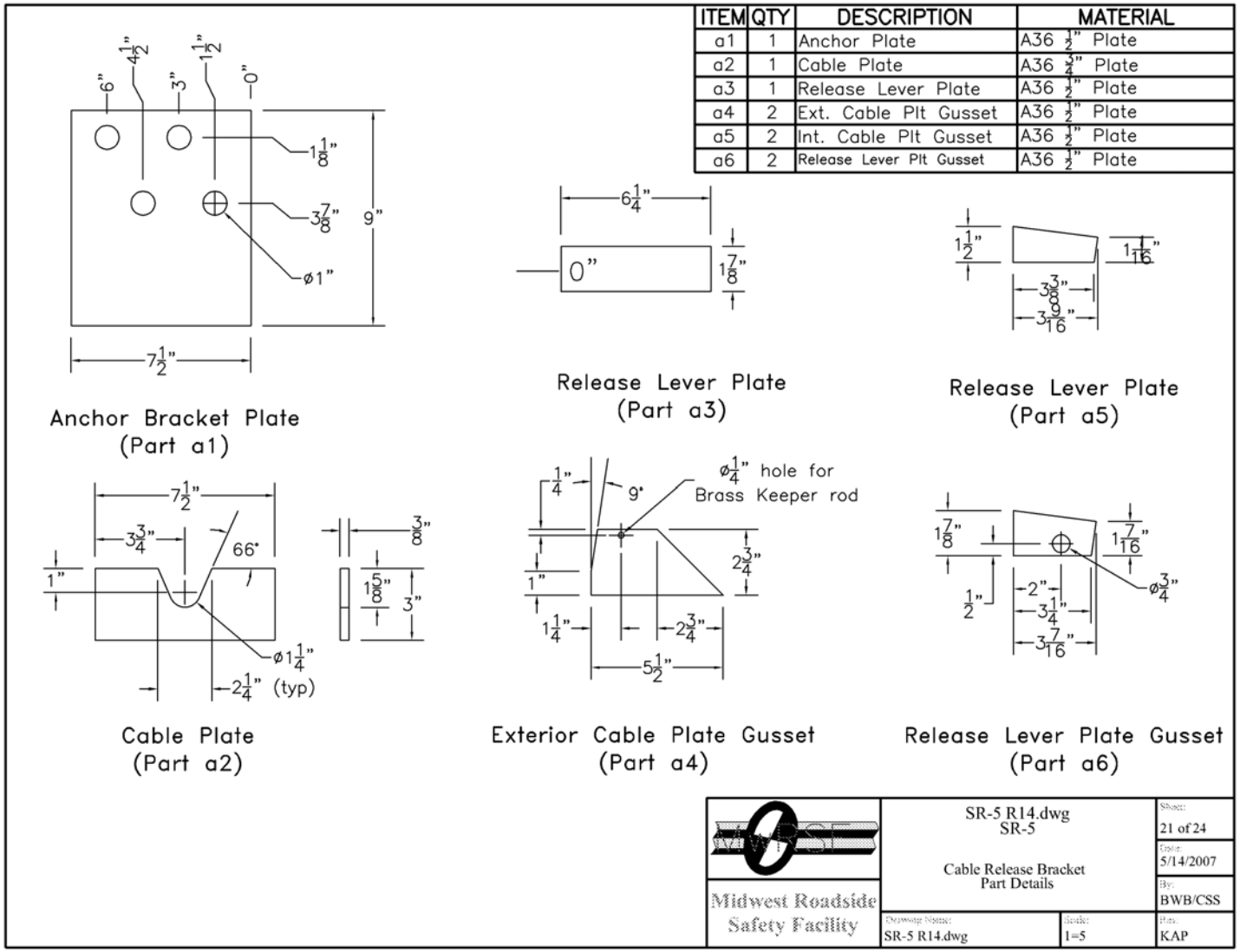

Figure A-21. Cable Release Bracket Details (English), Test SR-5

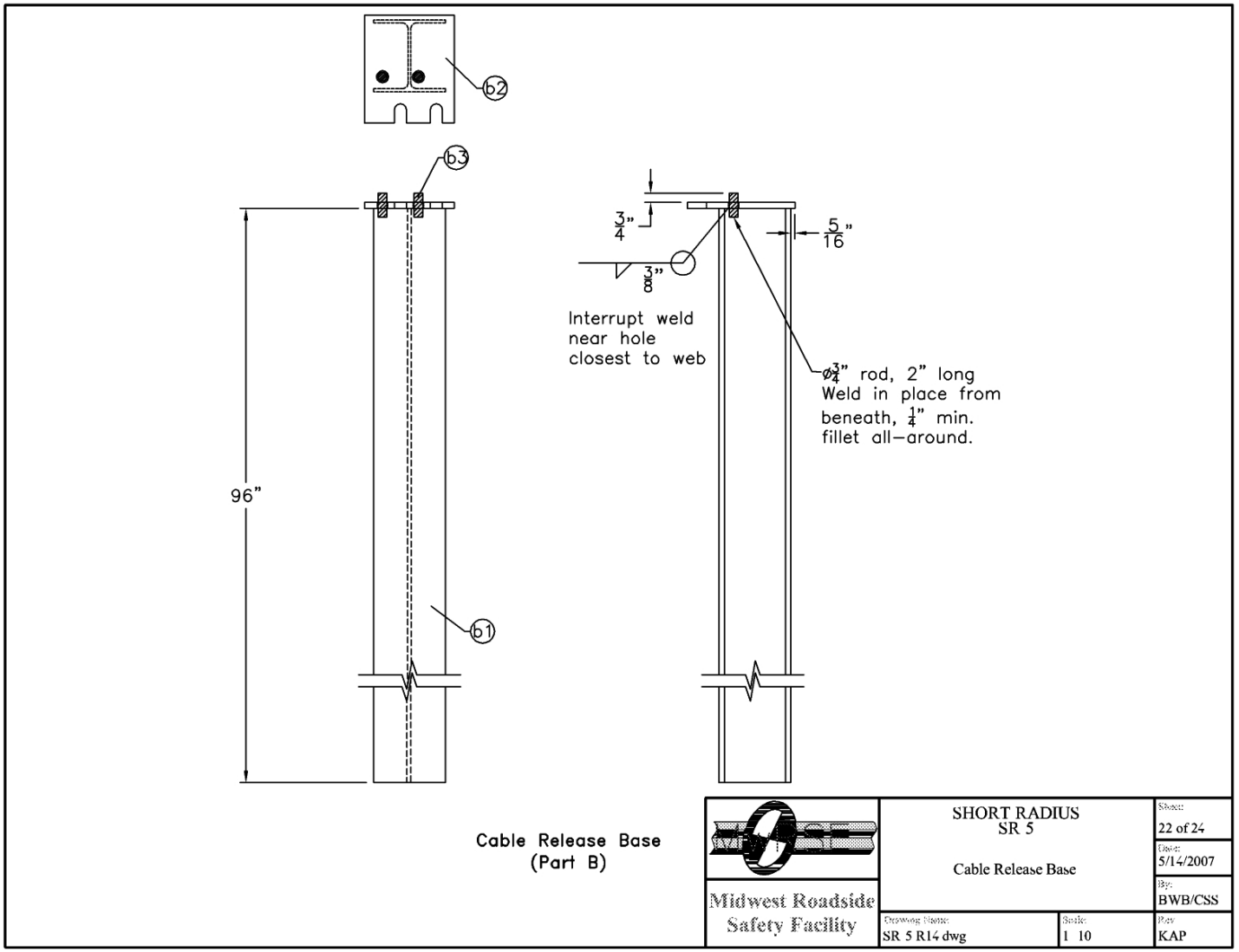

Figure A-22. Cable Release Base (English), Test SR-5

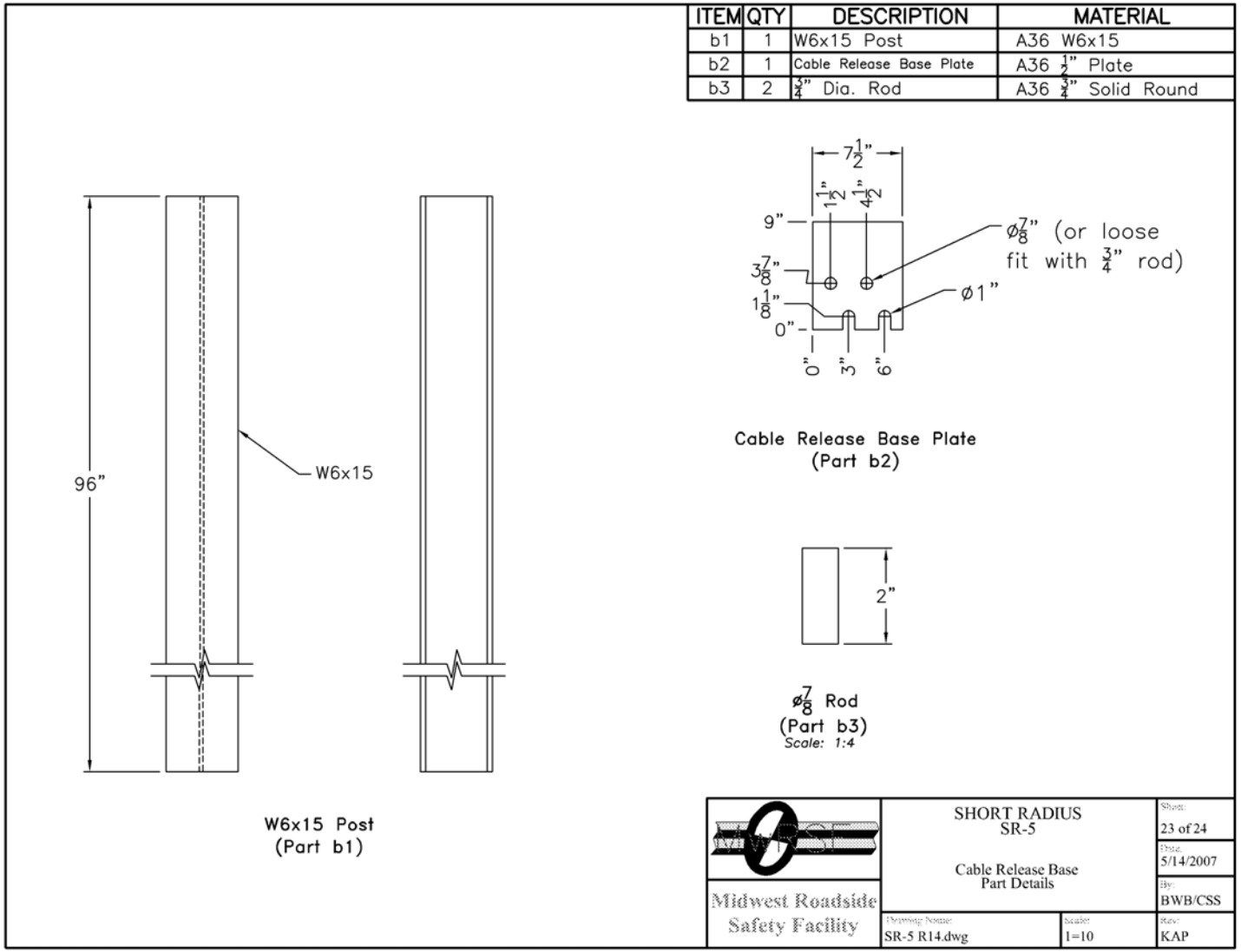

Figure A-23. Cable Release Base Details (English), Test SR-5

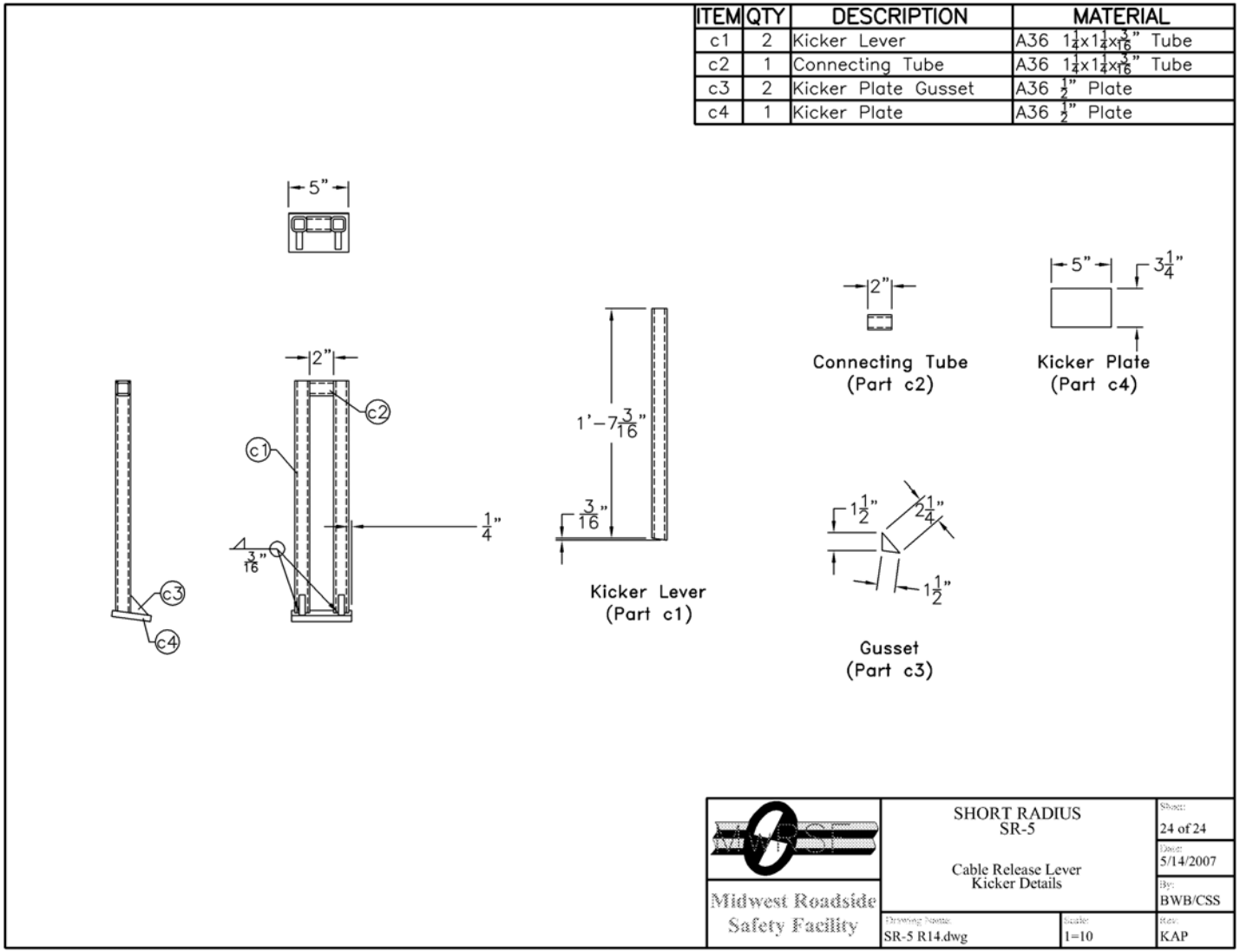

Figure A-24. Cable Release Lever Kicker Details (English), Test SR-5

APPENDIX B

Test Summary Sheets in English Units

Figure B-1. Summary of Test Results and Sequential Photographs (English), Test SR-5
Figure B-2. Summary of Test Results and Sequential Photographs (English), Test SR-6

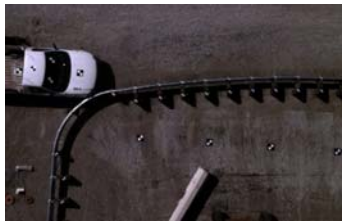

0.000 sec

0.104 sec

0.216 sec

0.342 sec

0.484 sec

- Test Number SR-5
- Date 4/4/2005
- Test Article
  - Type . . . . . Short-Radius Guardrail
  - Key Elements . . . Four 6-ft 6-in. long curved and slotted thrie beam guardrail sections (parabolic flare)
    One 6-ft 6-in. long straight thrie beam guardrail section
    31 in. top rail height
    18 breakaway posts
    Iowa steel post transition
    Simulated tangent W-beam guardrail end terminal
    Additional upstream anchor for primary side
  - Orientation . . . . . Centerline truck with back of post no. 13P
- Soil Type . . . . . Grading B - AASHTO M 147-65 (1990)
- Vehicle Model . . . . . 1997 Ford F-250 pickup truck
  - Curb . . . . . 4,105 lb
  - Test Inertial . . . . . 4,412 lb
  - Gross Static . . . . . 4,412 lb
- Vehicle Speed
  - Impact . . . . . 63.2 mph
  - Exit . . . . . 53.1 mph
- Vehicle Angle
  - Impact . . . . . 0.9 deg
  - Exit . . . . . 12.6 deg
- Vehicle Stability . . . . . Satisfactory
- Occupant Ridedown Deceleration (10 msec avg.)
  - Longitudinal . . . . . 5.72 Gs < 20 Gs
  - Lateral (not required) . . . . . 5.37 Gs < 20 Gs
- Occupant Impact Velocity
  - Longitudinal . . . . . 13.37 ft/s < 40 ft/s
  - Lateral (not required) . . . . . 10.43 ft/s < 40 ft/s
- THIV (not required) . . . . . 16.26 ft/s
- PHD (not required) . . . . . 7.35 Gs
- Vehicle Damage
  - TAD[20] 1-FR-3
  - SAE[21] 1-FRAW5
- Vehicle Stopping Distance 137 ft-6 in. downstream
  35 ft-5 in. right
- Test Article Damage . . . . . Moderate
- Maximum Deflections
  - Permanent Set . . . . . 58.4 in.
  - Dynamic . . . . . 87.4 in.
  - Working Width . . . . . 89.0 in. laterally from primary side

Figure B-1. Summary of Test Results and Sequential Photographs (English), Test SR-5

0.000 sec 0.079 sec 0.172 sec 0.313 sec 0.404 sec

- Test Number SR-6
- Date 10/7/2005
- Test Article
  - Type . . . . . Short-Radius Guardrail
  - Key Elements . . . . Four 12-ft 6-in. long curved and slotted thrie beam guardrail sections (parabolic flare)
    One 12-ft 6-in. long straight thrie beam guardrail section
    31 in. top rail height
    18 breakaway posts
    Iowa steel post transition
    Simulated tangent W-beam guardrail end terminal
    Cable anchor for primary side tension development
  - Orientation . . . . . Right quarter-point vehicle with centerline nose
- Soil Type . . . . . Grading B - AASHTO M 147-65 (1990)
- Vehicle Model . . . . . 1996 Geo Metro
  - Curb . . . . . 1,708 lb
  - Test Inertial . . . . . 1,803 lb
  - Gross Static . . . . . 1,969 lb
- Vehicle Speed
  - Impact . . . . . 61.8 mph
  - Exit . . . . . NA (Did not exit)
- Vehicle Angle
  - Impact . . . . . 0.8 deg
  - Exit . . . . . NA (Did not exit)
- Vehicle Stability . . . . . Satisfactory
- Occupant Ridedown Deceleration (10 msec avg.)
  - Longitudinal . . . . . -20.73 Gs > 20Gs
  - Lateral . . . . . 12.05 Gs < 20 Gs
- Occupant Impact Velocity
  - Longitudinal . . . . . 30.84 ft/s < 39.4 ft/s
  - Lateral . . . . . 0.43 ft/s < 12 m/s
- THIV (not required) . . . . . 30.97 ft/s
- PHD (not required) . . . . . 23.97 Gs
- Vehicle Damage . . . . . Extensive
  - TAD[20] 12-FD-6
  - SAE[21] 12-FDAW6
- Vehicle Stopping Distance 14 ft 9 in. downstream
  4 ft 10 in. right
- Test Article Damage . . . . . Moderate
- Test Article Deflections
  - Permanent Set . . . . . 91.5 in.
  - Dynamic . . . . . 99.3 in.
  - Working Width . . . . . 21 ft 3 in. downstream of secondary side
    13 ft 1 in. right of primary side

Figure B-2. Summary of Test Results and Sequential Photographs (English), Test SR-6

APPENDIX C

Occupant Compartment Deformation Data, Test SR-5

Figure C-1. Occupant Compartment Deformation Data - Set 1, Test SR-5
Figure C-2. Occupant Compartment Deformation Data - Set 2, Test SR-5
Figure C-3. Occupant Compartment Deformation Index (OCDI), Test SR-5

VEHICLE PRE/POST CRUSH INFO
Set-1

TEST: SR-5
VEHICLE: 1997 Ford F250

Note: If impact is on driver side need to enter negative number for Y

POINT	X	Y	Z	X'	Y'	Z'	DEL X	DEL Y	DEL Z
1	58.75	9.75	6.5	Bad Data	9.25	7.5	Bad Data	-0.5	1
2	58.75	13.5	6.5		12.75	7.75		-0.75	1.25
3	58.75	16	6.5		15.25	8		-0.75	1.5
4	58.75	18.75	6.75		18	8		-0.75	1.25
5	59	26	6.5		25.25	7.5		-0.75	1
6	59	26.75	6.75		26.25	7.25		-0.5	0.5
7	53.25	8.25	5.25		8	6		-0.25	0.75
8	54.25	12	9		11.5	9.75		-0.5	0.75
9	54.25	16.25	9		16	9.5		-0.25	0.5
10	54.25	20.25	9		19.5	10		-0.75	1
11	54.25	23.75	9		22.75	10.25		-1	1.25
12	54.25	28.5	9		27.5	10		-1	1
13	45.75	6.75	4		6.75	4.5		0	0.5
14	46.25	10.25	9.25		10.25	9.75		0	0.5
15	46.5	14.75	9.25		14.5	10		-0.25	0.75
16	46.75	19	9.25		18.75	8.75		-0.25	-0.5
17	46.75	22.75	9.25		22.25	9.75		-0.5	0.5
18	46.75	27.25	9.25		26.5	10.5		-0.75	1.25
19	35.75	9	9.5		9	9.5		0	0
20	35.75	13.75	9.5		13.75	9.5		0	0
21	35.75	18.5	9.25		18.25	9.5		-0.25	0.25
22	35.75	23.75	9.25		23.75	9.25		0	0
23	36.25	28.75	9.5		28.25	9.75		-0.5	0.25
24	28.5	8.75	7.8		8.75	7		0	-0.8
25	28.5	16	7.25		16.25	7.25		0.25	0
26	28	26.25	6.75		26.5	6.5		0.25	-0.25
27	21.75	10.5	8		10.5	7.75		0	-0.25
28	21.75	19.5	7.75		19.5	7.5		0	-0.25
29									
30									

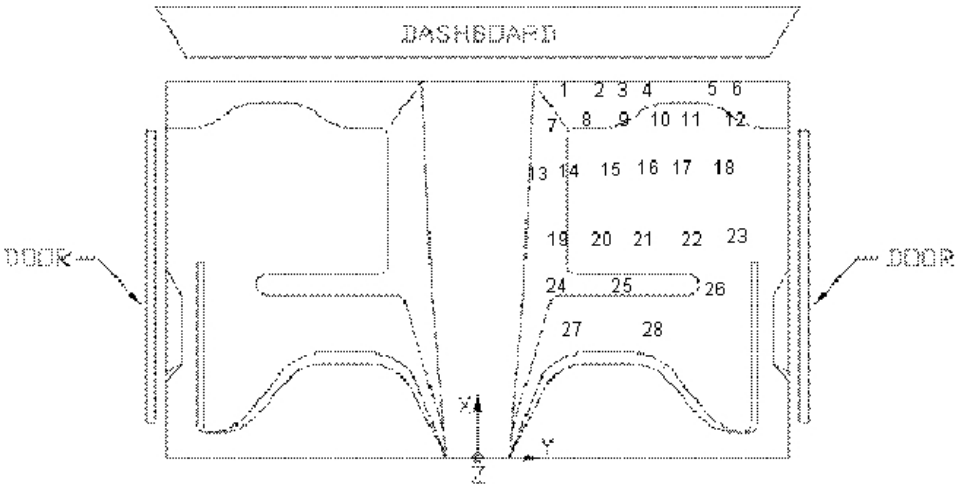

Figure C-1.Occupant Compartment Deformation Data - Set 1, Test SR-5

VEHICLE PRE/POST CRUSH INFO
Set-2

TEST: SR-5
VEHICLE: 1997 Ford F250

Note: If impact is on driver side need to enter negative number for Y'

POINT	X	Y	Z	X'	Y'	Z'	DEL X	DEL Y	DEL Z
1	50.5	19.75	7	50.5	20.25	6.5	0	0.5	-0.5
2	50.5	23.5	7.25	50.75	23.75	7	0.25	0.25	-0.25
3	50.5	28	7.25	51	25.5	7.25	0.5	-0.5	0
4	50.5	28.75	7.25	51	28.5	7	0.5	-0.25	-0.25
5	50.75	36	7	50.75	35.5	6.75	0	-0.5	-0.25
6	50.75	38.75	7	50.25	38.5	6.5	-0.5	-0.25	-0.5
7	45	18.25	6	45	18.5	5.5	0	0.25	-0.5
8	46	22	9.5	46	21.75	8.75	0	-0.25	-0.75
9	46	26.25	9.5	46	26	8.75	0	-0.25	-0.75
10	46	30.25	9.5	46.25	29.75	9.25	0.25	-0.5	-0.25
11	46	33.75	9.5	46.25	33	9.75	0.25	-0.75	0.25
12	46	38.5	9.25	46.25	37.5	9.75	0.25	-1	0.5
13	37.5	16.75	4.5	37.5	16.75	3.75	0	0	-0.75
14	38	20.25	9.75	38.25	20.25	9.25	0.25	0	-0.5
15	38.25	24.75	9.75	38.5	24.75	9.25	0.25	0	-0.5
16	38.5	29	9.5	38.25	29	8.25	-0.25	0	-1.25
17	38.5	32.75	9.5	38.5	32.5	9.25	0	-0.25	-0.25
18	38.5	37.25	9.5	38.75	36.5	10	0.25	-0.75	0.5
19	27.5	19	9.75	27	19	9.25	-0.5	0	-0.5
20	27.5	23.75	9.5	27.25	23.75	9.25	-0.25	0	-0.25
21	27.5	28.5	9.5	27.25	28.5	9.25	-0.25	0	-0.25
22	27.5	33.75	9	27.25	33.75	9	-0.25	0	0
23	28	38.75	9.25	27.5	38.5	9.75	-0.5	-0.25	0.5
24	20.25	18.75	7.25	20.25	19	6.75	0	0.25	-0.5
25	20.25	26	7.5	20.25	26	7.25	0	0	-0.25
26	19.75	36.25	6.5	19.75	36.5	6.5	0	0.25	0
27	13.5	20.5	8	13.5	20.75	8	0	0.25	0
28	13.5	29.5	7.75	13.5	30	7.75	0	0.5	0
29									
30									

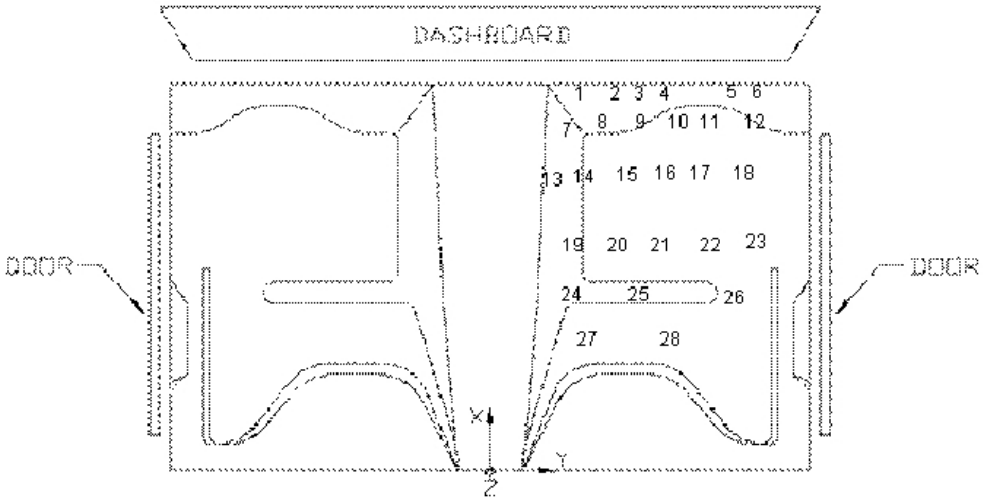

Figure C-2.Occupant Compartment Deformation Data - Set 2, Test SR-5

Occupant Compartment Deformation Index (OCDI)

Test No. SR-5
Vehicle Type: 2000p

OCDI = XXABCDEFGHI

XX = location of occupant compartment deformation

A = distance between the dashboard and a reference point at the rear of the occupant compartment, such as the top of the rear seat or the rear of the cab on a pickup

B = distance between the roof and the floor panel

C = distance between a reference point at the rear of the occupant compartment and the motor panel

D = distance between the lower dashboard and the floor panel

E = interior width

F = distance between the lower edge of right window and the upper edge of left window

G = distance between the lower edge of left window and the upper edge of right window

H= distance between bottom front corner and top rear corner of the passenger side window

I= distance between bottom front corner and top rear corner of the driver side window

Severity Indices

0 - if the reduction is less than 3%
1 - if the reduction is greater than 3% and less than or equal to 10 %
2 - if the reduction is greater than 10% and less than or equal to 20 %
3 - if the reduction is greater than 20% and less than or equal to 30 %
4 - if the reduction is greater than 30% and less than or equal to 40 %

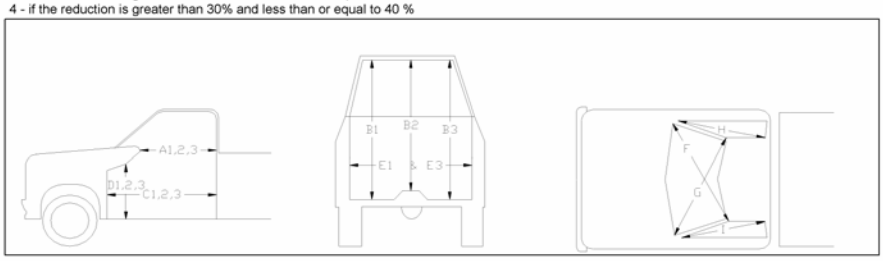

where,
1 = Passenger Side
2 = Middle
3 = Driver Side

Location:

Measurement	Pre-Test (in.)	Post-Test (in.)	Change (in.)	% Difference	Severity Index
A1	44.25	44.50	0.25	0.56	0
A2	46.00	46.00	0.00	0.00	0
A3	49.75	49.75	0.00	0.00	0
B1	48.00	48.00	0.00	0.00	0
B2	44.00	43.75	-0.25	-0.57	0
B3	48.50	48.00	-0.50	-1.03	0
C1	64.50	64.75	0.25	0.39	0
C2	62.75	63.00	0.25	0.40	0
C3	63.50	62.75	-0.75	-1.18	0
D1	19.50	19.50	0.00	0.00	0
D2	11.75	11.75	0.00	0.00	0
D3	15.75	17.00	1.25	7.94	1
E1	63.50	62.25	-1.25	-1.97	0
E3	64.50	64.50	0.00	0.00	0
F	59.00	59.00	0.00	0.00	0
G	58.50	58.75	0.25	0.43	0
H	42.75	42.50	-0.25	-0.58	0
I	42.25	42.00	-0.25	-0.59	0

Note: Maximum sevrity index for each variable (A-I) is used for determination of final OCDI value

	XX A B C D E F G H I
Final OCDI:	RF 0 0 0 1 0 0 0 0 0

Figure C-3.Occupant Compartment Deformation Index (OCDI), Test SR-5

APPENDIX D

Accelerometer and Rate Transducer Data Analysis, Test SR-5

Figure D-1. Graph of Longitudinal Deceleration, Test SR-5
Figure D-2. Graph of Longitudinal Occupant Impact Velocity, Test SR-5
Figure D-3. Graph of Longitudinal Occupant Displacement, Test SR-5
Figure D-4. Graph of Lateral Deceleration, Test SR-5
Figure D-5. Graph of Lateral Occupant Impact Velocity, Test SR-5
Figure D-6. Graph of Lateral Occupant Displacement, Test SR-5
Figure D-7. Graph of Roll, Pitch, and Yaw Angular Displacements, Test SR-5

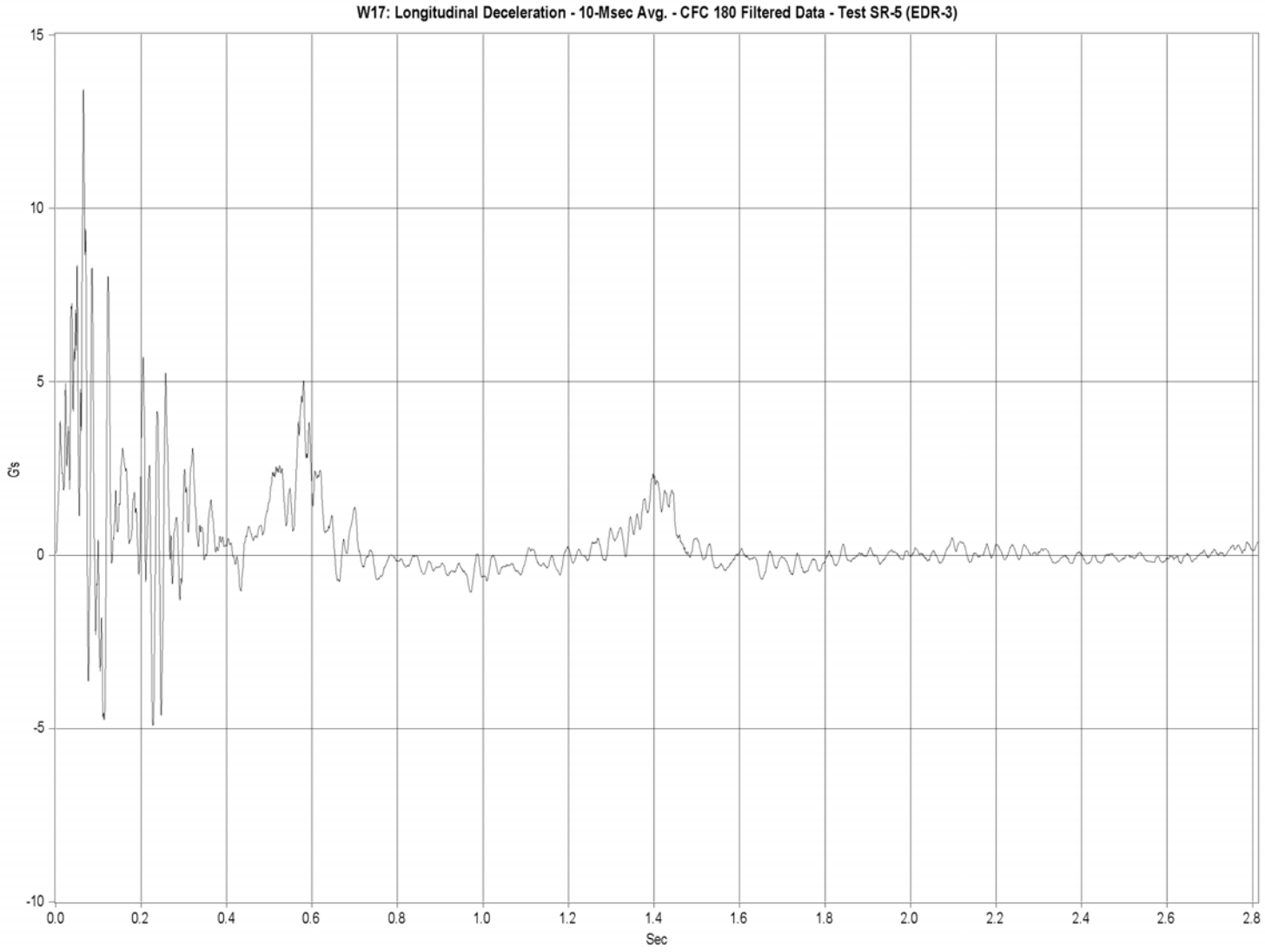

.Figure D-1. Graph of Longitudinal Deceleration, Test SR-5

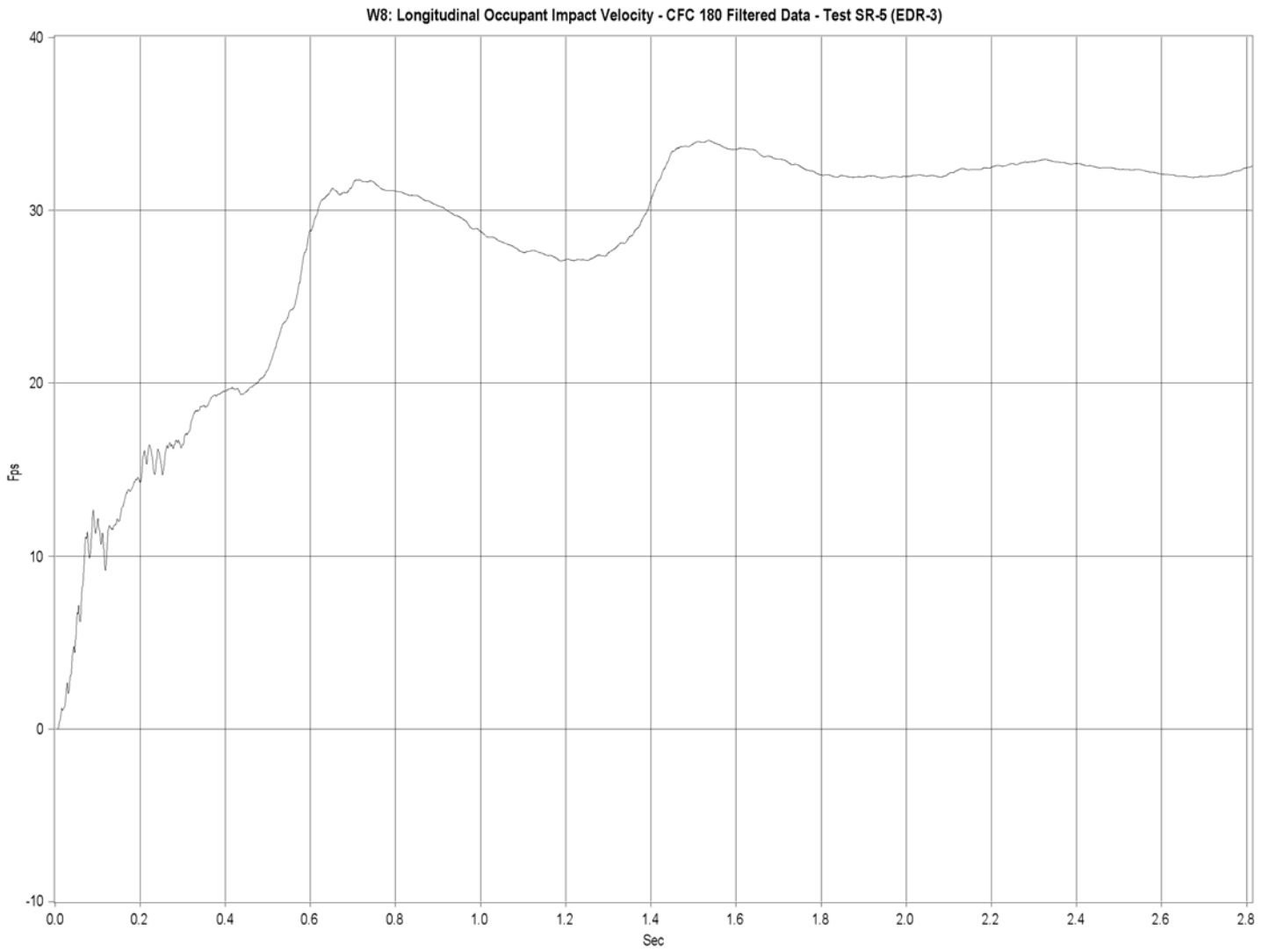

Figure D-2. Graph of Longitudinal Occupant Impact Velocity, Test SR-5

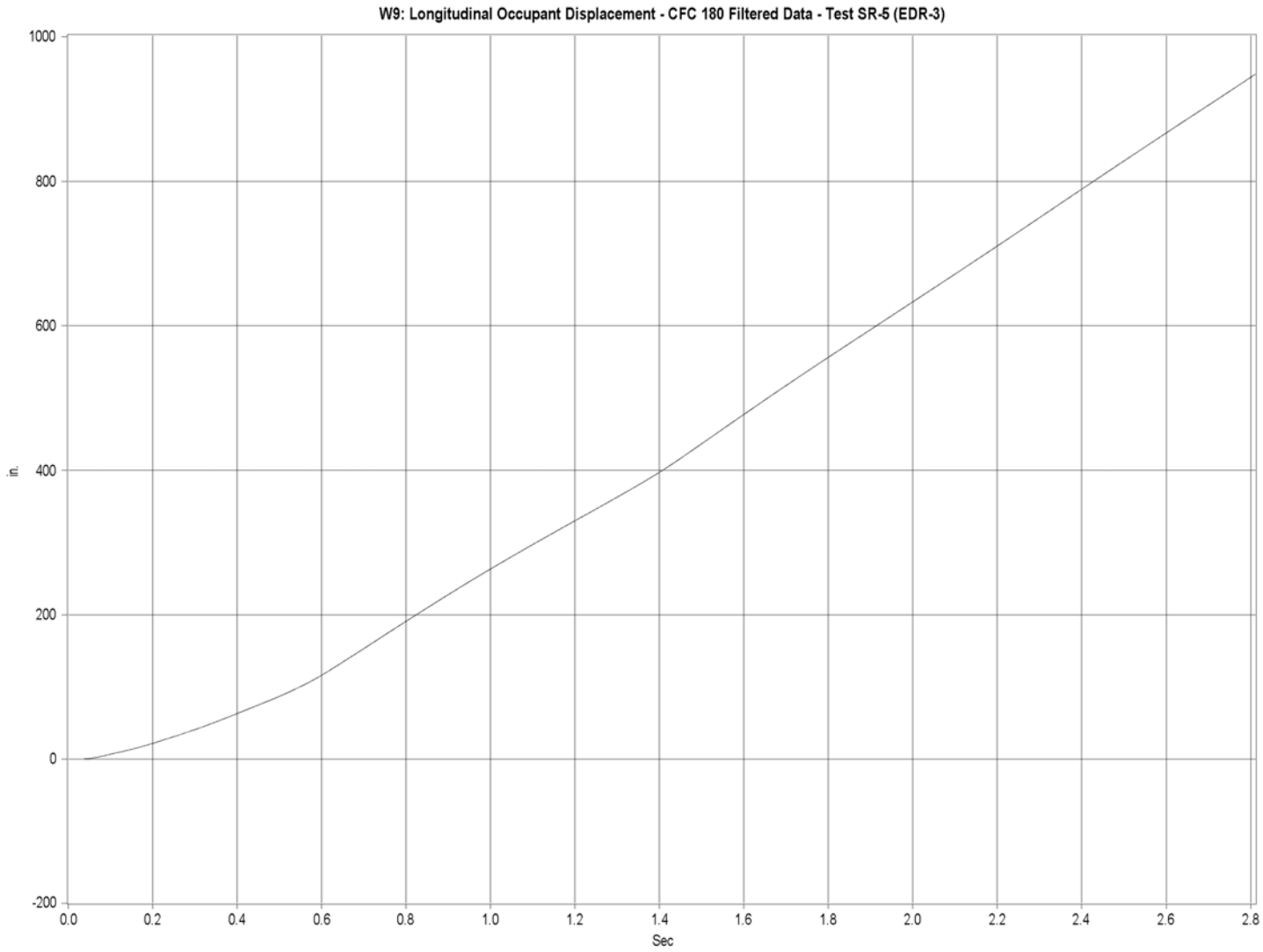

Figure D-3. Graph of Longitudinal Occupant Displacement, Test SR-5

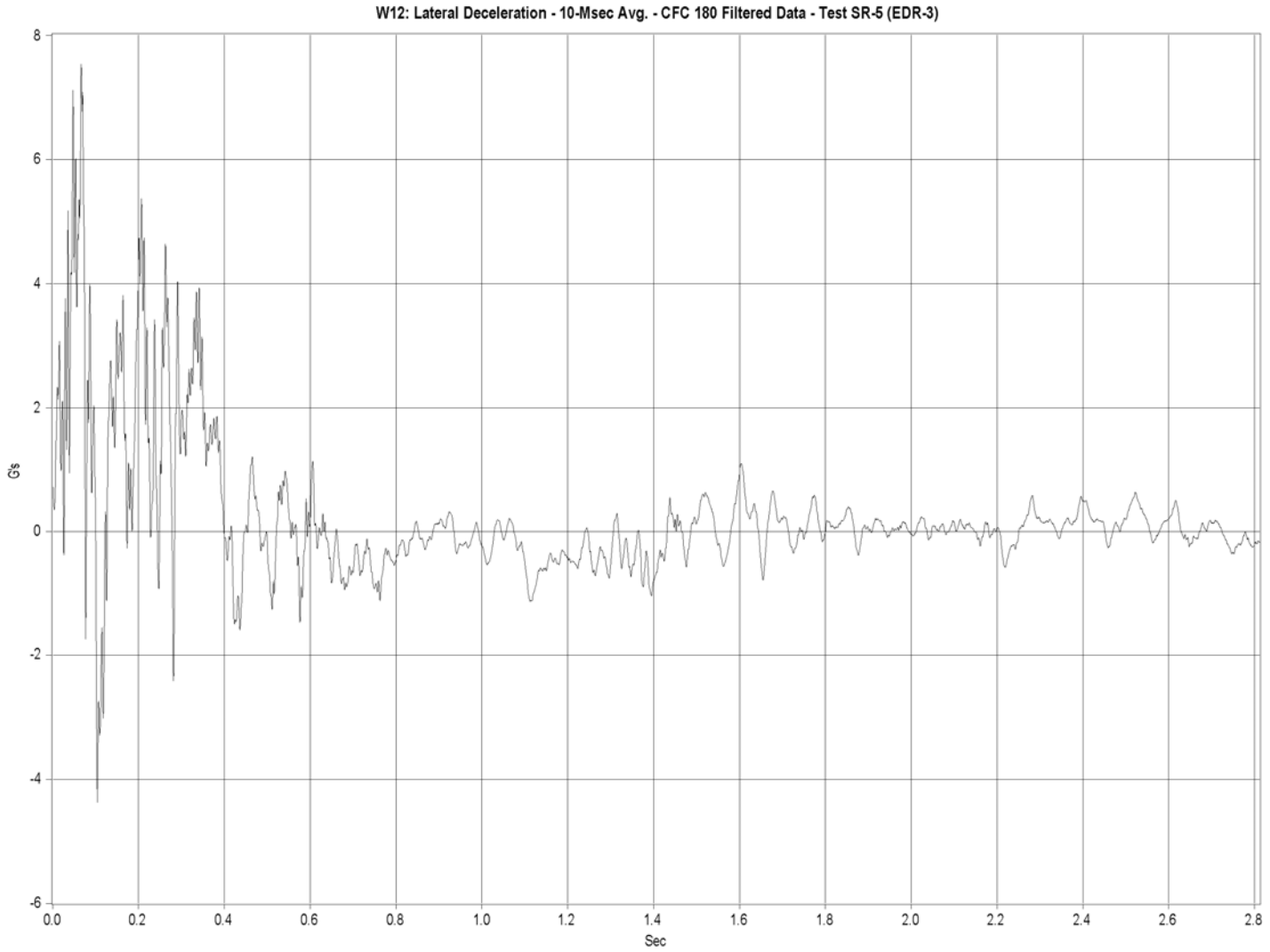

Figure D-4. Graph of Lateral Deceleration, Test SR-5

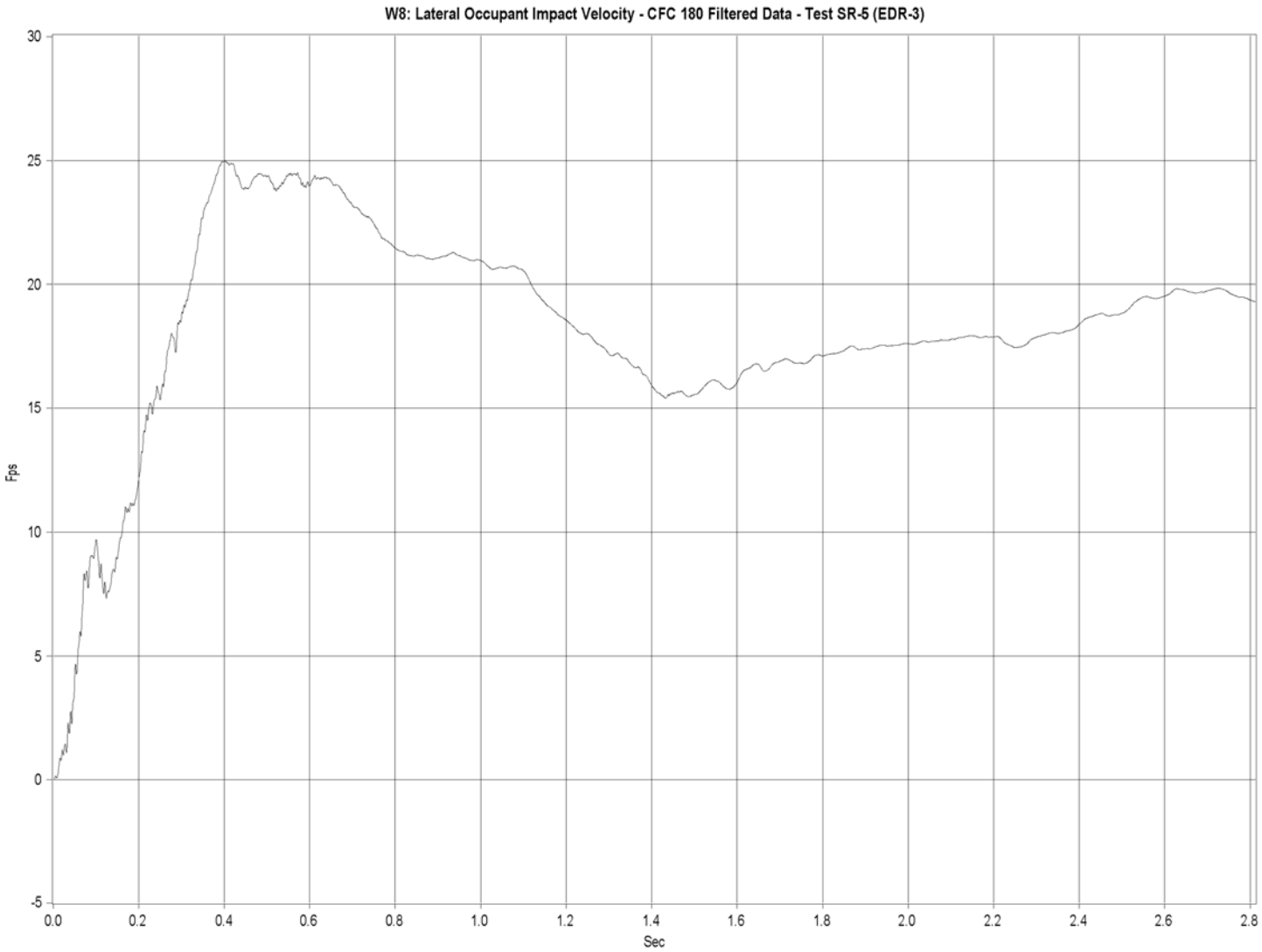

Figure D-5. Graph of Lateral Occupant Impact Velocity, Test SR-5

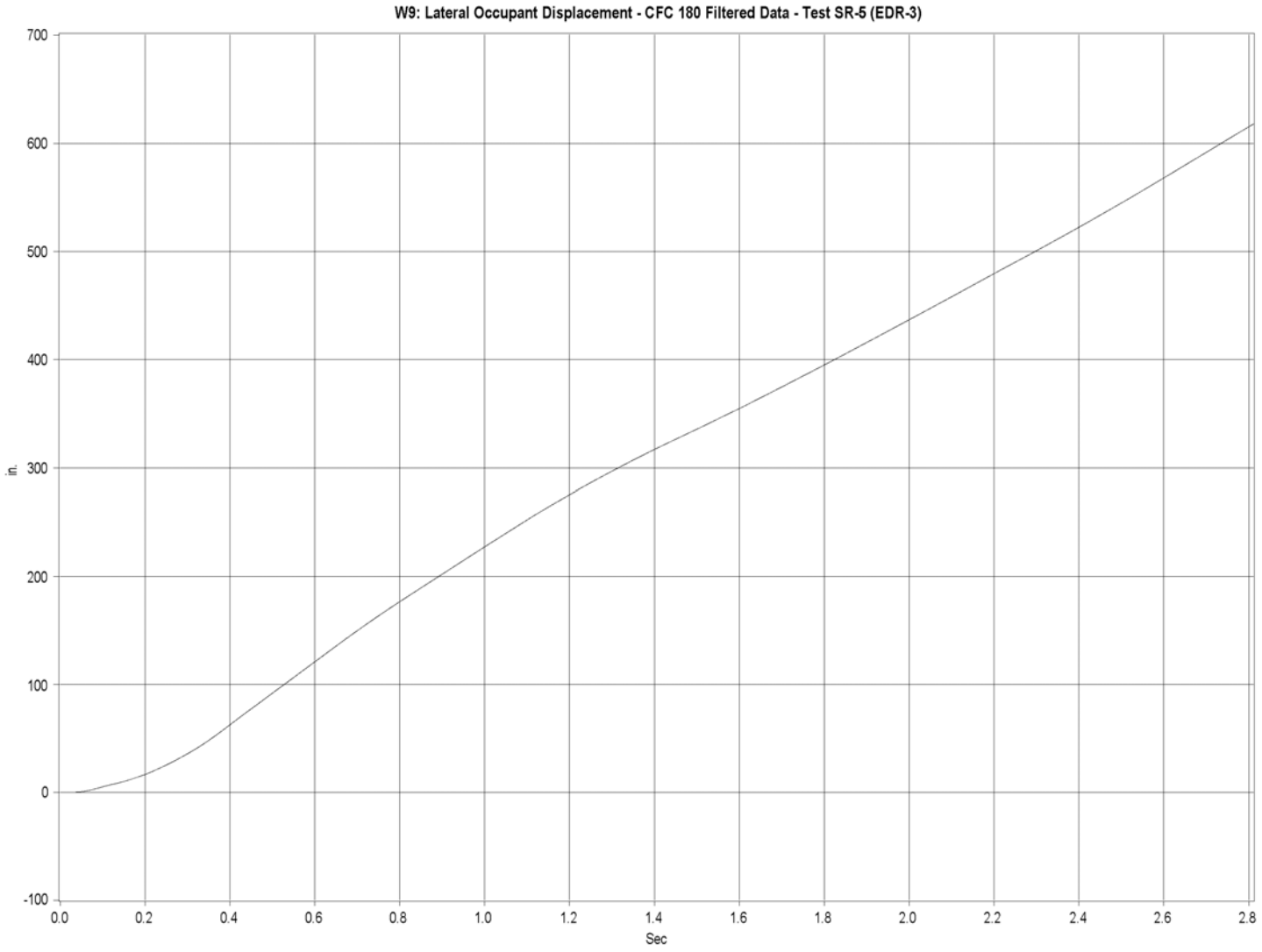

Figure D-6. Graph of Lateral Occupant Displacement, Test SR-5

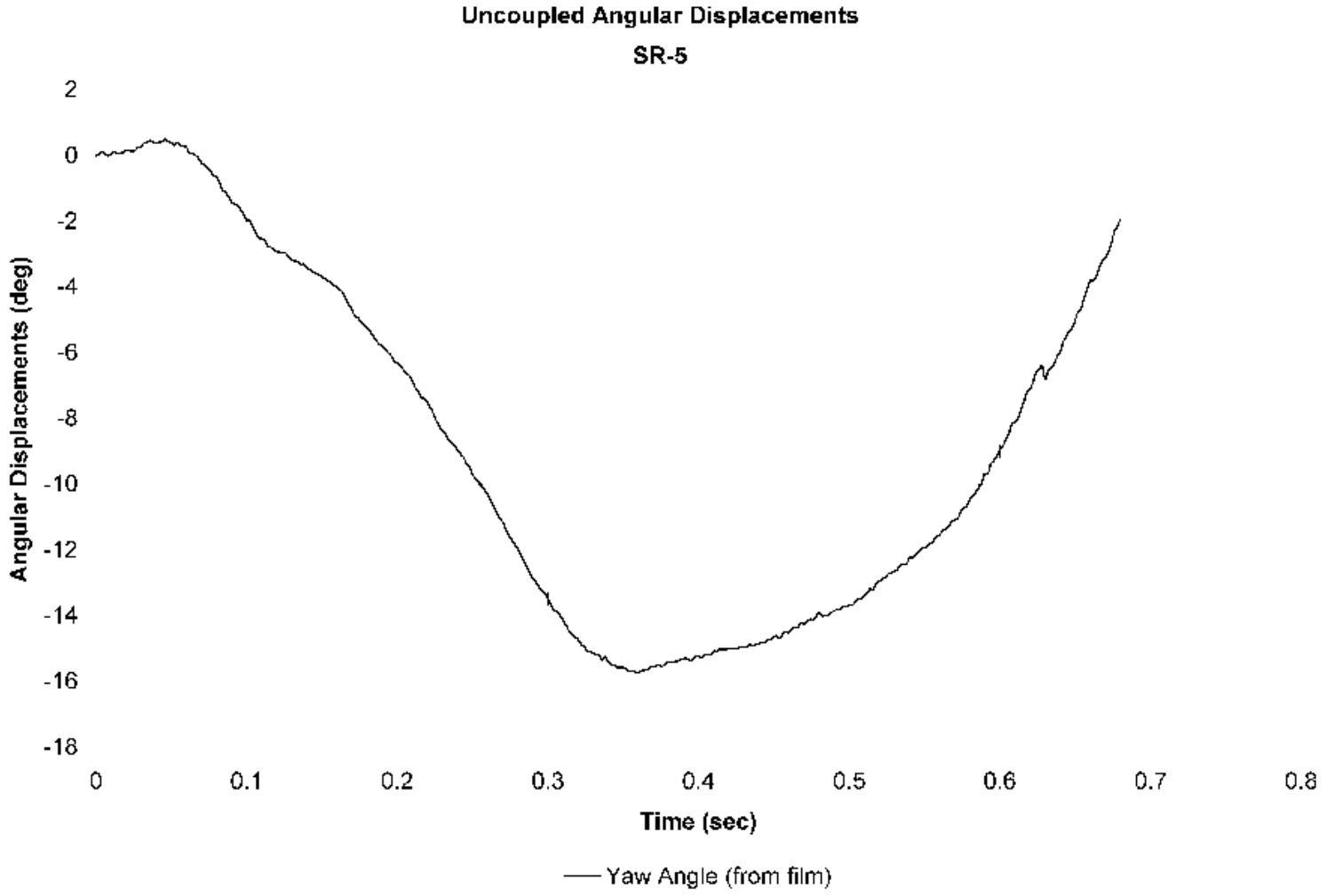

Figure D-7. Graph of Roll, Pitch, and Yaw Angular Displacements, Test SR-5

APPENDIX E

Metric-Unit System Drawings, Test SR-6

Figure E-1. Short-Radius Design Details, Test SR-6
Figure E-2. Secondary Side Design Details, Test SR-6
Figure E-3. Primary Side Design Details, Test SR-6
Figure E-4. Primary Side End Anchorage Details, Test SR-6
Figure E-5. Cable Anchor Details, Test SR-6
Figure E-6. Cable Anchor Details, Test SR-6
Figure E-7. Nose Cable Anchor Plate Details, Test SR-6
Figure E-8. MGS and Thrie Beam Foundation Tube Details, Test SR-6
Figure E-9. Wood Post Details, Test SR-6
Figure E-10. Wood Post Details, Test SR-6
Figure E-11. Wood Post Details, Test SR-6
Figure E-12. Iowa Steel Post Transition Details, Test SR-6
Figure E-13. Primary Side End Anchorage Details, Test SR-6
Figure E-14. Anchorage Post Details, Test SR-6
Figure E-15. Rail Slot Pattern No. 1 Details, Test SR-6
Figure E-16. Rail Slot Pattern No. 2 Details, Test SR-6
Figure E-17. Rail Curvature, Rail Section No. 1, Test SR-6
Figure E-18. Rail Curvature, Rail Section Nos. 2 and 3, Test SR-6
Figure E-19. Rail Curvature, Rail Section No. 4, Test SR-6

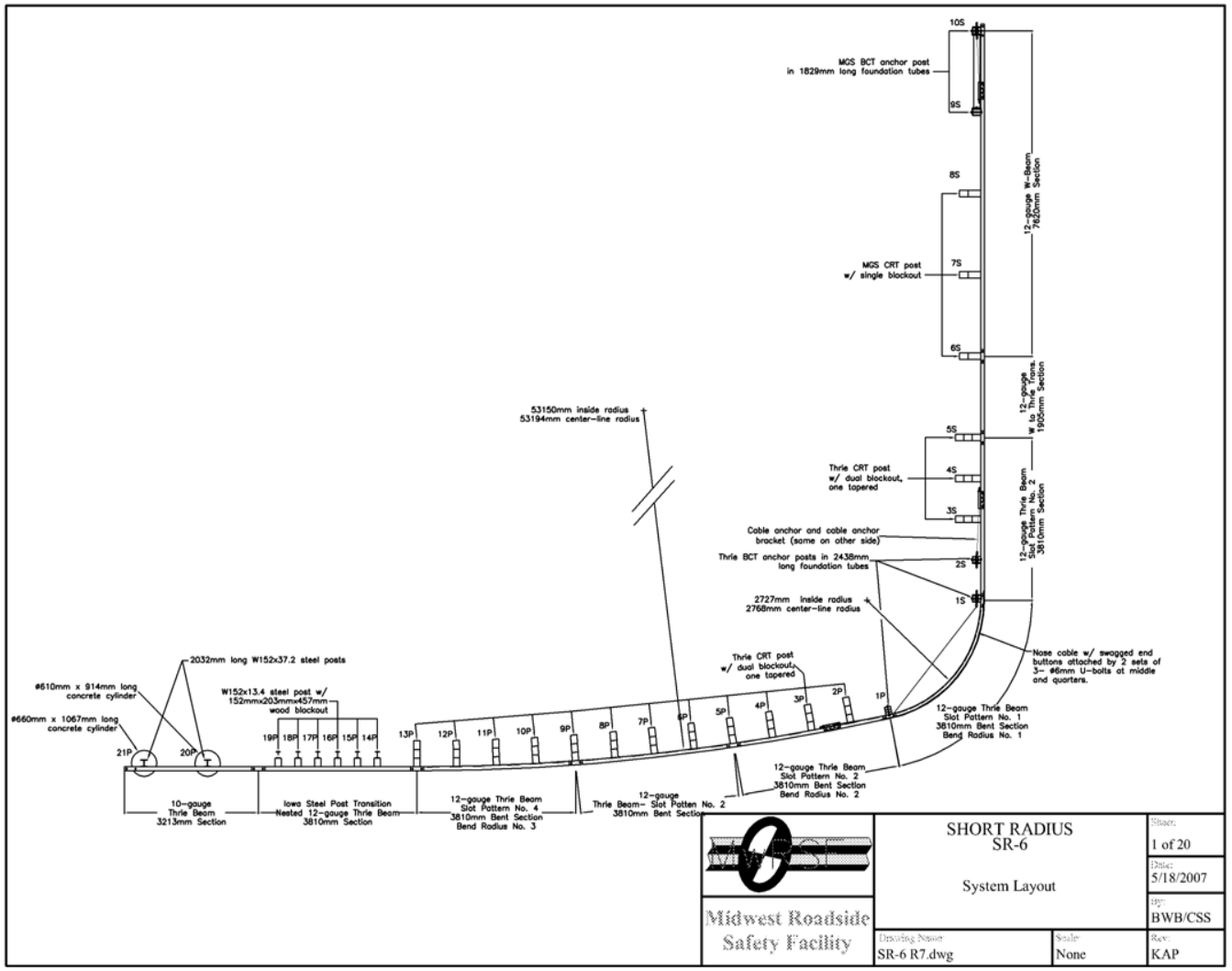

Figure E-1. Short-Radius Design Details, Test SR-6

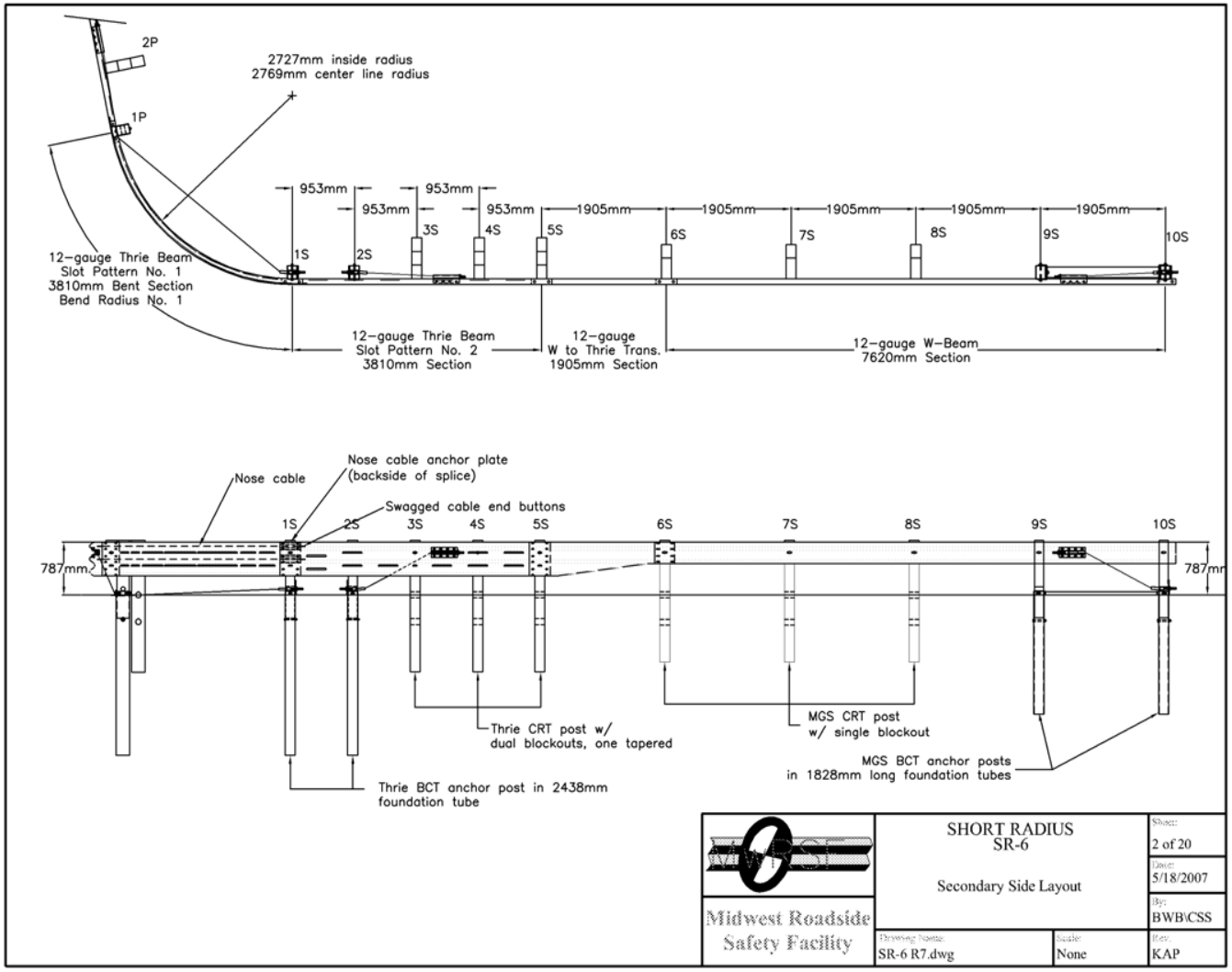

Figure E-2. Secondary Side Design Details, Test SR-6

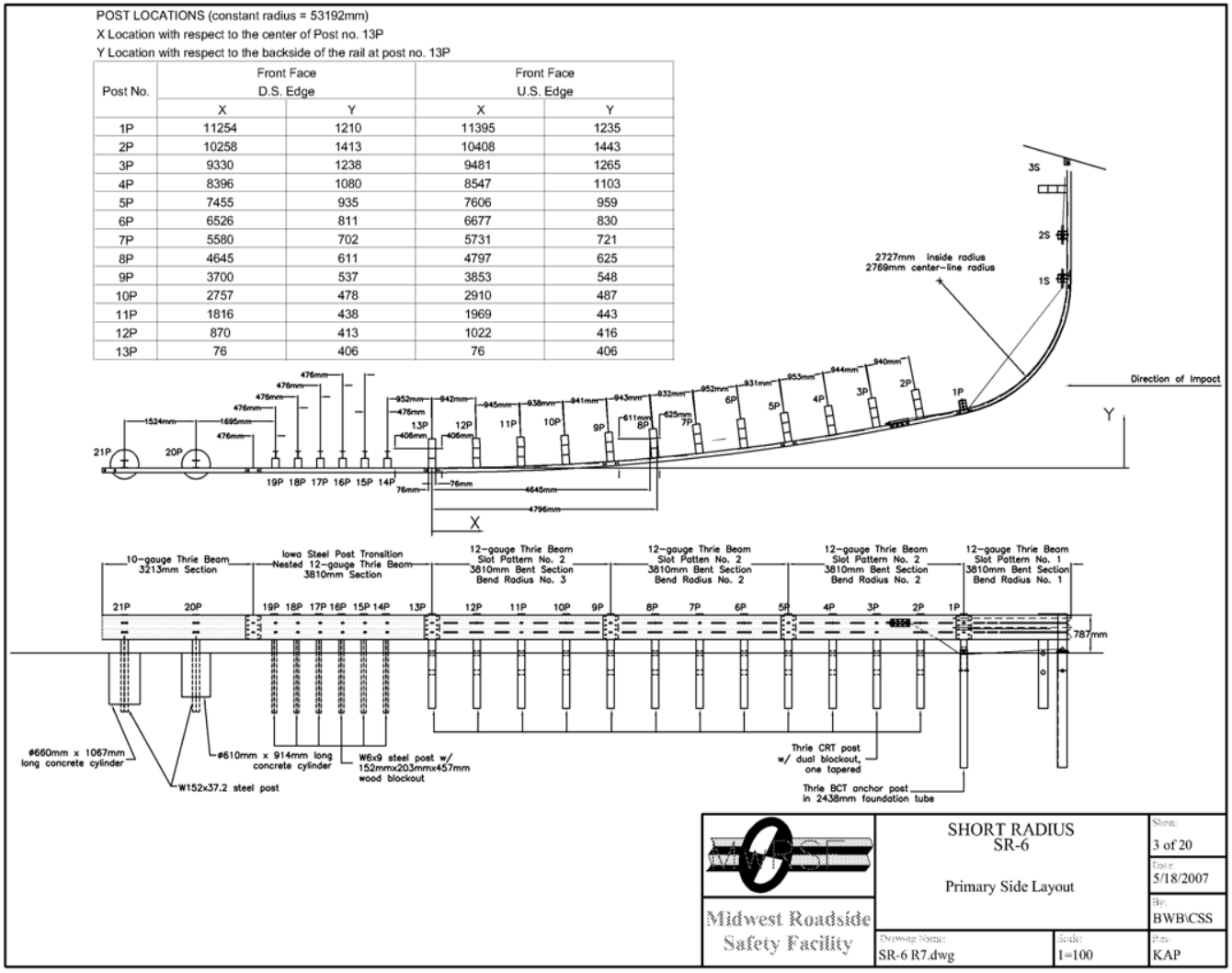

Figure E-3. Primary Side Design Details, Test SR-6

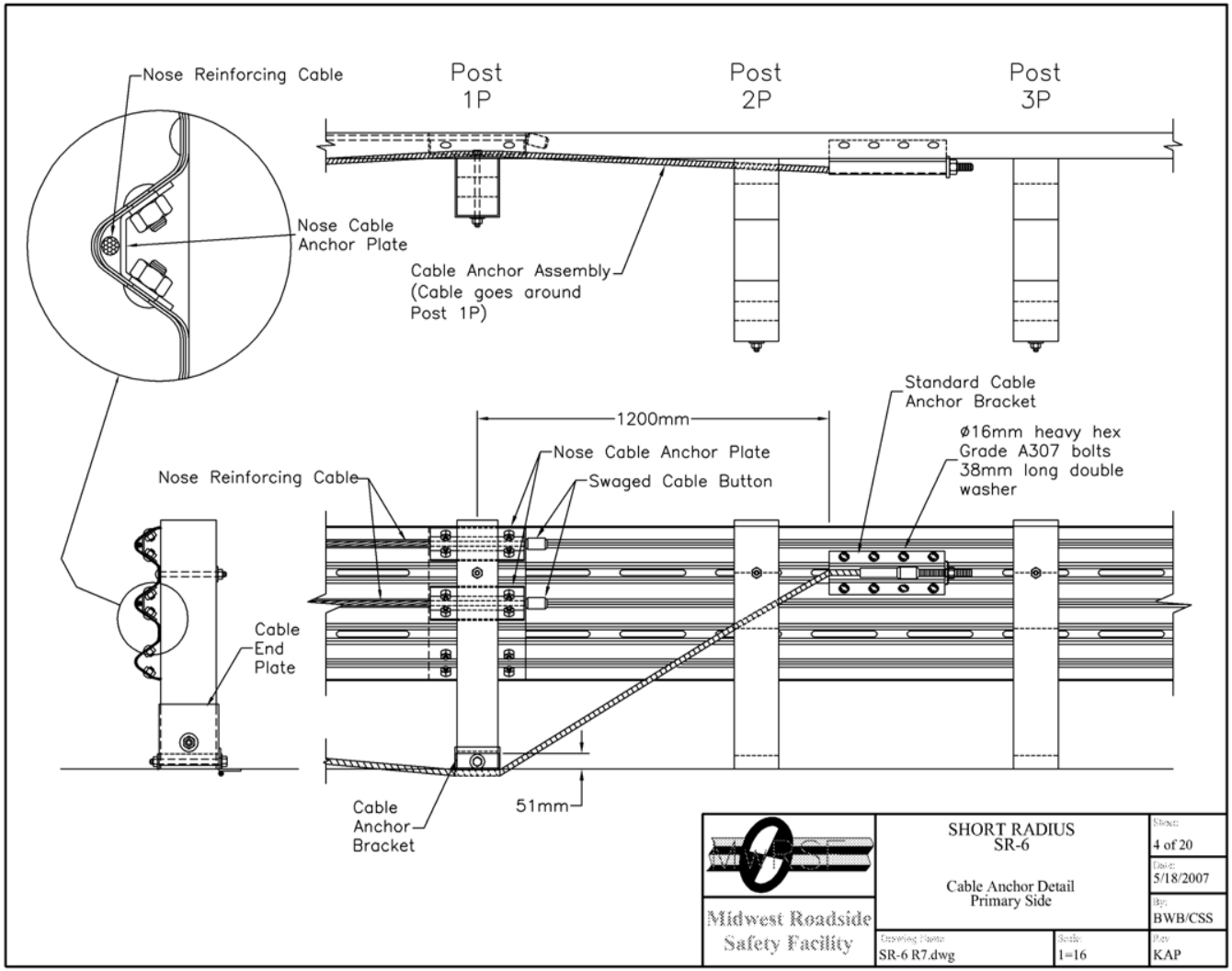

Figure E-4. Primary Side End Anchorage Details, Test SR-6

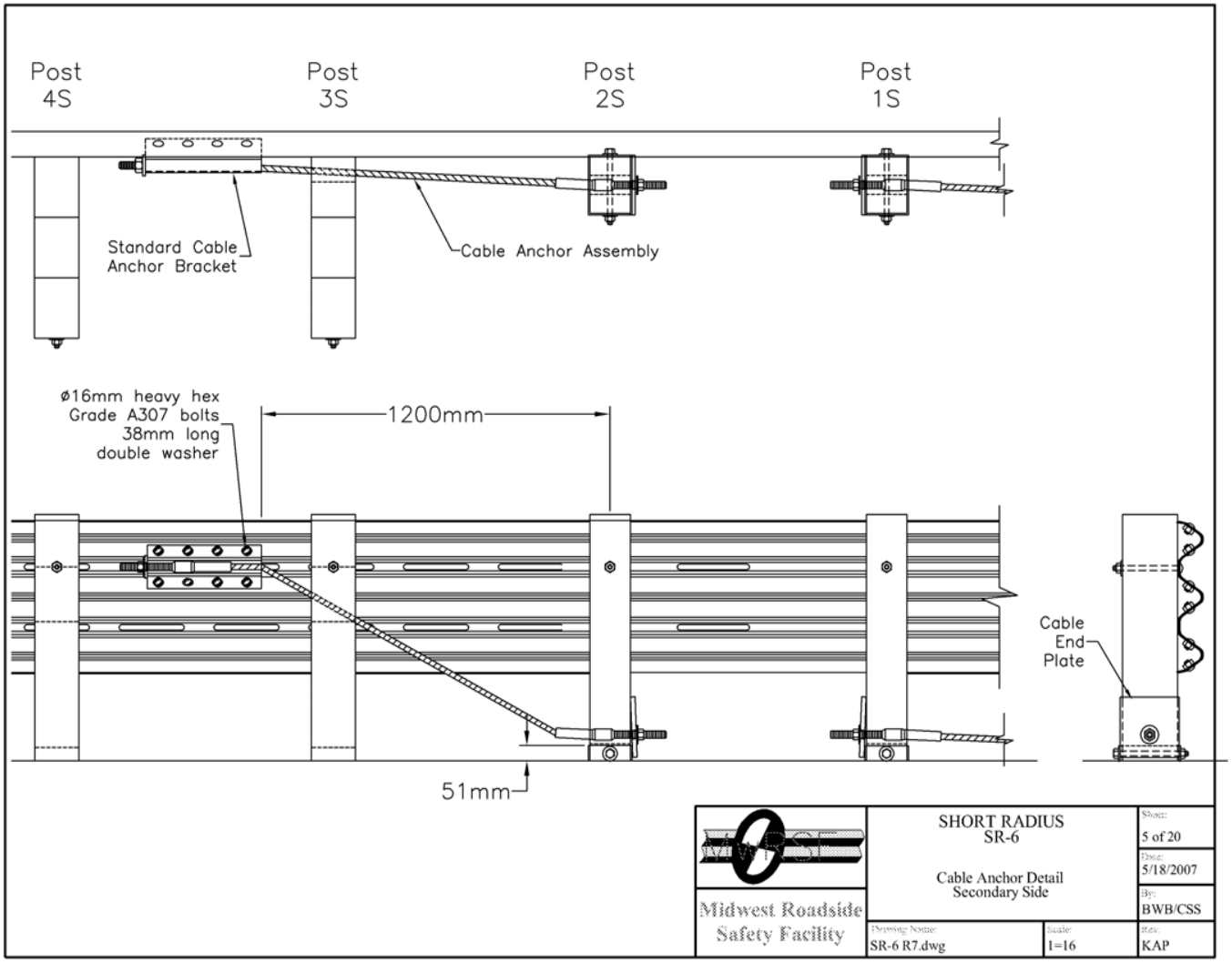

Figure E-5. Cable Anchor Details, Test SR-6

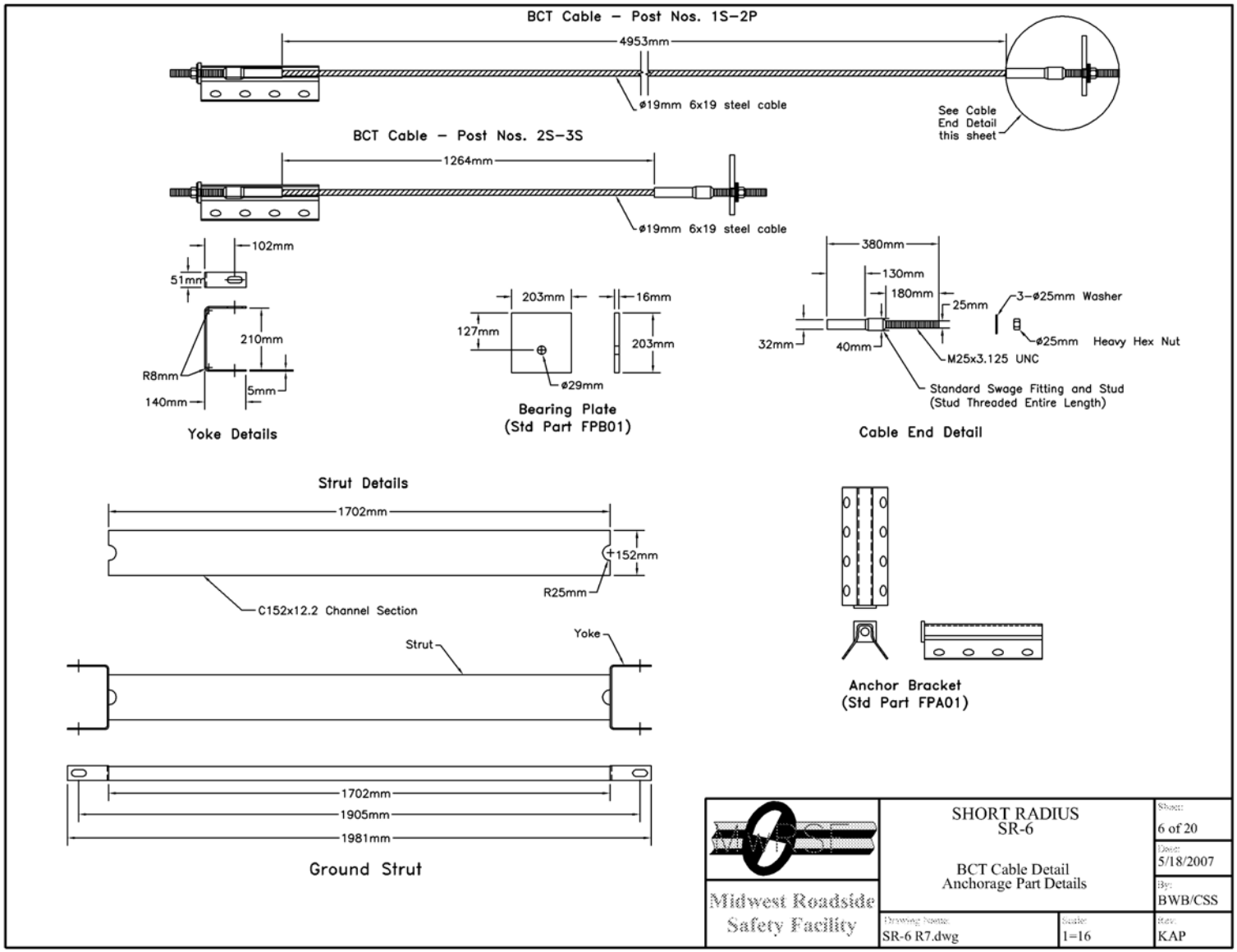

Figure E-6. Cable Anchor Details, Test SR-6

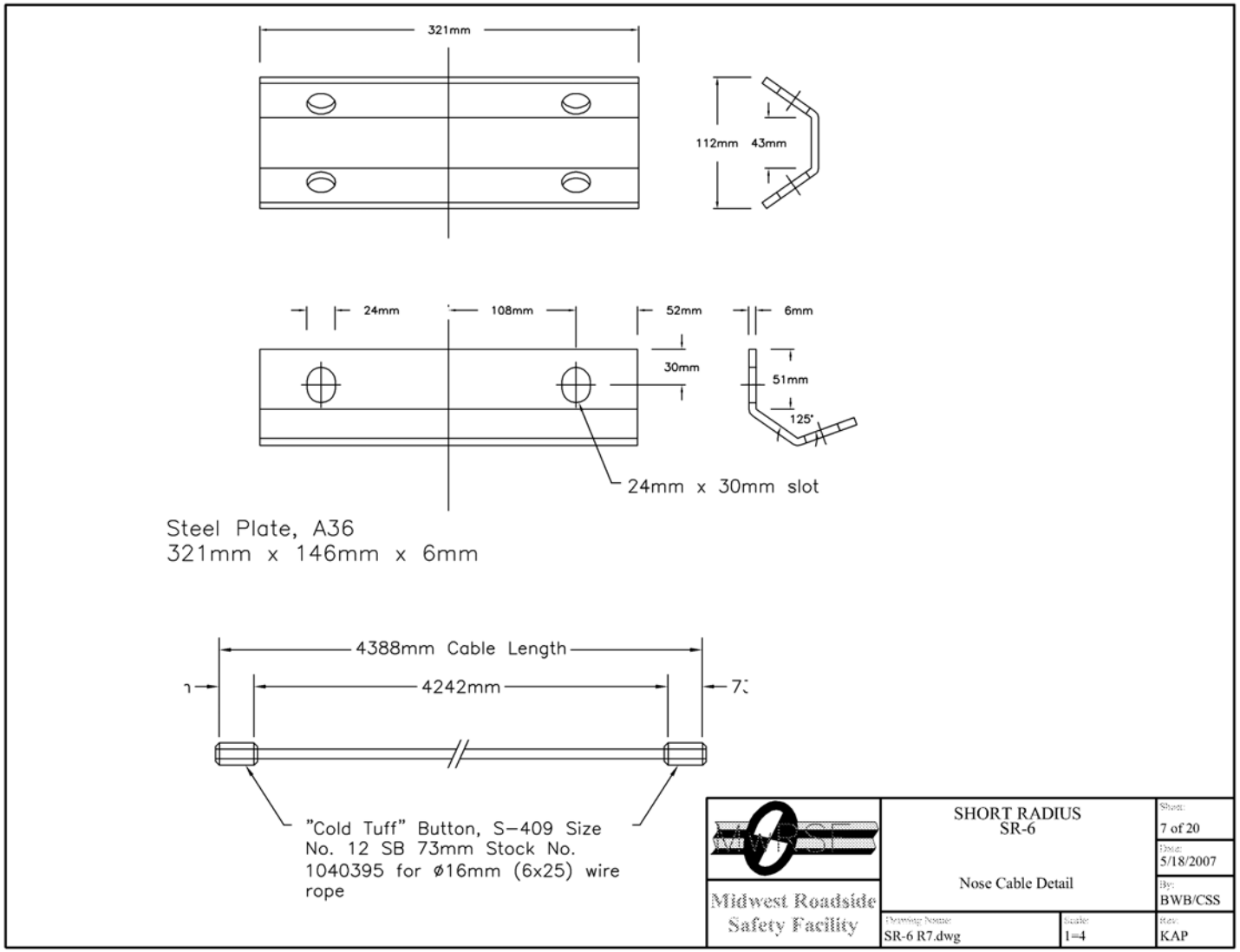

Figure E-7. Nose Cable Anchor Plate Details, Test SR-6

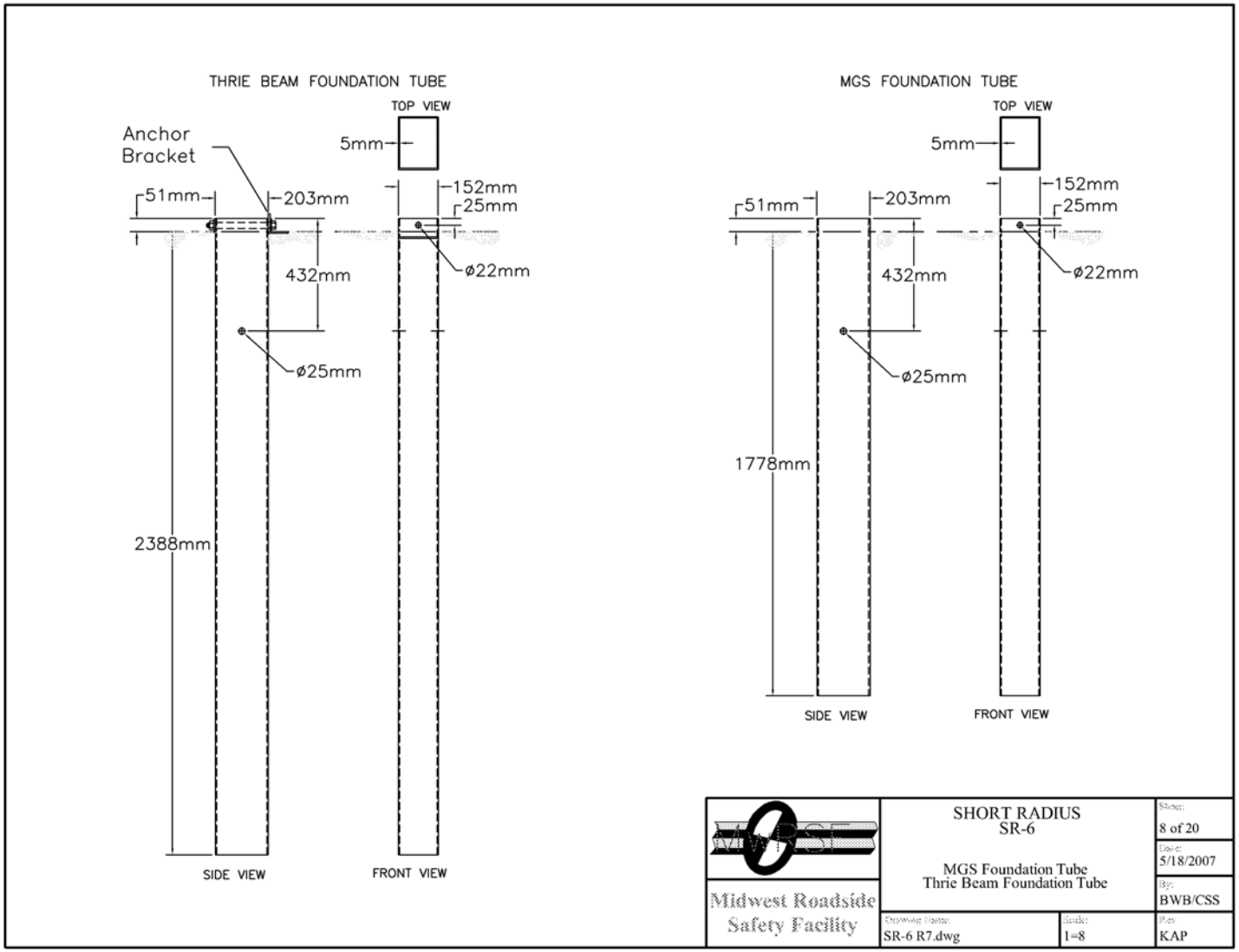

Figure E-8. MGS and Thrie Beam Foundation Tube Details, Test SR-6

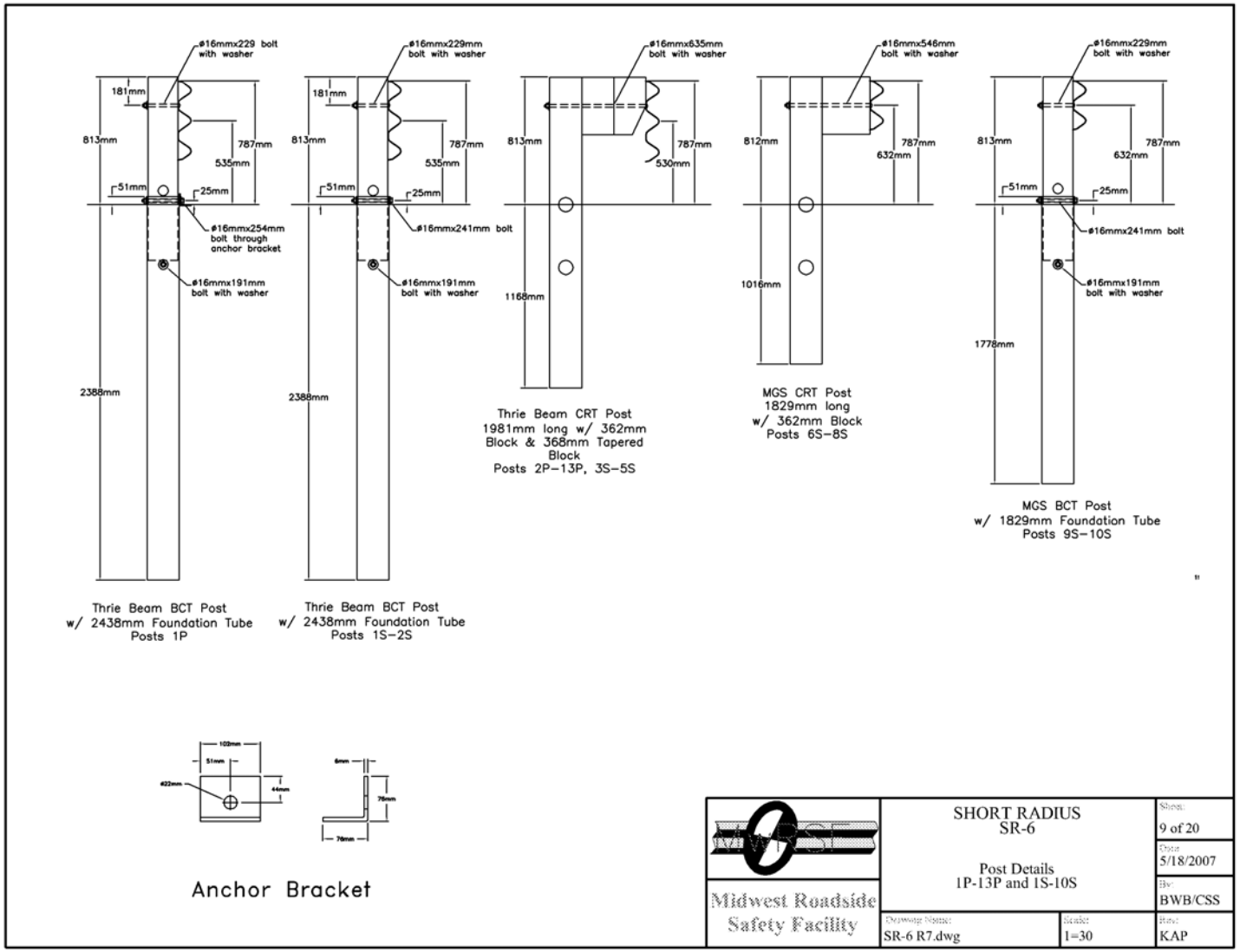

Figure E-9. Wood Post Details, Test SR-6

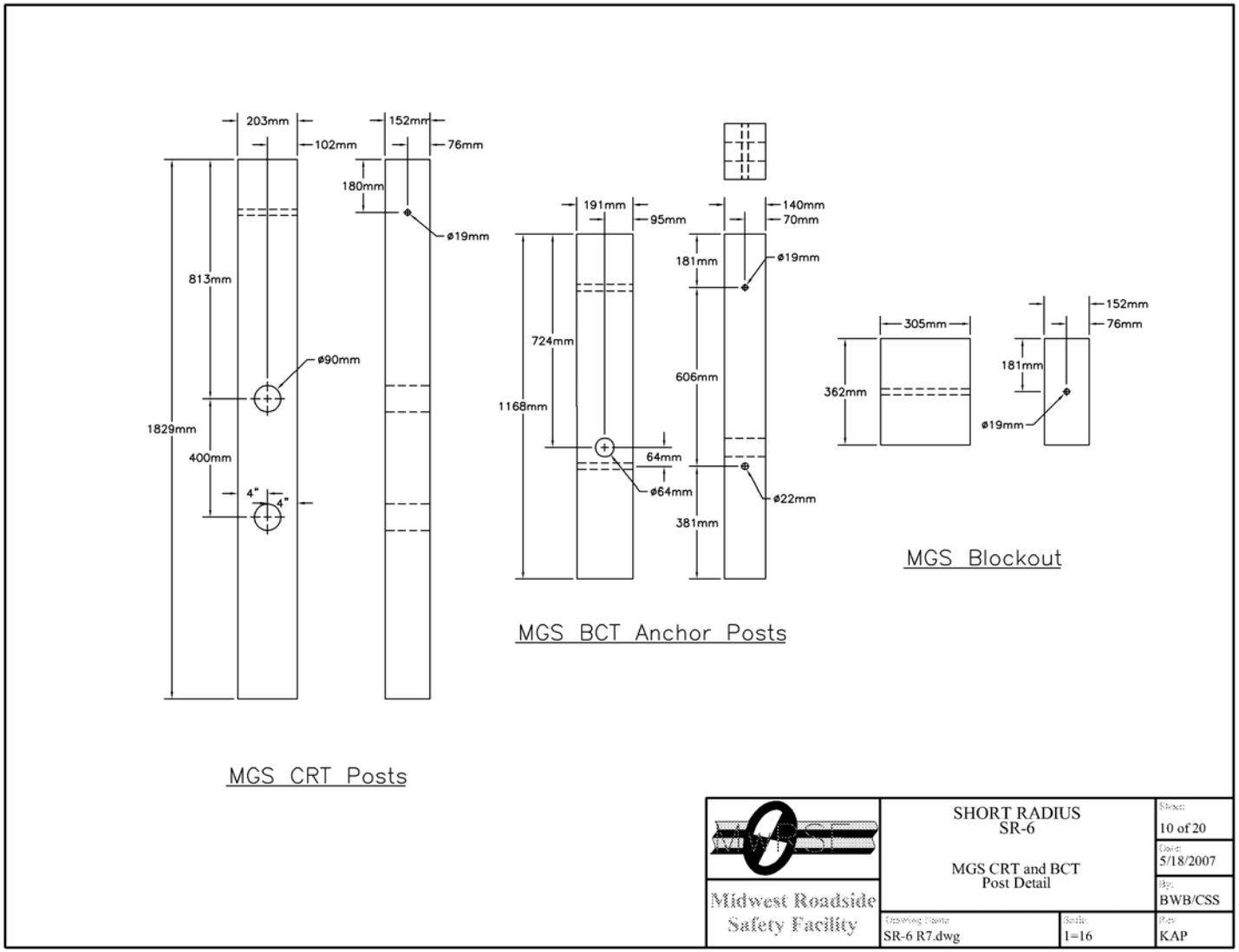

Figure E-10. Wood Post Details, Test SR-6

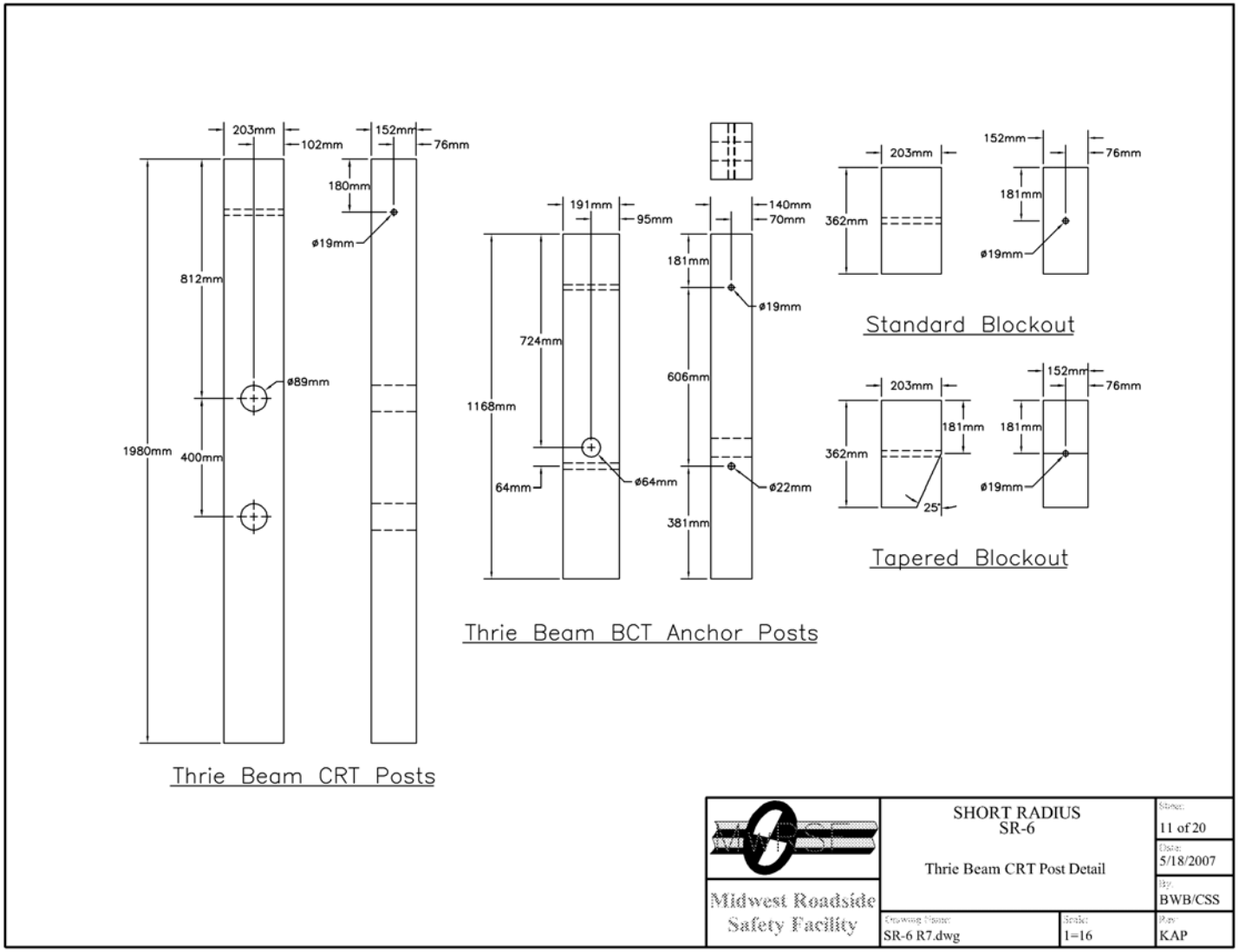

Figure E-11. Wood Post Details, Test SR-6

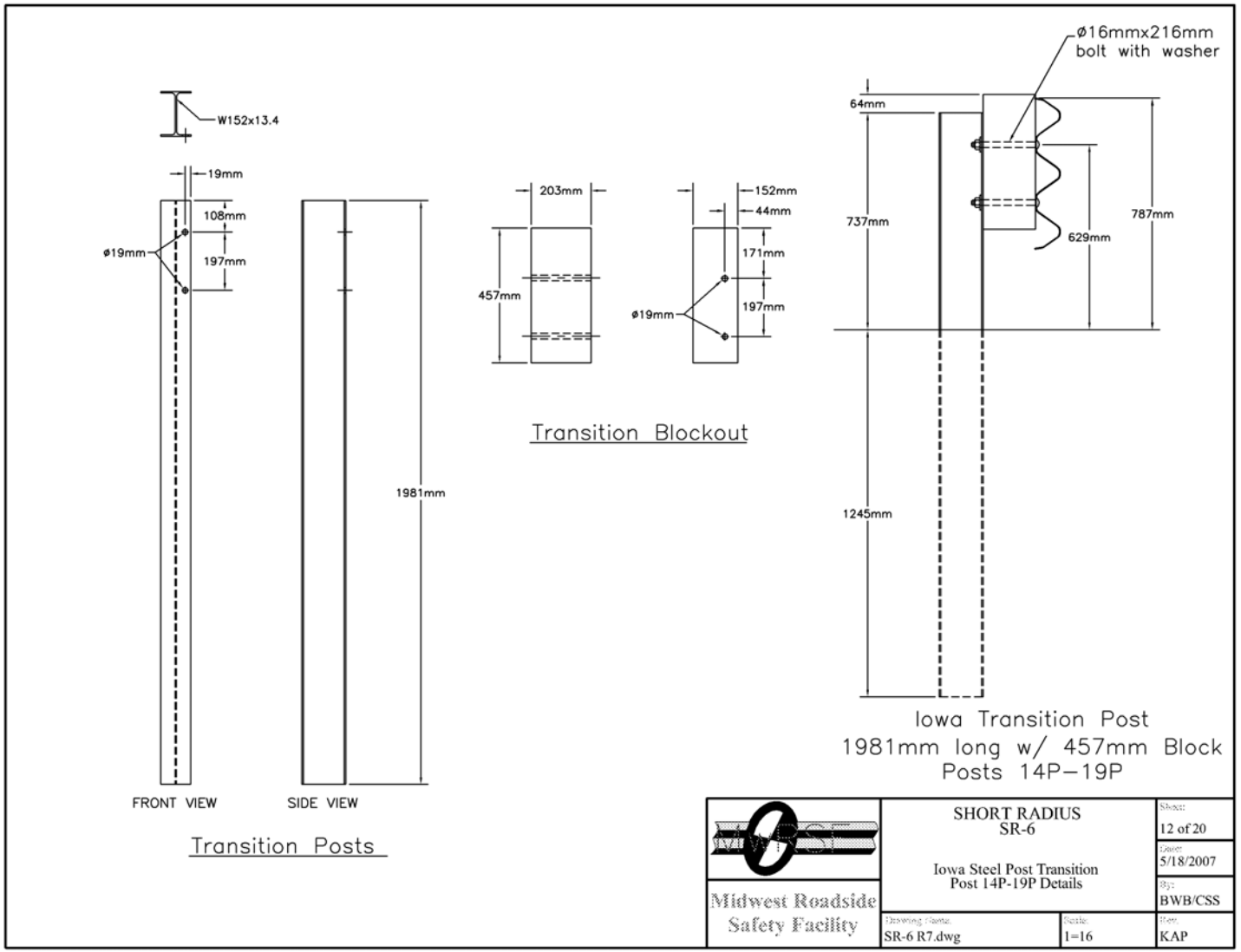

Figure E-12. Iowa Steel Post Transition Details, Test SR-6

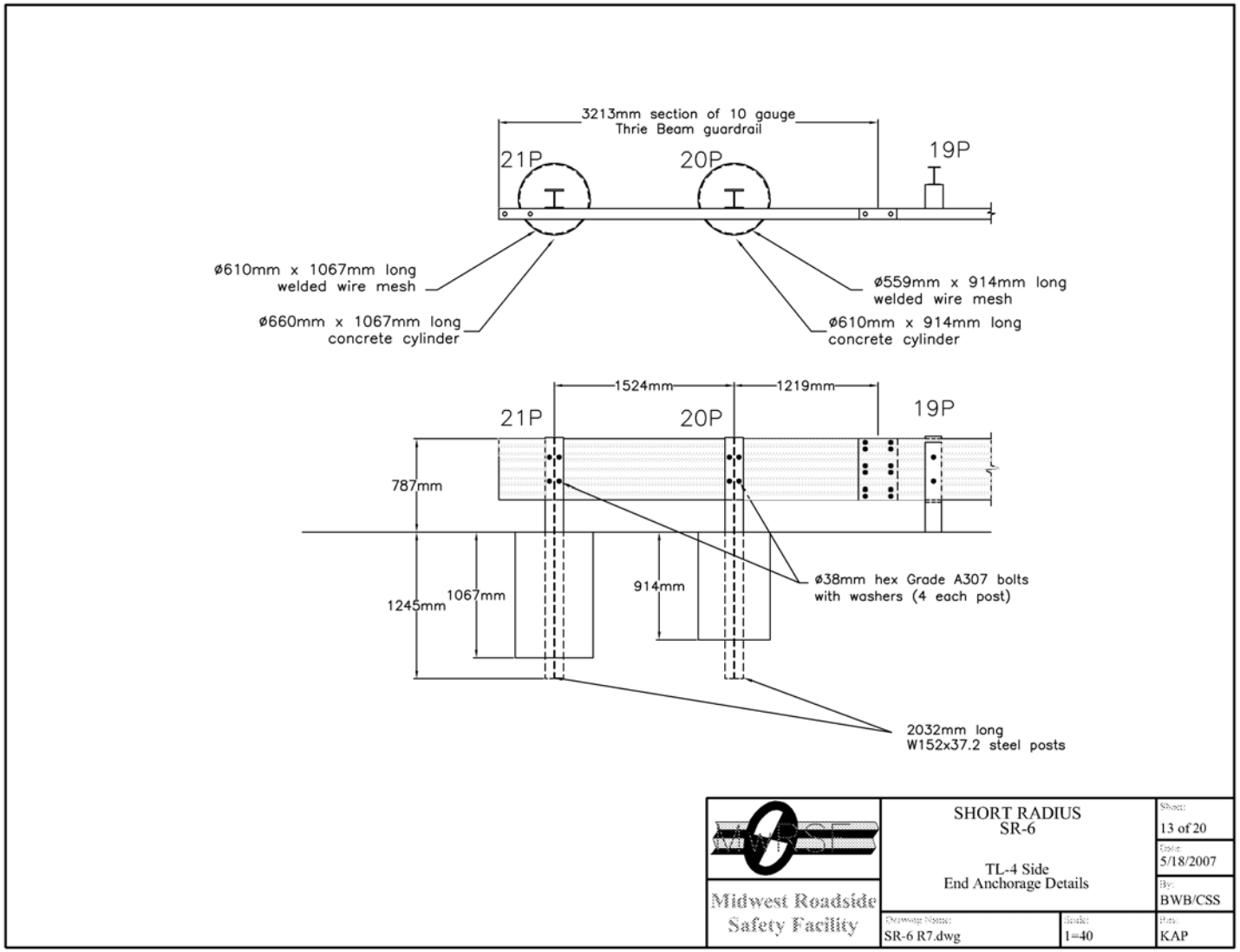

Figure E-13. Primary Side End Anchorage Details, Test SR-6

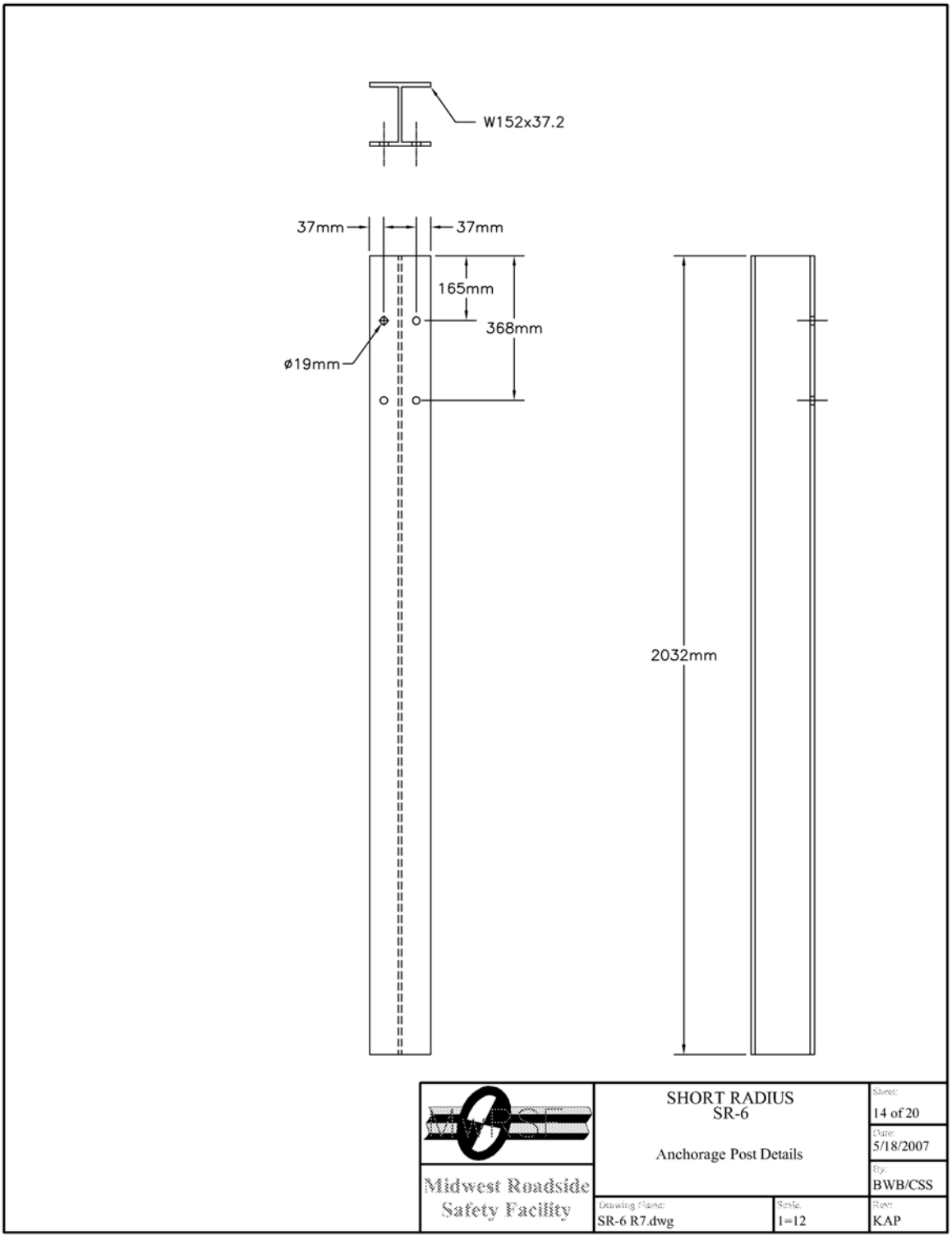

Figure E-14. Anchorage Post Details, Test SR-6

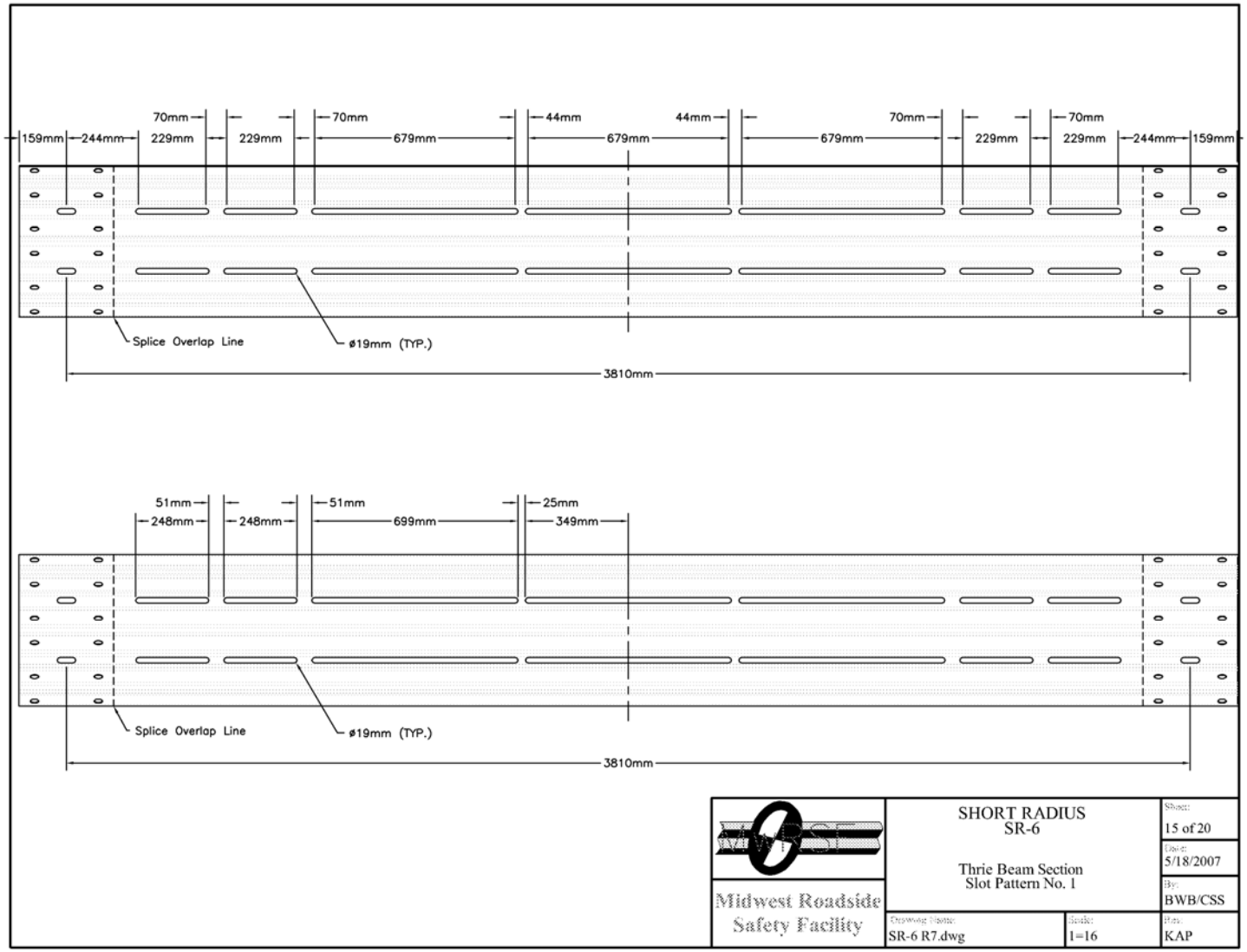

Figure E-15. Rail Slot Pattern Details, Rail Section No. 1, Test SR-6

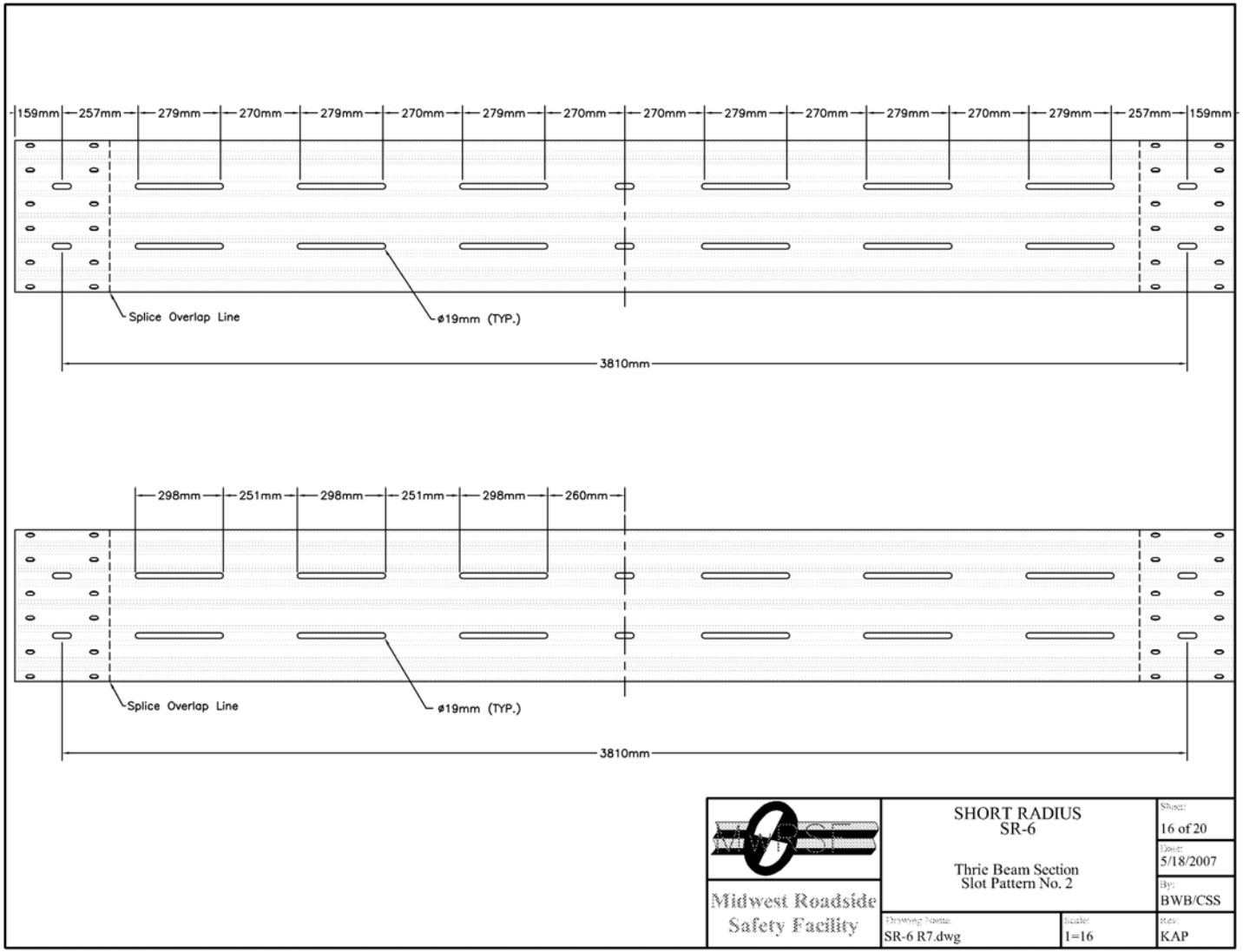

Figure E-16. Rail Slot Pattern Details, Rail Section No. 2, Test SR-6

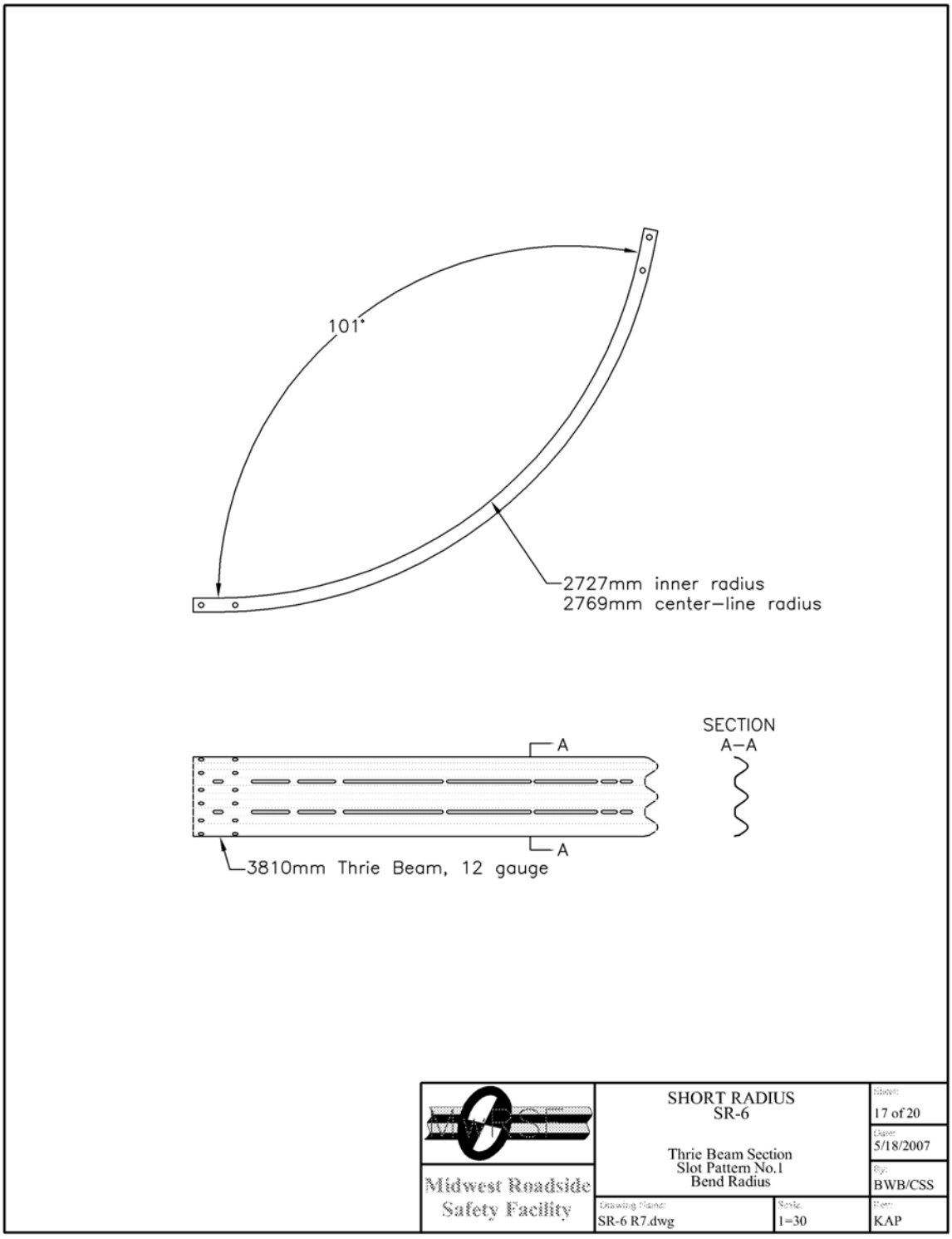

Figure E-17. Rail Curvature, Rail Section No. 1, Test SR-6

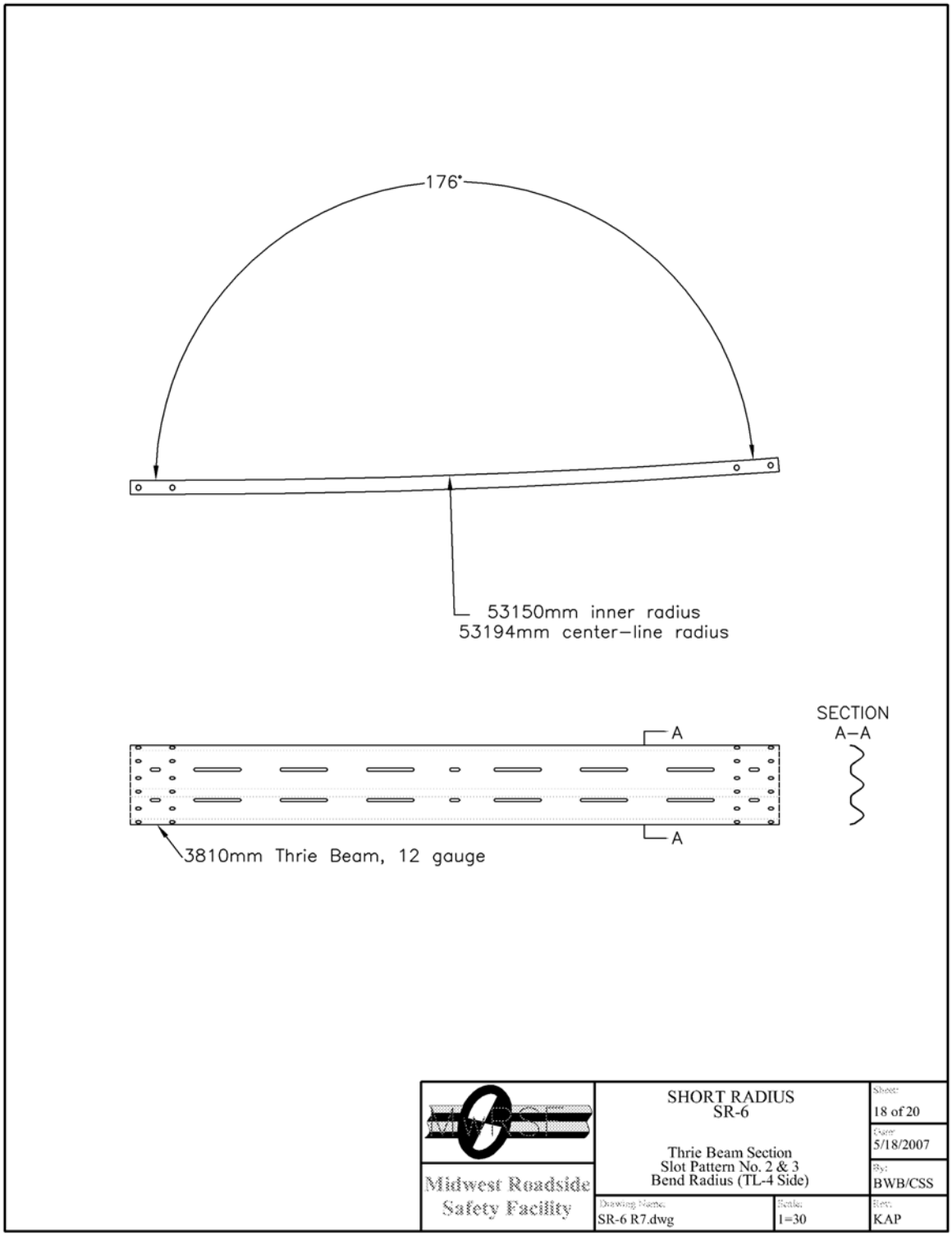

Figure E-18. Rail Curvature, Rail Section Nos. 2 and 3, Test SR-6

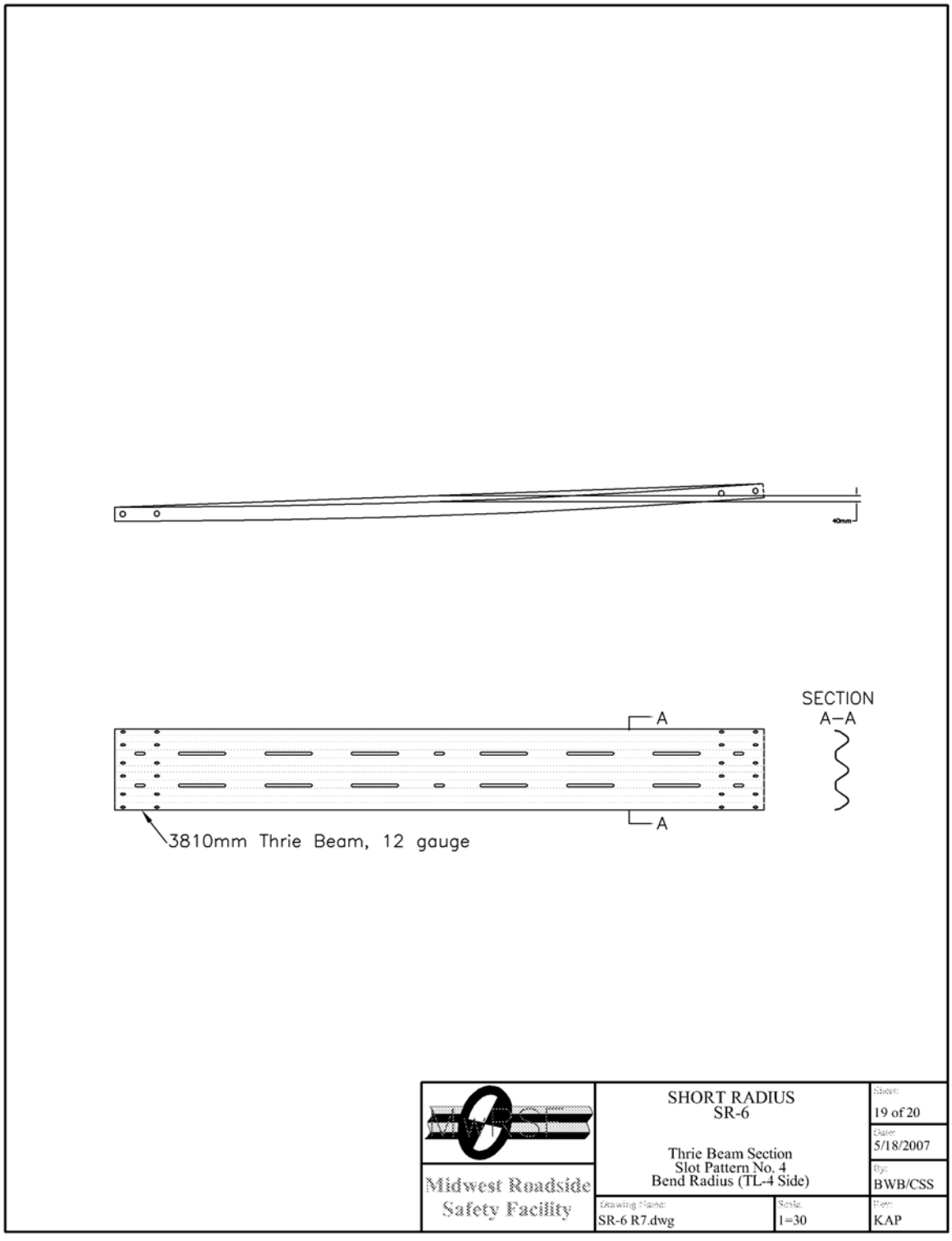

Figure E-19. Rail Curvature, Rail Section No. 4, Test SR-6

APPENDIX F

English-Unit System Drawings, Test SR-6

Figure F-1. Short-Radius Design Details (English), Test SR-6
Figure F-2. Secondary Side Design Details (English), Test SR-6
Figure F-3. Primary Side Design Details (English), Test SR-6
Figure F-4. Primary Side End Anchorage Details (English), Test SR-6
Figure F-5. Cable Anchor Details (English), Test SR-6
Figure F-6. Cable Anchor Details (English), Test SR-6
Figure F-7. Nose Cable Anchor Plate Details (English), Test SR-6
Figure F-8. MGS and Thrie Beam Foundation Tube Details (English), Test SR-6
Figure F-9. Wood Post Details (English), Test SR-6
Figure F-10. Wood Post Details (English), Test SR-6
Figure F-11. Wood Post Details (English), Test SR-6
Figure F-12. Iowa Steel Post Transition Details (English), Test SR-6
Figure F-13. Primary Side End Anchorage Details (English), Test SR-6
Figure F-14. Anchorage Post Details (English), Test SR-6
Figure F-15. Rail Slot Pattern Details, Rail Section No. 1 (English), Test SR-6
Figure F-16. Rail Slot Pattern Details, Rail Section No. 2 (English), Test SR-6
Figure F-17. Rail Curvature, Rail Section No. 1 (English), Test SR-6
Figure F-18. Rail Curvature, Rail Section Nos. 2 and 3 (English), Test SR-6
Figure F-19. Rail Curvature, Rail Section No. 4 (English), Test SR-6

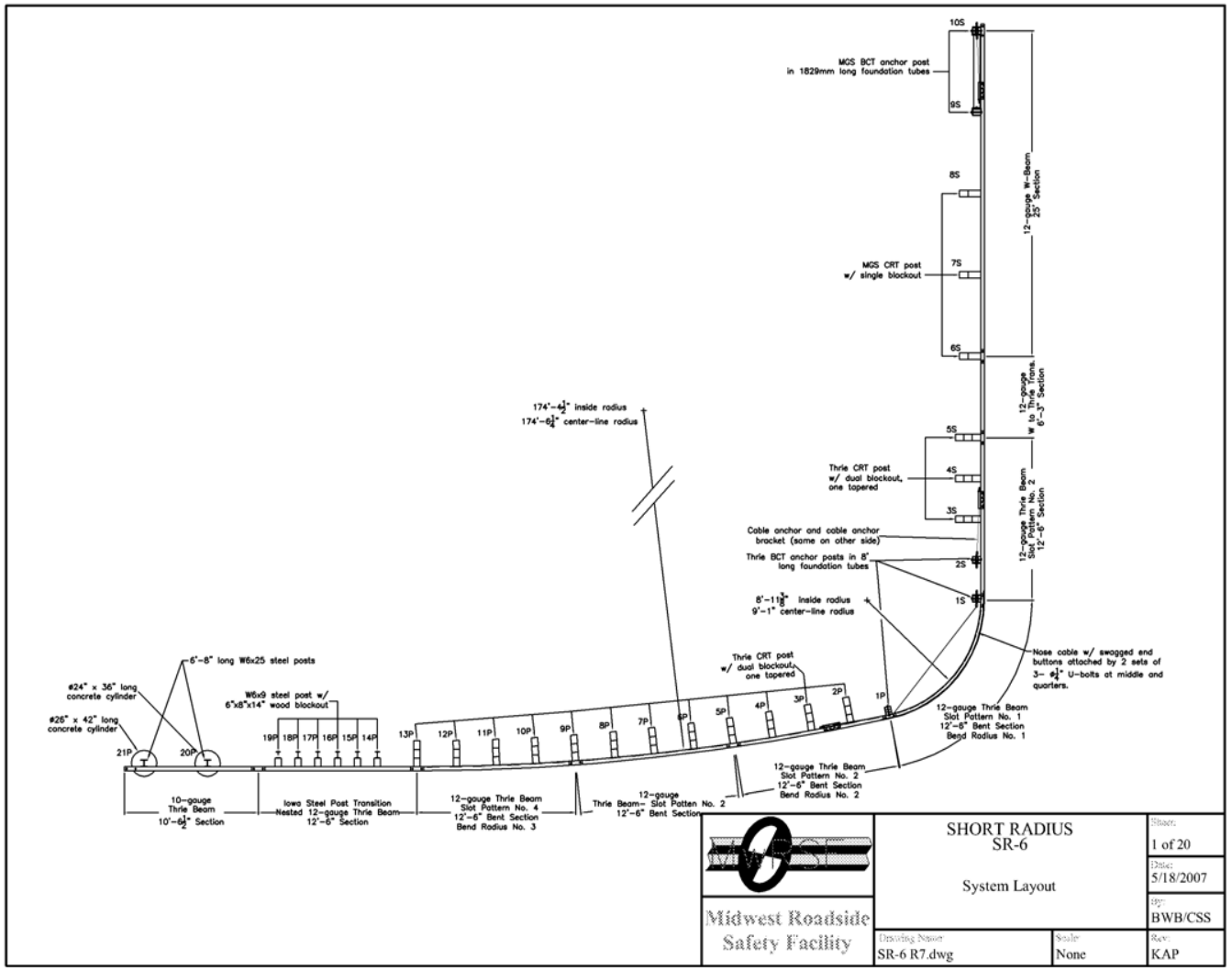

Figure F-1. Short-Radius Design Details (English), Test SR-6

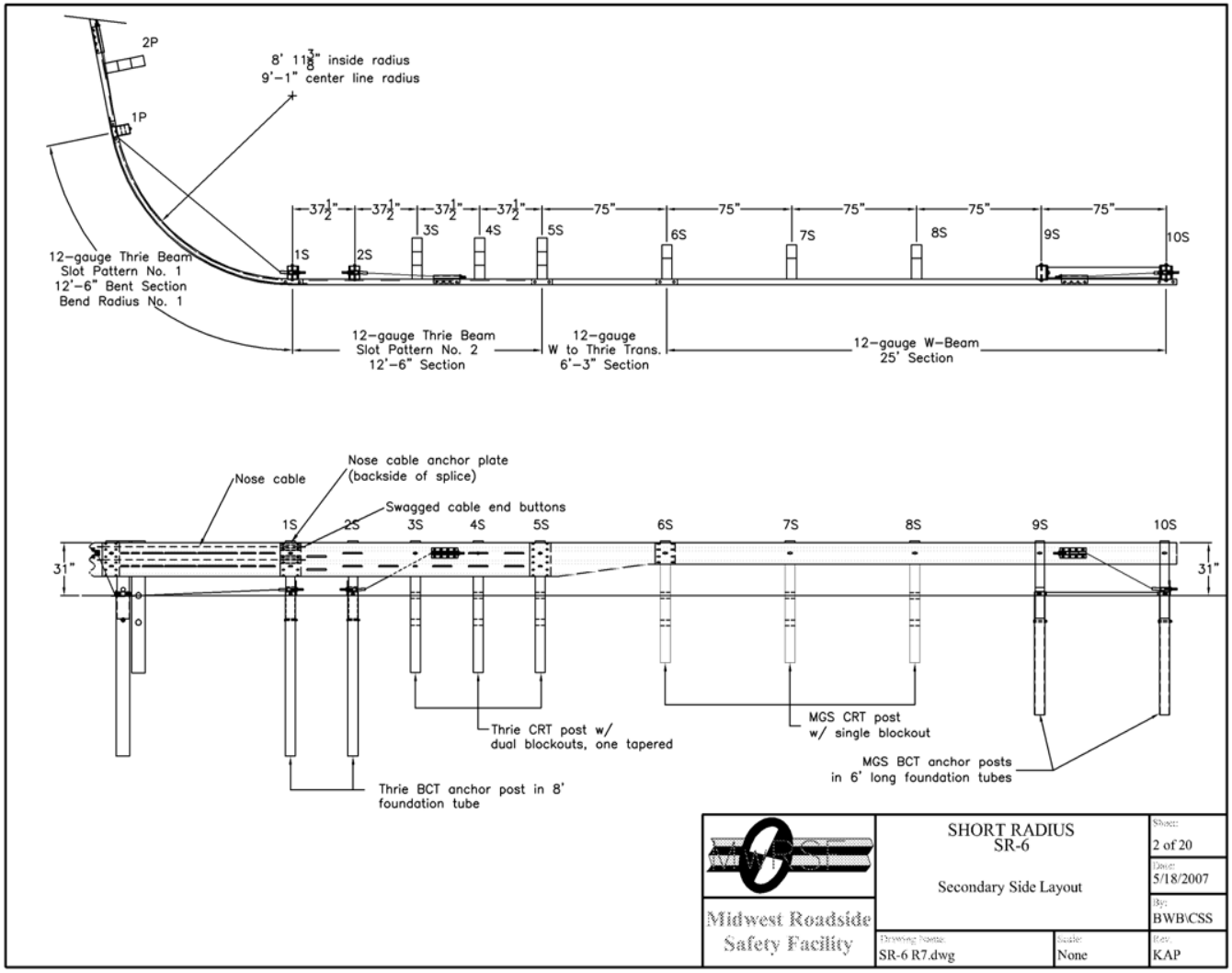

Figure F-2. Secondary Side Design Details (English), Test SR-6

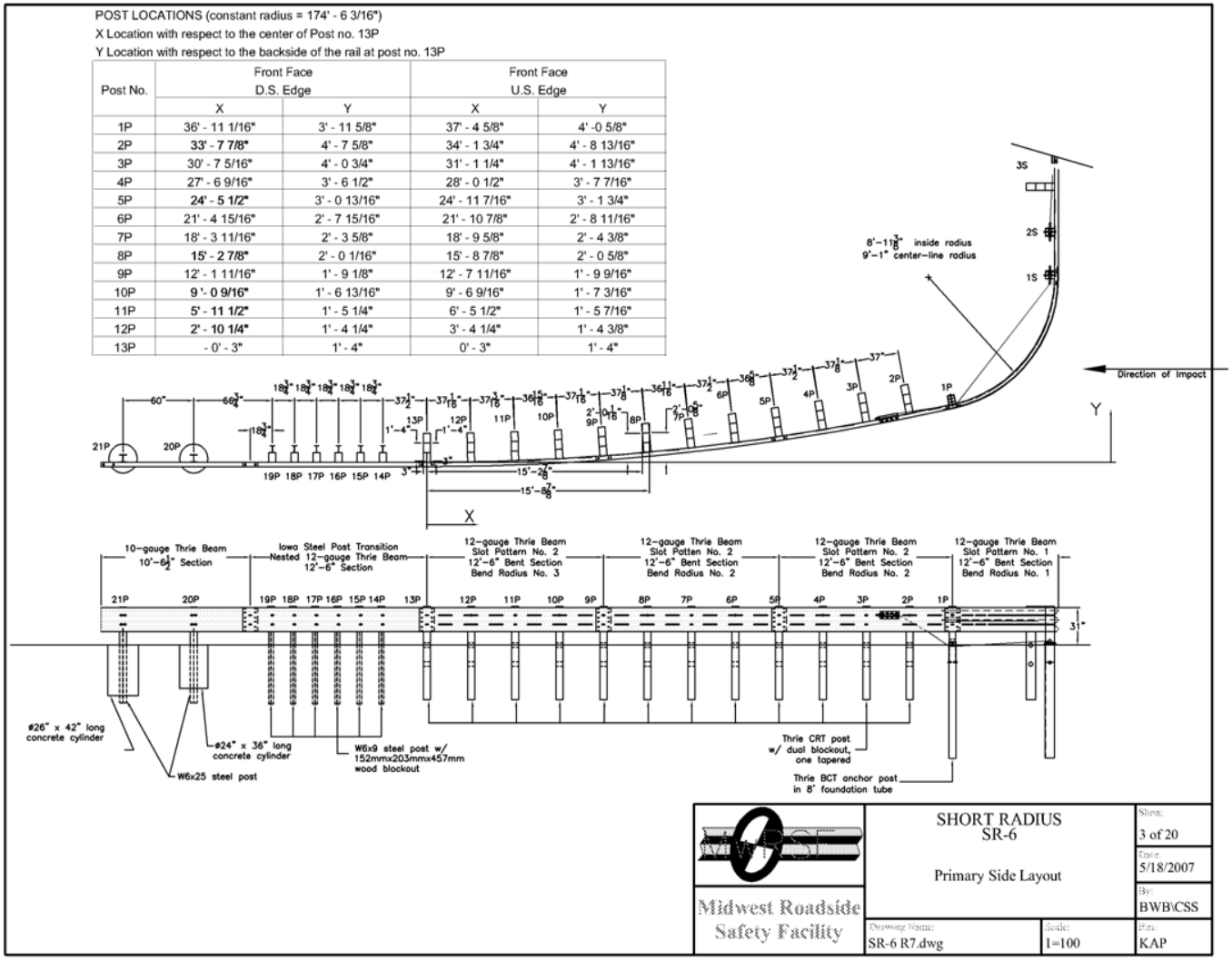

Figure F-3. Primary Side Design Details (English), Test SR-6

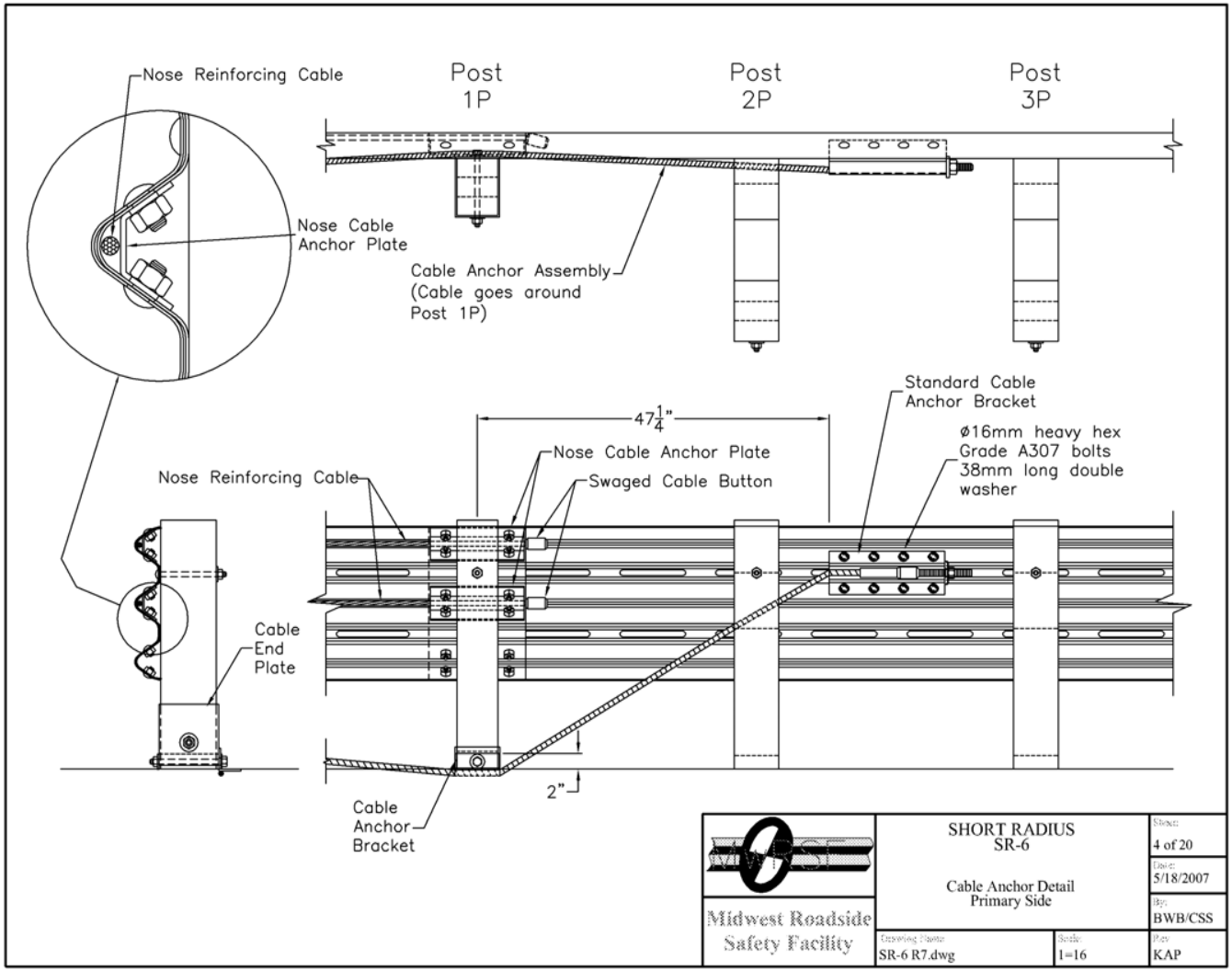

Figure F-4. Primary Side End Anchorage Details (English), Test SR-6

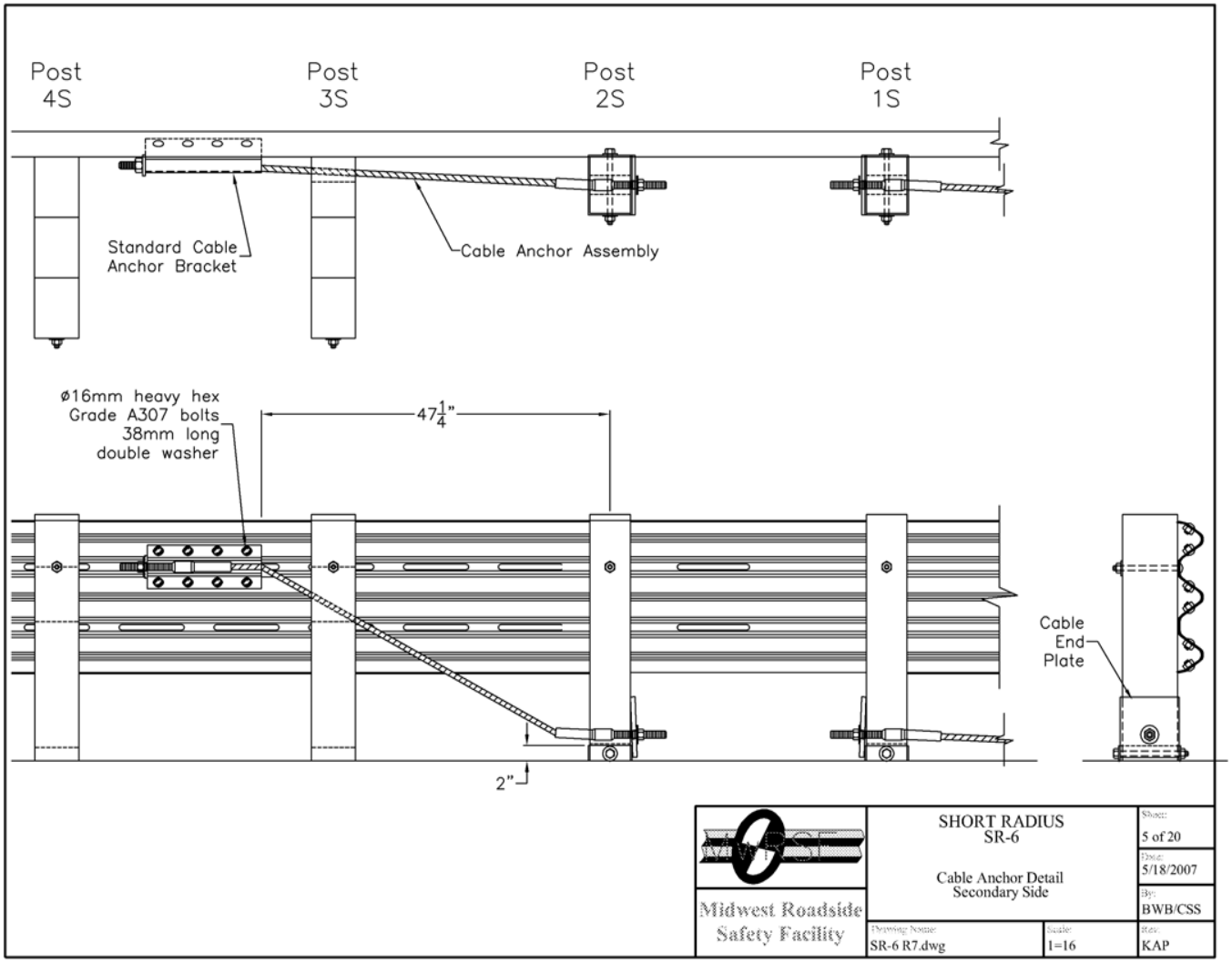

Figure F-5. Cable Anchor Details (English), Test SR-6

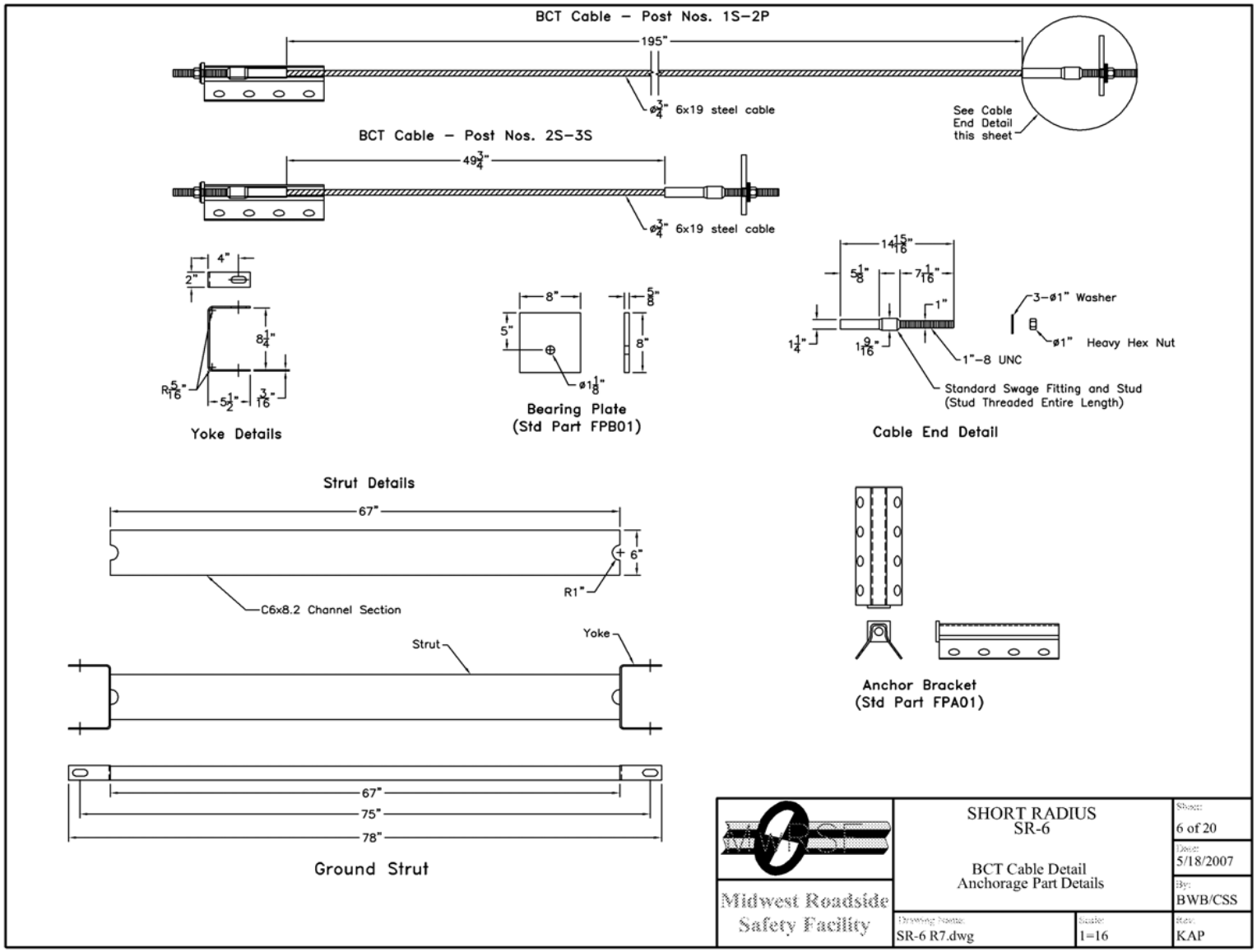

Figure F-6. Cable Anchor Details (English), Test SR-6

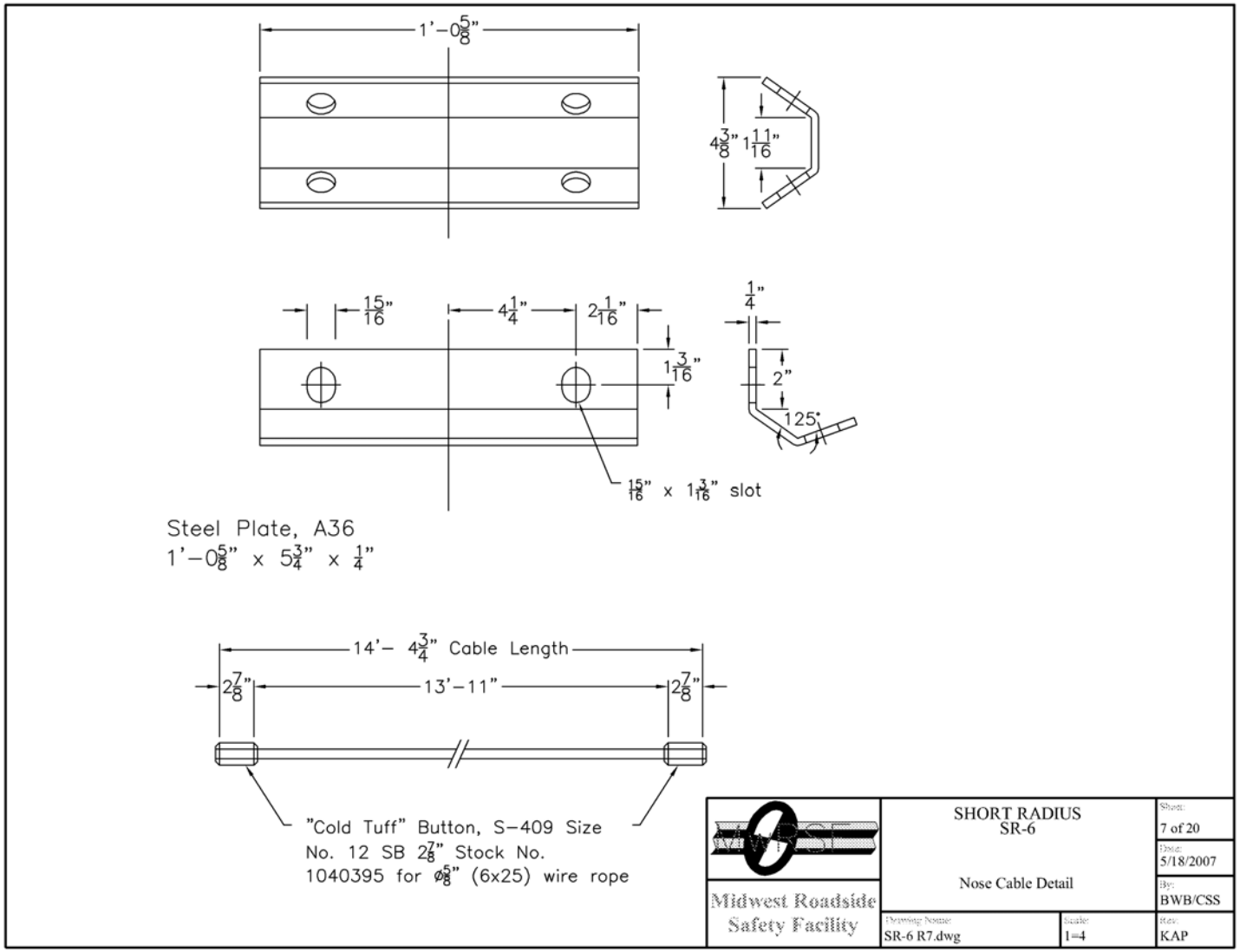

Figure F-7. Nose Cable Anchor Plate Details (English), Test SR-6

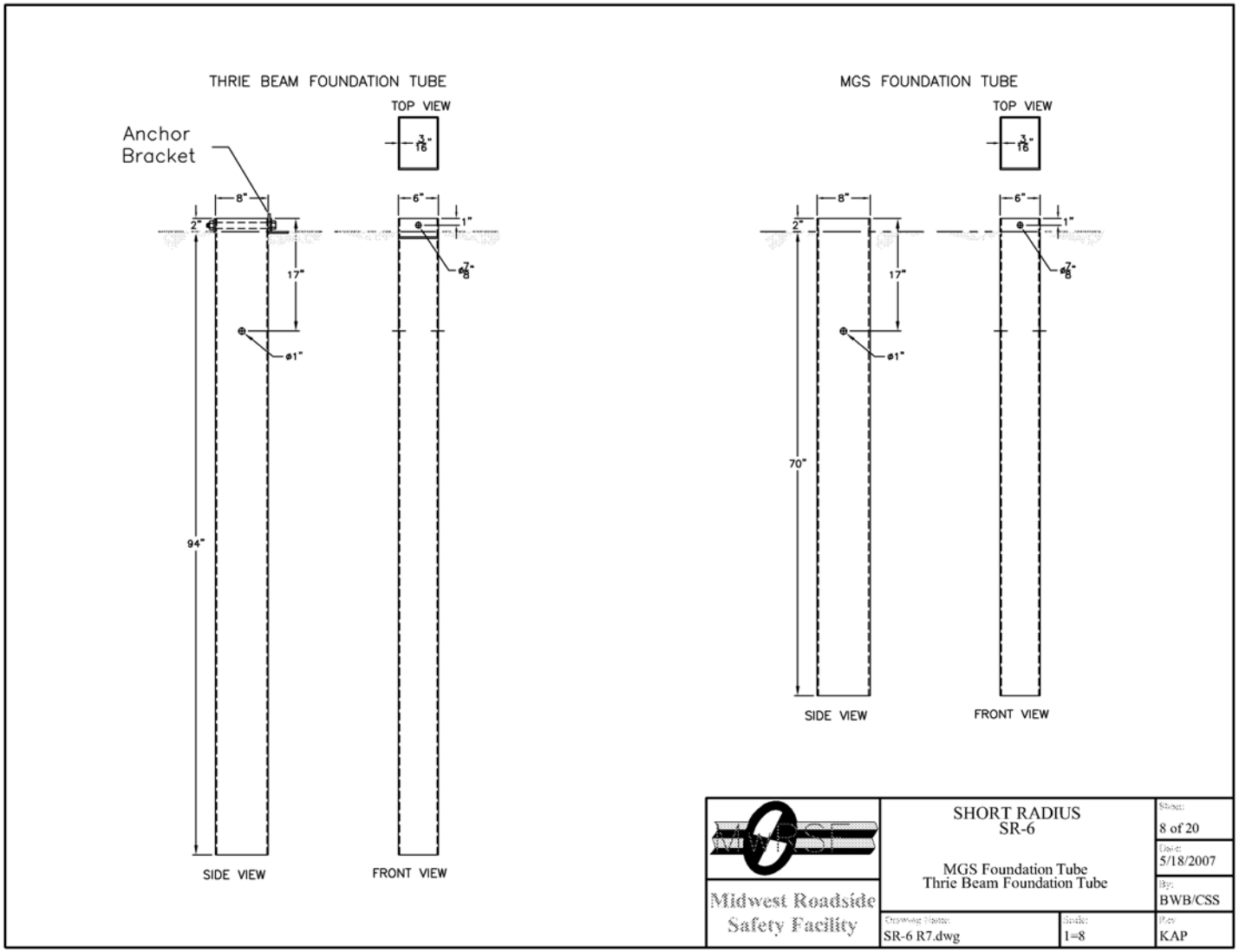

Figure F-8. MGS and Thrie Beam Foundation Tube Details (English), Test SR-6

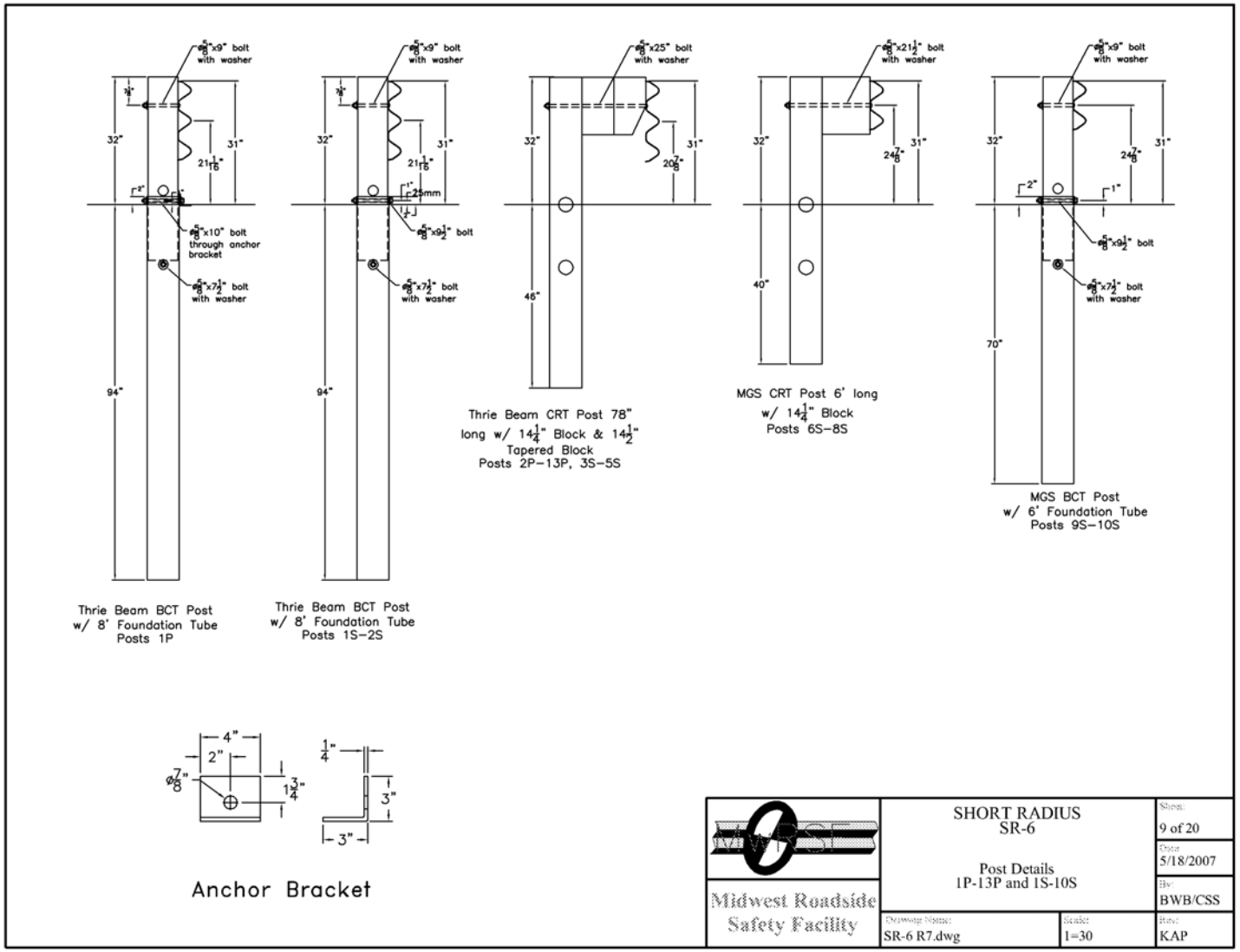

Figure F-9. Wood Post Details (English), Test SR-6

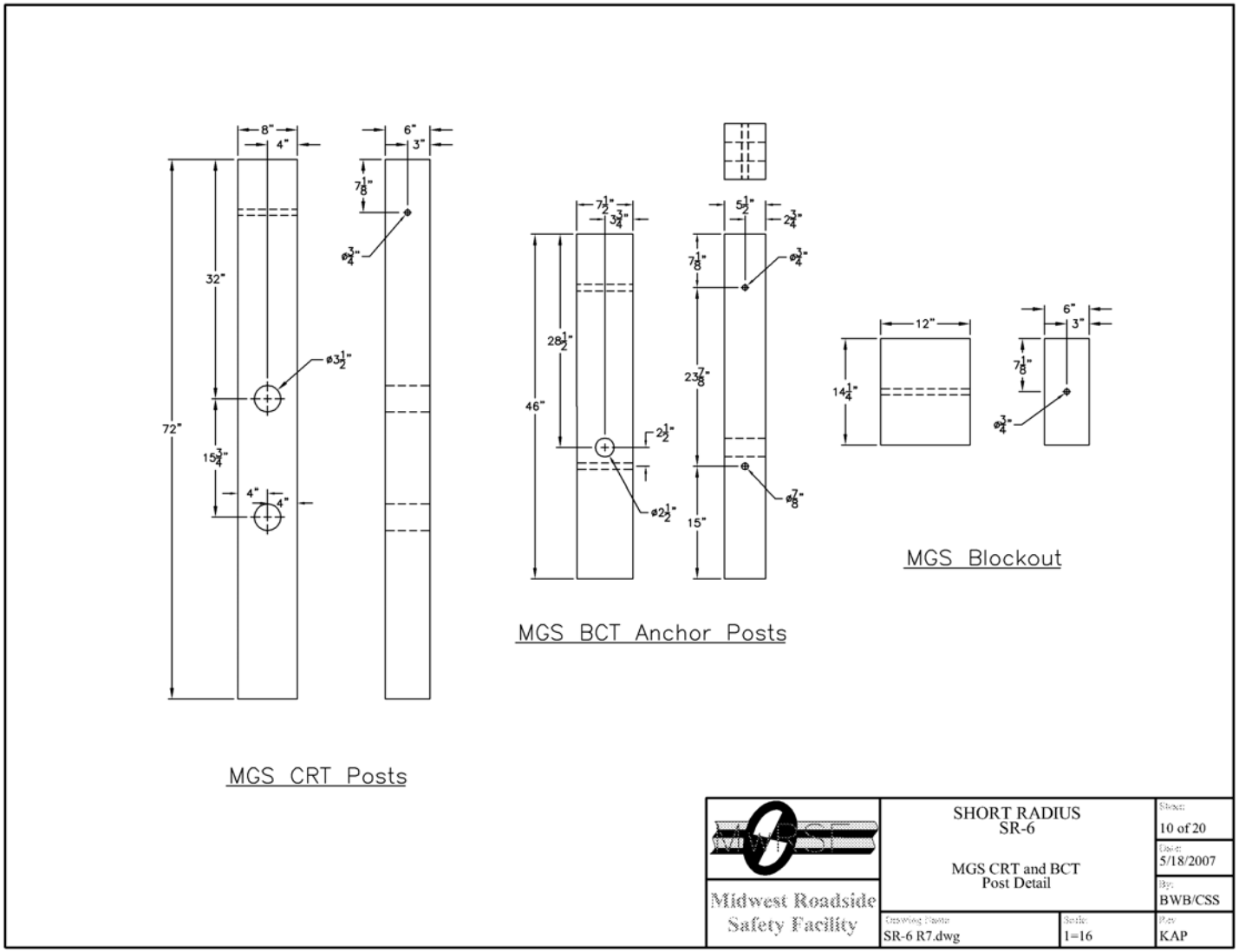

Figure F-10. Wood Post Details (English), Test SR-6

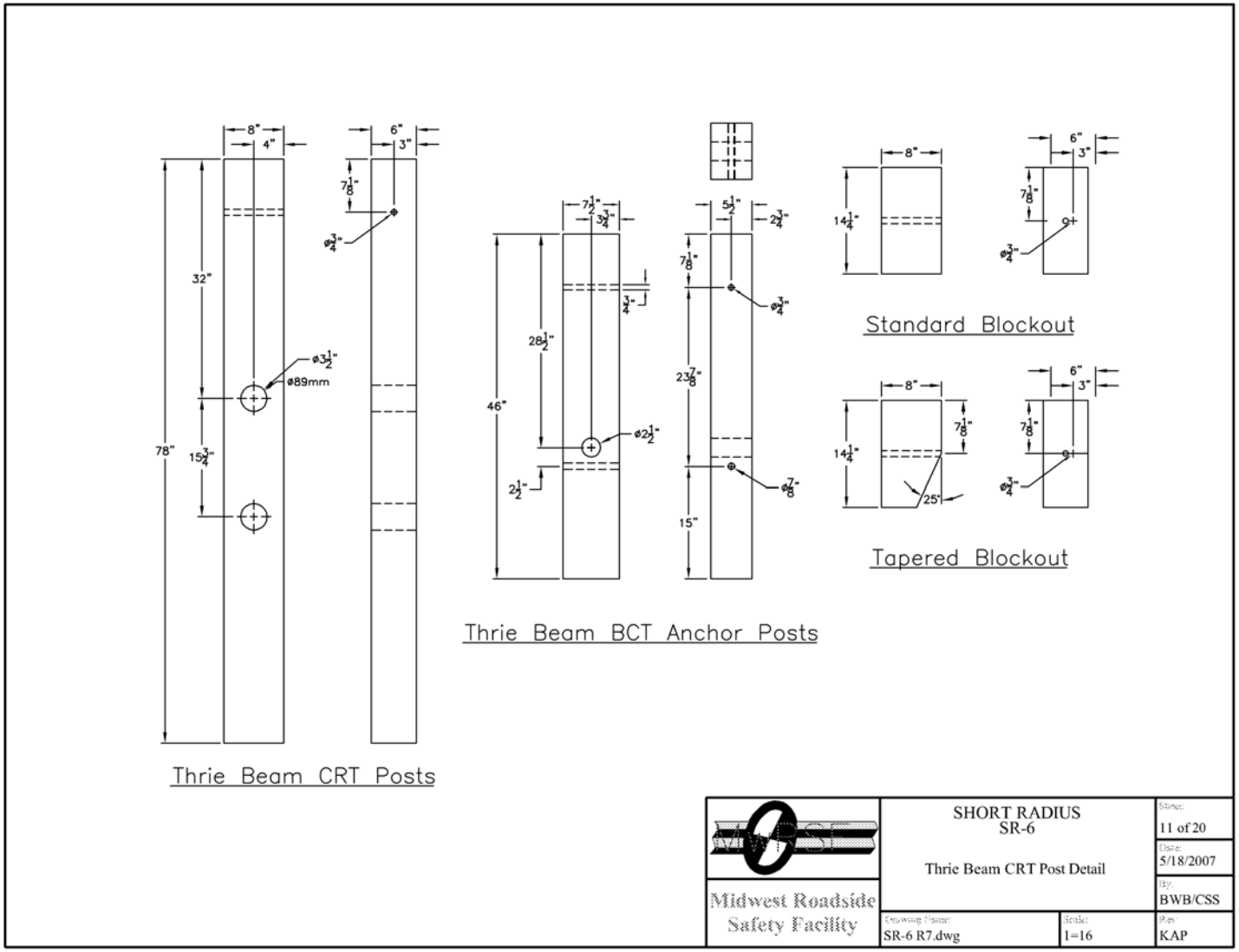

Figure F-11. Wood Post Details (English), Test SR-6

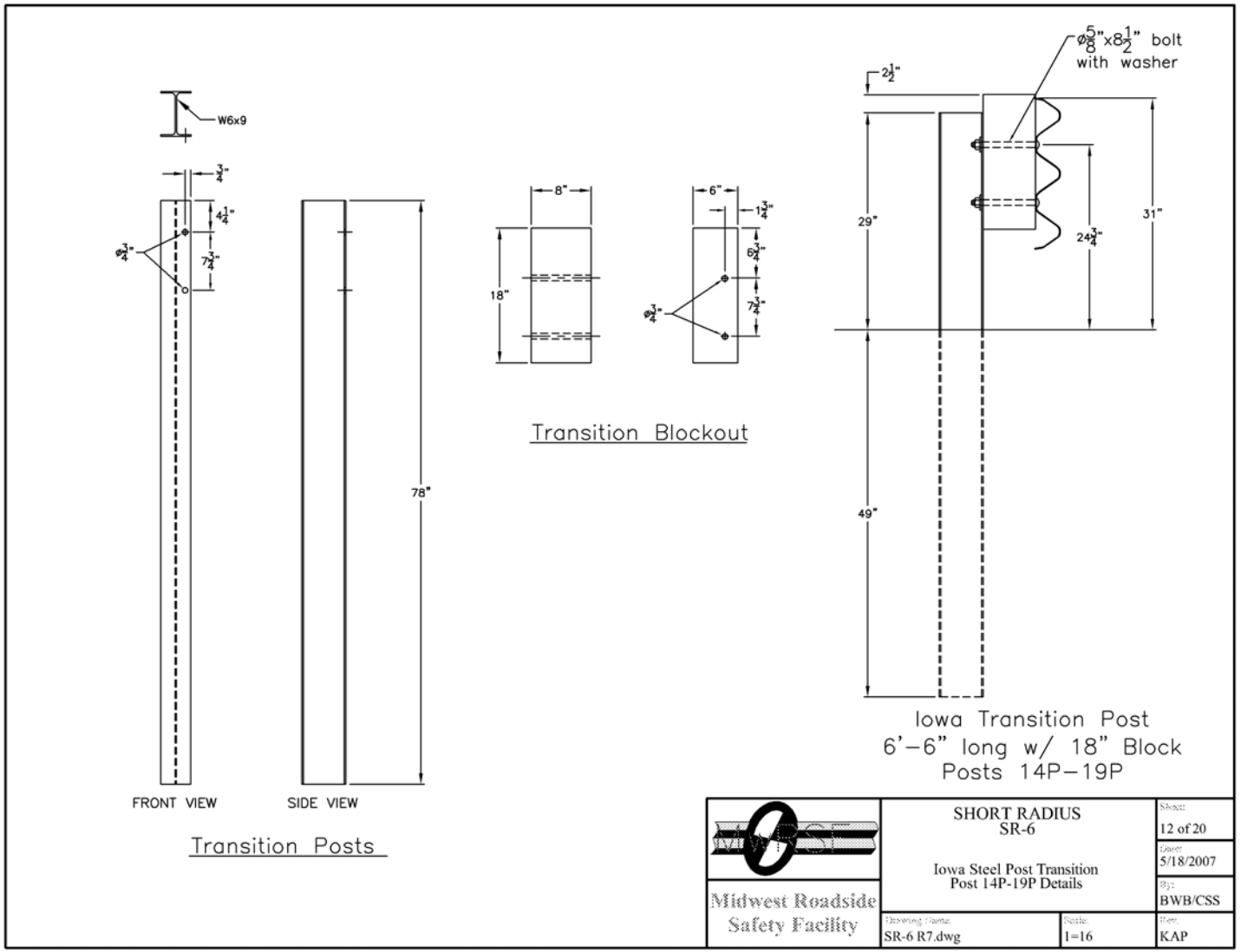

Figure F-12. Iowa Steel Post Transition Details (English), Test SR-6

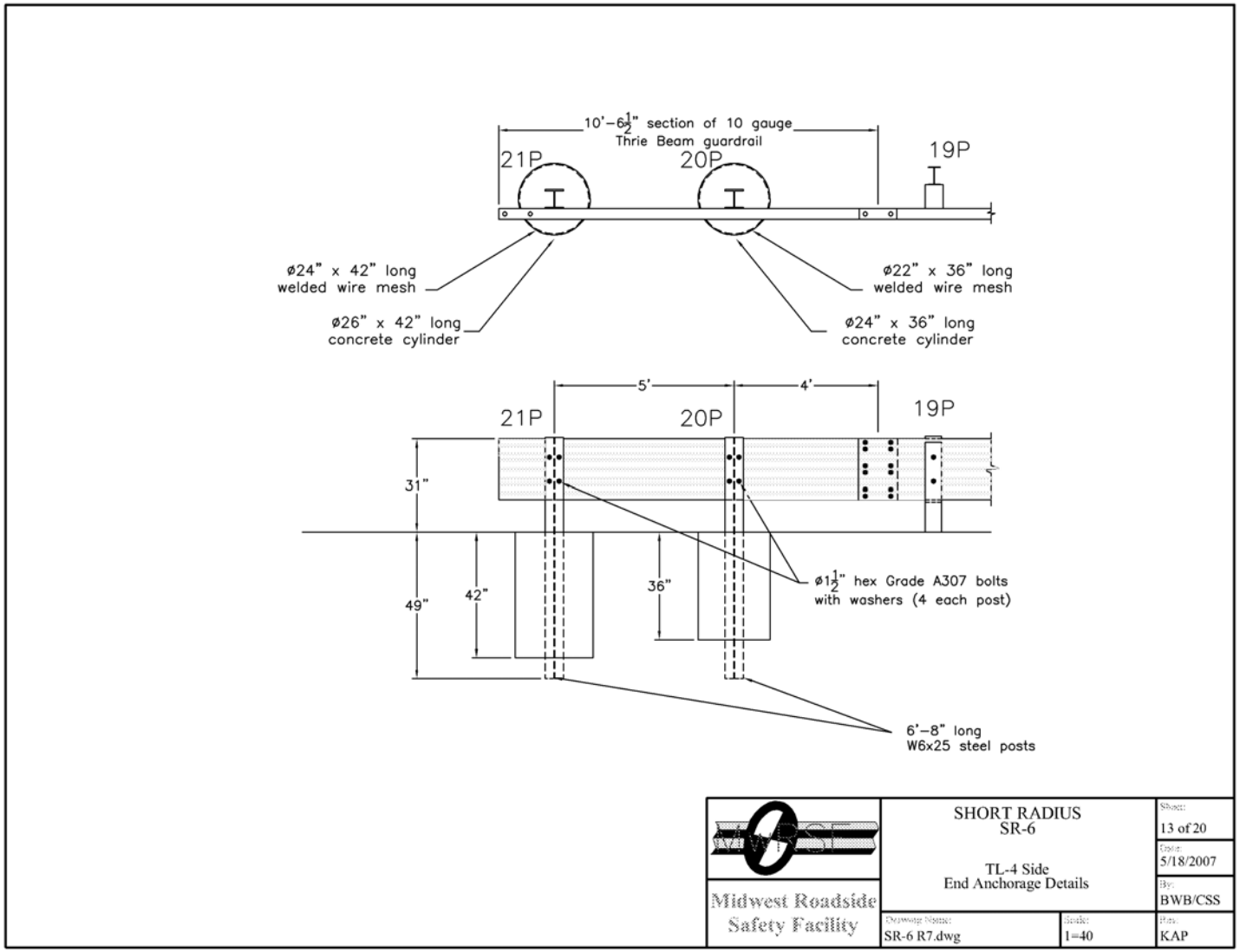

Figure F-13. Primary Side End Anchorage Details (English), Test SR-6

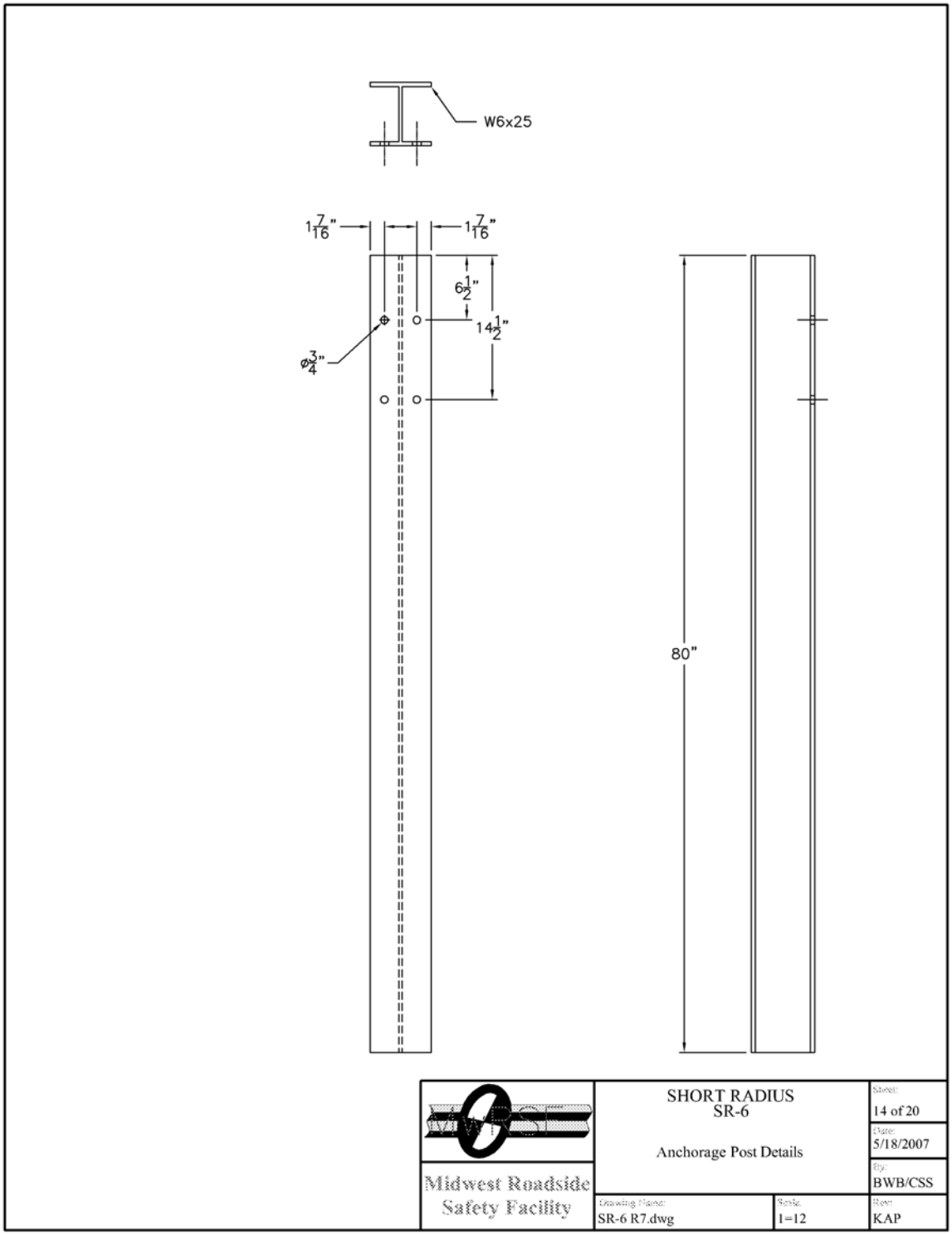

Figure F-14. Anchorage Post Details (English), Test SR-6

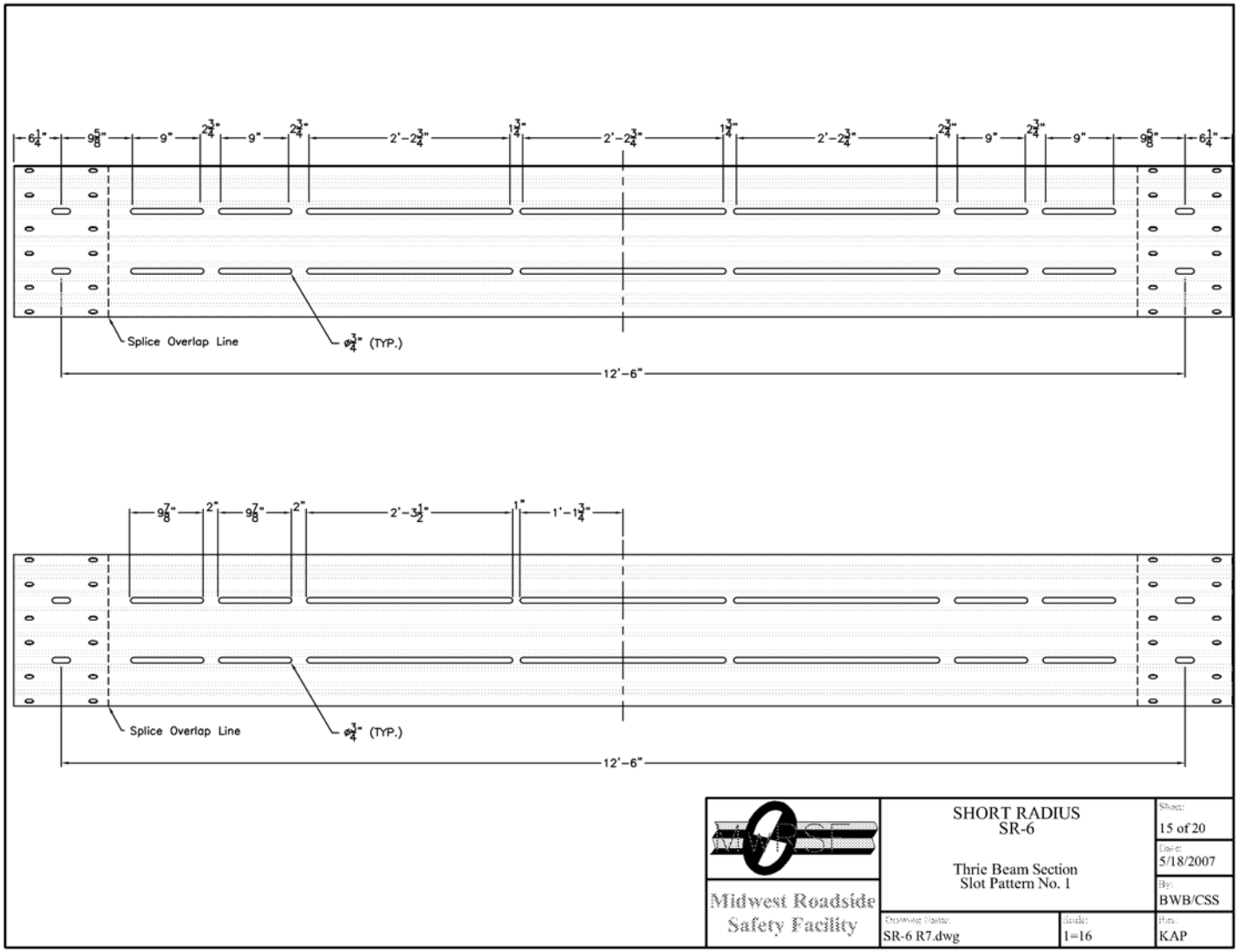

Figure F-15. Rail Slot Pattern Details, Rail Section No. 1 (English), Test SR-6

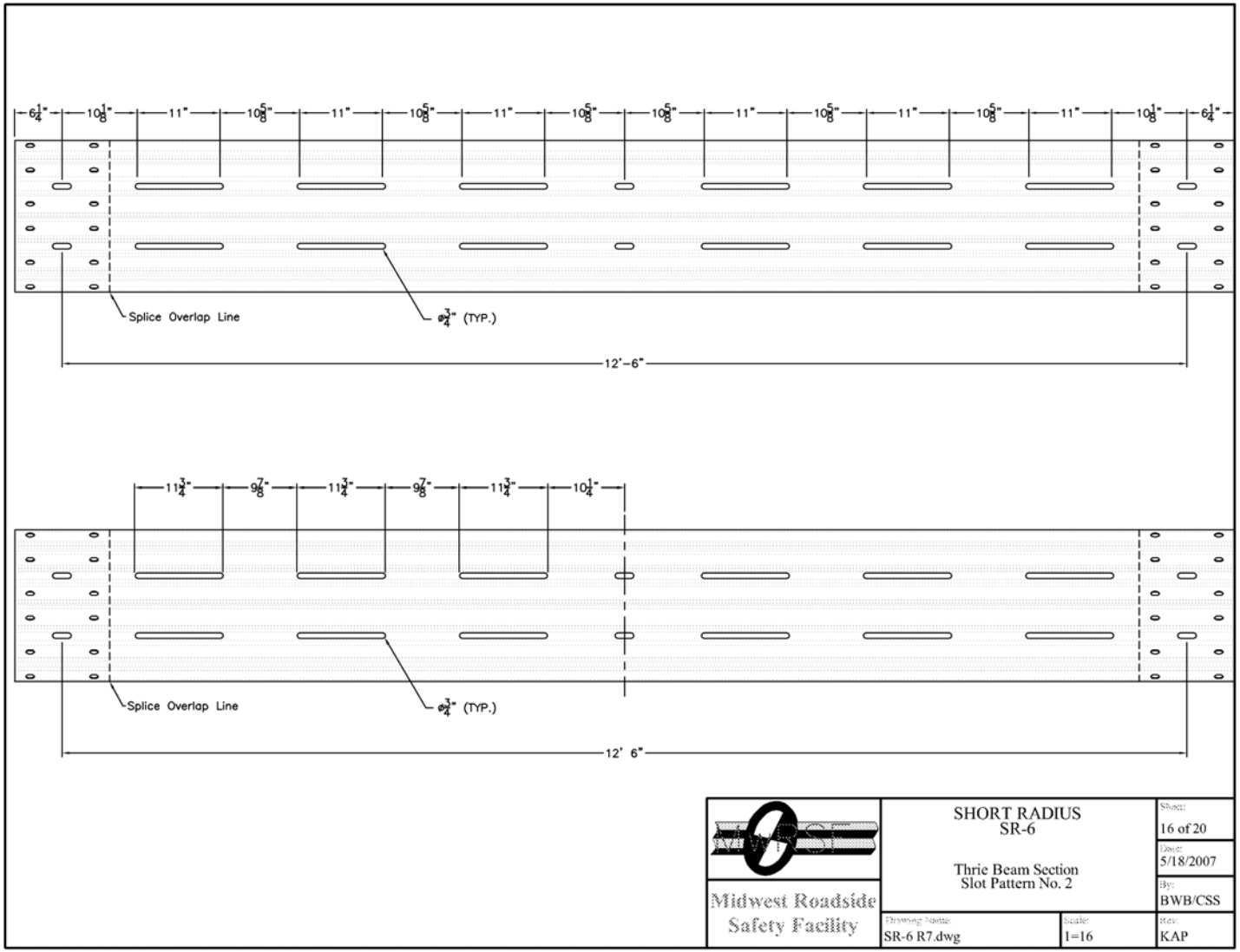

Figure F-16. Rail Slot Pattern Details, Rail Section No. 2 (English), Test SR-6

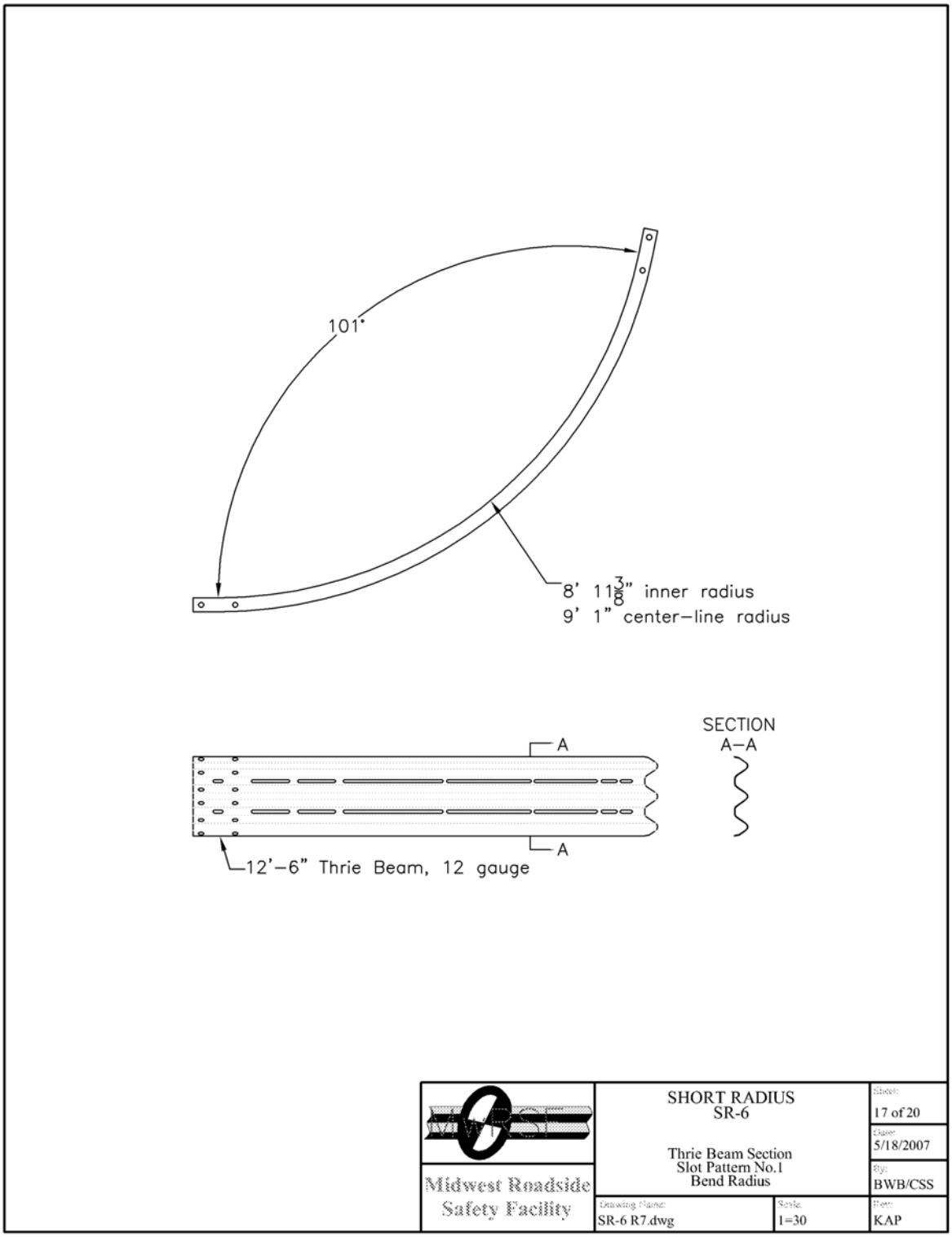

Figure F-17. Rail Curvature, Rail Section No. 1 (English), Test SR-6

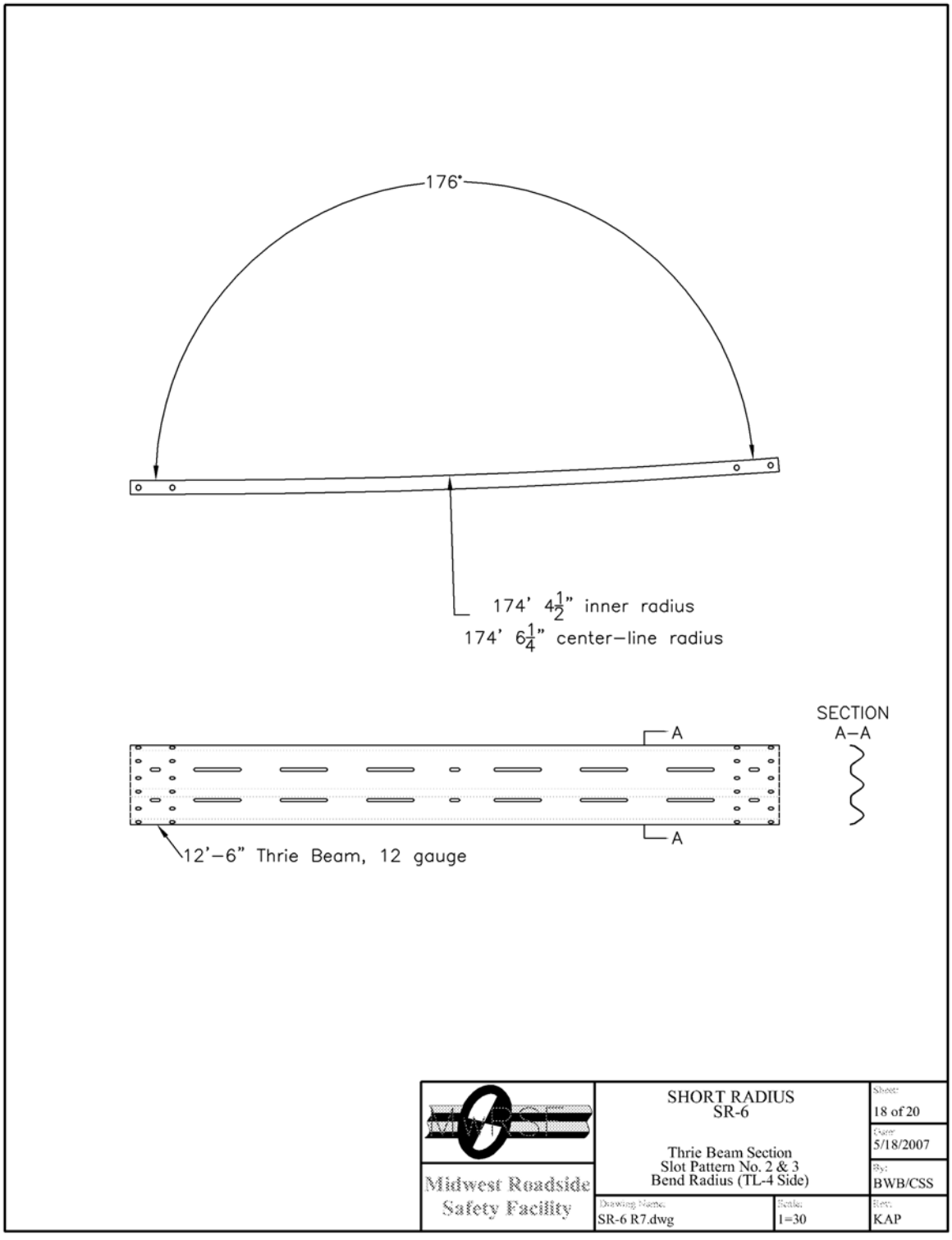

Figure F-18. Rail Curvature, Rail Section Nos. 2 and 3 (English), Test SR-6

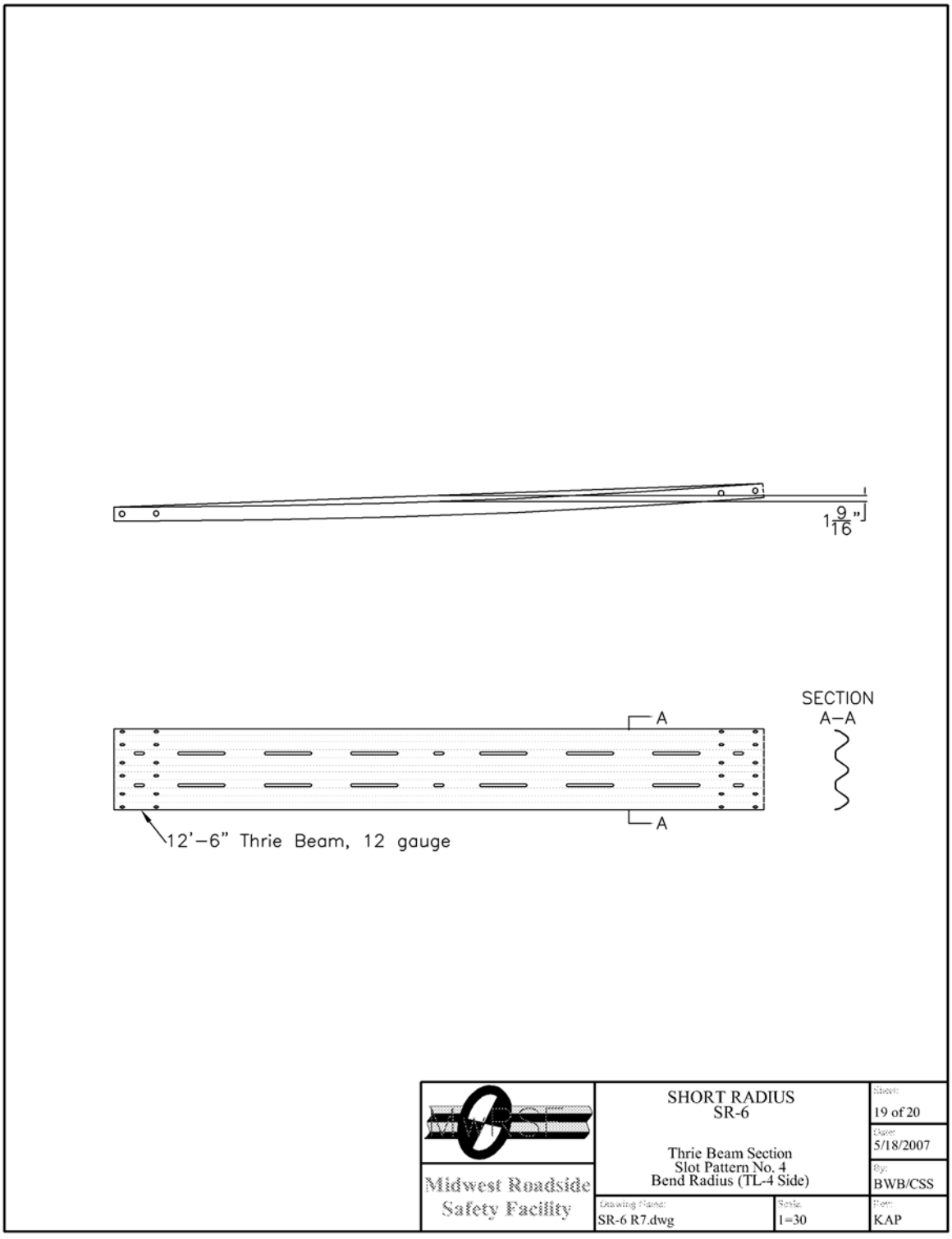

Figure F-19. Rail Curvature, Rail Section No. 4 (English), Test SR-6

APPENDIX G

Accelerometer and Rate Transducer Data Analysis, Test SR-6

Figure G-1. Occupant Compartment Deformation Index (OCDI), Test SR-6

Occupant Compartment Deformation Index (OCDI)

Test No. SR-6
Vehicle Type: 820c / Metro

OCDI = XXABCDEFGHI

XX = location of occupant compartment deformation

A = distance between the dashboard and a reference point at the rear of the occupant compartment, such as the top of the rear seat or the rear of the cab on a pickup

B = distance between the roof and the floor panel

C = distance between a reference point at the rear of the occupant compartment and the motor panel

D = distance between the lower dashboard and the floor panel

E = interior width

F = distance between the lower edge of right window and the upper edge of left window

G = distance between the lower edge of left window and the upper edge of right window

H= distance between bottom front corner and top rear corner of the passenger side window

I= distance between bottom front corner and top rear corner of the driver side window

Severity Indices

0 - if the reduction is less than 3%
1 - if the reduction is greater than 3% and less than or equal to 10 %
2 - if the reduction is greater than 10% and less than or equal to 20 %
3 - if the reduction is greater than 20% and less than or equal to 30 %
4 - if the reduction is greater than 30% and less than or equal to 40 %

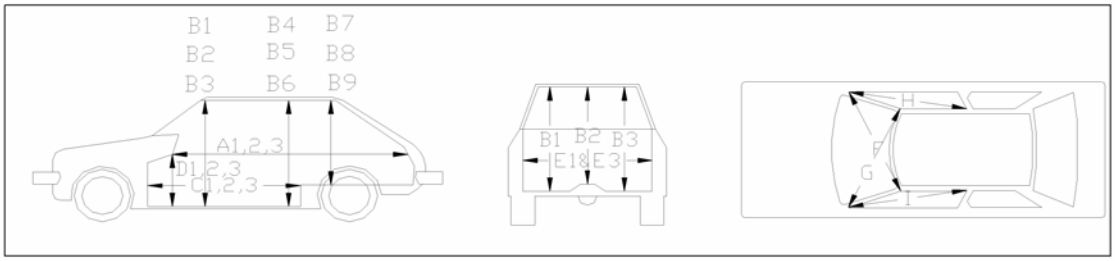

where,
1 = Passenger Side
2 = Middle
3 = Driver Side

Location:

Measurement	Pre-Test (in.)	Post-Test (in.)	Change (in.)	% Difference	Severity Index
A1	85.00	85.00	0.00	0.00	0
A2	85.50	85.25	-0.25	-0.29	0
A3	82.25	82.50	0.25	0.30	0
B1	40.25	40.50	0.25	0.62	0
B2	40.00	40.00	0.00	0.00	0
B3	41.25	41.50	0.25	0.61	0
C1	55.00	54.00	-1.00	-1.82	0
C2	59.75	59.00	-0.75	-1.26	0
C3	54.75	55.00	0.25	0.46	0
D1	14.00	14.25	0.25	1.79	0
D2	14.50	14.50	0.00	0.00	0
D3	13.00	13.00	0.00	0.00	0
E1	49.25	49.50	0.25	0.51	0
E3	49.50	49.50	0.00	0.00	0
F	48.75	48.50	-0.25	-0.51	0
G	48.25	48.25	0.00	0.00	0
H	39.50	39.75	0.25	0.63	0
I	40.50	40.50	0.00	0.00	0

Note: Maximum sevrity index for each variable (A-I) is used for determination of final OCDI value

	XX A B C D E F G H I
Final OCDI:	RF 0 0 0 0 0 0 0 0 0

Figure G-1. Occupant Compartment Deformation Index (OCDI), Test SR-6

APPENDIX H

Accelerometer and Rate Transducer Data Analysis, Test SR-6

Figure H-1. Graph of Longitudinal Deceleration, Test SR-6
Figure H-2. Graph of Longitudinal Occupant Impact Velocity, Test SR-6
Figure H-3. Graph of Longitudinal Occupant Displacement, Test SR-6
Figure H-4. Graph of Lateral Deceleration, Test SR-6
Figure H-5. Graph of Lateral Occupant Impact Velocity, Test SR-6
Figure H-6. Graph of Lateral Occupant Displacement, Test SR-6
Figure H-7. Graph of Roll, Pitch, and Yaw Angular Displacements, Test SR-6

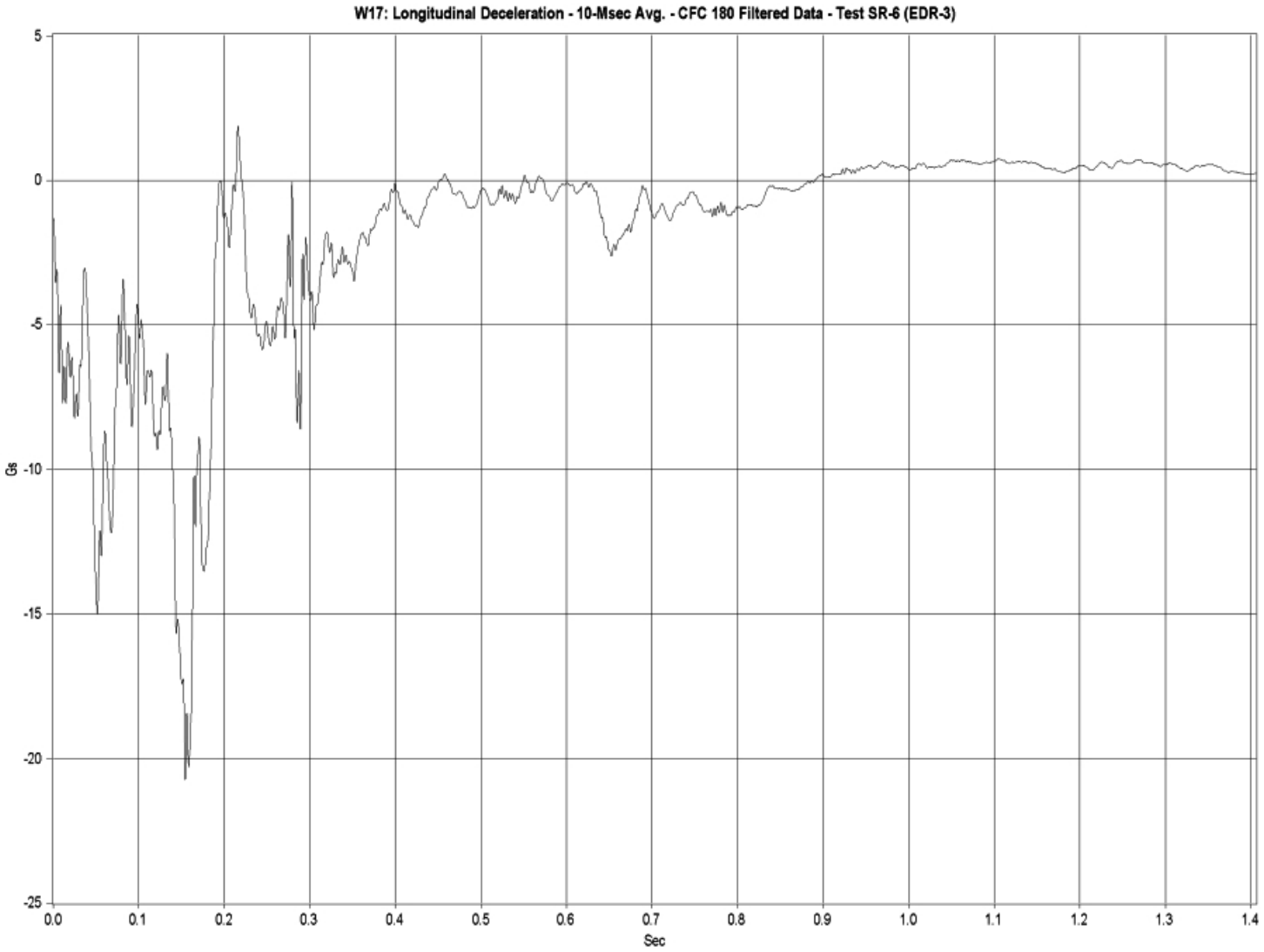

Figure H-1. Graph of Longitudinal Deceleration, Test SR-6

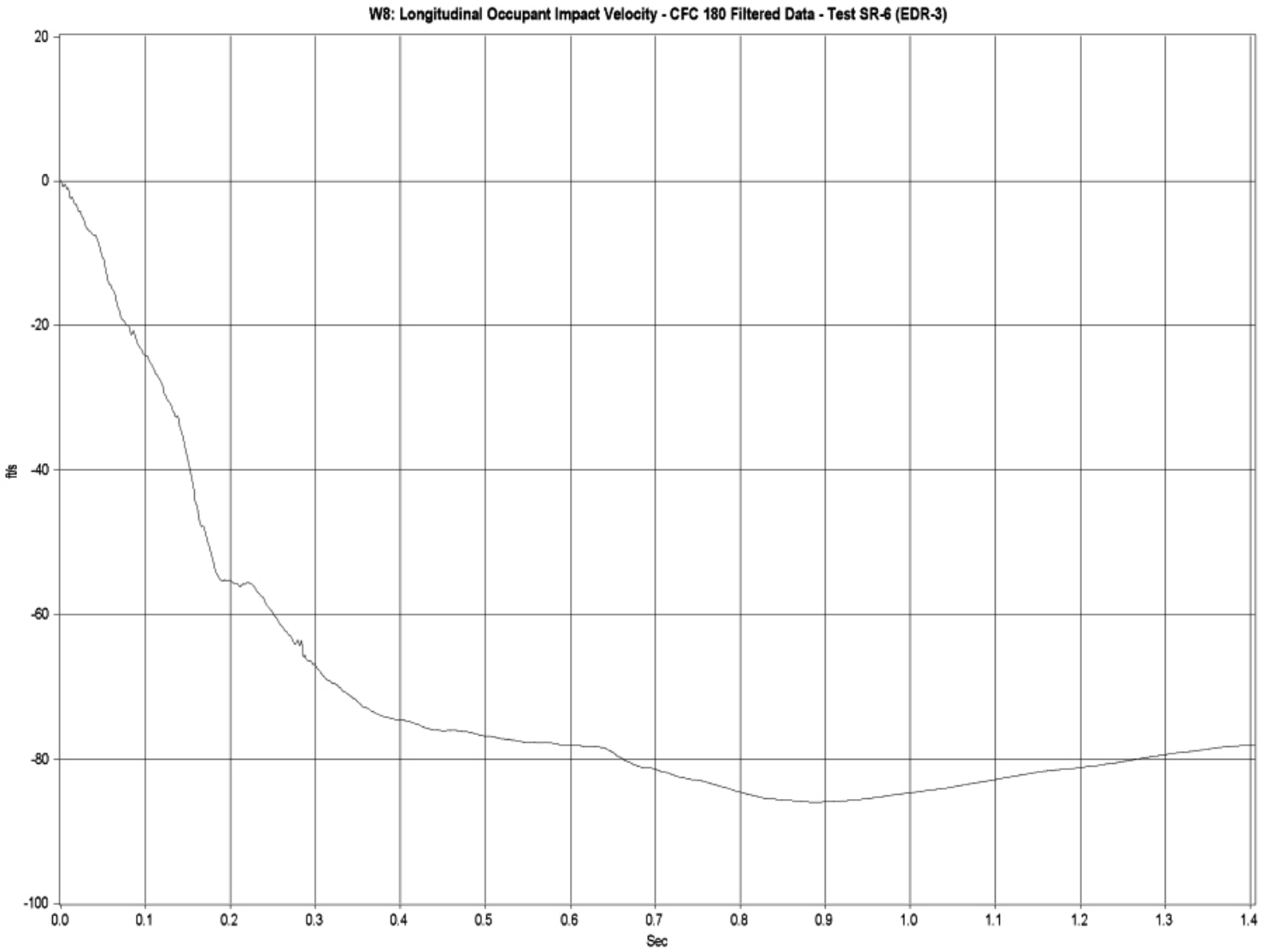

Figure H-2. Graph of Longitudinal Occupant Impact Velocity, Test SR-6

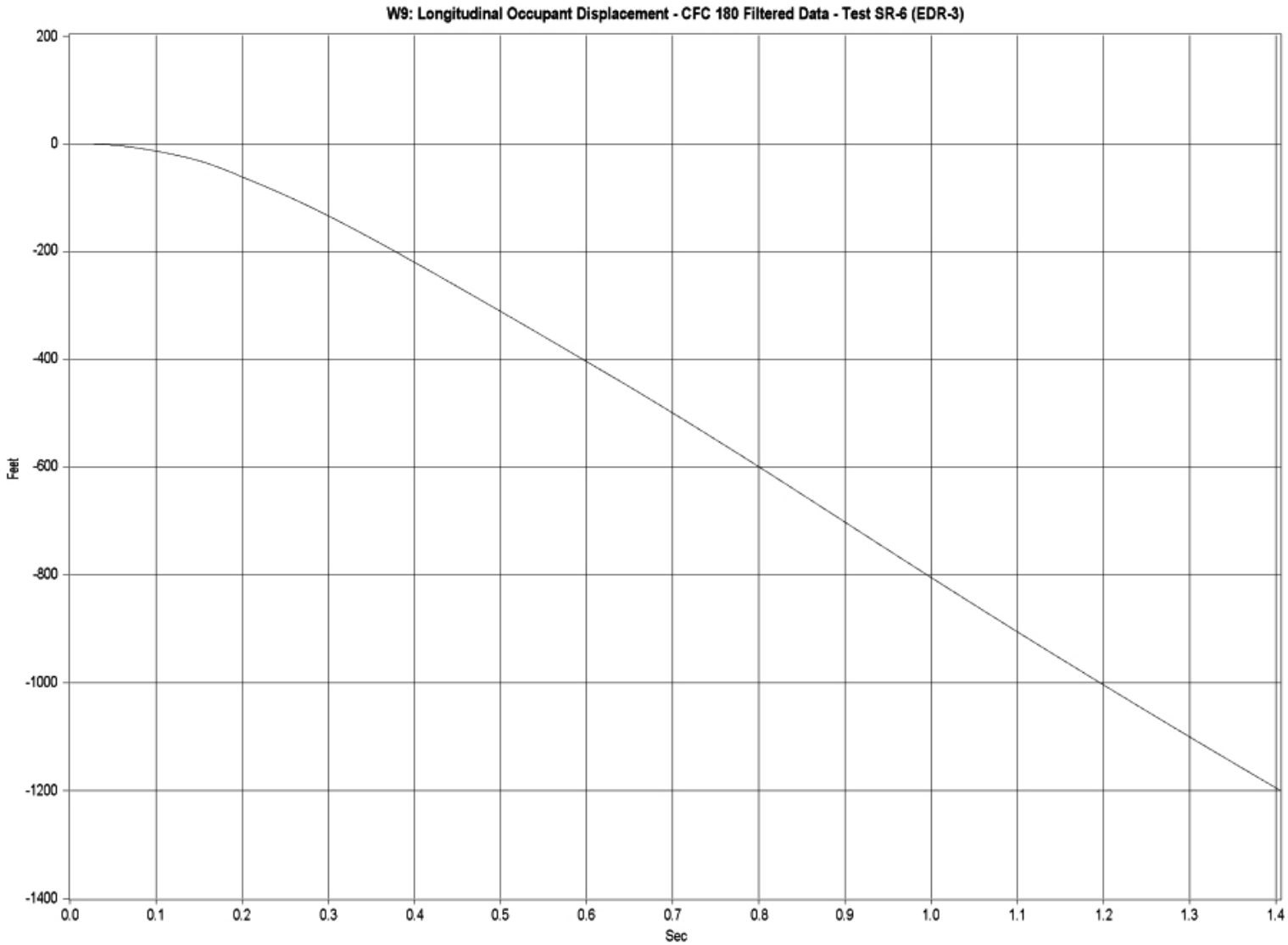

Figure H-3. Graph of Longitudinal Occupant Displacement, Test SR-6

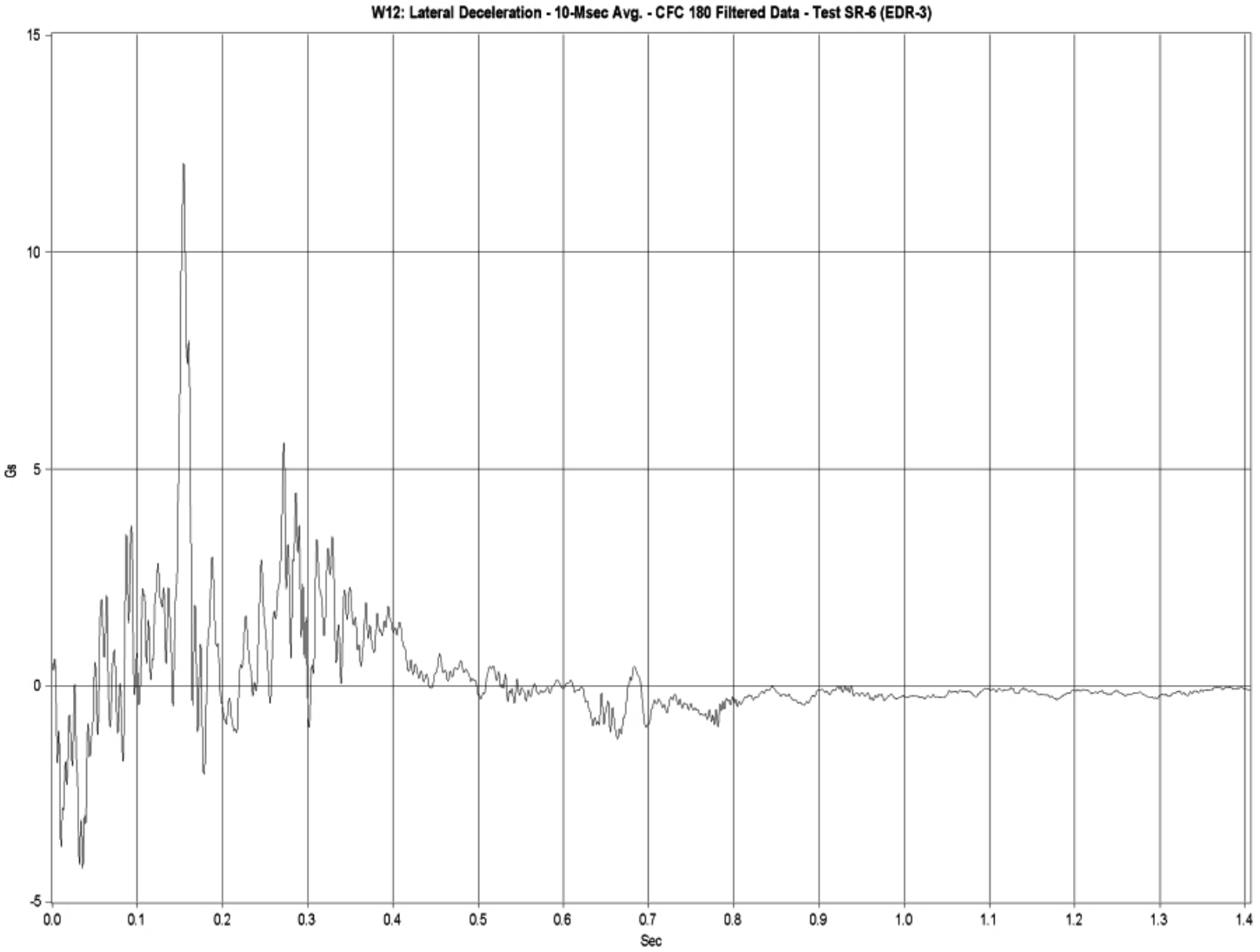

Figure H-4. Graph of Lateral Deceleration, Test SR-6

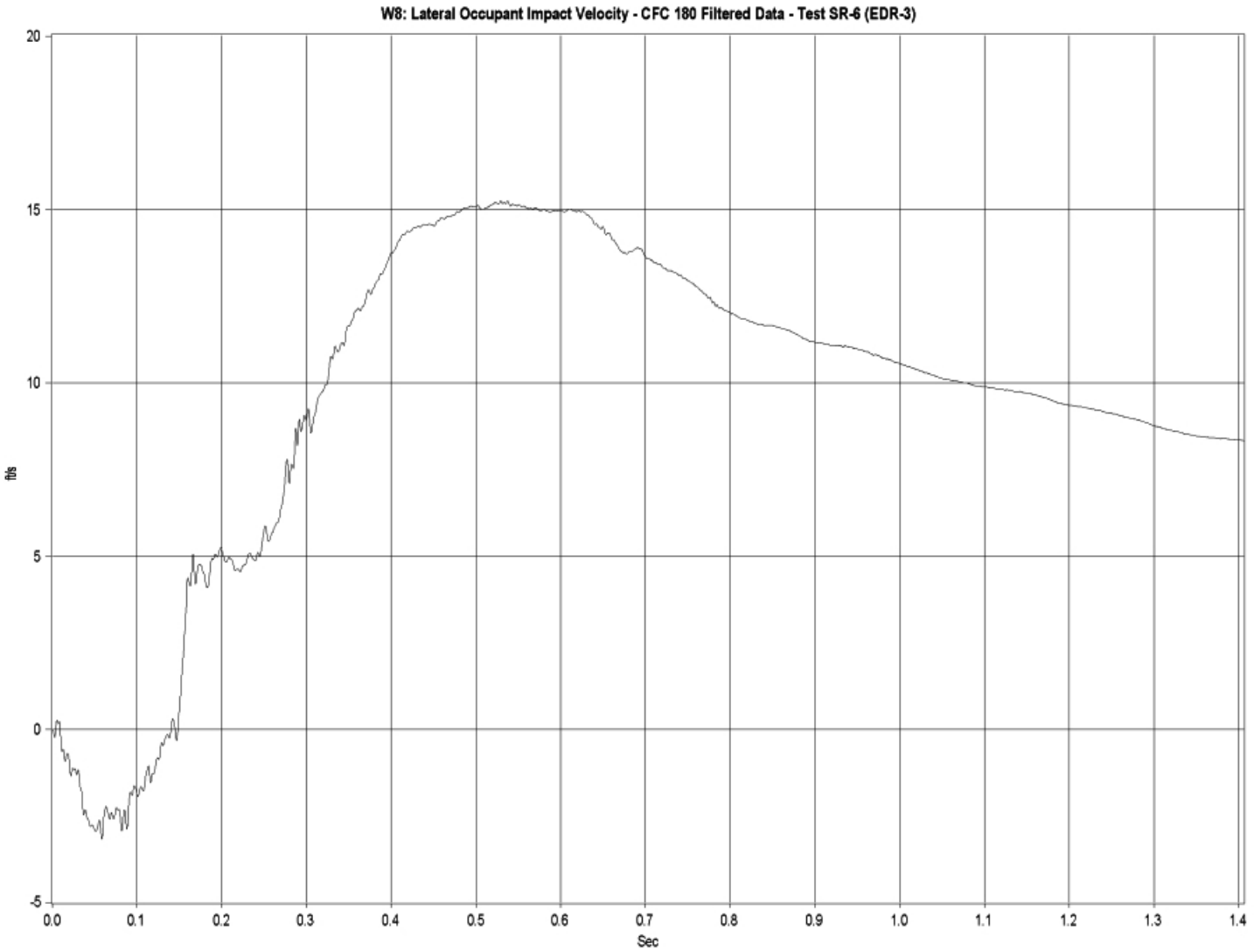

Figure H-5. Graph of Lateral Occupant Impact Velocity, Test SR-6

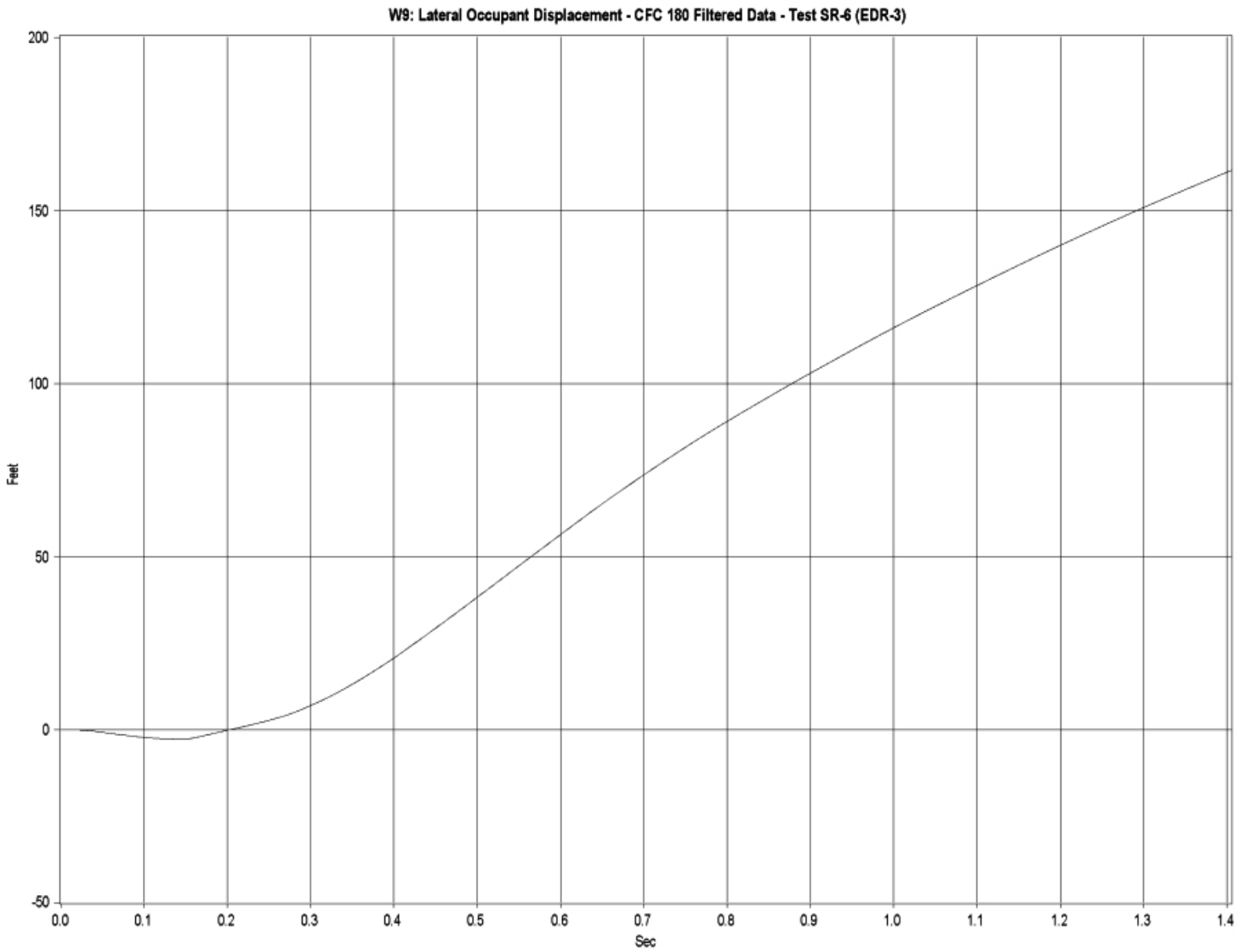

Figure H-6. Graph of Lateral Occupant Displacement, Test SR-6

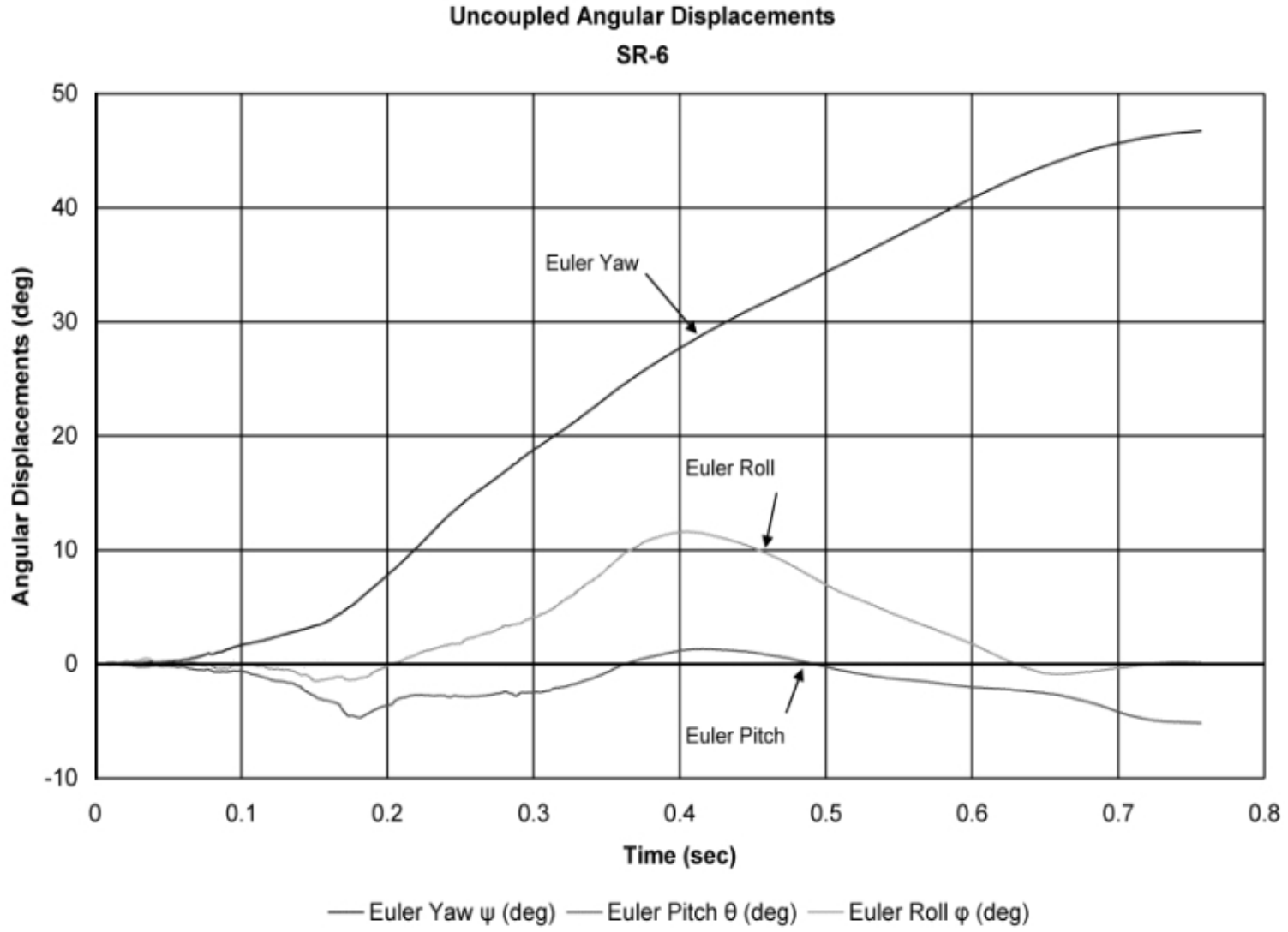

Figure H-7. Graph of Roll, Pitch, and Yaw Angular Displacements, Test SR-6